



**Nuran Cihangir Martin**

**Computational techniques and model accuracy  
for electric power transmission and distribution  
solo and coordinated system-operational  
problems**

**Tese de Doutorado**

Thesis presented to the Programa de Pós-graduação em Engenharia de Produção, of PUC-Rio in partial fulfillment of the requirements for the degree of Doutor em Engenharia de Produção.

Advisor: Prof. Bruno Fânzeres dos Santos

Rio de Janeiro  
April 2024



**Nuran Cihangir Martin**

**Computational techniques and model accuracy  
for electric power transmission and distribution  
solo and coordinated system-operational  
problems**

Thesis presented to the Programa de Pós-graduação em Engenharia de Produção of PUC-Rio in partial fulfillment of the requirements for the degree of Doutor em Engenharia de Produção. Approved by the Examination Committee:

**Prof. Bruno Fânzeres dos Santos**

Advisor

Departamento de Engenharia Industrial – PUC-Rio

**Prof. Peter Palensky**

TU Delft

**Dr. Arild Helseth**

SINTEF

**Dr. David Pozo**

European Commission

**Prof. Nikolaos Paterakis**

TU Eindhoven

**Prof. Davi Michel Valladão**

Departamento de Engenharia Industrial – PUC-Rio

Rio de Janeiro, April 11th, 2024

All rights reserved.

### **Nuran Cihangir Martin**

Nuran Cihangir Martin works as a Grid Strategist at a Distribution System Operator in the Netherlands, Stedin. She is a member of the European Distribution System Operator's Association (E.DSO) and the Netherlands National Committee for CIGRE C6 - Active Distribution Systems. She obtained her B.Sc. degree in Mathematics from the Middle East Technical University (METU), Ankara, Türkiye, and M.Sc. degree in the area of quantitative methods in Financial Economics, from Istanbul Bilgi University, Istanbul, Türkiye. Her current research interests include electric power distribution and transmission systems planning and operations, and applications of optimisation and computational techniques.

#### Bibliographic data

Martin, Nuran Cihangir

Computational techniques and model accuracy for electric power transmission and distribution solo and coordinated system-operational problems / Nuran Cihangir Martin; advisor: Bruno Fânzeres dos Santos. – 2024.

187 f: il. color. ; 30 cm

Tese (doutorado) - Pontifícia Universidade Católica do Rio de Janeiro, Departamento de Engenharia Industrial, 2024.

Inclui bibliografia

1. Engenharia Industrial – Teses. 2. Unit Commitment com restrita de rede AC e fluxo de potência. 3. Coordenação DSO-TSO. 4. Gerenciamento de congestionamento e tensão. 5. Otimização distribuída. 6. Técnicas computacionais. I. Santos, Bruno Fânzeres dos. II. Pontifícia Universidade Católica do Rio de Janeiro. Departamento de Engenharia Industrial. III. Título.

CDD: 658.5

To My Parents,  
for their felt support, life guidance and eternal love; to their homelands in  
the Eastern Black Sea with kemenche music and horon dances, and the  
Eastern Mediterranean with its davul and colourful folklore; to Gelibolu  
(Gallipoli) where our early memories began...

## Acknowledgments

To My Parents, who were not able to be there physically, but their support, life guidance and eternal love were always felt during the whole Ph.D. process.

To my advisor Prof. Bruno Fanzeres, for his valuable insights, patience and always being there to support this work, inspiring me, and teaching me the pathway towards being a researcher, scientist and engineer.

To esteemed Members of the Thesis Committee who provided valuable insights, support and time.

To all my mathematics Professors from the Middle East Technical University, Istanbul Bilgi University, and other Professors and teachers all along the way, my father to discover mathematics, philosophy and scientific thought, and my mother for her wisdom.

To Prof. Teresia Diana Lewé van Aduard de Macedo Soares and Prof. Luiz Brandão and other Professors of PUC-Rio for rekindling the motivation towards doing science, and to Prof. Alexandre Street for inspiring me to shift my research ideas towards power systems and engineering, and flourishing the fascinating idea of describing laws of physics with mathematics.

To Prof. Marco Antonio Guimarães Dias, for the lectures on game theory, and his life-changing advise on being resilient and not giving up.

To Professors of DTU and NTNU, particularly Prof. Stein-Erik Fleten for much appreciated discussions on research ideas, and Prof. Jalal Kazempour and his students for the intriguing power systems courses.

To Professors of Brazilian Institute for Pure and Applied Mathematics, IMPA, specifically to Prof. Luciano Irineu de Castro Filho, Arnaldo Nascimento of PUC-Rio for refreshing courses, Luiza Ribeiro for the first power systems modelling insights and to students and employees of PUC-Rio, special thanks to Cláudia Teti, for their kindness.

To Felipe Cotta and his Carnaval Group for teaching and captivating me with Brazilian rhythms and surdo drum, and to Pelé da Praia and his students for the philosophical beach volleyball courses.

To Stedin, and Sander Harmsen for being supportive.

To Roland Martin, Selçuk Cihangir, Gülden Mert and their families for always willing to be there to provide their support in every situation.

To all my dear friends, other beloved ones, unnamed people, countries, places, and their literature, art, music and dances with all the wisdom and inspirations they brought into this thesis.

To PUC-Rio, for the aids granted.

This study was financed in part by the Coordenação de Aperfeiçoamento de Pessoal de Nível Superior - Brasil (CAPES) - Finance Code 001.

## Abstract

Martin, Nuran Cihangir; Santos, Bruno Fânzeres dos (Advisor). **Computational techniques and model accuracy for electric power transmission and distribution solo and coordinated system-operational problems**. Rio de Janeiro, 2024. 187p. Tese de Doutorado – Departamento de Engenharia Industrial, Pontifícia Universidade Católica do Rio de Janeiro.

To counter climate change, modern power systems are undergoing a decarbonisation-based transition involving vast deployment of renewable energy sources and electrification of societies. For this transition to succeed, various challenges associated with renewable power production need to be addressed in power system operations. These challenges stem from high output variability along with limited predictability and controllability, leading to flexibility needs in power system operations. Optimal power flow (OPF) and unit commitment (UC) are amongst the most important computational tools for system operators to determine the state of the power system. This computation is performed to optimise various decisions on the grid, to dispatch the components in the network, and to reconfigure them. Additionally, the computation is used to price the services provided by large scale generators and, progressively, by decentralised entities such as households and small enterprises which, apart from consuming, also generate and store power, and thus, have a role in energy balancing through their flexibility. Various simplifications are made in OPF and UC to tackle the computational burden of the models, which tends to be high for realistic systems. Model inaccuracy due to simplification of power flow equations or ignoring stochasticity, is increasingly causing high costs for system operations, as the real situation deviates from the forecast implying costly actions by system operators in real-time.

This thesis focuses on challenges in modern power system operations, such as coordinated congestion and voltage management, energy and reserve scheduling as well as price computation. Firstly, the thesis constructs methods and algorithms to enhance computational capability and model accuracy for Alternating Current (AC) Network-Constrained UC and OPF problems through devising an improved approximation of the physical laws governing power flows. Secondly, it applies these methods and algorithms to the coordination problem amongst multiple Distribution System Operators (DSO) and

Transmission System Operators (TSO), introducing novel decentralised optimisation techniques for managing congestion and voltage problems as well as addressing network information exchange aspects. Finally, the thesis proposes new pricing mechanisms, endogenously tackling the non-convex operational decisions for energy and reserve scheduling for day-ahead planning, considering stochasticity of renewable energy generation. Computational and accuracy benefits are illustrated in case studies by employing various metrics developed.

## **Keywords**

AC Network Constrained Unit Commitment and Optimal Power Flow; DSO-TSO Coordination; Congestion and Voltage Management; Distributed Optimisation; Computational Techniques.

## Resumo

Martin, Nuran Cihangir; Santos, Bruno Fânzeres dos. **Técnicas computacionais e precisão de modelos para problemas de operação de sistemas individuais e coordenados de transmissão e distribuição de energia elétrica**. Rio de Janeiro, 2024. 187p. Tese de Doutorado – Departamento de Engenharia Industrial, Pontifícia Universidade Católica do Rio de Janeiro.

Para combater as alterações climáticas, os sistemas energéticos modernos estão a passar por uma transição baseada na descarbonização, envolvendo uma vasta implantação de fontes de energia renováveis e a electrificação das sociedades. Para que esta transição seja bem sucedida, vários desafios associados à produção de energia renovável precisam de ser abordados nas operações do sistema energético. Esses desafios decorrem da alta variabilidade de produção, juntamente com previsibilidade e controlabilidade limitadas, levando a necessidades de flexibilidade nas operações do sistema de energia. O fluxo de potência ideal (OPF) e o comprometimento da unidade (UC) estão entre as ferramentas computacionais mais importantes para os operadores do sistema determinarem o estado do sistema de potência. Este cálculo é realizado para otimizar diversas decisões na rede, para despachar os componentes da rede e para reconfigurá-los. Além disso, o cálculo é utilizado para precificar os serviços prestados por geradores de grande escala e, progressivamente, por entidades descentralizadas como famílias e pequenas empresas que, além de consumirem, também geram e armazenam energia, e assim, têm um papel no equilíbrio energético através de sua flexibilidade. Várias simplificações são feitas no OPF e no UC para lidar com a carga computacional dos modelos, que tende a ser elevada para sistemas realistas. A imprecisão do modelo devido à simplificação das equações de fluxo de potência ou ao ignorar a estocasticidade, está causando cada vez mais altos custos para as operações do sistema, à medida que a situação real se desvia da previsão, implicando ações dispendiosas por parte dos operadores do sistema em tempo real.

Esta tese centra-se nos desafios das operações dos sistemas de energia modernos, tais como gestão coordenada de congestionamento e tensão, programação de energia e reservas, bem como cálculo de preços. Em primeiro lugar, a tese constrói métodos e algoritmos para melhorar a capacidade computacional e a precisão do modelo para problemas de UC e OPF com restrita

de rede e corrente alternada (AC) através do desenvolvimento de uma aproximação melhorada das leis físicas que governam os fluxos de potência. Em segundo lugar, aplica estes métodos e algoritmos ao problema de coordenação entre múltiplos Operadores de Redes de Distribuição (DSO) e Operadores de Redes de Transmissão (TSO), introduzindo novas técnicas de otimização descentralizada para gerir problemas de congestionamento e tensão, bem como abordar aspectos de troca de informação de rede. Por fim, a tese propõe novos mecanismos de precificação, abordando endogenamente as decisões operacionais não convexas de energia e programação de reservas para o planejamento do dia seguinte, considerando a estocasticidade da geração de energia renovável. Os benefícios computacionais e de precisão são ilustrados em estudos de caso, empregando diversas métricas desenvolvidas.

## **Palavras-chave**

Unit Commitment com restrita de rede AC e fluxo de potência; Coordenação DSO-TSO; Gerenciamento de congestionamento e tensão; Otimização distribuída; Técnicas computacionais.

## Table of contents

<b>1</b>	<b>Introduction</b>	<b>16</b>
1.1	Context and motivation	16
1.2	Objectives	22
1.3	Research directions	23
1.4	Scientific contributions	27
1.5	Thesis outline	29
1.6	List of publications	30
<b>2</b>	<b>Methodological Background</b>	<b>32</b>
2.1	Convex relaxations and approximations for AC Optimal Power Flow	32
2.2	Outer approximation	51
2.3	Distributed, decentralised computation of Optimal Power Flow	55
2.4	Stochastic optimisation	60
2.5	Bi-linear optimisation	62
2.6	Risk measures and control	65
<b>3</b>	<b>Computational Techniques and Model Accuracy in Unit Commitment and AC Optimal Power Flow</b>	<b>68</b>
3.1	Background for Mathematical Formulations	68
3.2	Introduction	68
3.3	Mathematical Formulation	70
3.4	Solution Methodology	73
3.5	Numerical Experiments	78
<b>4</b>	<b>Computational Techniques and Model Accuracy in DSO-TSO Coordination Problems for Congestion and Voltage Management</b>	<b>90</b>
4.1	Background for Mathematical Formulations	90
4.2	Introduction	91
4.3	Mathematical Formulation	96
4.4	Solution Methodology	101
4.5	Numerical Experiments	113
<b>5</b>	<b>Computational Techniques and Model Accuracy in Energy and Reserve Pricing for Power Systems with Non-Convex Costs</b>	<b>126</b>
5.1	Stochastic Energy and Reserve Market Clearing Model with Cost Recovery	132
5.2	Solution Methodology: Hybrid McCormick Envelopes and Binary Expansion	145
5.3	Case Study	147
5.4	Chapter Conclusion	160
<b>6</b>	<b>Conclusions, Limitations and Future Perspectives</b>	<b>163</b>
6.1	Overview of conclusions	163

## List of figures

Figure 3.1	Total cost [\$] per iteration for medium-loading case.	79
Figure 3.2	Illustrative cut procedure.	81
Figure 3.3	Case 2: Constraint violation under the algorithm high-loading case.	83
Figure 3.4	Case 2: Constraint violation under the SOCP high-loading case.	83
Figure 3.5	Case 1, 5-bus, 24-hours: Computational performance curves plotting percentage of instances solved vs. runtime in natural logarithm of seconds of each instance solved.	86
Figure 3.6	Case 2, 240-bus, 24-hours: Computational performance curves plotting percentage of instances solved vs. runtime in natural logarithm of seconds of each instance solved.	87
Figure 3.7	Case 3, 118-bus, 24-hours: Computational performance curves plotting percentage of instances solved vs. runtime in natural logarithm of seconds of each instance solved.	87
Figure 3.8	Case 1, 5-bus, 24-hours: Constraint violations in p.u. for 100 instances under the algorithm high-loading case.	88
Figure 3.9	Case 1, 5-bus, 24-hours: Constraint violations in p.u. for 100 instances under the SOCP high-loading case.	89
Figure 4.1	Illustration with 3-subsystems.	107
Figure 4.2	Standard ADMM with 3-subsystems.	107
Figure 4.3	Decentralised ADMM with 3-subsystems.	108
Figure 4.4	7-bus system with 3 sub-systems.	115
Figure 4.5	Case 1 with 2 sub-systems: Optimality gap per iteration for standard ADMM results with different values of $\rho$ .	116
Figure 4.6	Case 1 with 2 sub-systems: Optimality gap per iteration standard ADMM vs. 2-level ADMM results with $\rho = 8$ .	117
Figure 4.7	Total demand and renewable generation per hour in MW.	123
Figure 4.8	Active power flow P per hour at the interface nodes between subsystems in MW.	123
Figure 4.9	Reactive power flow Q per hour at the interface nodes between subsystems in MVar.	124
Figure 4.10	SOC [MWh] storage system-1 per hour at the distribution systems.	124
Figure 4.11	SOC [MWh] storage system-2 per hour at the distribution systems, representative also for storage system-3 and 4.	124
Figure 5.1	Technology-specific revenue cap, adapted from [162].	143
Figure 5.2	Flowchart of the proposed model.	144
Figure 5.3	Illustrative 3-bus system.	148
Figure 5.4	Case 2: Congestion DA-energy prices per node (\$ / MWh)	157
Figure 5.5	Case 2: Lost opportunity cost per generator (\$)	157
Figure 5.6	Case 3: Lost opportunity cost per generator ( $\times 10$ \$)	159

## List of tables

Table 3.1	5-Bus generation data.	78
Table 3.2	5-Bus line and demand data.	79
Table 3.3	Proposed Algorithm - Case 1, Total costs, computational time, number of iterations and Max. ConsViol for each system-loading level.	80
Table 3.4	SOCP - Case 1, Total costs, computational time and Max. ConsViol for each system-loading level.	80
Table 3.5	Case 2, 240-Bus generation data.	81
Table 3.6	Proposed Algorithm - Case 2, Total costs, computational time, number of iterations and Max. ConsViol for each system-loading level.	82
Table 3.7	SOCP - Case 2, Total costs, computational time and Max. ConsViol. for each system-loading level.	82
Table 3.8	Descriptive statistics for computational time under Algorithm for each system-loading level.	85
Table 3.9	Descriptive statistics for computational time under SOCP for each system-loading level.	86
Table 4.1	7-Bus system branch data.	115
Table 4.2	7-Bus system 2-Case studies.	116
Table 4.3	7-Bus system computational results.	116
Table 4.4	IEEE-118-bus transmission system coupled with one IEEE-33 bus distribution system; DC power flow 1-hour without flexible resources computational results for $\rho = 8$ .	119
Table 4.5	IEEE-118-bus transmission system coupled with two IEEE-33 bus distribution systems; DC power flow 1-hour without flexible resources computational results for $\rho = 8$ .	120
Table 4.6	IEEE-118-bus transmission system coupled with two 33-bus distribution systems; AC power flow 24-h with flexible resources computational results: 'Two-level ADMM with Linearisation-Algorithm 1 & 2 vs. 'Standard ADMM with Standard SOCP'	125
Table 5.1	3-Bus thermal generation data.	149
Table 5.2	Case 1: Energy & Res. Market: DA-energy, reserve, and RT-prices (\$ / MWh).	149
Table 5.3	Case 1: Energy & Res. Market: Consumer payment (\$), Expected cost of supplying energy (\$), and Duality gap (%).	150
Table 5.4	Case 1: Energy & Res. Market: Opportunity cost under different pricing schemes (\$).	150
Table 5.5	Case 1: Energy-only market case: DA and RT prices (\$ / MWh).	151
Table 5.6	Case 1: Energy-only market case: Consumer payment (\$), Expected cost of supplying energy (\$), and Duality gap (%).	151
Table 5.7	Case 1: Energy-only market case: Opportunity cost under different pricing schemes (\$).	151
Table 5.8	Case 1: Congestion case: Consumer payment (\$), Expected cost of supplying energy (\$) and Duality gap (%).	152

Table 5.9	Case 1: Congestion case: Opportunity cost under different pricing schemes (\$).	153
Table 5.10	Case 1: Risk aversion case: DA-energy, reserve and RT-prices (\$/MWh).	153
Table 5.11	Case 1: Risk aversion case: Consumer payment (\$), Expected cost of supplying energy (\$), and Duality gap (%).	154
Table 5.12	Case 1: Risk aversion case: Opportunity cost under different pricing schemes (\$).	154
Table 5.13	Case 1: Illustration of benefit of risk-aversion.	154
Table 5.14	Case 2: Risk-neutral Energy and Reserve: Consumer payment (\$), Expected cost of supplying energy (\$), and Duality gap (%).	155
Table 5.15	Case 2: Average profit per generator under different pricing schemes and market, operational case (\$).	156
Table 5.16	Case 2: Risk-neutral Energy and Reserve with Congestion: Consumer payment (\$), Expected cost of supplying energy (\$), and Duality gap (%).	156
Table 5.17	Case 2: Risk-Averse Energy and Reserve: Consumer payment (\$), Expected cost of supplying energy (\$), and Duality gap (%).	158
Table 5.18	Case 2: Risk-neutral Energy Only: Consumer payment (\$), Expected cost of supplying energy (\$), and Duality gap (%).	158
Table 5.19	Case 3: Risk-neutral Energy and Reserve: Consumer payment (\$), Expected cost of supplying energy (\$), and Duality gap (%).	158
Table 5.20	Case 3: Risk-neutral Energy and Reserve with Congestion: Consumer payment (\$), Expected cost of supplying energy (\$), and Duality gap (%).	159
Table 5.21	Case 3: Risk-Averse Energy and Reserve: Consumer payment (\$), Expected cost of supplying energy (\$), and Duality gap (%).	159
Table 5.22	Case 3: Risk-neutral Energy Only: Consumer payment (\$), Expected cost of supplying energy (\$), and Duality gap (%).	160
Table 5.23	Case 2: Computational Analysis	160

*...it is not at all natural that "laws of nature"  
exist, much less that man is able to discover  
them.*

**Wigner, E.P. (1960).**, *"The unreasonable effectiveness of mathematics in the natural sciences. Richard Courant lecture in mathematical sciences delivered at New York University, May 11, 1959". Communications on Pure and Applied Mathematics. 13 (1): 1-14.*

# 1

## Introduction

### 1.1

#### Context and motivation

Climate change and its irreversible hazards, e.g., heat waves, floods, wildfires and floods, are pressing the need for restraining emission of greenhouse gases. This has been stimulated by international agreements. In Paris in 2016, at the UN Climate Change Conference (COP21), 196 countries adopted an international treaty on climate change. Ambitious strategies have been formulated, such as the EU's Green Deal which aims to achieve climate neutrality within the EU by 2050, setting intermediate objectives of an at least 55% reduction in greenhouse gas emissions by 2030, relative to 1990 [1]. Implementation requires an economic, industrial and social transformation. Governments have initiated institutional, legal and market reforms, they invest in grid infrastructure, and create incentives to stimulate renewable energy generation, its integration into power grids, as well as technological progress required to catalyse the green transition.

Power systems are at the heart of the energy transition, as the core of the decarbonisation agenda involves boosting renewable power production, and, to the extent possible, electrification of industries, mobility and households. This poses several and significant challenges to power grid operations, which must be addressed to make the transition successful.

The conventional structure of power systems, their evolution and technical challenges in view of the energy transition are outlined next:

#### *The structure of power systems*

Power systems are traditionally operated vertically, and power flows are to a large extent predictable, uni-directional, and from top to bottom. Physical layer of power systems is built on four subsystems, consisting of generation, transmission, distribution, and supply [2]. At the top, the generation subsystem incorporates all energy-production facilities. The transmission subsystem is the network of electricity freeways transporting bulk quantities of electrical energy from production locations to the distribution areas. Transmission takes place through alternating current (AC) transmission lines with a high voltage level of 100 kV to 600 kV, or through direct current (DC) power lines for very long distances, typically at 500 kV. The transmission subsystems tend to be meshed

networks, involving loop structured circuits with buses (nodes) and lines. The distribution subsystem channels electrical power from the transmission subsystem into consumption areas at the bottom. This network operates at 20kV and characteristically has a radial, tree-like structure, for robustness and protection reasons. Finally, the supply subsystem supplies the generated power to the end-user with protection and metering equipment. The system uses low voltage - typically 100 V in the USA and 200 V in Europe.

Power transformers in each subsystems interconnect the different voltage levels, e.g., from generation to transmission and transmission to distribution etc. Transmission, distribution, and supply subsystems are commonly operated and monitored by different entities, so-called network, or system operators.

Conventionally, distribution networks have been passive, and reliant on the transmission network for energy supply, frequency control and voltage regulation.

#### *Decarbonisation strategies – impact on power systems and grids*

The green ambitions are, for example in the EU-countries and the US, pushed forward through incentives and industrial policies, aimed at households, the private sector, research and technological progress. Together with the potentially low, theoretically zero, per unit (marginal) cost of renewable generation this has spurred renewable power generation in recent times.

This trend has severe implications for power systems and modern grid design, due to growing renewable production and electricity consumption leading to developments on both the supply and the demand side.

On the latter side these developments are driven by growing demand from households, businesses, industry and for mobility. On the supply side, renewable power generation is, apart from hydro and biomass, non-dispatchable. In other words, the control over production is, partly or fully, not at the producer's discretion [3]. At the same time, the output has weather-dependency, limited predictability, and is stochastic. Renewable energy generators are connected to the network via power-electronic interfaces converting DC output power into AC, which demonstrate a different behaviour compared with conventional synchronous generators, among others due to their low inertia. As a consequence, the total inertia of the system may become insufficient to compensate for disturbances of power balance, leading to relatively large frequency deviations which affects dynamic stability of the system in case of faults and disturbances [4]. These features differ from generation with conventional sources such as coal, natural gas or nuclear.

Furthermore, large-scale generators at the high- or medium- voltage levels

are nowadays joined by units acting both on the generation and consumption side who thus bring bi-directional power flows to the grid. This latter group consists of households and businesses producing energy via, e.g., photovoltaic (solar) systems, cogenerating plants, wind turbines, small hydro plants, fuel cells and microgeneration as well as using storage systems (such as batteries), electric vehicles and heat pumps. These so-called distributed energy resources (DERs) are mainly located at a medium- or low-voltage level, at the edge of the grid and often behind-the-meter because of being located on the client's side of the utility meter [5].

These trends imply new dynamics for which grids were not designed. On the transmission level, net-demand structures are becoming more volatile, e.g., due to timing mismatch between industrial-scale renewable generation and consumption. At the same time, system operators need to balance demand and supply at any point in time.

#### *Network congestion and flexibility*

The described new, growing and unpredictable loads through, e.g., heat pumps and electric vehicles, as well as volatile renewable generation give rise to system bottlenecks, such as network congestion and voltage problems [6].

Network congestion is defined as a situation in which demand for active power is higher than the transfer capacity of the network [7]. Grid congestion has conventionally been managed by transmission system operators, but it is becoming a task of distribution system operators as well, because of bi-directional and unpredictable power flows by DERs and proactive demand. Congestion in distribution systems is traditionally mitigated through grid reinforcement by increasing the hosting capacity for cables, feeders, and transformers. According to the European Standard (EN50160), voltage deviations measured on a 10-minutes granularity should not exceed  $\pm 10\%$  of its nominal value on a weekly basis [8]. This has become challenging to maintain in modern distribution grids.

Flexibility is defined as the ability of the grid to react to price or activation signals to increase or decrease generation or consumption. At transmission system level, flexibility can provide stability, frequency control and energy supply management, whereas at the distribution level, it may be used to mitigate congestion and voltage fluctuations. Storage systems such as batteries potentially assist in mitigating these bottlenecks, as they enable the shifting of excess generation towards low demand hours [2]. Additionally, especially in case of a large number of DERs in the system, energy storage can assist in compensating for disturbances of power balance leading to relatively

large frequency deviations, as the total inertia of the system may become insufficient [4].

If coordinated, the above-mentioned DERs at-the-edge can jointly provide services to the grid, such as providing fast-reacting ancillary reserves to the transmission system or congestion management services to the distribution system. These services have an activation time of fractions of a second to months and even years for long-term adequacy [9]. Acting as a bottom-up flexibility provider these coordinated DERs can reduce or increase consumption, and hence pro-actively participate in grid operations from the demand-side. These actions are typically based on price signals aimed to be reflective of grid conditions at any given point in time.

#### *Modernization of grids*

Due to the green agenda and the various interlinked developments surrounding renewable power generation described above, the grids are to be modernised to continue to effectively play their role. To facilitate modernisation of aging grid, there is a need to reinforce the grid, replace existing components and investment in digitalisation, or so-called smart grid deployment. Smart grids include advanced communication of control technologies to enable an efficient and economically viable grid management. This applies particularly to distribution grids, as transmission networks to a large extent already possess these technologies [2]. Monitoring smart grids has lately been the focus with a vast deployment of phasor measurement units (PMUs), advanced substations and smart meters (globally) [10] to foster situational awareness of grids which are exposed to instant dynamics of loads and electro-mechanical interactions of generators. In fact, a rapid adoption rate of digital grid edge technologies to monitor DERs, which are power electronics interfaced, is anticipated within the coming decade.

#### *Power system operations*

Power system operations concern short-term decisions made by transmission or distribution system operators customarily within a time frame of one month to minutes or seconds ahead of actual power delivery, and tend to base on one most likely generation or demand scenario. Planning within a month period involves, for instance, preventive maintenance of components. Day-ahead planning refers to the procurement of reserves as a backup against potential contingencies in the network as well as the scheduling of generators. Intraday decisions concern certain adjustments to day-ahead dispatch made by operators to account for changes in forecast and procure additional reserves

if needed. Operating decisions finally, which take place within minutes prior to actual delivery, focus mainly on security and control related activities by actual dispatching of generators to ascertain that technical grid-requirements are met, such as voltage levels and transmission line capacity limits.

Current system-operational tools for short-term planning are mainly based on a steady-state situation of the grid with the ability to stay in equilibrium following a gradual change of system state, indicated on the basis of voltage and current levels, and phase angles at the nodes of the grid.

Power systems are transitioning from 'vertically operated' structures into 'horizontally operated' structures. Large, uneconomical or aged power plants are being decommissioned, which gives rise to a power system with a large number of DERs at the distribution networks with a horizontal, bidirectional power flows [4]. As a consequence of this, the foremost objective of the transmission system is becoming interconnecting the 'active distribution networks', i.e., networks which are able to control DERs where their flexibility is used by distribution system operators to operate and regulate system parameters, without much support from transmission networks. Voltage stability of such a system is a challenge, which is no longer imposed by large generation units.

#### *Power flow computation*

Power flow, or load flow, computation is among the most significant tools for system operators determining the steady-state behaviour [11] by specifying voltage magnitude and phase angle at each bus of the grid at a given generation and consumption. The computation typically incorporates voltage magnitude constraints per bus as well as power losses and is based on the laws of physics, namely Kirchhoff's Laws and Ohm's Law.

Within this general class of computation problems, optimal power flow (OPF) computation typically seeks to obtain voltage magnitude, phase angle and other operational constraints, e.g., generator minimum and maximum output, transmission stability, and line capacity limits, under an objective of minimum costs. Decisions on switching of components, e.g. in case of equipment failure or simply to start-up or shut-down a running unit, are also included in the formulation. This inclusion is relevant for planning purposes, namely to decide upon how much power to dispatch or how to schedule the equipment to generate sufficient power to meet forecast demand. Such a scheduling related optimisation problem is called a unit commitment (UC), commonly used for day-ahead planning of system operations. Its formulation with network constraints is called network-constrained UC (or NCUC). Inclusion of contingency related aspects makes the problem security-constrained unit com-

mitment (SCUC), commonly solved for control purposes minutes or seconds before power delivery. These problems are solved by system operators multiple times a day in each electrical control center. A computationally fast, robust and scalable technique is still not available to solve these problems [12, 13]. Often, in fact, approximations, decompositions, or simply judgement is used to seek a reasonably acceptable solution. Inaccuracy of the obtained solutions, can lead to environmental hazard because of carbon emissions due to, e.g., unnecessary activation of non-renewable-based sources, wasted energy as well as other inefficiencies or costs for using resources such as additional re-dispatch.

In electrical terms, power flow is alternating current (AC). The optimal power flow formulations which apply exact AC equations are called AC OPF. Due to computational complexity for solving AC OPF or related problems such as AC NCUC, simplifications involving linearisation of power flow equations are made. Among the most common simplifications is direct current (DC) optimal power flow (DC OPF), or for unit commitment DC NCUC.<sup>1</sup> DC OPF, among others, assumes that voltage magnitudes are close to constant and do not vary significantly, and voltage angles are close to zero.

#### *Modern power systems and model accuracy*

This thesis does not focus on a power system of any specific country or jurisdiction, and attempts to provide methods which are as generalisable as possible. The market structures are based on liberalised electricity markets. Modern power systems refer to systems in which technological innovations, such as inverter- or power electronics- based distributed energy generation, renewable energy sources, energy storage systems as well as advanced communication systems are available.

In modern power systems, due to variability and power electronics-related components, the system operating state can be subject to instant or structural deviations causing branch congestion and voltage problems. Therefore, the underlying assumptions for simplified power flow models, such as DC OPF, may not be realistic in a more dynamic grid. Improved accuracy of power flow models, on the other hand, enhance effectiveness of system operational control [14]. In addition, anticipated usage of modern power systems towards their limits through capacity optimisation, accuracy and efficiency of power flow computation techniques becomes increasingly important to determine steady state behaviour of the network for a given level of demand and supply. Furthermore, accuracy of the models assists in maintaining value of the system

<sup>1</sup>Note that DC OPF is a naming for this simplification, is not equal to a power flow solution to a DC network [12]

components through more effective control for their degradation.

Model accuracy, in fact, is a significant challenge in modern power systems. Because of unpredictability of various parameters, such as wind speed and solar irradiation, models can provide outputs which can be far from reality [15], sometimes measurable by smart devices. The latter can give rise to inaccurate conclusions, expose system design and decision making to risks. Complex optimisation problems need to be solved to achieve a higher accuracy, e.g., for prediction of power flows, incorporation of DER-driven uncertainties.

*Zero marginal cost renewables and non-convexities from market perspective*

Furthermore, day-ahead energy and reserve scheduling for at least some modern power systems, such as in the United States, is performed out of a solution to a least-cost DC network-constrained unit commitment (DC NCUC) problem [16, 17, 18]. Market clearing price is based on marginal costs and per location or node in the network in some jurisdictions, named as locational marginal pricing (LMP). One of the challenges in modern power systems with massive renewables is the fact that the prices can drop to zero and negative when such generation is abundant. The latter is due to close to zero marginal costs for renewables. On the other hand, if the production is not sufficient, then prices can rise to a significant amount. These can be aggravated in case the grid is subject to bottlenecks, such as congestion. One of the aspects which the regulators are concerned about, e.g., in the European Union, is how to remunerate generation assets. Operational switching decisions leading to non-convex mathematical optimisation problems. The clearing prices in the current applications do not consider the non-zero duality gap of these non-convex problems, causing incentive misalignment. Non-convexity as well as incorporation of stochasticity to the decision-making framework for system operators induces complex optimisation problems which can be hard to solve within the time limits available to operators for day-ahead and real-time scheduling purposes.

## 1.2 Objectives

This thesis explores challenges in modern power system operations and pricing, where an improved approximation of the physical laws governing power flows, incorporation of stochasticity and addressing non-convexity in the pricing models and more efficient computational methods to tackle these points can provide benefits to efficiency and effectiveness of power system

operations. The main objective of the thesis is as follows:

To improve computational capability and model accuracy for

i) AC Network-Constrained Unit Commitment (AC NCUC) and Optimal Power Flow (OPF) for solo operations as well as coordinated transmission and distribution system operations to mitigate congestion and voltage problems with a limited network information interchange;

ii) locational marginal pricing (LMP) for DC NCUC for transmission systems under non-convex operational decisions and stochastic renewable generation (RES).

Both objectives are grouped into research directions, and detailed next.

### 1.3

#### Research directions

This main objective is grouped into three research directions:

**Chapter 3:** The first research direction concentrates on the methodological foundation for reducing computational load in AC unit commitment and optimal power flow calculations.

**Chapter 4:** The second research direction applies these methodological principles to the coordination problem amongst multiple Distribution System Operators (DSOs) and Transmission System Operators (TSOs), introducing novel techniques for managing congestion and voltage problems with computational savings, thereby enabling more efficient power system operations.

**Chapter 5:** The last research direction proposes a new price computation mechanism within a similar framework. The complexities here principally stem from addressing the pricing of non-convex operational decisions and stochasticity, where conventional marginal-pricing approaches reach their limits.

These three research directions can demonstrate the significance of employing AC optimal power flow models, coordination amongst multiple DSO and TSO entities, endogenous pricing of non-convex energy and reserve scheduling involving uncertainties in modern power systems, and the computational challenges associated with such modeling. The thesis proposes metrics for evaluating these benefits and computational methods that enhance the current state-of-the-art techniques for such complex mathematical models.

The specific background for the three research directions is detailed next.

### 1.3.1

#### **Computational techniques and model accuracy in AC NCUC and optimal power flow**

In modern power systems, existing modelling frameworks for power flow modelling mainly based on DC linear approximation, ignoring reactive power and voltage, is becoming insufficient, necessitating more detailed modeling. A key aspect of this involves simplifying the power flow equations describing physical laws, namely Kirchhoff's laws, which are non-convex. The feasible region for OPF problems, being non-convex, results in the possibility of non-unique local optimal solutions. One main difficulty is which local solution to choose and how good they are [19], and they tend to result in solutions close to their initialisation set-points [13]. One of the main frameworks for simplification of power flow equations striving towards obtaining globally optimal decision-variables is based on convex relaxation techniques, i.e., approximating the feasibility region of a non-convex problem represented by a tightest possible convex region.

Second-order cone programming (SOCP) is one of the common convexification-based techniques used to solve AC network-constrained unit commitment (AC NCUC) and optimal power flow problems [20]. The main shortcoming of this approach is the computational complexity increasing exponentially with the system size. Noted is also that at least under normal operating conditions for various cases the power injections and flows computed from the convex relaxations may be close to those of the true global solution to the original non-convex problem. However, even under such conditions, the optimal voltage phase results tend to deviate from the global solution. Additionally, especially under high-system loading conditions, the optimisation results from convex relaxations may not be exact, i.e., deviation between the global solution to the non-convex problem and that of the relaxed problem [13]. Computing power flow as a convex relaxation, such as semi-definite programming (SDP) and its variants regarded as the tightest of such relaxations under certain conditions, entail prohibitively high computational burden with increasing network size [19]. This aspect motivates usage of second-order-cone programming-based techniques in practice, though they tend to be, in general, weaker than SDP.

Following these arguments, this research line focuses on enhancing power grid operations by employing a more accurate model of the physical laws governing power grids, namely the AC power flow. More specifically, this thesis addresses how model accuracy for AC NCUC and OPF (non-convex) be enhanced so that a minimum deviation from a true global solution can be

obtained with computational savings against established convex relaxations, such as Second-Order-Cone Programming (SOCP).

### 1.3.2

#### **Computational techniques and model accuracy in multi-agent DSO-TSO coordination for congestion and voltage management**

Power systems are traditionally operated under a centralised approach, i.e., a central operator - typically a transmission system operator - that has a perfect knowledge of the transmission system, with economical and technical data required, viewing distribution system as a passive load with power flows with one direction from transmission into distribution [2]. Applying optimal control principles, the operator plans and operates the system by matching demand and supply at a minimum cost. The operator takes necessary decisions and inform generators and consumers on what and when to do. Similarly, distribution systems are traditionally reliant on transmission systems for power supply. Both systems ignore the state of each other in their planning.

Smart electric power systems' physical structure, however, is increasingly distributed with bi-directional power flows. Various entities, such as distribution and transmission system operators and market actors, interact in this system as well as take responsibility in a certain part of the system.

Congestion and voltage management are becoming increasingly important for operations and control in transmission and distribution systems with a large share of renewable generation [21]. Such control procedures can be effectively incorporated in AC optimal power flow and unit commitment as energy management algorithms. A variety of solution techniques are available for such algorithms, such as centrally as a problem of one single controlling entity. This approach is not realistic because of being reliant on optimisation of system costs cumulatively through a central-planner assuming to have full visibility or direct control of the overall power system [22, 23]. It also ignores the individual optimisation of system operators, and their competition with one another, and may not always scale well for computational purposes [24]. The privacy of network data amongst the involved entities as well as the DERs may not be maintained. Interconnectedness of systems, such as transmission, and distribution managed by different entities, also implies that control decisions of one entity would affect the other. The involved entities need to coordinate for efficiency and effectiveness of control in order to assure system reliability.

Distributed algorithms often lack convergence guarantees for multiple sub-systems, which is in practice the case, and suffer from numerical issues, and their performance depend on the choice of *a priori* decision-dependent penalty

parameters. In the general case, a necessity to have a central coordinator for data communication may not be practicable, or data storage and transfer may not be optimal.

To address these issues, distributed solution algorithms are proposed for AC OPF or NCUC, where a coordinating entity may need to aggregate the variables which are to be coordinated between the entities to reach to a system goal, such as minimisation of system costs while reliable operations can be assured for the entire system. Distributed approaches enable computation of equilibrium set-points for different systems concerned while balancing the common resources [25]. Another advantage of distributed solution algorithms is in terms of cybersecurity, data storage and grid data privacy. There are numerous reasons why data in relation to power grid are preferably not shared. For instance, grid data can reveal some vulnerabilities of the grid, and an attacker can make use of this to manipulate grid operations [26]. Minimum data transfer between different entities, locations or smart devices can assist safeguarding important data. Hence, these algorithms enable scalable, reliable solutions and have advantages in terms of communication requirements between entities or components [27].

Based on this background, this research line investigates how distributed and decentralised optimisation algorithms can be applied to mitigate congestion and voltage problems in a coordinated way between distribution and transmission as well as amongst multiple distribution systems with reduced data interchange needs while computational capability and model convergence are enhanced. It also addresses AC optimal power flow computation accuracy, which can bring benefits for multi-agent DSO-TSO coordination by optimising the power flows at the interface of the entities.

### 1.3.3

#### **Computational techniques and model accuracy in energy scheduling and pricing in power systems**

This research line explores the challenges for integrating renewable sources into power systems in terms of operation and pricing, particularly regarding energy and reserve scheduling with associated market design.

High levels of renewable penetration into power systems as well as operational features of system components or one-off cost structures represented by binaries are increasingly inducing misalignment between operations and prices [28, 29]. It is because existing energy scheduling schemes inherently have non-convex features which are not adequately captured in existing modelling. Accordingly, *post*-clearance settlements such as uplift are applied in order to

remunerate generators for these one-off costs. However, uplift payments are not reflected in the clearing prices, distorting price signals.

Additionally, electricity market-clearing around the globe is based on a deterministic modelling approach that relies on a single, most likely scenario. This is challenged by variability of renewable generation and demand, leading to large forecast errors in jurisdictions, e.g., Australia where renewables are deployed on a massive scale [30, 28]. Additionally, unpredictable congestion or bottlenecks can occur when generation in real-time is much higher than anticipated exceeding the hosting capacity of the network. Accordingly, a costly balancing might be needed in the system through re-dispatch of expensive generation sources in real-time. In order to accommodate the forecast imprecision, a stochastic modeling approach is applied, which considers the nature of uncertainty represented by a probability distribution. Due to this feature, it is considered to be an appropriate decision-making approach for systems with a high share of renewable sources [31]. On top of this, system operators need a certain degree of robustness in their decisions to be able to meet demand and supply at a least possible deviation from social welfare under unexpected scenarios [32].

Energy-only markets, mainly applied in the European countries, do not schedule reserves during the day-ahead stage, and assume that they are available in real-time. However, it is shown by [33] that a co-optimisation between energy and reserves at that stage can decrease costs for supplying energy. This practice, according to [30], increase efficiency, transparency, and fairness.

Furthermore, such DC NCUC optimisation problems for energy and reserve scheduling with stochastic variables on real large-scale power transmission systems accounting for bottlenecks and real-time re-dispatch of generation may not be efficiently solved by commercial solvers or standard algorithms [34], and are typically NP-hard [35].

On the back of these, this research line addresses how model accuracy and computational capability for energy and reserve scheduling be improved in a risk-controlled manner to derive locational marginal pricing (LMP) for DC transmission systems with non-convex operational features and stochastic renewable generation.

## 1.4

### Scientific contributions

The main contributions of this work are as follows:

A) **Chapter 3:** To devise a framework and an algorithm in relation to enhancement of accuracy for AC OPF / UC (non-convex) so that global optimal solutions to the convexified problem can be obtained with computational savings against established convex relaxations, such as Second-Order-Cone Programming (SOCP).

i) To develop a decomposition algorithm to approximate the non-convex feasibility region for the AC unit commitment and optimal power flow problem.

ii) To perform computational experiments in the form of performance curves benchmarking the proposed algorithm against solving SOCP formulation with off-the-shelf commercial solvers.

B) **Chapter 4:** To propose a decentralised optimisation algorithm to mitigate congestion and voltage problems in a coordinated way between distribution and transmission systems with a limited network information interchange while computational capability, convergence guarantees towards an approximate stationary solution for multi-block problems, and model accuracy for AC optimal power flow are enhanced.

i) To develop a computationally efficient global optimal solution procedure for the convexified DSO-TSO congestion management and voltage control coordination problem, based on a two-level nested decentralised ADMM framework requiring limited network data interchange with convergence guarantees to an approximate stationary solution for multi-block problems.

ii) To enhance the power flow modelling in DSO-TSO coordination for congestion and voltage management in order to closely align transmission and distribution system operations.

iii) To implement the linearisation and decomposition of AC UC OPF method proposed in Contribution A) within the context of a DSO-TSO coordination problem for the accuracy of modelling for power flow at the interface of the system operators.

C) **Chapter 5:** To propose a risk-controlled solution framework for the improvement of DC-NCUC model accuracy and computational capability to derive locational marginal pricing (LMP) for transmission systems with non-convex operational structures and stochastic renewable generation.

i) To address the day-ahead energy and endogenous reserve scheduling as a multi-commodity product taking into account the stochastic balancing stage

and scale-up the numerical analysis to larger power networks to gain insights on realistic systems.

ii) To incorporate a risk aversion profile to the system operator for meeting demand and supply under uncertain renewable power generation, mimicking the daily decision process of operators in practice.

iii) To provide a comparison of the energy and reserve scheduling outcomes from the perspective of provision of cost recovery or limiting windfall profits via a revenue cap for the generation companies under different pricing schemes.

iv) To design an efficient procedure to tackle the bi-linear optimisation problem to improve the computational compatibility to handle the energy and reserve scheduling process.

## 1.5

### Thesis outline

**Chapter 2** presents methodological background for all contributions. Particularly, the Chapter starts by introducing and comparing Convex relaxation and approximation techniques for optimal power flow in relation to [Paper A]-[Paper B]. Namely, linear- and quadratic- programming based approaches, DC power flow, second-order cone programming, semi-definite programming and hybrid approaches are presented. Later in the Chapter an outer approximation, linked to [Paper A]-[Paper B], is outlined. Furthermore, distributed optimisation is introduced and the general approach of the alternating directional method of multipliers, related to [Paper B], is presented. Later of the Chapter is devoted to the methodological aspects of [Paper C]-[Paper D]. These are in relation to stochastic optimisation, bi-linear optimisation as well as risk measures to control risk in these problems. **Chapter 3** presents thesis contributions to a more accurate convex approximation of AC unit commitment and optimal power flow when compared to the widely applied and reasonably accurate technique under mild conditions, Second-Order Cone Programming, a computationally efficient decomposition algorithm according to [Paper A]. This Chapter introduces the AC unit commitment and optimal power problem in its general form, for which the SOCP reformulation is driven. The proposed approximation and linearisation technique is presented. Later part of the Chapter is devoted to constructing an algorithm for the purpose of efficiency of the proposed procedure.

**Chapter 4** presents thesis contributions on efficient solutions to solve a multi-agent DSO-TSO coordination problem at the interface of high-voltage network with battery energy storage systems and medium-voltage levels for ad-

addressing congestion and voltage management problems with a limited network information interchange between operators. This chapter relates to [**Paper B**]. This Chapter introduces centralised and decentralised mathematical optimisation problems for each system operator, based on an optimal power flow type of modelling. The Chapter is further devoted into distributed and decentralised algorithms striving towards minimum data transfer. In addition, accuracy and computational efficiency of the power flow modelling is addressed based on [**Paper A**].

Chapter 5 presents thesis contributions towards accuracy of pricing non-convex unit commitment problems to schedule energy and reserves for the day-ahead stage considering a stochastic approach on the balancing stage as well as a robustness of system-operator decisions. The Chapter proposes various pricing schemes and a computationally efficient procedure to solve such mixed integer bi-linear programming problems. It provides main results of [**Paper C**] - [**Paper D**].

Chapter 6 provides a summary of the overall main results, limitations of the thesis and future research directions.

## 1.6

### List of publications

#### Publications part of the thesis

The following publications constitute the core of this thesis:

[**Paper A**] Martin, N. C., & Fanzeres, B. (2023, June). Linearisation Based Decomposition Method for Circle Approximation in AC Network Constrained Unit Commitment. In 2023 IEEE Belgrade PowerTech (pp. 1-6). IEEE.

[**Paper B**] Martin, N. C., & Fanzeres, B. A Two-Level ADMM Algorithm for Multi-Agent DSO-TSO Congestion Management and Voltage Control Coordination with Limited Information Exchange. *In process of publication*.

[**Paper C**] Martin, N. C., & Fanzeres, B. (2023). Stochastic risk-averse energy and reserve scheduling and pricing schemes with non-convexities and revenue caps. *Electric Power Systems Research*, 225, 109858.

[**Paper D**] Martin, N. C., & Fanzeres, B. (2023, September). A Stochastic Risk-Averse Model to Price Energy in Pool-Based Electricity Markets with

Non-Convex Costs and Revenue Caps. In 2023 International Conference on Smart Energy Systems and Technologies (SEST) (pp. 1-6). IEEE.

## 2

### Methodological Background

This section will provide a background on the main methodological concepts applied in the thesis, namely i) convex relaxations and approximations for AC optimal power flow; ii) outer approximation; iii) distributed, decentralised computation of optimal power flow; iv) stochastic optimisation; bi-linear optimisation; and, v) risk measures and control.

#### 2.1

##### Convex relaxations and approximations for AC Optimal Power Flow

###### *Power flow computation*

Power flow formulations establish relationship between voltage phasors and power injections at nodes (buses) in any power system [13]. These equations are fundamental for power system operational optimisation- and control-related problems, such as optimal power flow (OPF), unit commitment (UC), state estimation, dynamic stability and voltage stability assessment or short-term security or contingency analysis. In addition, they are also incorporated in medium- and long-term planning models, e.g., for maintenance scheduling and generation or transmission expansion planning [2].

Power flow computation analyses the power system in its steady-state, i.e., focuses on a snapshot of power system operations, not its dynamic evolution.

###### *Radial and meshed network configurations*

Before going into further details on power flow computation, a description of the most common network configuration, namely radial and meshed, is provided next:

Radial configuration is a tree-like network structure where there are no closed loops. It is the simplest and cheapest network topology. In a radial system, generators at the starting point are linked to the load center by means of distribution transformers. Circuit protection scheme for radial networks is straightforward in terms of design and coordination as well as implementation of a reactive power compensation [36]. Since substation tends to be close to loads, a radial network configuration is easy to analyse and operate. Low cost and such straightforwardness of radial configuration make it interesting especially for low-voltage networks. Its principal disadvantage is its limited flexibility in view of system planning, since in case new generation and loads

to be added to the system, new cables and other components need to be installed. In addition, connected parties in such a network are reliant on a single feeder, and any fault leads to interruption for the entire users connected to the feeder. Power availability for each load can be lower compared to, e.g., meshed networks because of the complexity of maintenance.

Meshed networks allow an alternative route with redundant circuits. A meshed distribution network is based on a ring structure, starting from a generator through various loads and back to the generator. All buses are interlinked in such a way that they constitute a closed loop, supplying distribution transformers or loads, and go back to the same substation. Power can be supplied to the loads in any direction, which makes it advantageous for isolating faults and supplying loads in case of a failure.

### *Optimal power flow*

As a power flow computation method, OPF is defined as a mathematical optimisation problem which seeks to minimise an objective function - e.g, total generation cost, power loss - subject to Kirchhoff's laws, capacity, stability and security constraints [37]. OPF problem was first put forward by [38]. Since then, there has been a rich body of research for solving OPF and related problems in different power system configurations. In fact, this thesis focuses on a balanced, radial, single-phase-equivalent distribution networks as well as transmission networks. Therefore, this Chapter mainly outlines optimisation-based techniques applicable to these settings. Note that most power systems tend to be not radial in practice [19]. Especially transmission networks and medium-voltage distribution networks are commonly meshed. However, because of radial networks' sparsity and simplicity compared to meshed networks, they are assumed to be the case in the literature especially in the analysis of distribution networks. In practice power systems tend to be sparse, having less than 0.05% connections between the buses [13].

Optimal power flow is frequently applied in combination with unit commitment variables, i.e., in order to schedule energy and reserve providing generation sources to meet demand.

The main difficulty of solving OPF is the fact that active and reactive power flows in a branch or transmission line is a non-convex function of bus voltages and phase angles. This difficulty can magnify when binary variables related to UC are also incorporated. Problems such as OPF and UC are classified as NP-hard even when radial networks are involved [39].

Accuracy of power flow modelling is of great importance, because network lines can become dangerously congested if for instance the calculated power

flow underestimates the actual power flowing through the lines. An overestimate of congestion can imply additional market costs for re-dispatch. In both cases, system security monitoring would be impacted [40]. For instance, power flows estimated under a DC approximation in MW can be sometimes just a few percentages different than AC estimates, but the differences can also be at times alarmingly high [40]. When the power flow calculations on potentially binding network elements differ from reality, this is critical. In general, inaccuracy of power flow can cause distortion of system dispatch and Locational Marginal Pricing (LMP). DC model can result in infeasible or sub-optimal solutions [41].

First solution method for the OPF problem was introduced by [42] based on a Newton's method and its variants. AC OPF for distribution networks are, for instance, solved by Newton-Raphson (NR) method. This method, however, tends to converge slowly and there is no convergence guarantee to a solution [43].

*Local optimal vs. global optimum solutions to optimal power flow*

At least some OPF formulations with non-convex constraints can be solved via non-linear solvers directly. Local optimal or stationary points using non-linear techniques, such as based on interior point methods or metaheuristic techniques are applied. The feasible region being non-convex gives rise to the possibility of non-unique local optimal solutions, not a global optimum solution to the OPF problem. Nor may these solutions provide any evidence on how good the obtained solution is [19]. In [44], it is observed in some examples having multiple local optima that interior point algorithms tend to converge to local solutions which are closest to the initial guess. In general, a 'high-voltage, small-angle-difference' is typically more interesting for finding a good operating point. 'Low-voltage, large-angle-difference' solutions are typically used for specific purposes, such as stability analysis [13, 44, 45]. Nevertheless, global optimum solution to OPF problems can tend to be much slower than local optimal ones [44], being their disadvantage. Hence, it is important to develop efficient globally optimal methods for solving OPF and related problems [19]. Global optimal techniques to OPF problems are still in their infancy, and much research is needed searching for computationally efficient solutions [19]. This section of the thesis focuses on convex relaxations and approximations, rather than non-linear optimisation techniques.

It is worth to mention that, other than local optima and global optimal solution-seeking type of algorithms, there is also a third category which attempts to compromise between the two by making use of the lower and upper

bounds provided while with the ambition to obtain nearly global optimal solutions. For instance, a branch-and-bound type algorithm applied by [46] combines a Lagrangian-relaxation-based approach to obtain a lower bound and an interior-point based approach to obtain upper bounds to the global optimal solution. It is shown that under the proposed approach, the duality gap is observed to be zero for the test cases used. Because of the existence of ramping constraints of the generation units in power systems, the generation in the following period would have a limited degression from the previous period. This feature also motivates analysis of lower bounds for the possibly local solutions [19].

#### *Convex relaxations and approximations to optimal power flow*

In order to search for computationally efficient solutions to the OPF, relaxations or approximations for the non-convex feasible space of the original problem are applied [13]. Using the convexity property to achieve a global optimum solution for the relaxed problem, there are a broad range of 'convex relaxation' techniques for AC OPF problems, which approximate AC power flow constraints by a convex outer approximation [47]. Details can be found in the survey [13]. Convex relaxations provide a lower bound to the optimal objective value for the original non-convex OPF. In addition, if certain conditions are satisfied in some cases exactness of the relaxation is possible [19]. Note that exactness of a relaxation is defined as one such that it gives a bound equivalent to the global objective value. In other words, the obtained solution has a zero optimality gap compared to the solution to the original non-convex problem. Exactness does not imply that the obtained optimal decision variables from the relaxation would give the global optimal decision variables to the original problem. It is because in case the solution set for the relaxation is a connected subset of the relaxation's feasible space. all these non-unique solutions would provide the same objective value to the relaxed problem, though some of these solutions might be infeasible in the original non-convex problem [13].

Furthermore, convex relaxations can provide important information on the problem itself. If the relaxed problem is infeasible, then, the original problem is also infeasible. However, if the relaxation is feasible, it is not a sufficient condition to guarantee that the original problem is feasible [13].

Relaxations typically extend the non-convex feasible region into a convex region, namely 'convex envelope', because of the convenience of the convexity property for optimisation purposes. Hence, they typically do not cut original feasibility space.

Approximations, on the other hand, make assumptions regarding certain

parameters and quantities, and simplify the power flow equations. The validity of assumptions are important in order for the approximations to adequately represent power system behaviour. Depending on the assumptions, in some cases the approximations can cut the original feasibility space and some originally feasible operating points may not be represented. Various approximations tend to sufficiently depict power flow under normal operating conditions.

Neither relaxations nor approximations exactly satisfy the power flow equations, and they can give infeasible solutions. Nevertheless they try to provide tractable solutions with sufficient representation of physical aspects of the network.

Convex relations in general are based on i) linear or quadratic programming; ii) Second-order cone programming (SOCP); and iii) semi-definite programming (SDP).

Power flow equations can be formulated in a broad number of ways, in order to explore different features of power systems or for computational reasons, etc. There are two main broad categories: i) branch flow models; ii) bus injection models. The latter is sub-grouped into I-V as well as voltage based formulations. These are outlined in the next Section.

### 2.1.1

#### **OPF model formulations**

Different power flow equations are obtained by formulating and using different representations of, e.g., admittance matrix, voltage phasors and power injections. Additionally distinct focus on set of variables used or graph theoretical representations of the network can be applied to reach to other formulations.

#### 2.1.1.1

##### **Branch flow OPF models**

Branch flow OPF formulations focus on current or power on each branch (or line) variables rather than injected power quantities at each bus. Branch flow formulations are mainly used for (low-voltage) distribution networks due to the fact that they tend to be radial [48].

'Bus injection' type of OPF models, on the other hand, are more standard-applied model type, and they focus on nodal variables, such as voltage and power injections per bus.

Both type of formulations are equivalent, and both contain non-convex power flow equations. We observe, however, that in the literature though 'bus injection' is a common type, modal formulations with nodal variables can also

include branch power flow variables. This is done by writing the Kirchhoff current laws per branch level, instead of bus level. Both models are just a representation of the Kirchhoff law for the same network. More details on formal formulations as well as equivalence of both models can be found in [48]. Numerous relaxations are devised in the literature for both formulations.

### *DistFlow equations*

The DistFlow equations, as a branch flow model, is proposed by [49, 50]. These equations are exact analytical expressions for balanced, single-phase equivalent model of a radial network. For meshed networks, one needs to enforce additional constraints to address the consistency in the angles around orientation of each phase angle. As such, the DistFlow equations provide relaxed solutions when applied to meshed networks.

A power network is composed of various components, such as buses, lines, generators and loads. Network is represented as a 'directed graph' for this formulation. Given  $\mathcal{L}$  set of branches (i.e., lines) as 'directed' links, and  $n \rightarrow m$  denote a branch between sending bus  $n$  and receiving bus  $m$ , where  $m$  is located downstream compared to  $n$ , i.e., more distant from the substation in a radial distribution system. Active and reactive power flows from  $n$  to  $m$  are denoted by  $p_{n,m}$  and  $q_{n,m}$ , respectively so that apparent power  $S_{n,m} = p_{n,m} + i \cdot q_{n,m}$ . Demanded power at the bus  $m$  is denoted by  $p_m + i \cdot q_m$  so that  $S_m = p_m + i \cdot q_m$ . Let  $l_{n,m} = |I_{n,m}|^2$  be the squared quantity of current flow  $I_{n,m}$ , from bus  $n$  to  $m$ . Lines are modelled as series impedances  $\mathbf{R}_{n,m} + i \cdot \mathbf{X}_{n,m}$ . The DistFlow equations are given by [13]:

$$p_{n,m} = R_{n,m} \cdot l_{n,m} - p_m + \sum_{k:n \rightarrow k} p_{n,k}, \forall (n, m) \in \mathcal{L}; \quad (2-1)$$

$$q_{n,m} = X_{n,m} \cdot l_{n,m} - q_m + \sum_{k:n \rightarrow k} q_{n,k}, \forall (n, m) \in \mathcal{L}; \quad (2-2)$$

$$|V_m|^2 = |V_n|^2 - 2 \cdot (R_{n,m} \cdot p_{n,m} + X_{n,m} \cdot q_{n,m}) + (R_{n,m}^2 + X_{n,m}^2) \cdot l_{n,m}, \\ \forall (n, m) \in \mathcal{L}; \quad (2-3)$$

$$l_{n,m} \cdot |V_n|^2 = p_{n,m}^2 + q_{n,m}^2, \forall (n, m) \in \mathcal{L}; \quad (2-4)$$

Note that the equations (2-3) – (2-4) are linear in  $|V_n|^2$ . By setting this term equal to a variable, one can get rid of the squared term, and obtain a linear set of equations - except for (2-4) which is non-convex.

### 2.1.1.2

#### Bus injection OPF models

Bus injection OPF models are principally formulated based on active and reactive power injected at each bus, rather than current flows at each line. Different type of bus injection models exists, such as, I-V formulation or voltage based formulation as broader categories. These fundamental formulations are mathematically equivalent. Various formulations are possible, and in fact, an active area of research is to capture and efficiently solve different power system problems.

##### *I-V formulation for OPF*

I-V formulation captures the fundamental aspects of AC power systems - namely, linear relationship between the voltage phasors and current injection phasors, as well as, power defined as a complex variable. In other words,

$$I_n = \sum_{m \in \mathcal{N}_n} \mathbf{Y}_{n,m} \cdot V_m, \quad \forall n \in \mathcal{N}; \quad (2-5)$$

$$p_n + i \cdot q_n = V_n \cdot \bar{I}_n, \forall n \in \mathcal{N}; \quad (2-6)$$

where each line  $\langle n, m \rangle \in \mathcal{L}$  has an admittance given by the complex number in rectangular coordinates  $Y_{n,m} = G_{n,m} + i \cdot B_{n,m}$ , where the parameters  $G_{n,m}$  is the line susceptance and  $B_{n,m}$  is the line conductance.

Note that in this formulation the equation (2-6) is non-convex, due to a bi-linear term. One of the advantages of the I-V formulation is the fact that it is purely formulated at each bus level without any variables coupling different buses [51].

Important to note that the formulation of admittance matrix  $\mathbf{Y}$  constrains the network components to be voltage-controlled [41, 52]. Such a fixed admittance matrix may not adequately represent elements such as ideal circuit breakers, since current through the component as a function of voltage cannot be expressed in the formulation when the circuit is closed. I-V formulations aim to incorporate such features.

##### *Voltage-based OPF formulations*

Commonly applied polar coordinate formulation of OPF introduces non-linear and non-convex constraints because of the power flow equations describing Kirchhoff's laws and Ohm's law. Kirchhoff's current law describes that for any node in an electrical circuit, the sum of currents flowing into that node is equal to the sum of currents flowing out of that respective node. Kirchhoff's voltage

law states that the directed sum of the voltages (or potential differences) around any loop is equal to zero. Ohm's law puts forward that electric current through a conductor between two points is directly proportional to the voltage across the two points.

OPF can be formulated as polar or rectangular coordinates, which are equivalent to each other. The rectangular form can sometimes be preferred due to the fact that the Hessian matrix of the constraints is constant, which is convenient for applying interior point methods [19]. In case voltage magnitudes are fixed at some of the buses, the polar formulation can yield some advantages [19, 53].

Polar formulation uses voltage magnitude and phase angle at each bus, active and reactive power flows as variables. Any angle can be changed by a multiple of  $2\pi$  without adjusting other variables [44], resulting in the same solutions due to the properties of sinus and cosinus. This thesis uses a polar coordinate formulation, which is the most common one. In the rectangular coordinate formulation of OPF, bus voltages, being complex numbers, are represented by their real and imaginary components.

A power network can be regarded as an 'undirected graph' (hence, 'bus injection' formulation) where the set of buses  $\mathcal{N}$  are the nodes of the graph and the set of lines  $\mathcal{L}$  are its edges [41]. Each bus  $n \in \mathcal{N}$  has two features: a voltage given by  $V_n = v_n + i.vq_n$ , and a power  $S_n = p_n + i.q_n$ , both being complex numbers so that  $i = \sqrt{-1}$ . Variables  $v_n$  and  $p_n$  in real numbers represent real voltage and power components, whereas  $vq_n$  and  $q_n$  represent imaginary voltage and power components. As in the I-V formulation, let receiving bus be denoted by  $m$  connected to sending bus  $n$ , so that  $m \in \mathcal{N}_n$ . Each line  $\langle n, m \rangle \in \mathcal{L}$  has an admittance given by the complex number given in rectangular coordinates, hence a 'rectangular voltage coordinate' formulation of power flow,  $Y_{n,m} = G_{n,m} + i.B_{n,m}$ , where the parameters  $G_{n,m}$  is the line susceptance and  $B_{n,m}$  is the line conductance, respectively. These network parameters are connected with each other by two fundamental physical laws, Kirchhoff's Current Law, given by:

$$\tilde{S}_n = \sum_{(n,m) \in \mathcal{L}} S_{n,m}, \forall n \in \mathcal{N} \quad (2-7)$$

and Ohm's Law, given by,

$$S_{n,m} = V_n \cdot \bar{V}_n \cdot \bar{Y}_{n,m} - V_n \cdot \bar{V}_m \cdot \bar{Y}_{n,m}, \forall (n, m) \in \mathcal{L} \quad (2-8)$$

All variables shown with  $\overline{(\cdot)}$  represent the complex conjugate of the corresponding complex conjugate variable. An important point to note is the fact that AC line power flows are not symmetric (which is a different feature than DC), i.e.,  $S_{n,m} \neq -S_{m,n}$ . Due to this, set  $\mathcal{L}$  consists of both  $(n, m)$  and  $(m, n)$  for each line of the network. In addition, network components are assumed to be voltage-controlled.

Different power flow equations are obtained by formulating and using different representations of admittance matrix, voltage phasors and power injections. A polar form can be written in an equivalent exponential way by applying Euler's formula given by  $e^{i\theta_n} = \text{Cos}(\theta_n) + i.\text{Sin}(\theta_n)$ . Hence, voltage per bus can be represented by  $V_n = |V_n|.e^{i\theta_n} = |V_n|\angle\theta_n$ , where  $|V_n|$  is the modulus of the complex number  $V_n$ , where  $\theta = \text{arctan}(vq/v)$  measured in radians and  $\theta_n \in (-\pi, \pi]$ , and  $|V_n| = \sqrt{v_n^2 + (vq)_n^2} > 0$ , as well as  $|V_n|^2 = V_n.\overline{V}_n$ . Note that it is a common way of formulating such problems because power systems tend to operate near a nominal voltage, i.e.,  $\overline{V}_n \approx 1.0\angle 0$ . Let  $\mathcal{N}_n$  be the set of nodes which are receiving nodes for power flowing from node  $n$ .

$$p_n = \sum_{m \in \mathcal{N}_n} p_{n,m}, \quad \forall n \in \mathcal{N}; \quad (2-9)$$

$$q_n = \sum_{m \in \mathcal{N}_n} q_{n,m}, \quad \forall n \in \mathcal{N}; \quad (2-10)$$

$$p_{n,m} = G_{n,m}.|V_n|^2 - |V_n|.|V_m|. (G_{n,m}.\text{Cos}(\theta_n - \theta_m) + B_{n,m}.\text{Sin}(\theta_n - \theta_m)), \quad \forall m \in \mathcal{N}_n, n \in \mathcal{N}; \quad (2-11)$$

$$q_{n,m} = -B_{n,m}.|V_n|^2 + |V_n|.|V_m|. (B_{n,m}.\text{Cos}(\theta_n - \theta_m) - G_{n,m}.\text{Sin}(\theta_n - \theta_m)), \quad \forall m \in \mathcal{N}_n, n \in \mathcal{N}; \quad (2-12)$$

### 2.1.2

#### Linear-Programming approximations for AC Optimal Power Flow, DC approximation

Large number of works in the literature restrict their attention to active power flow especially given its computational advantages. To this end, non-convex AC power flow equations are approximated by a number of linear equations describing a DC power flow model [41]. Under normal operating conditions and applying some adjustments to account for line losses, it is observed that the DC power flow model leads to a fairly accurate approximation of the inherently non-convex AC power flow equations for active power [40]. These can be incorporated into different power system problems, such as techno-economic analysis, market clearing type of purposes - e.g., a

Unit Commitment problem, making it a mixed-integer problem. Approximated by a DC power flow model, this results in a Mixed Integer Linear Programming (MILP) problem, for the solution of which the solvers have made significant progress over the last decades [54, 55]. It is particularly noted the progressive increase of computational capacity and maturity level of the solvers to solve MILPs.

Furthermore, non-convex or convexified AC power flow models can fail to converge in case of severe contingency and standard re-dispatch of generators following the changes in loading level [40]. This would be problematic in real-world applications when, for instance post contingency occurs, and the security limits of the system is still to be monitored.

Albeit its computational advantages, the DC power flow approximation to AC power flow focuses on active power flow, and does not model reactive power and voltage. Hence, it cannot be applied for some power system problems, such as voltage management, capacitor placement. The DC power flow model, in general, ignores transmission losses. In addition, the accuracy of the DC approximation beyond normal operating conditions is debatable [56, 40]. Its accuracy for transmission systems is case-specific, and depends on the power system, loading-conditions, flow patterns and transmission elements. Some extensions in the literature provide approximations to transmission losses, e.g., as in reference [57].

In case of a low voltage network and at a collapsing voltage level, AC and DC results can be significantly different [40].

In addition, for distribution systems with high resistance to reactance ratio  $R/X$  DC approximation is often not valid [58].

There are three main assumptions of the DC power flow model [59], so that the approximation can be used with a degree of accuracy:

- i) Voltage angle differences are small, i.e.,  $\sin(\delta) = \delta$ , so that

$$\sin(\theta_n - \theta_m) \approx \theta_n - \theta_m; \quad (2-13)$$

$$\cos(\theta_n - \theta_m) \approx 1 \quad (2-14)$$

Although it is said that above approximations can only hold for weakly loaded systems [59], empirical data on the voltage angle differences on the Belgian HV system shows that these differences tend to be indeed small, on average of 2%. Therefore, this condition 1 can be satisfied in practice.

- ii) Line resistance is negligible, reactance is much larger than resistance i.e.,  $R \ll X$ , implying lossless lines.  $X/R$  ratio is the tangent of the angle created by reactance and resistance in a circuit. This condition, (negligibility of

line resistance), is difficult to hold in practice except high voltage transmission networks. It is because effect of resistance increases when voltage decreases. Typical  $X/R$  ratio in a Belgian HV network is observed to be in the range of 0.8 to 12.5 depending on the voltage level. For the accuracy of DC power flow, it is empirically shown on a Belgian HV system that  $X/R > 4$  would be needed.

iii) Flat voltage profile, i.e., all voltages are equal and close to 1.0 per unit (p.u.), and do not vary significantly. Deviations from the predefined value is the most important issue here, rather than nominal values. Voltage deviations result in line voltage differences, which cannot be captured in DC power flow. This gives rise to an inaccurate estimate for the active power flow, which is highly responsive to voltage variations. Flat voltage profile assumption is shown to be most critical one for the accuracy of DC power flow [59]. For DC power flow accuracy, it is shown that a voltage deviation, measured as a standard deviation of 0.01, is empirically shown to be needed in the Belgian HV system.

When these above 3 assumptions are applied to non-convex AC active and reactive power flow equations for  $p_{n,m}$  and  $q_{n,m}$ , then they reduce to the following DC power flow equations:

$$p_{n,m} = -B_{n,m} \cdot (\theta_n - \theta_m), \forall \langle n, m \rangle \in \mathcal{L} \quad (2-15)$$

### 2.1.3

#### Other Linear and Quadratic Programming approximations for AC Optimal Power Flow

Linearisation approaches for power flow equations are typically based on first and second order Taylor series expansion of state variables, namely, voltage and phase angle. Examples of one-step approaches based on this expansion are [60, 61, 62]. Respectively in these references, Taylor series expansion of the state variables in different spaces, a generalized function of these variables or tight convex approximations of line flow constraints are proposed. There are also sequential linear programming (SLP) models are proposed, which enhance the relaxations or approximations sequentially per iteration. Notable sequential approaches in the literature are current voltage (I-V) formulation-based OPF [51], using penalty function and the respective slack variables, second-order cone programming relaxation which is tightened dynamically via linear cuts as a sequence of hyperplanes [63] or forming trust regions around the calculated set points [64]. A recent paper, [65] for instance, extends [60] into a sequential

algorithm, and tightens critical constraints per iteration.

A linear-programming approximation for power flow is presented in [41] incorporating reactive power and voltage. This model is based on a polyhedral relaxation of the cosine terms in the AC equations and Taylor series expansion of the other non-linear terms.

### 2.1.3.1

#### Linearised DistFlow approximation

Linearised DistFlow approximation is a widely applied because of its computational advantages as a linear programming problem. The DistFlow equations are exact for radial distribution systems. Linearised DistFlow assumes that the active and reactive power losses are much smaller compared to active and reactive power flows in a given branch, i.e.,  $R_{n,m} \cdot I_{n,m} \ll p_{n,m}$  and  $X_{n,m} \cdot I_{n,m} \ll q_{n,m}$ . Therefore, these losses are ignored in the formulation, which results in:

$$p_{n,m} = -p_m + \sum_{k:n \rightarrow k} p_{n,k}, \forall \langle n, m \rangle \in \mathcal{L}; \quad (2-16)$$

$$q_{n,m} = -q_m + \sum_{k:n \rightarrow k} q_{n,k}, \forall \langle n, m \rangle \in \mathcal{L}; \quad (2-17)$$

$$|V_m|^2 = |V_n|^2 - 2 \cdot (R_{n,m} \cdot p_{n,m} + X_{n,m} \cdot q_{n,m}), \\ \forall (n, m) \in \mathcal{L}; \quad (2-18)$$

### 2.1.4

#### Second-order cone programming relaxation

The first SOCP formulation for OPF problems was derived by [66] and it was applied on a radial distribution network.

The canonical form of a second-order cone programming can be written as [67]:

$$\min_{\mathbf{x}} c^T \cdot \mathbf{x}; \quad (2-19)$$

subject to:

$$\| \mathbf{E}_i \cdot \mathbf{x} + \mathbf{b}_i \|_2^2 \leq g_i^T + d_i, \forall i = 1, \dots, r; \quad (2-20)$$

$$\mathbf{A} \cdot \mathbf{x} = \mathbf{b}; \quad (2-21)$$

$$\mathbf{x} \geq 0; \quad (2-22)$$

Rotated SOCP constraints are also used in the context of power flow formulations, which can equivalently represent canonical SOCP constraints. These rotated SOCP constraints are defined as

$$\mathbf{x} \cdot \mathbf{y} \geq \|\mathbf{z}\|_2^2; \quad (2-23)$$

$$\mathbf{x} \geq 0, \mathbf{y} \geq 0; \quad (2-24)$$

SOCP relaxation is obtained by applying some changes of variables in the power flow equations, as the followings:

$$c_{n,n} = |V_{n,t}|^2, \quad \forall n \in \mathcal{N}; \quad (2-25)$$

$$c_{n,m} = |V_m| \cdot |V_n| \cdot \text{Cos}(\theta_n - \theta_m) = v_n \cdot v_m + v_{q_n} \cdot v_{q_m}, \\ \forall m \in \mathcal{N}_n, n \in \mathcal{N}; \quad (2-26)$$

$$s_{n,m} = |V_m| \cdot |V_n| \cdot \text{Sin}(\theta_n - \theta_m) = -v_n \cdot v_{q_m} + v_m \cdot v_{q_n}, \\ \forall m \in \mathcal{N}_n, n \in \mathcal{N}; \quad (2-27)$$

$$|V_n| = \sqrt{v_n^2 + (v_{q_n})^2} > 0, \text{ as well as } |V_n|^2 = V_n \cdot \bar{V}_n.$$

$$p_n = \sum_{m \in \mathcal{N}_n} p_{n,m}, \quad \forall n \in \mathcal{N}; \quad (2-28)$$

$$q_n = \sum_{m \in \mathcal{N}_n} q_{n,m}, \quad \forall n \in \mathcal{N}; \quad (2-29)$$

$$p_{n,m} = G_{n,m} \cdot c_{n,n} - G_{n,m} \cdot c_{n,m} + \\ - B_{n,m} \cdot s_{n,m}, \quad \forall m \in \mathcal{N}_n, n \in \mathcal{N}; \quad (2-30)$$

$$q_{n,m} = -B_{n,m} \cdot c_{n,n} + B_{n,m} \cdot c_{n,m} + \\ - G_{n,m} \cdot s_{n,m}, \quad \forall m \in \mathcal{N}_n, n \in \mathcal{N}; \quad (2-31)$$

$$c_{n,m} = c_{m,n}, \quad \forall n \in \mathcal{N}, \forall m \in \mathcal{N}_n; \quad (2-32)$$

$$s_{n,m} = -s_{m,n}, \quad \forall n \in \mathcal{N}, \forall m \in \mathcal{N}_n; \quad (2-33)$$

$$c_{n,m}^2 + s_{n,m}^2 = c_{n,n} \cdot c_{m,m}, \quad \forall n \in \mathcal{N}, \forall m \in \mathcal{N}_n; \quad (2-34)$$

The above is an exact analytic formulation for radial networks. Non-convexity arises because of (2-34). SOCP relaxation is obtained as a rotated cone formulation:

$$c_{n,m}^2 + s_{n,m}^2 \leq c_{n,n} \cdot c_{m,m}, \forall n \in \mathcal{N}, \forall m \in \mathcal{N}_n; \quad (2-35)$$

It is shown that SOCP relaxation is tight for radial (tree) networks under various voltage and load conditions [39]. Under high-loading conditions relaxations and approximations, such as the SOCP relaxation, tend to be inexact [14].

Sufficient conditions for the exactness of SOCP relaxation, e.g. based on [66], is well-studied. These sufficient conditions are also valid for tighter relaxations than SOCP, e.g., semi-definite type relaxations scaled diagonally-dominant sum-of-squares (SDSOS), Shor relaxation, quadratic constrained (QC) relaxation, moment relaxation, and 'strong SOCP' relaxation. Below sufficiency conditions only apply to problems where balanced single-phase equivalent network models are used.

i) As in [68], SDP relaxation, as a dual of a convex relaxation for the OPF problem. Whenever the duality gap is zero, a global optimum solution of the convex dual problem can be derived. Relaxation is shown in [68] to be tight for the networks where the resistance is very low,  $10^{-5}$  per unit for each transformer, and with no reactive loads where demand can be over met provided that dual is a positive number. Zero duality gap can be satisfied under certain conditions, tested on some benchmark systems. These imply that under normal operating conditions SDP relaxation could be tight. [69] provides a counterexample, however, showing that the approach in [68] can lead to physically meaningless solutions with non-zero duality gap.

ii) For meshed networks [70] shows that allowing for oversatisfaction of load where adequate number of virtual phase-shifters are available in the system, or other non-trivial technical assumptions SDP relaxation is exact.

iii) [71] show for radial networks that when no lower bounds are enforced on active and reactive power generation limits at any bus, while voltage, line losses and line flows are considered. [72] and [73] findings support this conclusion when line limits constraints are not enforced.

iv) [74] show that for radial networks if voltage magnitudes are fixed and real power lower bounds enforced, but not the reactive power lower bounds, angle is limited by practical bounds, then the convex relaxations become tight.

Furthermore, some approaches are proposed in the literature to increase the tightness of SOCP, which is in general not guaranteed to be tight. An example is the sequential tightness algorithm [58]. This tightness algorithm iteratively shrinks the upper bounds for power loss constraints which violate tightness criteria set. Interior point method is used to solve proposed SOCP model in polynomial time.

For radial networks, [19] shows that in the presence of generation lower bounds for active and reactive power under which conditions SOCP relaxation would be i) exact, ii) inexact or iii) feasible though the original non-convex

OPF is infeasible.

SOCP, in general, demonstrates computational advantages compared to, e.g., SDP. Mixed-integer SOCP, which can be for instance the case for UC problems, solvers are rather recent and not so mature compared to MILP solvers [13].

### 2.1.5

#### Semi-definite programming relaxation

SDPs are generalised forms for SOCP as well as linear programming problems. Unlike linear programming and SOCP in which the decision variables are represented by vectors, SDP decision variables are symmetric matrices, name  $\mathbf{X}$ . Given  $\mathbf{X} \succeq 0$  representing its positive semi-definite property of the decision matrix  $\mathbf{X}$ , i.e., non-negativity of all diagonal entries. Semi-definite programming in its canonical form is given by [67, 13]:

$$\min_{\mathbf{X}} \text{tr}(\mathbf{C}.\mathbf{X}); \quad (2-36)$$

subject to:

$$\text{tr}(\mathbf{A}_i.\mathbf{X}) = b_i, \forall i = 1, \dots, r; \quad (2-37)$$

$$\mathbf{X} \succeq 0; \quad (2-38)$$

where  $\text{tr}(\cdot)$  is the trace operator,  $\mathbf{A}_i$  and  $\mathbf{C}$  are square and symmetric matrices, and  $b_i$  are scalars. Trace operator, defined as  $\text{tr}(\mathbf{A}.\mathbf{B}) = \sum_i \sum_k \mathbf{A}_{i,k}.\mathbf{B}_{k,i}$ , makes the constraint (2-37) linear in variable  $\mathbf{X}$ .

Due to the fact that SDP solvers are not yet mature [13], which is also the case for SOCP compared to LP, the preference in model formulations is also the reverse order of this, i.e., first LP, SOCP and finally SDP.

The work [68] is amongst the earliest works popularising usage of SDP for OPF problems.

SDP can be formulated both in real or complex variables. Complex variables arise due to phasor representation of voltages in the power flow equations. Some formulations use the property of Hermitian matrices, whose eigen values are real-values, which makes the positive semi-definiteness aspect well-defined.

SDP relaxation to OPF is solvable in general in polynomial time [19]. This result is generalised in [70] with not only quadratic cost functions but also arbitrary convex cost functions.

In case of exactness conditions are satisfied for SDP relaxation, a global optimal solution to the OPF problem can be obtained. Efficient algorithms

to solve SDP relaxation, however, are still to be found [58], and they tend to be prohibitively computationally expensive when the network size becomes larger [19]. This feature motivates usage of SOCP-based techniques in practice, though they are in general weaker than SDP, recognising that SDP is a powerful method. Both SDP and SOCP yield the same lower bound for the OPF problem applied to radial networks even if the relaxation is inexact, i.e., exactness conditions are not satisfied.

It is shown that for radial networks, the SOCP relaxation is equivalent to SDP relaxation [75].

SDP relaxations are exact for a limited number of problems, sometimes under not realistic network assumptions especially in modern power systems such as non-responsive demand or when load oversatisfaction is allowed or when generation lower bounds are ignored. Therefore, if SDP relaxation is not tight then the obtained solution may sometimes be not meaningful or practicable. Like any other relaxations, SDP can result in infeasible or inexact solutions [19].

SDP relaxation for non-convex quadratically constrained quadratic programs (QCQPs) are first proposed in the seminal work [76], so-called 'Shor relaxation'. The first paper applied SDP in OPF problem was [77]. Later on after the work [68], the SDP for OPF problems became more widespread. For the Shor Relaxation, it is more convenient to express power flow equations in their 'rectangular voltage coordinates, such that  $\tilde{V}_n = v_n + i.vq_n$ . Admittance matrix expressed here throughout in rectangular coordinates.

This formulation of power flow, namely on the basis of rectangular admittance as well as voltage coordinates provides the active and reactive power flow formulations as in (2-39) - (2-43). Note that this formulation has real and imaginary part of voltage as variables (unlike the rectangular admittance and polar voltage coordinate formulation provided earlier at the beginning of the chapter). This results in the following power flow equations:

$$p_n = \sum_{m \in \mathcal{N}_n} p_{n,m}, \quad \forall n \in \mathcal{N}; \quad (2-39)$$

$$q_n = \sum_{m \in \mathcal{N}_n} q_{n,m}, \quad \forall n \in \mathcal{N}; \quad (2-40)$$

$$p_{n,m} = v_n \cdot \left( G_{n,m} \cdot v_m - B_{n,m} \cdot v q_m \right) + v q_n \cdot \left( B_{n,m} \cdot v_m + G_{n,m} \cdot v q_m \right) + G_{n,m} \cdot \left( |V_m|^2 \right), \quad \forall m \in \mathcal{N}_n, n \in \mathcal{N}; \quad (2-41)$$

$$q_{n,m} = v_n \cdot \left( -B_{n,m} \cdot v_m - G_{n,m} \cdot v q_m \right) + v q_n \cdot \left( G_{n,m} \cdot v_m - B_{n,m} \cdot v q_m \right) + B_{n,m} \cdot \left( |V_m|^2 \right), \quad \forall m \in \mathcal{N}_n, n \in \mathcal{N}; \quad (2-42)$$

$$|V_n|^2 = v_n^2 + (v q_n)^2, \quad \forall n \in \mathcal{N}; \quad (2-43)$$

Firstly, power flow equations are formulated in such a way that all non-convexity is incorporated into a rank constraint. Thereafter, that constraint is relaxed, forming an SDP-type relaxation, namely Shor relaxation.

Shor relaxation can be written in real-valued or complex-valued formulations, which are equivalent in the sense that they provide the same objective value as well as an optimal solution to real formulation based relaxation can be formed by using the complex-valued formulation based relaxation, or vice versa. Solely the formulation for the real-valued relaxation is provided here for expository purposes. Complex-valued formulations can be found in reference [13]. The latter is constructed on the basis of Hermitian matrices.

Given  $\mathbf{e}_m$  the  $m^{\text{th}}$  standard basis vector in  $\mathbb{R}^{|\mathcal{N}|}$ . For each bus  $n \in \mathcal{N}$ , matrices  $\mathbf{L}_{p,m}$ ,  $\mathbf{L}_{q,m}$ ,  $\mathbf{M}_m$  and  $\mathbf{N}_m$  are formed given as follows, with  $m$  standing for the receiving bus.

$$\mathbf{L}_{p,m} = \frac{1}{2} \cdot \begin{bmatrix} \operatorname{Re}\left(\mathbf{Y}^T \cdot \mathbf{e}_m \cdot \mathbf{e}_m^T + \mathbf{e}_m \cdot \mathbf{e}_m^T \cdot \mathbf{Y}\right) & \operatorname{Im}\left(\mathbf{Y}^T \cdot \mathbf{e}_m \cdot \mathbf{e}_m^T - \mathbf{e}_m \cdot \mathbf{e}_m^T \cdot \mathbf{Y}\right) \\ \operatorname{Im}\left(\mathbf{e}_m \cdot \mathbf{e}_m^T \cdot \mathbf{Y} - \mathbf{Y}^T \cdot \mathbf{e}_m \cdot \mathbf{e}_m^T\right) & \operatorname{Re}\left(\mathbf{Y}^T \cdot \mathbf{e}_m \cdot \mathbf{e}_m^T + \mathbf{e}_m \cdot \mathbf{e}_m^T \cdot \mathbf{Y}\right) \end{bmatrix}; \quad (2-44)$$

$$\mathbf{L}_{q,m} = -\frac{1}{2} \cdot \begin{bmatrix} \operatorname{Im}\left(\mathbf{Y}^T \cdot \mathbf{e}_m \cdot \mathbf{e}_m^T + \mathbf{e}_m \cdot \mathbf{e}_m^T \cdot \mathbf{Y}\right) & \operatorname{Re}\left(\mathbf{e}_m \cdot \mathbf{e}_m^T \cdot \mathbf{Y} - \mathbf{Y}^T \cdot \mathbf{e}_m \cdot \mathbf{e}_m^T\right) \\ \operatorname{Re}\left(\mathbf{Y}^T \cdot \mathbf{e}_m \cdot \mathbf{e}_m^T - \mathbf{e}_m \cdot \mathbf{e}_m^T \cdot \mathbf{Y}\right) & \operatorname{Im}\left(\mathbf{Y}^T \cdot \mathbf{e}_m \cdot \mathbf{e}_m^T + \mathbf{e}_m \cdot \mathbf{e}_m^T \cdot \mathbf{Y}\right) \end{bmatrix}; \quad (2-45)$$

$$\mathbf{M}_m = \begin{bmatrix} \mathbf{e}_m \cdot \mathbf{e}_m^T & \mathbf{0} \\ \mathbf{0} & \mathbf{e}_m \cdot \mathbf{e}_m^T \end{bmatrix}; \quad (2-46)$$

$$\mathbf{N}_m = \begin{bmatrix} \mathbf{0} & \mathbf{0} \\ \mathbf{0} & \mathbf{e}_m \cdot \mathbf{e}_m^T \end{bmatrix}; \quad (2-47)$$

Then the power flow formulated on the basis of rectangular admittance as well as voltage coordinates can be equivalently written as

$$p_n = \operatorname{tr}(\mathbf{L}_{p,m} \cdot \mathbf{W}), \quad \forall n \in \mathcal{N}, m \in \mathcal{N}_n; \quad (2-48)$$

$$q_n = \operatorname{tr}(\mathbf{L}_{q,m} \cdot \mathbf{W}), \quad \forall n \in \mathcal{N}, m \in \mathcal{N}_n; \quad (2-49)$$

$$|V_n|^2 = \operatorname{tr}(\mathbf{M}_m \cdot \mathbf{W}), \quad \forall n \in \mathcal{N}, m \in \mathcal{N}_n; \quad (2-50)$$

$$0 = \operatorname{tr}(\mathbf{N}_1 \cdot \mathbf{W}); \quad (2-51)$$

$$\mathbf{W} = \mathbf{x} \cdot \mathbf{x}^T; \quad (2-52)$$

where  $x = [v_1 \dots v_n; vq_1 \dots vq_n]^T$ . Equation (2-43) sets the reference angle to 0.

The SDP relaxation, based on Shor relaxation as applied in [68] relaxes the constraint in relation to rank, i.e., number of linearly independent columns of the matrix  $\mathbf{W}$ . For this, (2-45) is replaced by

$$\mathbf{M} \succeq 0; \quad (2-53)$$

If the optimal solution  $\mathbf{W}^*$  to the SDP-relaxed problem fulfills the following, then the relaxation is exact and the globally optimal solutions to the original problem can be obtained from the solution to the relaxed-problem.

$$\operatorname{rank}(\mathbf{W}^*) = 1; \quad (2-54)$$

Shor relaxation is shown to be exact in a number of power system OPF

applications [68]. However, it is also shown that it can fail to be exact [69]. Exactness of Shor relaxation can be impacted by the objective function chosen as well as constraints in which, e.g., the way the power flow is formulated. Since it is demonstrated that there are test power systems for which Shor relaxations are not exact, though they do not satisfy the so far known sufficient conditions imply that there can be other sufficient conditions which are not known, constituting a potential research direction. Various sufficient conditions are derived with regard to SOCP, which also apply to SDP. Specific sufficient conditions can be found in references, such as [78, 79, 80]. Some of these sufficiency conditions may not be practicable, such as no limits on reactive power injections or power flows [80].

SDP is a computationally challenging method in general, especially due to the positive semi-definite constraint (2-53) in the real-valued formulation. The complex-valued formulation tends to have similar computational challenges. Several methods focus on graph theoretical concepts, such as utilising 'chordal sparsity' of the network to reduce computational burden. These methods may suffer from numerical ill-conditioning. Such techniques as 'facial reduction' are applied to improve this aspect [81].

Other than Shor relaxation, especially for the cases it is inexact, Lasserre hierarchy applied to real-valued polynomial optimisation problems and related moment, or sum-of-squares relaxation hierarchies are proposed [82, 83]. Furthermore, moment relaxation hierarchy in complex numbers are also proposed, computationally superior to Lasserre hierarchy due to smaller matrices used, but at the cost that in general such relaxations are less tight than Lasserre. However, it is worthwhile to highlight that SDP solvers with complex numbers are even less mature than those solvers SDP applied to real-valued problems. As a trade-off to accuracy and computational burden, some further relaxations to Lasserre hierarchy are proposed, such as SDP/ SOCP hierarchy [84]. The latter is based on the idea that SOCP constraints necessary but not sufficient conditions for SDP constraints obtained from higher order moment relaxations. The proposed mixed SOCP/SDP model makes use first-order relaxation by making use of SDP constraints and higher-order relaxation of the SOCP constraints. Another type of relaxation to Lasserre hierarchy is named as Scaled Diagonally Dominant Sum-of-Squares (SDSOS) [85]. This method is based on polynomial optimisation through which hierarchy of SOCP relaxations are provided.

Off-the-shelf SDP solvers, such as MOSEK, typically apply interior point methods based on second-order derivatives and provide local optimal solutions. Along with interior point algorithm other methods, such as coordinate-descent,

ADMM are also applied. Enhancements to model formulations as well as other computational advances are still welcome for solving SDP-type problems.

## 2.2

### Outer approximation

This section presents a general form of outer approximation-based algorithms.

Optimisation problems, in which the objective and constraints are represented by linear and non-linear functions of both continuous and integer variables, are named as mixed-integer non-linear programming problems (MINLP) [86]. There is a large variety of optimisation problems which can be represented by a MINLP. A specific class of MINLP are named as "convex MINLP" to describe problems which are convex when the integer variables are relaxed into continuous. Despite this naming, any optimisation problem with a discrete feasible space is by definition non-convex.

"Convex MINLP" are an important class in which convexity property, when relaxed, can be used and decomposition algorithms can be applied. Amongst the decomposition algorithms for MINLP, outer approximation (OA) and its variants, such as single-tree OA [87], quadratic cuts OA [88], conic-based OA [89], are widely applied.

Most successful algorithms to solve "Convex Mixed Integer Nonlinear Programming" problems are based on linear approximation [55, 86]. OA is one of the most efficient methods, and several solvers apply this method. One of the shortcomings is that there can be instabilities and some jumps can be experienced in the search space. Some regularisation methods are proposed in the literature to tackle this issue [90].

The principal idea is to approximate non-linear functions by valid linear functions of nonlinear constraints using gradients. These linearisations are identical to the first-order Taylor series expansions of the non-linear functions in the constraints. Because of the convexity of the approximated function, this linearisation results in a relaxation for the original problem. It is due to the fact that the polyhedral set constructed by these linear approximation is larger than the original feasibility set of the non-convex constraints.

Outer approximation (OA) algorithm is first proposed by [91], and later enhanced by [92]. It is a highly popular approach to solve mixed integer non-linear problems due to its interpretability and straightforward implementation and convergence guarantees in a finite number of iterations [55]. As the number of integer solutions is assumed to be finite, it requires relatively few number of iterations and hence leads to fast convergence.

OA attempts to construct an upper bound for the original mixed integer non-linear problem by fixing the integer variable. It differentiates whether the solution to the problem by fixing the integer variable is feasible or not. Gap between the best upper and lower bounds are used as a stopping criteria. As in [92], assuming that KKT conditions are satisfied when the integer variables are fixed at obtained optimal values, a solution for the integer variable is not considered for a second time by the algorithm unless that solution is part of the optimal solution set. In the latter case, it would be visited for the second time at maximum. This implies that the OA needs relatively few number of iterations for convergence.

MINLPs can be abstracted as follows:

$$\min_{\mathbf{x}, \mathbf{y}} f(\mathbf{x}, \mathbf{y}); \quad (2-55)$$

subject to:

$$g_j(\mathbf{x}, \mathbf{y}) \leq 0, \forall j = 1, \dots, l; \quad (2-56)$$

$$\mathbf{A}\mathbf{x} + \mathbf{B}\mathbf{y} \leq \mathbf{b}, \forall \mathbf{x} \in \mathbb{R}^n, \mathbf{y} \in \mathbb{Z}^m; \quad (2-57)$$

The objective function can be transformed into an epigraph form as a constraint such that,  $f(\mathbf{x}, \mathbf{y}) \leq \mu$ . and  $\mu$  stands for the objective value.

For global convergence reasons typically convexity and continuous differentiability of the functions  $f, g_1, \dots, g_l : \mathbb{R}^n \times \mathbb{R}^m \rightarrow \mathbb{R}$ , bounded search space (e.g., polyhedron) for the linear constraints, and constraint qualification for each feasible integer combination, e.g., Slater's condition are assumed to hold [86]. Albeit these, OA can also be applied in non-convex functions [93].

As outlined in [86] in detail, OA proceeds firstly by an initialisation by a set of trial solutions,  $\{\mathbf{x}^i, \mathbf{y}^i\}_{i=0}^k$ , linear relaxation can be obtained by the constraints

$$f(\mathbf{x}^i, \mathbf{y}^i) + \Delta f(\mathbf{x}^i, \mathbf{y}^i)^\top \cdot \begin{bmatrix} \mathbf{x} - \mathbf{x}^i \\ \mathbf{y} - \mathbf{y}^i \end{bmatrix} \leq \mu, \forall i = 1, \dots, k; \quad (2-58)$$

$$g(\mathbf{x}^j, \mathbf{y}^i) + \Delta g_j(\mathbf{x}^i, \mathbf{y}^i)^\top \cdot \begin{bmatrix} \mathbf{x} - \mathbf{x}^i \\ \mathbf{y} - \mathbf{y}^i \end{bmatrix} \leq 0, \forall i = 1, \dots, k, \forall j \in \mathcal{I}_i; \quad (2-59)$$

where  $\mathcal{I}_i$  are index sets consisting of active non-linear constraints when the trial solution  $(\mathbf{x}^i, \mathbf{y}^i)$  applied. The above constraints given by (2-58)–(2-59) represent a polyhedral and they are an outer approximation to the non-linear constraints. The linear constraints generated in order to approximate the non-

convex feasible space is called 'cuts'. It is because they cut off the search space by eliminating the parts which are found to be infeasible.

The consecutive integer solution candidates,  $\mathbf{y}^{k+1}$ , are derived by solving:

$$\min_{\mathbf{x}, \mathbf{y}, \mu} \mu; \quad (2-60)$$

subject to:

$$f(\mathbf{x}^i, \mathbf{y}^i) + \Delta f(\mathbf{x}^i, \mathbf{y}^i)^\top \cdot \begin{bmatrix} \mathbf{x} - \mathbf{x}^i \\ \mathbf{y} - \mathbf{y}^i \end{bmatrix} \leq \mu, \forall i = 1, \dots, k; \quad (2-61)$$

$$g(\mathbf{x}^j, \mathbf{y}^i) + \Delta g_j(\mathbf{x}^i, \mathbf{y}^i)^\top \cdot \begin{bmatrix} \mathbf{x} - \mathbf{x}^i \\ \mathbf{y} - \mathbf{y}^i \end{bmatrix} \leq 0, \forall i = 1, \dots, k, \forall j \in \mathcal{I}_i; \quad (2-62)$$

$$\mathbf{A} \cdot \mathbf{x} \leq \mathbf{b}; \quad (2-63)$$

$$\mathbf{x} \in \mathbb{R}^n, \mathbf{y} \in \mathbb{Z}^m, \mu \in \mathbb{R}; \quad (2-64)$$

Since convexity is assumed in the problem, the optimal solution obtained from the problem (2-60) – (2-64) gives a valid lower bound for the original MINLP problem. Define  $LB^{k+1}$  is a lower bound.

In order to derive valid upper bounds to the original MINLP problem, two situations are considered. Firstly, if the integer  $\mathbf{y}^{k+1}$  is feasible, the continuous variable  $\mathbf{x}^{k+1}$  can be obtained through the solution to the convex NLP problem

$$\min_{\mathbf{x} \in \mathbb{R}^n} f(\mathbf{x}, \mathbf{y}^{k+1}); \quad (2-65)$$

subject to:

$$g_j(\mathbf{x}, \mathbf{y}^{k+1}) \leq 0, \forall j = 1, \dots, l; \quad (2-66)$$

$$\mathbf{A} \cdot \mathbf{x} + \mathbf{B} \cdot \mathbf{y}^{k+1} \leq \mathbf{b}; \quad (2-67)$$

A feasible solution to the problem given by (2-65) – (2-67) provides an upper bound to the original MINLP problem,  $UB^{k+1}$ .

In case this latter optimisation problem is infeasible, a feasibility problem which is outlined herebelow, needs to be solved to obtain  $\mathbf{x}^{k+1}$ . The feasibility problem is a minimisation problem on the norm of the constraint violations, usually  $l_{\text{inf}}$  or  $l_1$ . By fixing at the optimal integer values for  $\mathbf{y}$ , the feasibility problem can be solved over the variables  $\mathbf{x}$  and  $\mathbf{s}$  such that

$$\min_{\mathbf{x} \in \mathbb{R}^n, \mathbf{s} \in \mathbb{R}_+^l} \|\mathbf{s}\|_p; \quad (2-68)$$

subject to:

$$g_j(\mathbf{x}, \mathbf{y}^{k+1}) \leq s_j, \forall j = 1, \dots, l; \quad (2-69)$$

$$\mathbf{A}\mathbf{x} + \mathbf{B}\mathbf{y}^{k+1} \leq \mathbf{b}; \quad (2-70)$$

The OA algorithm proceeds in such a way that at each iteration a new MILP optimisation problem is solved having an additional cut compared to the previous iteration. To increase the efficiency of this process for searching integer variable candidate and not to solve too many similar problems, some works such as [87], incorporate other procedures into the OA - e.g., branch-and-bound.

Pseudo code of the OA algorithm is provided below:

---

**Algorithm 1** Outline of Outer Approximation Algorithm

---

1. *Initialisation:*
    - 1.1 Solve a continuous relaxation of the MINLP problem, store optimal solutions  $\bar{\mathbf{x}}, \bar{\mathbf{y}}$ ;
    - 1.2 Cut generation at the points  $\bar{\mathbf{x}}, \bar{\mathbf{y}}$  using (2-58)–(2-59), construct master OA-MILP problem (2-60)–(2-64);
    - 1.3 Set iteration counter  $\nu \leftarrow 1$ , set  $UB^0 \leftarrow \infty$ , set  $LB^0 \leftarrow -\infty$ ;
  2. *Convergence check, repeat until  $UB^{\nu-1} - LB^{\nu-1} \leq \epsilon$  tolerance level:*
    - 2.1 Solve OA-MILP (2-60)–(2-64), get  $\mathbf{y}^\nu, LB^\nu$ ;
    - 2.2 Solve NLP-I (2-65)–(2-67) with integer variables  $\mathbf{y}$  fixed at  $\mathbf{y}^\nu$ , get  $\mathbf{x}^\nu$ ;
      - 2.2.1 If problem NLP-I (2-65)–(2-67) feasible,  $UB^\nu = \min\{f((\mathbf{x}^\nu, \mathbf{y}^\nu), UB^{\nu-1})\}$ ;
      - 2.2.2 If problem NLP-I infeasible, solve feasibility problem NLP-f given by (2-68)–(2-70), get  $\mathbf{x}^\nu$ , set  $UB^\nu \leftarrow UB^{\nu-1}$ ;
    - 2.3 Generate cuts at the points  $\mathbf{x}^\nu, \mathbf{y}^\nu$  using (2-58)–(2-59), add to master OA-MILP problem (2-60)–(2-64);
    - 2.4 Set iteration counter  $\nu \leftarrow \nu + 1$ ;
  3. *Return best found solutions given tolerance level.*
-

## 2.3

### **Distributed, decentralised computation of Optimal Power Flow**

Smart electric power systems' physical structure is increasingly distributed. Various entities, such as distribution and transmission system operators and market actors, interact in this system as well as take responsibility in a certain part of the system. Since these systems are physically interconnected, control decisions of one entity would impact the other. These entities need to coordinate for efficiency and effectiveness of control in order to assure system reliability. Hence, centralised control and energy management algorithms may not be adequate for operation and control purposes [23]. Since a centralised problem, where an agent knows all variables and constraints for transmission and distribution networks, is not realistic. Accordingly, the DSO-TSO coordination related contribution focuses on decentralised or distributed computing.

As previously discussed, optimal power flow and unit commitment function as energy management algorithms. Despite various solution techniques are proposed to solve such problems centrally as a problem of one single controlling entity, distributed and decentralised techniques are also extensively studied. The paper [23] provides a thorough outline of these techniques. Within the latter context, the OPF problem is usually studied from the perspective of how one controlling entity would coordinate with the neighbouring entity so that reliable operations can be assured for the entire system.

Distributed and decentralised techniques differ from each other in terms of whether a central coordinator is needed or not, as defined in [23]. Distributed optimisation requires a coordinator which coordinates different independent entities. Entities themselves do not communicate with each other. One can talk about two different hierarchy level, one with controlling entities, and the other with the coordinator. Hence, in distributed OPF algorithms, communication network, is different from the electric network topology itself. Decentralised techniques, on the other hand, do not have a coordinator. Each entity exchanges information with the next entity. In decentralised algorithms, there is no hierarchy involved, and all entities have independent and same hierarchy level. Despite the fact that in these algorithms, often the network topology and communication network would be the same, it is not necessarily always the case.

There are six widely applied decentralised or distributed optimisation algorithms to OPF type of problems: analytical target cascading (ATC) [94], alternating direction method of multipliers (ADMM), proximal message passing (PMP) [95], auxiliary problem principle (APP), optimality condition

decomposition (OCD) [96], and consensus and innovations (CI) [97]. ATC and ADMM are distributed algorithms with a coordinator, whereas the remaining are decentralised algorithms.

This thesis applies an ADMM-type of algorithm, and proposes a decentralised structure in order to mitigate the need for a central controller, being a limitation of distributed algorithms. The choice of ADMM as a method in the respective contribution of the thesis is because of the fact that it allows computation of equilibrium set points of the agents with a limited information interchange and without any hierarchy amongst the agents. Other methods to compute equilibrium set points, such as Nash equilibrium, may require a central agent.

A general version of the ADMM is described in the next subsection.

Other than these classifications in terms of distributed and decentralised nature of algorithms, there is another classification in terms of offline and online algorithms [13]. Offline algorithms are distributed algorithms in which iterations continue on all variables in the cyber environment until a convergence is achieved. Interim iterations may not necessarily comply with Kirchhoff's laws or operating constraints.

Real-time or online algorithms, on the other hand, provide advantages for real large-scale power systems involving dynamic DERs. In these models, the iterations are performed solely on variables of controllable devices as a feedback to the network. A set of algebraic equations or differential equations are applied to the power flow problem and optimisation model is with the objective to control. These models can capture changing network topology and conditions. Some of such algorithms are to a certain degree decentralised and model-free, i.e., not depending on system parameters but rather on the measurement data from smart devices.

### 2.3.1

#### **Alternating directional method of multipliers**

Other than the earlier described physical structure of smart grids, namely the entities being responsible for their own part while interconnected with each other, there are time limitations for system operators to take operational decisions, such as for energy management or market clearance purposes etc. These factors motivate consideration of a decomposition mechanism which can facilitate finding a solution within the tolerated error limits.

In distributed optimisation, in general, how to perform a decomposition and respective update procedure is of importance to gain algorithmic efficiencies [98]. One of the common distributed approaches is the Dual Decomposition

with dual sub-gradient ascent method enabling distributed computation, which is reported to be slow. Method of Multipliers is an alternative approach, which is characterised to be robust and with favourable convergence properties. The Alternating Direction Method of Multipliers (ADMM) provides a trade-off between these two approaches [13]. ADMM and its variants are reviewed by a recent survey [99].

Similar to the Dual Decomposition, the ADMM is based on the minimisation of the Lagrangian function, - performed on its augmented form -, and update of dual variables. The Dual Decomposition method minimises the Lagrangian function with regard to the primal variables jointly. In the ADMM, the primal variable updates are performed in an alternating or sequential manner. First, augmented Lagrangian function is formed. Then, it is decomposed and minimised over sequential Gauss-Seidel iterations.

ADMM is applied in OPF and UC type of problems, particularly for large-scale power systems [100]. ADMM performs a decomposition and coordination process in which a large problem is divided into sub-problems in which the solution process is coordinated, and overall it provides the solution of the original large scale-problem [101], in case convergence is achieved, which is not always for granted.

Even though in its standard form ADMM requires a coordinator, and as such it is a distributed algorithm, there are works in the literature which attempts to remove this coordinator need and apply a decentralised algorithm. Examples to this are works by [101] and [102]. In addition, there are some decentralised techniques proposed combining ADMM with some convexification procedures such as in [103].

Given a general problem with two-blocks, i.e., a problem ultimately separable into two optimisation problems when necessary modifications are made, a compact form is formulated as follows:

$$\min_{\mathbf{x}, \mathbf{y}} (f(\mathbf{x}) + g(\mathbf{y})) \quad (2-71)$$

subject to:

$$\mathbf{C}.\mathbf{x} + \mathbf{D}.\mathbf{y} - \mathbf{b} = \mathbf{0} \quad : \boldsymbol{\pi} \quad (2-72)$$

$$\mathbf{x}, \mathbf{y} \succeq 0 \quad (2-73)$$

where  $\mathbf{C}$ ,  $\mathbf{D}$  are matrices,  $\mathbf{x}$ ,  $\mathbf{y}$ ,  $\mathbf{b}$ , and  $\boldsymbol{\pi}$  are vectors. the Lagrangian function is constructed as follows:

$$\mathcal{L}_\rho(\mathbf{x}, \mathbf{y}, \boldsymbol{\pi}) = (f(\mathbf{x}) + g(\mathbf{y}) + \boldsymbol{\pi}^T . (\mathbf{C}.\mathbf{x} + \mathbf{D}.\mathbf{y} - \mathbf{b}) + \frac{\rho}{2} . \| \mathbf{C}.\mathbf{x} - \mathbf{D}.\mathbf{y} - \mathbf{b} \|_2^2); \quad (2-74)$$

where  $\rho > 0$  is a penalty parameter controlling the violation of feasibility of the relaxed linking constraints as well as the step size for the Lagrangian multiplier update problem. The choice of  $\rho$  is a research area, and its varying update per iteration  $\nu$  may improve the convergence of the decomposed problem [100, 104], though case-dependent. Under mild conditions, it is demonstrated that the ADMM converges for all values of  $\rho > 0$  [105] for convex problems. The ADMM iterates between the variable updates of the problem, corresponding to the elements of the vectors  $\mathbf{x}$  and  $\mathbf{y}$  using Gauss-Seidel, and the updates of the dual of the relaxed constraints given by the vector  $\boldsymbol{\pi}$  [23].

Primal-variable update is performed by:

$$\mathbf{x}^{\nu+1} = \operatorname{argmin}_{\mathbf{x}} \mathcal{L}_{\rho}(\mathbf{x}, \mathbf{y}^{\nu}, \boldsymbol{\pi}^{\nu}); \quad (2-75)$$

$$\mathbf{y}^{\nu+1} = \operatorname{argmin}_{\mathbf{y}} \mathcal{L}_{\rho}(\mathbf{x}^{\nu}, \mathbf{y}, \boldsymbol{\pi}^{\nu}); \quad (2-76)$$

Dual-variable update is performed by:

$$\boldsymbol{\pi}^{\nu+1} := \boldsymbol{\pi}^{\nu} + \rho \cdot (\mathbf{C} \cdot \mathbf{x}^{\nu+1} + \mathbf{D} \cdot \mathbf{y}^{\nu+1} - \mathbf{b}); \quad (2-77)$$

The consensus ADMM algorithm stops when the primal and dual residuals in each sub-problem is sufficiently small with an error tolerance level of  $\epsilon$ :

$$\| \mathbf{s}^{\nu+1} \|_2^2 = \| \rho \cdot (\mathbf{C} \cdot \mathbf{x}^{\nu+1} + \mathbf{D} \cdot \mathbf{y}^{\nu+1} - \mathbf{b}) \|_2^2 \leq \epsilon; \quad (2-78)$$

$$\| \mathbf{r}^{\nu+1} \|_2^2 = \| \boldsymbol{\pi}^{\nu+1} - \boldsymbol{\pi}^{\nu} \|_2^2 \leq \epsilon; \quad (2-79)$$

Note that  $\mathbf{x}$ - and  $\mathbf{y}$ -update above can be done in a decentralised way, since they are independent of each other. Dual variable,  $\boldsymbol{\pi}$ , -update, however, requires a centralised coordination. A central coordinator collects all shared variables from all sub-problems, the coordinator calculates the dual variables (multipliers) and sends them back to the sub-problems which needs to be updated. Furthermore, since letting in the algorithm  $x^{\nu}$  instead of  $x^{\nu+1}$ , makes parallel computing possible. The procedure is iteratively repeated until a convergence is found under a set tolerance level.

Noted, in general, is that if the objective function is convex and satisfying other properties as described in [100], the residual under the equality constraint, which is relaxed and augmented into the objective function, is guaranteed to converge to zero, and objective values of the iterates approach the

original problem's optimal value.

ADMM can also be used for non-convex problems. However, the convergence of the algorithm may not be guaranteed, though it is reported to behave well in some problems, though case-specific. Various works attempt to improve convergence of mixed-integer problems, e.g., by introducing tight bounds on the problem.

### 2.3.1.1 Consensus ADMM

In two- or multi-block optimisation problems in general the agents may have shared decision variables on the value of which they need to reach to a consensus albeit having own objectives. This problem can be formulated as [99]:

$$\min_{\mathbf{x}} \sum_{i \in \mathcal{I}} (f_i(\mathbf{x})) \quad (2-80)$$

subject to:

$$\mathbf{C} \cdot \mathbf{x} - \mathbf{b} = \mathbf{0} \quad (2-81)$$

$$\mathbf{x} \succeq 0 \quad (2-82)$$

where  $f_i : \mathbb{R}^n \rightarrow \mathbb{R}$  is a function representing the individual objectives of each agent  $i$ ,  $\mathbf{x} \in \mathbb{R}^n$  is the vector of shared decision variables between the agents. This problem can be reformulated as:

$$\min_{\mathbf{x}} \sum_{i \in \mathcal{I}} (f_i(\mathbf{x}_i)) \quad (2-83)$$

subject to:

$$\mathbf{C} \cdot \mathbf{x}_i - \mathbf{b} = \mathbf{0}, \quad (2-84)$$

$$\mathbf{x}_i = \mathbf{z} \quad : \quad \boldsymbol{\pi}_i \quad (2-85)$$

$$\mathbf{x}_i, \mathbf{z} \succeq 0 \quad (2-86)$$

where  $\mathbf{x}_i \in \mathbb{R}^n$  is the local decision copy held by agent  $i$  and  $\mathbf{z} \in \mathbb{R}^n$  is the global decision variable or consensus variable which ensures consistency of decision copies of individual agents. This consensus variable  $\mathbf{z}$  requires to be managed by a central coordinator. Accordingly, the Lagrangian function is constructed

as follows:

$$\mathcal{L}_\rho(\mathbf{x}_i, \mathbf{z}, \boldsymbol{\pi}_i) = \sum_{i \in \mathcal{I}} (f_i(\mathbf{x}_i) + \boldsymbol{\pi}_i^T \cdot (\mathbf{x}_i - \mathbf{z}) + \frac{\rho}{2} \cdot \|\mathbf{x}_i - \mathbf{z}\|_2^2); \quad (2-87)$$

By using the property that the  $z$  - *update* problem becomes an unconstrained optimisation problem, its analytic equivalent can be constructed. This would allow a simplified and convenient choice of  $\mathbf{z}^\nu$  at each iteration as  $\mathbf{z}^\nu = \bar{\mathbf{x}}^\nu$ , where  $\bar{\mathbf{x}}^\nu = \frac{1}{|\mathcal{I}|} \cdot \sum_i \mathbf{x}_i^\nu$ .

Accordingly, at each iteration  $\nu$ , primal variable update is performed by:

$$\mathbf{x}_i^{\nu+1} = \underset{\mathbf{x}_i}{\operatorname{argmin}} \left( f_i(\mathbf{x}_i) + \boldsymbol{\pi}_i^T \cdot \mathbf{x}_i + \frac{\rho}{2} \cdot \|\mathbf{x}_i - \bar{\mathbf{x}}^{\nu+1}\|_2^2 \right), \forall i; \quad (2-88)$$

Dual update is performed by:

$$\boldsymbol{\pi}_i^{\nu+1} := \boldsymbol{\pi}_i^\nu + \rho \cdot (\mathbf{x}_i^{\nu+1} - \bar{\mathbf{x}}^{\nu+1}), \forall i; \quad (2-89)$$

The consensus ADMM algorithm stops when the primal and dual residuals in each sub-problem  $i$  is sufficiently small with an error tolerance level of  $\epsilon$ :

$$\|\mathbf{s}^{\nu+1}\|_2^2 = \rho \cdot \|\mathbf{z}^{\nu+1} - \mathbf{z}^\nu\|_2^2 \leq \epsilon; \quad (2-90)$$

$$\|\mathbf{r}_i^{\nu+1}\|_2^2 = \|\boldsymbol{\pi}_i^{\nu+1} - \boldsymbol{\pi}_i^\nu\|_2^2 \leq \epsilon, \forall i; \quad (2-91)$$

## 2.4

### Stochastic optimisation

Lack of perfect information or unknown data is common in power system or any real-life problems. For instance, in day-ahead electricity scheduling the system operators will not perfectly know how much wind power would be generated the next day as it depends on wind speed. Since the decisions still need to be made throughout a decision horizon under the uncertainty of the realisation of the parameters, this triggers the application of stochastic optimisation. These uncertain parameters are modeled as a random variable. Random variables follow a stochastic process, which is defined as the process according to which the value of the random variable evolves. In a stochastic process, a set of dependent random variables are sequentially organised in time.

In stochastic optimisation inputs are represented by probability functions [106]. There are various ways how the decision-making can be formulated, e.g., by the expected values of the uncertain data represented by their probability

functions. Computationally, it is practical to represent stochastic processes through scenarios. Each scenario is a standalone occurrence of a stochastic process. Since input data is a collection of different sets of random variables, the objective function of the optimisation is also a random variable.

Stochastic optimisation increases the size, and hence, the computational aspects of the problem considerably. A large number of scenarios might be needed to sufficiently represent the plausible uncertainty of the random variables. This may lead to intractability of the problem.

Over the decision horizon, a number of stages is defined, representing a point in time the decisions are taken or where uncertainty is revealed. Therefore, information available to the decision-maker changes per stage. A stochastic optimisation can be two or multi-stage. In this thesis, a two-stage stochastic programming is considered.

### 2.4.1

#### Two-stage stochastic optimisation

Two-stage stochastic optimisation is defined as an optimisation problem where the decisions are taken in two stages. Define a stochastic process  $\lambda$  represented by a set of scenarios  $\lambda_s$ , and two decision variable vectors are given by  $\mathbf{x}$  and  $\mathbf{y}$ . Let  $\mathbf{x}$  be the variable for which the decision is first made. This is called the *first-stage* or *here-and-now* decisions [106, 107]. These decisions are taken before the revelation of the stochastic process  $\lambda(s)$ . The variable  $\mathbf{y}$  is decided after the decision  $\mathbf{x}$  is made and the stochastic process  $\lambda(s)$  represented by a set of scenarios  $s$  has materialised. Therefore, the vector  $\mathbf{y}$  are the *second-stage* or *wait-and-see* decisions, and they depend on the variable  $\mathbf{x}$  and scenario  $s$ . The vector  $\mathbf{y}$  can be represented as  $\mathbf{y}(\mathbf{x}, s)$ . This decision process can be described as a decision tree with a set of nodes and branches. Nodes stand for states of the problem where decisions are taken at any given time. The node where the first stage decision is made is called the root node, where the planning horizon starts. Second-stage nodes are connected to the root node via so-called branches, which show different realisations of random variables. The final nodes in the scenario tree are called leaves. In the case of second-stage stochastic programming, second-stage decisions are the leaves of the tree.

Two-stage stochastic programming can be written as a stochastic linear programming problem in the following form:

$$\min_{\mathbf{x}} z = \mathbf{c}^T \cdot \mathbf{x} + \mathbb{E}_{\lambda}[Q(\mathbf{x}, \tilde{\lambda})]; \quad (2-92)$$

subject to:

$$\mathbf{A} \cdot \mathbf{x} = \mathbf{b}; \quad (2-93)$$

$$\mathbf{x} \in \mathcal{X}; \quad (2-94)$$

where:

$$Q(\mathbf{x}, \lambda_s) = \min_{\mathbf{y}} \left\{ \mathbf{q}(s)^T \cdot \mathbf{y}(s) \right\}; \quad (2-95)$$

subject to:

$$\mathbf{T}(s) \cdot \mathbf{x} + \mathbf{W}(s) \cdot \mathbf{y}(s) = \mathbf{h}(s); \quad (2-96)$$

$$\left. \mathbf{y}(s) \in \mathcal{Y} \right\}, \forall s \in \mathcal{S}; \quad (2-97)$$

where  $\mathbf{x}$  and  $\mathbf{y}(s)$  are vectors representing the first- and second- stage decision vectors, whereas  $\mathbf{c}$ ,  $\mathbf{q}(s)$ ,  $\mathbf{b}$ ,  $\mathbf{h}(s)$ ,  $\mathbf{A}$ ,  $\mathbf{T}(s)$  and  $\mathbf{W}(s)$  are matrices and vectors of parameters of suitable size. The nested problem given by (2-95) – (2-97) is named as recourse problem.

Let  $\phi_s$  be probability assigned to each scenario within a scenario set  $\mathcal{S}$ . Two-stage stochastic programming can be re-written in the following more compact form, so-called deterministic equivalent problem:

$$\min_{\mathbf{x}, \mathbf{y}(s)} z = \mathbf{c}^T \cdot \mathbf{x} + \sum_{s \in \mathcal{S}} \phi_s \cdot \left( \mathbf{q}(s)^T \cdot \mathbf{y}(s) \right); \quad (2-98)$$

subject to:

$$\mathbf{A} \cdot \mathbf{x} = \mathbf{b}; \quad (2-99)$$

$$\mathbf{T}(s) \cdot \mathbf{x} + \mathbf{W}(s) \cdot \mathbf{y}(s) = \mathbf{h}(s), \forall s \in \mathcal{S}; \quad (2-100)$$

$$\mathbf{x} \in \mathcal{X}, \mathbf{y}(s) \in \mathcal{Y}, \forall s \in \mathcal{S}; \quad (2-101)$$

## 2.5

### Bi-linear optimisation

Bi-linear optimisation problems arise when two decision variables, whether integer or continuous, multiply each other. This makes the optimisation problem non-convex, and hence, off-the-shelf linear programming solvers cannot be readily used. Although some modern solvers, such as Gurobi, can handle such problems their efficiency remain to be further tested. Continuous and mixed integer bi-linear programming problems are encountered in various

applications in engineering, and this problem is moderately well-studied in the optimisation literature [108]. A solution approach which is extensively applied is by constructing polyhedral relaxations using envelopes of each bi-linear term within a branch-and-bound framework [109, 110].

Optimisation problems with bi-linear terms can be in the objective functions or constraints. This thesis focuses on problems where the bi-linear terms are in the constraints and they are continuous.

Two widely used methods, namely McCormick Envelopes and binary expansion are outlined next.

### 2.5.1

#### McCormick envelopes

A standard way of solving bi-linear optimisation problems is by replacing such terms by their concave and convex envelopes, so-called McCormick envelopes [111]. McCormick envelopes is a relaxation technique for bi-linear non-convex nonlinear problems. The principal assumption is the fact that convex and concave envelopes can be constructed for a non-convex function which is to be optimised. The concave envelope (and convex envelope respectively) is the concave over-estimator (convex under-estimator) for the non-convex function which constructs the tightest feasible space to the function. Non-unique concave over-estimators and convex under-estimators may exist. However, there exists a unique concave envelope and a convex envelope for the non-convex objective function in question, which is the main idea of the McCormick envelopes.

For bounded continuous variables,  $x$  and  $y$  respectively, and a bi-linear variable  $w$ , such that  $w = x.y$ , define a bi-linear set  $\mathcal{P}$  consisting of two over-estimators and two under-estimators for  $w$ . Formulation follows [108].

$$\mathcal{P} =: \{(x, y, w) \in \mathbb{R} \times \mathbb{R} \times \mathbb{R} : w = x.y, \underline{x} \leq x \leq \bar{x}, \underline{y} \leq y \leq \bar{y}\} \quad (2-102)$$

Applying McCormick envelopes provides the set  $\mathcal{M}$  as follows:

$$\begin{aligned} \mathcal{M} =: & \{(x, y, w) \in \mathbb{R} \times \mathbb{R} \times \mathbb{R} : w \geq 0, \\ & w \leq \bar{x}.y, w \leq \bar{y}.x, w \geq \bar{y}.x + \bar{x}.y - \bar{x}.\bar{y}, \\ & w \geq \underline{y}.x + \underline{x}.y - \underline{x}.\underline{y}, w \leq \underline{y}.x + \bar{x}.y - \bar{x}.\underline{y}, w \leq \bar{y}.x + \underline{x}.y - \underline{x}.\bar{y}, \} \end{aligned} \quad (2-103)$$

McCormick envelopes are computationally straightforward to implement.

McCormick technique-based relaxation tends to be stronger than various convexification and linearisation techniques [112]. These features brings about their wide-spread applicability for bi-linear optimisation problems.

For the general case, McCormick envelops are the best possible linear cuts within the  $(x, y, w)$  space. The quality of McCormick-based relaxation, however, depends on the distance of  $x$  and  $y$  from their bounds [113, 114]. Pre-processing of variables or branching-based techniques are applied in the literature for a reduced domain for  $x$  and  $y$  aimed to obtain a tighter relaxation. Various global optimisation solvers apply variable bounding to diminish the search space of the relaxed problem under McCormick. Piecewise McCormick relaxation is proposed [114], which splits one of the bi-linear variables' domain into a number of partitions while keeping the global bounds of the other variable. Interval arithmetic, reduced cost and optimisation-based approaches are applied for bound tightening purposes. A global optimisation based bound tightening algorithm is proposed by [115], unlike some earlier works, without introducing new integer variables.

Other than these, some approaches in the literature blend different methods, such as McCormick envelops and unary expansion, as in [34] in order to combine advantages of the methods.

## 2.5.2

### Binary expansion

Another way of linearisation of bi-linear terms is binary (or unary) expansion.

Binary expansion of the continuous variable  $y$  proceeds as follows. Let  $y \in [\underline{y}, \bar{y}]$ .

Define binary expansion step size as  $\Delta y = (\bar{y} - \underline{y})/M1$ , where  $M1$  is a large integer. For the binary expansion, let  $M1 = 2^{K1}$ , where  $K1 > 0$ . Unary expansion can be obtained by applying a logarithm base of 10 in the formulation.

Furthermore, let the set  $\mathcal{K} = \{0, 1, \dots, K1\}$  and  $y = \underline{y} + \Delta y \cdot \sum_{l \in \mathcal{K}} 2^l \cdot z_l^1$ , where  $z_l^1 \in \{0, 1\}$ . Define  $w_l^1 \in \mathbb{R}$  such that  $v_l^1 = z_l^1 \cdot x$ .  $v_l^1$  is used to model the product  $x \cdot z_l^1$ . The following set can be obtained:

$$\begin{aligned} \mathcal{B} =: & \{(x, y, w, z, v) \in \mathbb{R} \times \mathbb{R} \times \mathbb{R} \times \{0, 1\}^{K1+1} \times \mathbb{R}^{K1+1} : \\ & y = x \cdot \underline{y} + \Delta y \cdot \sum_{l \in \mathcal{K}} 2^l \cdot v_l^1\}; \end{aligned} \quad (2-104)$$

The precision of binary expansion depends on the step size for the binary

expended term chosen [116]. A small step size implies a higher precision whereas with a higher computational burden due to larger number of binaries increasing the searching space of the optimisation problem.

## 2.6

### Risk measures and control

In stochastic optimisation, an uncertain parameter is modelled as a stochastic process, and hence the objective function which typically minimises costs is a random variable based on an assumed probability distribution. Optimisation is performed over a function specifying the distribution of this random variable, which is commonly based on its expected value. The main cons of this representation is the fact that it ignores other features, such as the tail risks of the distribution [106]. Hence, there exists a probability that the tail risk occurs, leaving the decision-maker with potentially substantial amounts of costs which may not be captured by the expected value representation. The latter is named as 'risk-neutral decision-making'. Risk measures are applied in the literature in order to control risk, which is coined as 'risk-averse decision-making'. Common metrics of risk are i) variance; ii) shortfall probability; iii) expected shortfall; iv) value-at-risk (VaR); v) conditional value-at-risk (CVaR). Variance is an intuitive and well-known metric, proposed by [117], which measures dispersion of costs, and can be incorporated into a stochastic optimisation problem. It minimises the probability of deviation from an expected costs. Its main cons is the fact that it penalises the scenarios at the higher end of the cost spectrum as well as those lower than expected cost. Shortfall probability and expected shortfall are linear risk measures which define risk as the probability of occurrence of cost which is higher than a benchmark, or the expected value of cost lower than the benchmark, respectively [118]. The drawback of these methods is the fact that they require a definition of a target cost value. In addition, they are not so-called 'coherent risk measures' [119], which is a desirable property. For a coherent risk measure, as defined in [119], all of the followings should hold: i) translation invariance; ii) subadditivity; iii) positive homogeneity; and iv) monotonicity.

Value-at-risk and conditional-value-at-risk, on the other hand, define a probability,  $(1 - \varphi)$ , representing the part of the probability distribution for which the risk is to be controlled. The VaR is the value corresponding to the  $(1 - \varphi)$ -quantile of the probability distribution for the loss function. CVaR corresponds to the expected value at the tail, beyond the  $(1 - \varphi)$ -quantile.

Other than these, stochastic dominance constraints can be incorporated into the stochastic optimisation formulation in order to control risk. The latter

approach is based on searching for 'acceptable' elements within a distribution of the cost function optimised, rather than a 'best' element. This approach facilitates the comparison between two random variables in terms of their acceptability, which one is better compared to a given benchmark 'acceptable' to the decision-taker. First- and second-order stochastic dominance constraints can be incorporated into the decision-making problem. First-order stochastic dominance constraints are applied by using a set of auxiliary binary variables. Second-order formulations are based on continuous variables. A principal shortcoming of stochastic dominance-based approaches is that it can be hard to specify a benchmark profile which leads to a feasible solution and its considerably higher computational burden.

Amongst all these risk measures CVaR is the most commonly applied one in optimisation problems because it is a coherent risk measure, and can be represented by a linear and continuous formulation, advantageous for optimisation and computational purposes [106].

### 2.6.1

#### Conditional value-at-risk

Given its convenient technical and computational features, in this thesis the quantile-based risk functional, Conditional Value-at-Risk (CVaR) [120], is applied to capture the risk aversion in the certainty equivalent optimisation problem. For a given percentile  $\varphi \in (0, 1)$  and probability over scenario  $s \in S$   $\phi_s$ ,  $CVaR(\varphi, f(\mathbf{x}, \tilde{\lambda}))$  - where  $f$  is a continuous function given vector  $\mathbf{x}$  and random vector  $\tilde{\lambda}$  - is computed as the expected loss in the  $(1 - \varphi)$  worst scenarios. The CVaR of a discrete distribution is defined as follows, where  $\mathbb{E}$  is an expected value function:

$$CVaR(\varphi, f(\mathbf{x}, \tilde{\lambda})) = \min \left\{ \beta + \frac{1}{1 - \varphi} \cdot \mathbb{E}_{\tilde{\lambda}}[(\min(\beta - f(\mathbf{x}, \tilde{\lambda}), 0)] \right\}; \quad (2-105)$$

$CVaR(\varphi, f(\mathbf{x}, \tilde{\lambda}))$  can be included into the stochastic risk-averse problem as follows [106]:

$$\begin{aligned} \min_{\underline{\mathbf{x}}} \quad & (1 - \Lambda) \cdot \left( \mathbf{c}^T \cdot \mathbf{x} + \sum_{s \in \mathcal{S}} \phi_s \cdot \mathbf{q}(s)^T \cdot \mathbf{y}(s) \right) + \\ & + \Lambda \cdot \left[ \beta + \frac{1}{1 - \varphi} \sum_{s \in \mathcal{S}} \phi_s \cdot \gamma_s^{CVaR} \right]; \end{aligned} \quad (2-106)$$

subject to:

$$\mathbf{A} \cdot \mathbf{x} = \mathbf{b}; \quad (2-107)$$

$$\mathbf{T}(s) \cdot \mathbf{x} + \mathbf{W}(s) \cdot \mathbf{y}(s) = \mathbf{h}(s), \forall s \in \mathcal{S}; \quad (2-108)$$

$$-\beta + \left( \mathbf{c}^T \cdot \mathbf{x} + \mathbf{q}(s)^T \cdot \mathbf{y}(s) \right) \leq \gamma_s^{CVaR}(s), \forall s \in \mathcal{S}; \quad (2-109)$$

$$\gamma_s^{CVaR}(s) \geq 0, \forall s \in \mathcal{S}; \quad (2-110)$$

$$\mathbf{x} \in \mathcal{X}, \mathbf{y}(s) \in \mathcal{Y}, \forall s \in \mathcal{S}; \quad (2-111)$$

where  $\beta$  is an auxiliary variable and  $\gamma_s^{CVaR}(s)$  is a continuous non-negative variable.

### 3

## Computational Techniques and Model Accuracy in Unit Commitment and AC Optimal Power Flow

This Chapter reuses the publication [Paper A] Martin, N. C., & Fanzeres, B. (2023, June). Linearisation Based Decomposition Method for Circle Approximation in AC Network Constrained Unit Commitment. In 2023 IEEE Belgrade PowerTech (pp. 1-6). IEEE, which is herewith referenced and cited as [20].

This contribution is principally motivated from the findings from the literature presented in Chapter 2 with regard to the need for computationally robust techniques for optimal power flow computation with enhanced model accuracy to represent physical laws describing these flows. This Chapter proposes a sequential-linearisation-based approximation method to convexify the non-convex power flow equations, and present its performance against a second-order-cone-programming convex relaxation as a benchmark. Convexification results in solution of the models in polynomial time and a provision of a lower bound for the optimisation problem [60].

### 3.1

#### Background for Mathematical Formulations

In this Chapter, a bus injection type, and voltage-based formulation of AC OPF is constructed when applicable. Voltage magnitudes at each bus  $n \in \mathcal{N}$ , are given by  $V_n$ , and are represented by a polar form, such that  $e^{i\theta_n} = \text{Cost}(\theta_n) + i \cdot \text{Sin}(\theta_n)$ , where  $\theta_n$  is the phase angle of the respective bus measured in radians,  $\theta_n \in (-\pi, \pi]$ ,  $\forall n \in \mathcal{N}$ . The notation is simplified such that instead of  $|V_n|$ , the notation  $V_n$  is used to represent voltage per bus.  $|V_n|$  is the modulus of the complex voltage  $V_n = |V_n| \cdot e^{i\theta_n}$ . Though not explicitly stated during the Chapter, admittance matrix formulation is on the basis of rectangular coordinates, such that  $\mathbf{Y}_{n,m} = \mathbf{G}_{n,m} + i \cdot \mathbf{B}_{n,m}$ . Balanced, single-phase equivalent model as well as steady-state conditions are assumed throughout.

### 3.2

#### Introduction

Unit Commitment (UC) models are widely used nowadays by utilities and system operators for minimum cost scheduling of energy and reserves [121]. This scheduling takes place under the assumption that the operation of

the power system is with a degree of precision. Various approximations to the system state are applied in practice, among others, a linear representation of the network via DC power flow. As these approximations are inexact, the state of the system in real-time may differ from the estimated state. Furthermore, DC power flow ignores reactive power scheduling, voltage management and other AC power flow-related constraints. The latter is increasingly important in view of the necessity to accommodate a larger share of weather-dependent generation and increased demand driven by electrification [14]. Additionally, a deviation between the predicted and the actual state of the system implies potentially costly corrective and *ad hoc* interventions by system operators [121]. Alignment of scheduling models with real operations is considered a key issue in today's principal power markets, such as the PJM [122].

The main challenges for solving AC network-constrained UC problems (AC-NCUC) are problem size and non-convexity [121, 14]. In fact, AC-NCUC problems are combinatorial optimisation problems whose computational complexity increases exponentially with the network size [123]. These problems entail mixed-integer variables representing on/off status of the generators, and power flow equations. As such, they are non-convex and non-linear, and, are classified as NP-hard [124]. Semi-definite programming [125] and second-order cone programming (SOCP) based relaxations [126, 127] are often applied. However, modern solvers cannot handle large-scale mixed-integer SOCP problems efficiently [14, 128]. Furthermore, SOCP results can be less precise with high system-loading conditions [129], characterised by voltage fluctuations and congestion of thermal limits. This occurs with an increased likelihood in power systems with a high level of renewable penetration [130].

In order to address the computational challenges, various algorithms are used in the literature, an outline of which can be found in [131]. Recent works [123] and [14] apply a Benders' type decomposition to the AC-NCUC problem. [123] solves a mixed-integer linear master problem, to which linear constraints for feasibility are included. These constraints can potentially cut integer solutions, which is a shortcoming of the approach. A semi-definite programming relaxation to the rectangular formulation of AC power flow is applied in the sub-problems. The algorithm in [14] requires a large information transfer between the two problems, causing in some instances a relatively high computational burden.

In view of the aforementioned considerations, the objective of this paper is to propose a linearisation for the circle approximation in AC-NCUC, which is an extension to the approach in [132] based on [133]. The resulting problem is a mixed-integer linear programming (MILP), for which the solution

methods used by state-of-the-art solvers are more mature compared to SOCP relaxations [128]. Such a linearisation is performed in earlier works on the basis of a discretisation, which is *a priori* and decision-dependent. To more efficiently solve the resulting large-scale MILP, as well as remove the *a priori* aspect of discretisation, an algorithm based on an outer approximation is designed. This algorithm selects the optimal lines from a continuous set at each iteration. Different than [14], the proposed decomposition needs solely an exchange of variables describing optimal cuts between the master and the sub-problems. Accordingly, the contributions of this paper can be summarised as follows:

1. To extend the linearisation approach in [133] into a quadratic relaxation of AC-NCUC problems. Such problems are usually solved by applying methods, such as SOCP. SOCP is less mature [134], computationally expensive in large scale, and may be less precise when loading conditions are on the high side. This motivates the linearisation.
2. To devise an efficient solution mechanism for the proposed linearisation on the basis of a circle approximation, which is an outer approximation type. This mechanism is capable of selecting optimal cuts from a continuous solution space, leading to convergence in a few iterations and enhancing standard SOCP results.

### 3.3

#### Mathematical Formulation

### 3.3.1 AC Non-Convex Unit Commitment Formulation

$$\min_{\Xi} \left( \sum_{t \in \mathcal{T}} \left( \sum_{i \in \mathcal{J}} \left( C_i \cdot g_{i,t} + C_{i,t}^{SU} + C_{i,t}^{SD} \right) + \sum_{d \in \mathcal{D}} \left( C_d^{\text{qshed}} \cdot g_{d,t}^{d,\text{shed}} \right) + \sum_{d \in \mathcal{D}} \left( C_d^{\text{shed}} \cdot q_{d,t}^{d,\text{shed}} \right) \right) \right); \quad (3-1)$$

subject to:

$$u_{i,t} \cdot \underline{G}_i \leq g_{i,t} \leq u_{i,t} \cdot \overline{G}_i, \quad \forall i \in \mathcal{J}, t \in \mathcal{T}; \quad (3-2)$$

$$0 \leq g_{k,t}^w \leq \overline{G}_k^w, \quad \forall t \in \mathcal{T}, k \in \mathcal{WP}; \quad (3-3)$$

$$u_{i,t} \cdot \underline{Q}_i \leq q_{i,t} \leq u_{i,t} \cdot \overline{Q}_i, \quad \forall i \in \mathcal{J}, t \in \mathcal{T}; \quad (3-4)$$

$$0 \leq q_{k,t}^w \leq \overline{Q}_k^w, \quad \forall t \in \mathcal{T}, k \in \mathcal{WP}; \quad (3-5)$$

$$\sum_{i \in \mathcal{J}_n} g_{i,t} - \sum_{d \in \mathcal{D}_n} g_{d,t} + \sum_{k \in \mathcal{J}_n} g_{k,t}^w + \sum_{d \in \mathcal{D}_n} g_{d,t}^{l,\text{shed}} - \sum_{m \in \mathcal{N}_n} p_{n,m,t} = 0, \quad \forall n \in \mathcal{N}, t \in \mathcal{T}; \quad (3-6)$$

$$p_{n,m,t} = G_{n,m} \cdot V_{n,t}^2 + V_{n,t} \cdot V_{m,t} \cdot (-G_{n,m} \cdot \text{Cos}\theta_{n,m,t} + B_{n,m} \cdot \text{Sin}\theta_{n,m,t}), \quad \forall m \in \mathcal{N}_n, n \in \mathcal{N}, t \in \mathcal{T}; \quad (3-7)$$

$$C_{i,t}^{SU} \geq (u_{i,t} - u_{i,0}) \cdot K_i^{SU}, \quad \forall i \in \mathcal{J}, t = 1; \quad (3-8)$$

$$C_{i,t}^{SD} \geq (u_{i,0} - u_{i,t}) \cdot K_i^{SD}, \quad \forall i \in \mathcal{J}, t = 1; \quad (3-9)$$

$$C_{i,t}^{SU} \geq (u_{i,t} - u_{i,t-1}) \cdot K_i^{SU}, \quad \forall i \in \mathcal{J}, t \in \mathcal{T} \setminus \{1\}; \quad (3-10)$$

$$C_{i,t}^{SD} \geq (u_{i,t-1} - u_{i,t}) \cdot K_i^{SD}, \quad \forall i \in \mathcal{J}, t \in \mathcal{T} \setminus \{1\}; \quad (3-11)$$

$$0 \leq g_{d,t}^{l,\text{shed}} \leq g_{d,t}, \quad \forall d \in \mathcal{D}, t \in \mathcal{T}; \quad (3-12)$$

$$0 \leq q_{d,t}^{l,\text{shed}} \leq q_{d,t}, \quad \forall d \in \mathcal{D}, t \in \mathcal{T}; \quad (3-13)$$

$$\sum_{i \in \mathcal{J}_n} q_{i,t} - \sum_{d \in \mathcal{D}_n} q_{d,t} + \sum_{k \in \mathcal{J}_n} q_{k,t}^{w,DA} + \sum_{d \in \mathcal{D}_n} q_{d,t}^{l,\text{shed}} - \sum_{m \in \mathcal{N}_n} q_{n,m,t} = 0, \quad \forall n \in \mathcal{N}, t \in \mathcal{T}; \quad (3-14)$$

$$q_{n,m,t} = (B_{n,m} - b_{n,m}^{\text{shunt}}) \cdot V_{n,t}^2 - V_{n,t} \cdot V_{m,t} \cdot (G_{n,m} \cdot \text{Sin}\theta_{n,m,t} + B_{n,m} \cdot \text{Cos}\theta_{n,m,t}), \quad \forall m \in \mathcal{N}_n, n \in \mathcal{N}, t \in \mathcal{T}; \quad (3-15)$$

$$p_{n,m,t}^2 + q_{n,m,t}^2 \leq \overline{S}_{n,m}^2, \quad \forall m \in \mathcal{N}_n, n \in \mathcal{N}, t \in \mathcal{T}; \quad (3-16)$$

$$\underline{V}_n^2 \leq V_{n,t}^2 \leq \overline{V}_n^2, \quad \forall n \in \mathcal{N}, t \in \mathcal{T}; \quad (3-17)$$

with  $\Xi = \{g_{i,t}, g_{k,t}^w, q_{i,t}, q_{k,t}^w, g_{d,t}^{l,shed}, p_{n,m,t}, u_{i,t} \in \{0, 1\}, C_{i,t}^{SU}, C_{i,t}^{SD}, q_{d,t}^{l,shed}, q_{n,m,t}, V_{n,t}, \theta_{n,m,t}\}$  is the set of primal decision variables. The formulation is not a contribution of this work. For more details refer to [14, 127]. The objective of the optimisation is depicted by (3-1), minimising total cost for a system operator for supplying energy, start-up/shut-down costs for generation, and, active/reactive power load-shedding costs. The constraints (3-2) and (3-3) refer to the minimum and maximum capacity for conventional and weather-dependent generators. Having multiplied by binary variables,  $u \in \{0, 1\}$ , implies that respective units are scheduled to start-up or shut-down when active. Constraints (3-4) and (3-5) relate to reactive power limits for conventional and weather-dependent generators. Constraint (3-6) is the active power balance equation. Equation (3-7) defines the active power flow with  $\theta_{n,m}$ , defined by:

$$\theta_{n,m} = \theta_n - \theta_m, \quad \forall m \in \mathcal{N}_n, n \in \mathcal{N}. \quad (3-18)$$

Equations (3-8), (3-9) activate start-up/shut-down costs when units are on/off, respectively for the initial hour, (3-10), (3-11) for the remaining hours. (3-12) and (3-13) depict the load-shed limits bounded by active/reactive power demand, respectively. Constraint (3-14) describes the reactive power balance. Equation (3-15) defines the reactive power flow. Equation (3-16) gives the apparent power limits for lines. Equation (3-17) provides the voltage limits for the nodes.

### 3.3.2 Second-Order Cone Reformulation

Constraints (3-7) and (3-15) are non-convex due to the trigonometric aspect of AC power flow given by cosine and sine functions. A reformulation of power flow [129] is obtained by defining new variables  $c_{n,m}$  and  $s_{n,m}$  as follows:

$$c_{n,n,t} = V_{n,t}^2, \quad \forall n \in \mathcal{N}, t \in \mathcal{T}; \quad (3-19)$$

$$c_{n,m,t} = V_{m,t} \cdot V_{n,t} \cdot \text{Cos}\theta_{n,m,t}, \\ \forall m \in \mathcal{N}_n, n \in \mathcal{N}, t \in \mathcal{T}; \quad (3-20)$$

$$s_{n,m,t} = V_{m,t} \cdot V_{n,t} \cdot \text{Sin}\theta_{n,m,t}, \\ \forall m \in \mathcal{N}_n, n \in \mathcal{N}, t \in \mathcal{T}; \quad (3-21)$$

Inserting these into the active and reactive power flow equations (3-7)

and (3-15), (3-22) and (3-23) are obtained:

$$p_{n,m,t} = G_{n,m} \cdot c_{n,n,t} - G_{n,m} \cdot c_{n,m,t} + B_{n,m} \cdot s_{n,m,t}, \quad \forall m \in \mathcal{N}_n, n \in \mathcal{N}, t \in \mathcal{T}; \quad (3-22)$$

$$q_{n,m,t} = (B_{n,m} - b_{n,m}^{\text{shunt}}) \cdot c_{n,n,t} - G_{n,m} \cdot s_{n,m,t} + B_{n,m} \cdot c_{n,m,t}, \quad \forall m \in \mathcal{N}_n, n \in \mathcal{N}, t \in \mathcal{T}; \quad (3-23)$$

By using the Pythagorean identity and the symmetric properties for sine and cosine functions [129], (3-24)–(3-26) are obtained [14]:

$$c_{n,m,t} = c_{m,n,t}, \quad \forall m \in \mathcal{N}_n, n \in \mathcal{N}, t \in \mathcal{T}; \quad (3-24)$$

$$s_{n,m,t} = -s_{m,n,t}, \quad \forall m \in \mathcal{N}_n, n \in \mathcal{N}, t \in \mathcal{T}; \quad (3-25)$$

$$c_{n,m,t}^2 + s_{n,m,t}^2 = c_{n,n,t} \cdot c_{m,m,t}, \quad \forall m \in \mathcal{N}_n, n \in \mathcal{N}, t \in \mathcal{T}; \quad (3-26)$$

The equality constraint (3-26) represents a non-convex region. Its second-order conic relaxation is given by the inequality constraint (3-27):

$$c_{n,m,t}^2 + s_{n,m,t}^2 \leq c_{n,n,t} \cdot c_{m,m,t}, \quad \forall m \in \mathcal{N}_n, n \in \mathcal{N}, t \in \mathcal{T}; \quad (3-27)$$

### 3.4

#### Solution Methodology

The model given by (3-1)–(3-6), (3-8)–(3-14), (3-16)–(3-17), (3-1), (3-6)–(3-7) and (3-11) is a mixed-integer SOCP relaxation for the non-convex AC-NCUC problem. The latter may not be efficiently solved with modern commercial solvers even when the instance size is medium to large [14]. Additionally, SOCP can become inexact under high demand, tight reactive power-generation limits, etc. [129, 135]. To address this, firstly, we linearise the quadratic relaxation for the conic (3-27) and quadratic (3-16) constraints. Next, we provide a circle (outer) approximation algorithm which makes a selection of optimal cuts at each iteration.

#### 3.4.1

##### Quadratic relaxation of SOCP-NCUC

The quadratic relaxation of SOCP AC-NCUC is given by inserting the valid bounds for  $c_{n,m,t}$  and  $s_{n,m,t}$  into (3-27) leading to (3-33). The resulting problem given by (3-28)–(3-34) is a mixed-integer quadratic problem, which is

hard to solve efficiently by commercial solvers [136]:

$$\min_{\underline{\Xi}} \text{Equation (3-1);} \quad (3-28)$$

subject to:

$$\text{Constraints: (3-2) – (3-6) and (3-8) – (3-14);} \quad (3-29)$$

$$\underline{V}_n^2 \leq c_{n,n,t} \leq \overline{V}_n^2, \quad \forall n \in \mathcal{N}, t \in \mathcal{T}; \quad (3-30)$$

$$c_{n,m,t} = c_{m,n,t}, \quad \forall m \in \mathcal{N}_n, n \in \mathcal{N}, t \in \mathcal{T}; \quad (3-31)$$

$$s_{n,m,t} = -s_{m,n,t}, \quad \forall m \in \mathcal{N}_n, n \in \mathcal{N}, t \in \mathcal{T}; \quad (3-32)$$

$$0 \leq c_{n,m,t}^2 + s_{n,m,t}^2 \leq \overline{V}_n^2 \cdot \overline{V}_m^2, \quad \forall m \in \mathcal{N}_n, n \in \mathcal{N}, t \in \mathcal{T}; \quad (3-33)$$

$$0 \leq p_{n,m,t}^2 + q_{n,m,t}^2 \leq \overline{S}_{n,m}^2, \quad \forall m \in \mathcal{N}_n, n \in \mathcal{N}, t \in \mathcal{T}; \quad (3-34)$$

### 3.4.2 Circle (outer) approximation

We apply the linearisation approach given in [133] to the quadratic constraints (3-33) and (3-34). To this end, let Set  $\mathcal{A}$  be a discretisation of a continuous range of  $(-\overline{S}_{n,m}, \overline{S}_{n,m})$ . Similarly, let Set  $\mathcal{A}'$  be a discretisation of a continuous range of  $(-\overline{V}_n \cdot \overline{V}_m, \overline{V}_n \cdot \overline{V}_m)$ . Then (3-35)–(3-36) linearly approximates (3-33) and (3-34).

$$-\frac{-\alpha_{n,m,t} \cdot p_{n,m,t} + \overline{S}_{n,m}^2}{\sqrt{\overline{S}_{n,m}^2 - \alpha_{n,m,t}^2}} \leq q_{n,m,t} \leq \frac{-\alpha_{n,m,t} \cdot p_{n,m,t} + \overline{S}_{n,m}^2}{\sqrt{\overline{S}_{n,m}^2 - \alpha_{n,m,t}^2}}, \quad \forall m \in \mathcal{N}_n, n \in \mathcal{N}, t \in \mathcal{T}, \alpha \in \mathcal{A}; \quad (3-35)$$

$$-\frac{-\alpha'_{n,m,t} \cdot c_{n,m,t} + \overline{V}_n^2 \cdot \overline{V}_m^2}{\sqrt{\overline{V}_n^2 \cdot \overline{V}_m^2 - \alpha'_{n,m,t}{}^2}} \leq s_{n,m,t} \leq \frac{-\alpha'_{n,m,t} \cdot c_{n,m,t} + \overline{V}_n^2 \cdot \overline{V}_m^2}{\sqrt{\overline{V}_n^2 \cdot \overline{V}_m^2 - \alpha'_{n,m,t}{}^2}}, \quad \forall m \in \mathcal{N}_n, n \in \mathcal{N}, t \in \mathcal{T}, \alpha' \in \mathcal{A}'; \quad (3-36)$$

The outlined linearisation, described by (3-35)–(3-36) is based on the

following concept. Let  $q_{n,m,t}$  be approximated by  $\alpha$  enumerated with its values within the Set  $\mathcal{A}$ . Any  $p$  tangent to the circle would satisfy (3-37):

$$p^2 + q^2 = \bar{S}^2, \quad (3-37)$$

This implies that the slope of the lines tangent to the circle is given by (3-38):

$$m = \frac{q}{p} = \pm \frac{\alpha}{\sqrt{\bar{S}^2 - \alpha^2}}, \quad (3-38)$$

The general equation of the tangents to a circle, e.g., formed by (3-37), is given by:

$$q = m.p \pm \bar{S} \cdot \sqrt{1 + m^2}, \quad (3-39)$$

By inserting the equation for slope  $m$  (3-38) into (3-39) we obtain the general equation, (3-40), describing the tangents to the circle, (3-37):

$$q = \pm \frac{\alpha}{\sqrt{\bar{S}^2 - \alpha^2}} \cdot p \pm \bar{S} \cdot \sqrt{1 + \frac{\alpha^2}{\bar{S}^2 - \alpha^2}}, \quad (3-40)$$

Similarly, the equation describing the tangent to the circle prescribing the feasible region for  $s_{n,m,t}$  and  $c_{n,m,t}$  can be drawn. The latter along with (3-40) with inequalities imposed, would result in (3-35) and (3-36). Consequently, (3-28)–(3-32) and (3-35)–(3-36) provide a circle outer linear approximation to the non-convex AC-NCUC problem. This is a MILP, which may require a large number of discrete values for  $\alpha$  and  $\alpha'$  enumerating its feasible values, which may not be efficiently solved. In addition, some of the lines may be redundant.

### 3.4.3

#### Algorithm

In order to address the efficiency aspects of the circle outer linear approximation approach illustrated in the previous section, we propose Algorithm 1, based on a master problem and sub-problems. The algorithm intrinsically selects the optimal cuts at each iteration. Therefore, after the *Initialisation* step, optimal lines are selected through the algorithm from a continuous set for feasible values of linearisation-related variables  $\alpha$  and  $\alpha'$ .

The cut procedure is outlined in Fig. 3.2. First, given optimal solutions  $(p_0, q_0)$  obtained from the master problem, a projection onto the circle describing the feasible region  $p^2 + q^2 \leq \bar{S}^2$  is taken. Let  $(p'_0, q_0)$  be this projection. A tangent (cut) to the circle passing through this point is drawn (*Tangent 1*). This cut is added to the master problem as a constraint at the following iteration. At the second iteration,  $(p_1, q_1)$  optimal solutions are drawn from the master problem. Similarly, its projection onto the circle is calculated,  $(p'_1, q_1)$ . A tangent to the circle going through this point is included as a constraint to

the master problem for the next iteration (*Tangent 2*). This process is repeated until the optimal point is sufficiently close to the circle under a tolerance level.

In the *Initialisation* step, the algorithm initialises the iteration counter,  $\nu$ , and, the initial set value for discretisation-related variables  $\alpha$  and  $\alpha'$ . A master problem is constructed by (3-41)–(3-47), which includes linearisation for circle approximation of SOCP constraints. Therefore, it becomes a MILP problem.

*Master problem solution:*

$$\min_{\underline{\Xi}} \text{Equation (3-1);} \quad (3-41)$$

subject to:

$$\text{Constraints: (3-2) – (3-6) and (3-8) – (3-14);} \quad (3-42)$$

$$\underline{V}_n^2 \leq c_{n,n,t} \leq \overline{V}_n^2, \quad \forall n \in \mathcal{N}, t \in \mathcal{T}; \quad (3-43)$$

$$c_{n,m,t} = c_{m,n,t}, \quad \forall m \in \mathcal{N}_n, n \in \mathcal{N}, t \in \mathcal{T}; \quad (3-44)$$

$$s_{n,m,t} = -s_{m,n,t}, \quad \forall m \in \mathcal{N}_n, n \in \mathcal{N}, t \in \mathcal{T}; \quad (3-45)$$

$$\begin{aligned} & -\frac{-\alpha_{n,m,t}^{(\mu)} \cdot p_{n,m,t} + \overline{S}_{n,m}^2}{\sqrt{\overline{S}_{n,m}^2 - \alpha_{n,m,t}^{(\mu)2}}} \leq q_{n,m,t} \leq \\ & \frac{-\alpha_{n,m,t}^{(\mu)} \cdot p_{n,m,t} + \overline{S}_{n,m}^2}{\sqrt{\overline{S}_{n,m}^2 - (\alpha_{n,m,t}^{(\mu)})^2}}, \\ & \forall m \in \mathcal{N}_n, n \in \mathcal{N}, t \in \mathcal{T}, \mu = 0, \dots, \nu; \end{aligned} \quad (3-46)$$

$$\begin{aligned} & -\frac{-\alpha'_{n,m,t}^{(\mu)} \cdot c_{n,m,t} + \overline{V}_n^2 \cdot \overline{V}_m^2}{\sqrt{\overline{V}_n^2 \cdot \overline{V}_m^2 - \alpha'_{n,m,t}^{(\mu)2}}} \leq s_{n,m,t} \leq \\ & \frac{-\alpha'_{n,m,t}^{(\mu)} \cdot c_{n,m,t} + \overline{V}_n^2 \cdot \overline{V}_m^2}{\sqrt{\overline{V}_n^2 \cdot \overline{V}_m^2 - \alpha'_{n,m,t}^{(\mu)2}}}, \\ & \forall m \in \mathcal{N}_n, n \in \mathcal{N}, t \in \mathcal{T}, \mu = 0, \dots, \nu; \end{aligned} \quad (3-47)$$

In **Step 1**, sub-problems are solved solely for the purpose of computing the projection of  $(p, q)$  and  $(c, s)$  onto their respective circular feasible regions given (3-33) and (3-34), respectively. Based on these projections, update of  $\alpha^{(\nu)}, \alpha'^{(\nu)}$  is performed for iteration  $\nu$ . More precisely  $\forall m \in \mathcal{N}_n, n \in \mathcal{N}, t \in \mathcal{T}$ , compute projection of  $(p_{n,m,t}, q_{n,m,t})$  onto its respective circle given by  $(p'_{n,m,t}, q_{n,m,t})$ :

$$\begin{aligned} (p'_{n,m,t})^{(\nu)} &= \overline{S}_{n,m}^2 - (q_{n,m,t})^{(\nu-1)}, \\ &\forall m \in \mathcal{N}_n, n \in \mathcal{N}, t \in \mathcal{T}; \end{aligned} \quad (3-48)$$

Similarly, compute projection of  $(c_{n,m,t}, s_{n,m,t})$ , defined by  $(c'_{n,m,t}, s'_{n,m,t})^{(\nu)}$  onto

its respective circle:

$$(c_{n,m,t}^{p^2})^{(\nu)} = \bar{V}_n^2 \cdot \bar{V}_m^2 - (s_{n,m,t}^2)^{(\nu-1)},$$

$$\forall m \in \mathcal{N}_n, n \in \mathcal{N}, t \in \mathcal{T}; \quad (3-49)$$

It is straightforward to show that the respective linearisation variables are to be chosen as:

$$\alpha_{n,m,t}^{(\nu)} \leftarrow p_{n,m,t}^{(\nu-1)}, \forall m \in \mathcal{N}_n, n \in \mathcal{N}, t \in \mathcal{T}; \quad (3-50)$$

$$\alpha_{n,m,t}^{s^{(\nu)}} \leftarrow c_{n,m,t}^{s^{(\nu-1)}}, \forall m \in \mathcal{N}_n, n \in \mathcal{N}, t \in \mathcal{T}; \quad (3-51)$$

In **Step 2** a convergence check is done based on a gap analysis, which is calculated as the distance to the circle described by the constraint (3-34).

When the *Gap* given by (3-52) is less than or equal to the tolerance level  $\epsilon$ , the algorithm stops. Otherwise, in **Step 3**, it updates the master by adding new cuts, (3-46) and (3-47). The algorithm goes on with **Step 1**.

$$\text{Gap} = (c_{n,m,t}^2)^{(\nu-1)} + (s_{n,m,t}^2)^{(\nu-1)} - \bar{V}_n^2 \cdot \bar{V}_m^2,$$

$$\forall m \in \mathcal{N}_n, n \in \mathcal{N}, t \in \mathcal{T}; \quad (3-52)$$

---

**Algorithm 1** Decomposition Algorithm for Linearisation of Circle Approximation of SOCP

---

*Initialisation:*

Set  $\mu \leftarrow 0$ ; Set  $\nu \leftarrow 0$ ;  
 Set  $\alpha_{n,m,t}^\nu \leftarrow \alpha_{n,m,t}^{\text{ini}}, \forall m \in \mathcal{N}_n, n \in \mathcal{N}, t \in \mathcal{T}$ ;  
 Set  $\alpha_{n,m,t}^{\nu'} \leftarrow \alpha_{n,m,t}^{\text{ini}'}, \forall m \in \mathcal{N}_n, n \in \mathcal{N}, t \in \mathcal{T}$ ;  
 Solve **master problem** given by (3-41)–(3-47), store its optimal solution  $(p_{n,m,t}^\nu, q_{n,m,t}^\nu, c_{n,m,t}^\nu, s_{n,m,t}^\nu)$ , and, objective function value  $\text{TotalCost}^{(\nu)}$ ;

*Iteration  $\nu \geq 1$*

**Step 1:** Run **sub-problems**.  $\forall m \in \mathcal{N}_n, n \in \mathcal{N}, t \in \mathcal{T}$ , compute projection of  $(p, q)$  on its respective circular region:  $((p')^{(\nu-1)}, q^{(\nu-1)})$ , where  $(p')^{(\nu-1)} = \bar{S}^2 - (q^2)^{(\nu-1)}$ . Similarly compute projection of  $(c, s)$  on its respective circle:  $(c')^{(\nu-1)}, s^{(\nu-1)}$  where  $(c')^{(\nu-1)} = \bar{V}_n^2 \cdot \bar{V}_m^2 - (s^2)^{(\nu-1)}$ . Set  $\alpha^{(\nu)} \leftarrow (p')^{(\nu-1)}$ . Set  $(\alpha')^{(\nu)} \leftarrow (c')^{(\nu-1)}$ . Store  $\alpha^{(\nu)}, \alpha'^{(\nu)}$ ;

**Step 2:** If  $\text{Gap} \leq \epsilon$ , then stop. Otherwise, go to **Step 3**;

**Step 3:**  $\forall \mu = 1, \dots, \nu$ , solve master problem consisting of (3-41)–(3-47). Store its optimal solution  $(p_{n,m,t}^{(\mu)}, q_{n,m,t}^{(\mu)}, c_{n,m,t}^{(\mu)}, s_{n,m,t}^{(\mu)})$ , and,

objective function value,  $\text{TotalCost}^{(\nu)}$ . Set  $\nu \leftarrow \nu + 1$ . Go to **Step 1**.

---

### 3.5 Numerical Experiments

In this section, we demonstrate the effectiveness of the proposed methodology in two case studies. All numerical experiments are performed on an Intel (R) Core (TM) i7-8550U CPU, 1.99 GHz with 8 GB of RAM machine under JuMP and CPLEX 22.1.0. The tolerance level for the stopping criteria is set to  $10^{-6}$  for all loading levels. Both case studies are run for a 6-hour period. The demand curve is constructed by applying a multiplier, namely the vector  $[1.034, 1.023, 0.986, 0.953, 0.943, 0.937]$ , to the base demand level. Two cases are tested under three system-loading conditions - low, medium and high.

#### 3.5.1 5-Bus System: Case Study 1

This case study is adapted from [32]. The illustrative system is made up of 5 buses, 6 transmission lines and 5 generators. The data are presented in Table 3.1. The apparent power limit of the lines is 200 MW. Start-up/shut-down costs are set at 50% of marginal costs. Reactive power limits of generators and reactive power demand are set at 20% of their active power limits and demand at the related node. Demand per node is considered to be 1.2 and 0.7 times that of the medium level reported in Table 3.2 for the high-loading and low-loading cases, respectively. The objective function's convergence behaviour is

Table 3.1: 5-Bus generation data.

Type	Max. capacity [MW]	Max. ramping [% / h]	Marginal cost [\$ / MW]	Bus number
G1	40	100	14	1
G2	170	100	15	1
G3	520	100	30	3
G4	200	70	40	4
G5	600	70	10	5

presented in Fig. 3.1.

Table 3.2: 5-Bus line and demand data.

Lines	From	To	$x$ [p.u.]	$r$ [p.u.]	Demand node	Demand [MW]
L1	1	2	2.81	0.06	D2	300
L2	1	4	3.04	0.31	D3	300
L3	1	5	0.64	0.23	D4	400
L4	2	3	1.08	0.24		
L5	3	4	2.97	0.51		
L6	4	5	2.97	0.12		

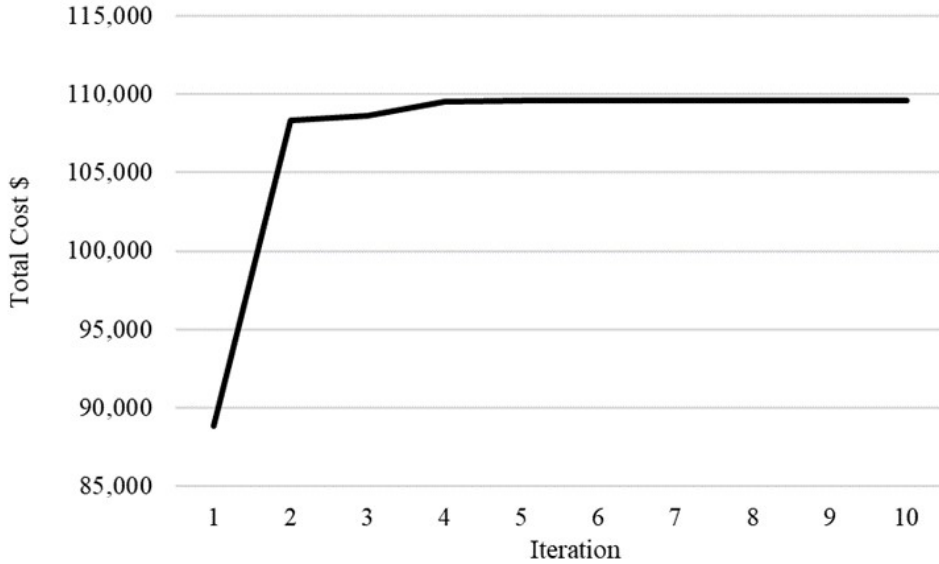


Figure 3.1: Total cost [\$] per iteration for medium-loading case.

Table 3.3 summarises the computational results, compared to the standard SOCP reported in Table 3.4. The algorithm needs 6–7 iterations to converge and generates computational savings under all loading levels of approximately 55-80%. Total cost is approximately the same for the low-loading level. The algorithm leads to 0.8% lower costs for the high, and, 3.9% for the medium case in relation to the SOCP results. A constraint violation, *ConsViol*, is defined which measures the deviation of the results with respect to the original non-convex equality constraint (3-26). This gives an indication of the quality of the obtained results. More precisely:

$$\text{ConsViol} = \| (c_{n,m,t}^2)^{(\nu-1)} + (s_{n,m,t}^2)^{(\nu-1)} - c_{n,n,t} \cdot c_{m,m,t} \|, \quad \forall m \in \mathcal{N}_n, n \in \mathcal{N}, t \in \mathcal{T}; \quad (3-53)$$

*Max. ConsViol* refers to the maximum observed constraint violation for all lines and time periods. Table 3.3 and Table 3.4 show that the algorithm provides more precision due to markedly lower constraint violations, constituting ca. 2-5% of that of SOCP. Intuitively, because the algorithm - as an outer

approximation - pushes solutions towards the circle's boundary.

Table 3.3: Proposed Algorithm - Case 1, Total costs, computational time, number of iterations and Max. ConsViol for each system-loading level.

	Total Cost [\$]	Max. ConsViol	Comp. Time [s]	# Iter
<b>High</b>	25,759.91	4.83	0.024	7
<b>Medium</b>	18,271.14	1.93	0.015	6
<b>Low</b>	9,959.92	5.68	0.018	6

Table 3.4: SOCP - Case 1, Total costs, computational time and Max. ConsViol for each system-loading level.

	Total cost [\$]	Max. ConsViol	Comp. Time [s]
<b>High</b>	25,972.02	119.82	0.052
<b>Medium</b>	19,002.86	112.95	0.082
<b>Low</b>	9,960.00	110.66	0.092

### 3.5.2

#### 240-Bus System: Case Study 2

A realistic 240-bus test system for California and the Western Electricity Coordinating Council (WECC) is applied, network data for which are outlined in [137]. It consists of 448 branches, 959 conventional and 35 weather-dependent generators with a total capacity of 99.745 GW. A total of 139 loads sums up to 62.45 GW, 49.872 and 39.898 GW under high-, medium-, low-loading, respectively.

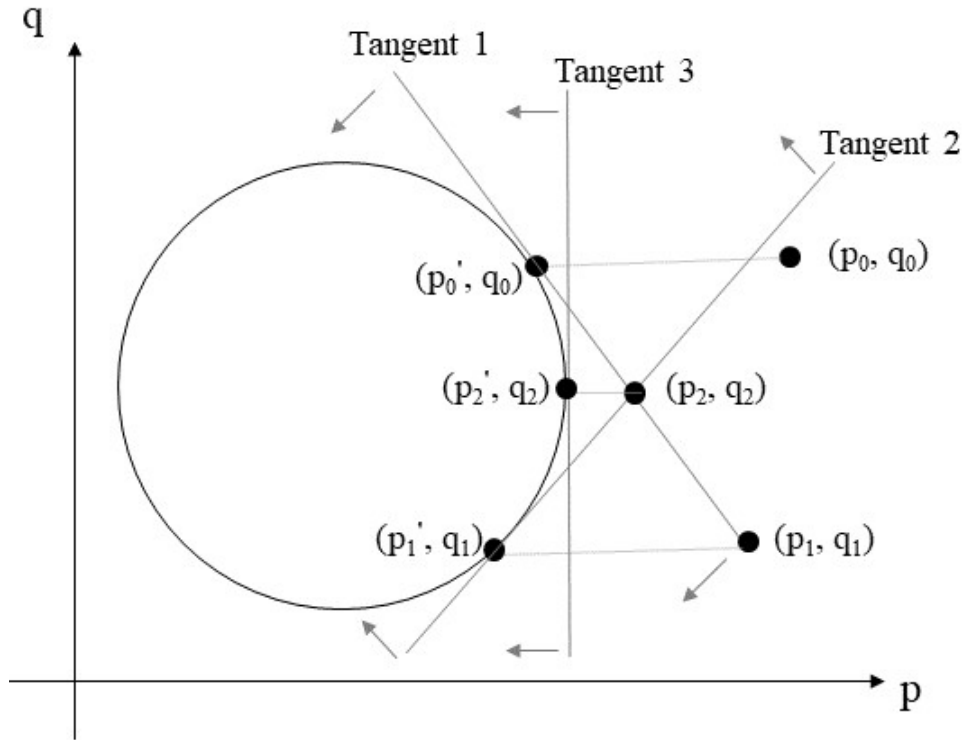


Figure 3.2: Illustrative cut procedure.

A summary of assumed operational constraints is provided in Table 3.5. Weather-dependent generation is considered deterministic. Load-shedding cost for active and reactive power is set at \$2,000 per MWh [116].

Table 3.5: Case 2, 240-Bus generation data.

Type	Max. ramping [% / h]	Start-up cost [\$ / MW]	Shut-down cost [\$ / MW]
Hydro	10	0	0
Gas	20	79	7.9
Coal	24	147	14.7
Other	10.00	0	0
Nuclear	27	160	160
Weather-dep.	100	0	0

Table 3.6 illustrates the results in relation to the devised algorithm under various system-loading levels. Under medium- and low-loading, the algorithm needs more time to search for feasible solutions. This is related with the master problem. Sub-problems solely check the solution quality given by the master and communicate new cuts back to the master. This characteristic, relying on minimum necessary exchange between master and sub-problems, seems beneficial in terms of computational time. Table 3.6 shows that the algorithm requires 2–3 iterations to converge. Total costs under the algorithm

and SOCP, latter reported in Table 3.7, are equal for low- and medium-loading, whereas high-loading outcomes differ. Computational time of the algorithm is solely 6.6% of the SOCP with medium-loading. *Max. ConsViol*, regarding the original non-convex constraint, indicates a lower dispersion of results under the algorithm for high- and medium-loading. With low-loading, however, maximum violation is 1.7 times more. The algorithm's average violation is 75% of SOCP.

Fig. 3.3, shows *ConsViol* per hour with all lines considered. Except for one extreme point above 90.0, the deviations are minimal, all less than 2.34. Compared to the SOCP, shown in Fig. 3.4, the devised algorithm gives rise to solutions with a notably lower *ConsViol*. This also implies it can yield more accuracy in power flow scheduling for a heavily-loaded system.

Table 3.6: Proposed Algorithm - Case 2, Total costs, computational time, number of iterations and Max. ConsViol for each system-loading level.

	Total Cost [MM\$]	Max. ConsViol	Comp. Time [s]	# Iter
<b>High</b>	97.93	94.18	24.01	2
<b>Medium</b>	2.52	3.06	50.67	2
<b>Low</b>	1.63	5,500.20	51.04	3

Table 3.7: SOCP - Case 2, Total costs, computational time and Max. ConsViol. for each system-loading level.

	Total cost [MM\$]	Max. ConsViol	Comp. Time [s]
<b>High</b>	99.20	3,383.81	24.59
<b>Medium</b>	2.52	3,121.68	767.64
<b>Low</b>	1.63	3,160.83	106.09

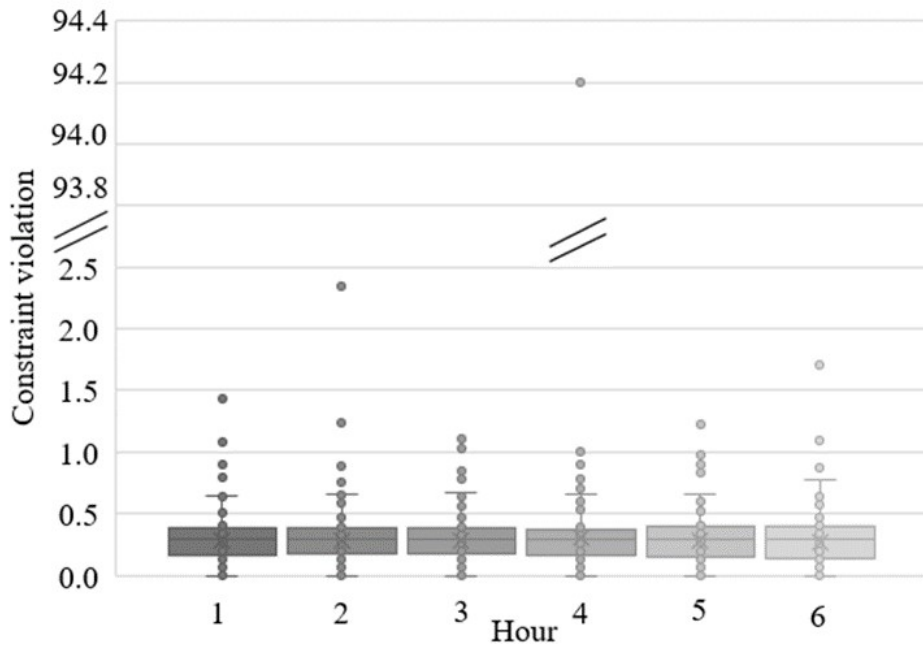


Figure 3.3: Case 2: Constraint violation under the algorithm high-loading case.

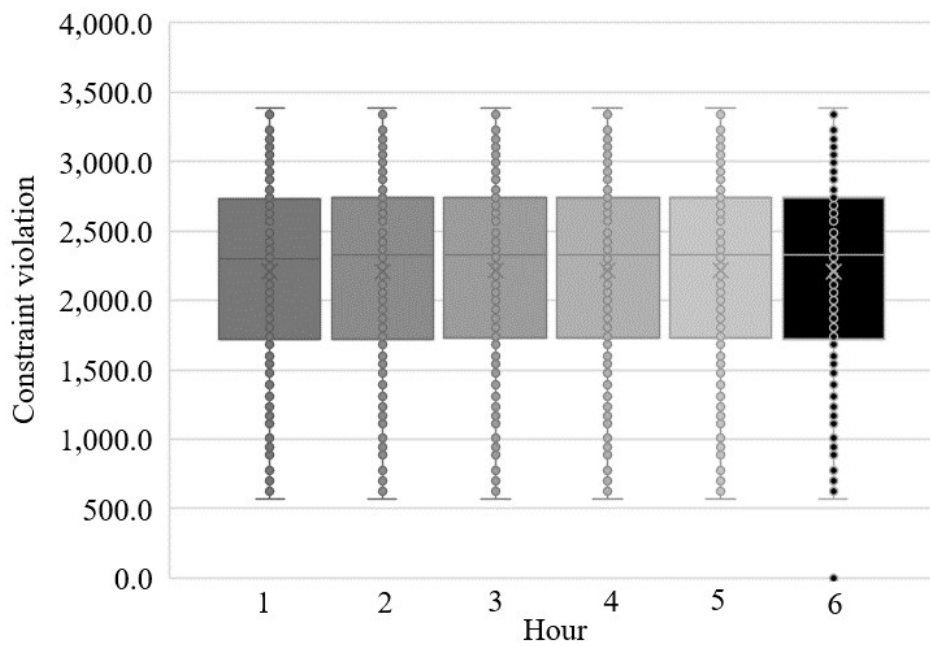


Figure 3.4: Case 2: Constraint violation under the SOCP high-loading case.

### 3.5.3

#### Computational performance curves appending numerical experiments

Note that this Section is not part of the publication [20]. However, it extends the analysis performed in the respective publication.

In this section, performance profiles are developed in order to evaluate, benchmark and compare optimisation outcomes under different approaches. A

set of metrics, such as wall-clock and CPU time and number of iterations are presented, which enable comparison of different algorithms. A certain chosen instance or minority of problems for which the results are populated may dominate the overall results. To address these, performance profiles are proposed in the literature. They are defined as (cumulative) distribution functions for a performance metric providing a means for visualising the performance differences amongst various solvers or algorithms, while circumventing choice of arbitrary parameters and explicitly showing failure of obtaining solutions for some instances [138]. In this thesis, the methodology to develop performance profiles follows works [138, 139].

For the numerical experiments, 5-Bus system of Case 1, 240-Bus System of Case 2 cover a 24-hour time horizon. As a Case 3, 118-Bus IEEE test system is included in order to further show the robustness of the method proposed.

In each Case, 100 instances for the load level are generated by applying a random multiplier,  $\rho$  to the fixed demand level in the earlier Sections, i.e.,  $\rho = (0.50, 0.70)$ ,  $\rho = (0.71, 1.20)$  and  $\rho = (1.21, 2.00)$  for low, medium and high loading-conditions of the system, respectively.  $(a, b)$  represents a continuous uniform distribution with the boundary values of  $a$  and  $b$ . For each instance, reactive power demand is set equal to 20% of the active power demand, which is a common procedure.

In the experiments, the time is measured as wall-clock-time, and in order to mitigate the effect of recompilation time the experiments are run twice, and the results for the second one are recorded where the recompilation effect is lower or minimal.

In Fig. 3.5, Fig. 3.6 and Fig. 3.7 performance curves are illustrated in Case 1, Case 2 and Case 3, respectively. The  $x$ -axis represents the total cumulative time in seconds in natural logarithmic scale for solving the corresponding percentage of 100 instances on the  $y$ -axis.

Fig. 3.5 in relation to Case 1 shows that low- and medium-loading the proposed algorithm outperforms the standard SOCP in varying degrees. After the first 25 instances the algorithm saves computational time in natural logarithm by 9.17% and 3.91%; after 50 instances 1.44%; 2.49%, 0.95%, 3.08% and at then end of 100 instances by 0.07% and 2.94%, in respective order of loading. The first 25 instances the savings are more considerable than when, for instance, all 100 are solved. Note that negative time in some first instances can appear because of the natural logarithmic scale used.

Note that the first instances under the SOCP take relatively long time albeit the fact that the compilation time aspect is mitigated by consecutive runs. It is most likely due to the fact that the first random problem instance

is relatively difficult to solve under the SOCP. Excluding this instance, would not change the overall conclusion.

Regarding the high-loading conditions, however, the proposed algorithm depicts a higher performance in the first three instances than the SOCP, thereafter this becomes no longer the case. The algorithm takes 16.91% more time than the standard SOCP when all 100 instances are run.

In Fig. 3.6, in relation to Case 2, one can observe that the algorithm depicts a higher performance under low- and high-loading, 2.51% and 1.81% of savings in natural logarithmic terms. For the medium-loading, between instances 3 until 12, the algorithm does not depict a better performance. Thereafter, it starts outperforming and saves 1.80% of time after having run all the instances.

In Fig. 3.7, regarding Case 3, the algorithm clearly depicts computational time savings after 100-instance-run - by 9.90%, 5.14% and 5.74% under low-medium-, and high-loading - in given order.

Note that mean value of the runtime could also be used for comparison purposes. However, it would not be able to capture the entire characteristics of computational time which can significantly differ in each instance.

Nevertheless, the descriptive statistics for computational time, given in seconds, regarding the algorithm is provided in Table 3.8 for Case 1, Case 2 and Case 3 as well as for different loading situations. Table 3.9, on the other hand, presents descriptive statistics for the standard SOCP.

Table 3.8: Descriptive statistics for computational time under Algorithm for each system-loading level.

Case #	Load	Computational time [s.] Algorithm				
		min.	25% quantile	50% quantile	75% quantile	max.
Case 1	low	0.370	0.446	0.618	0.783	1.231
	medium	0.555	0.637	0.729	0.897	1.905
	high	0.703	0.971	1.025	1.093	1.532
Case 2	low	23.869	29.065	32.510	44.171	106.888
	medium	13.426	22.234	28.770	48.138	109.310
	high	36.156	36.916	37.924	39.029	52.297
Case 3	low	12.468	13.118	13.952	16.169	86.189
	medium	12.859	13.796	14.128	14.828	28.240
	high	12.796	13.541	13.795	14.088	16.506

Also note that computing time is mainly related to the solution of the master problem. Sub-problems take very low computational time, since they are mainly for calculating the parameters for the cuts for which the inputs come from the master problem.

Table 3.9: Descriptive statistics for computational time under SOCP for each system-loading level.

Case #	Load	Computational time [s.] SOCP				
		min.	25% quantile	50% quantile	75% quantile	max.
Case 1	low	0.484	0.527	0.593	0.688	2.918
	medium	0.651	0.775	0.816	1.012	2.973
	high	0.357	0.410	0.471	0.531	2.869
Case 2	low	12.080	31.945	37.450	45.100	156.430
	medium	10.420	34.961	38.400	43.725	150.451
	high	14.280	35.900	38.800	45.275	150.719
Case 3	low	18.531	25.201	29.629	51.052	82.032
	medium	18.014	19.987	21.181	22.990	34.223
	high	14.913	19.096	21.156	22.620	43.689

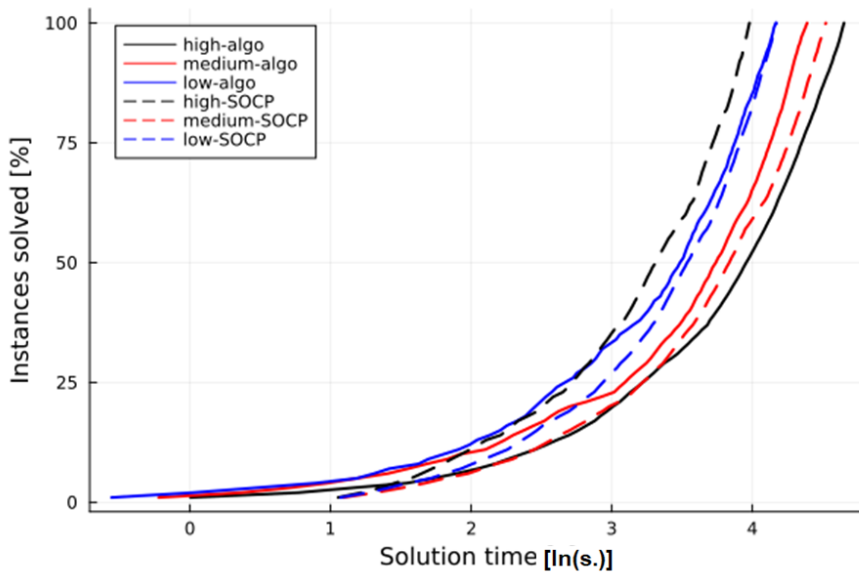


Figure 3.5: Case 1, 5-bus, 24-hours: Computational performance curves plotting percentage of instances solved vs. runtime in natural logarithm of seconds of each instance solved.

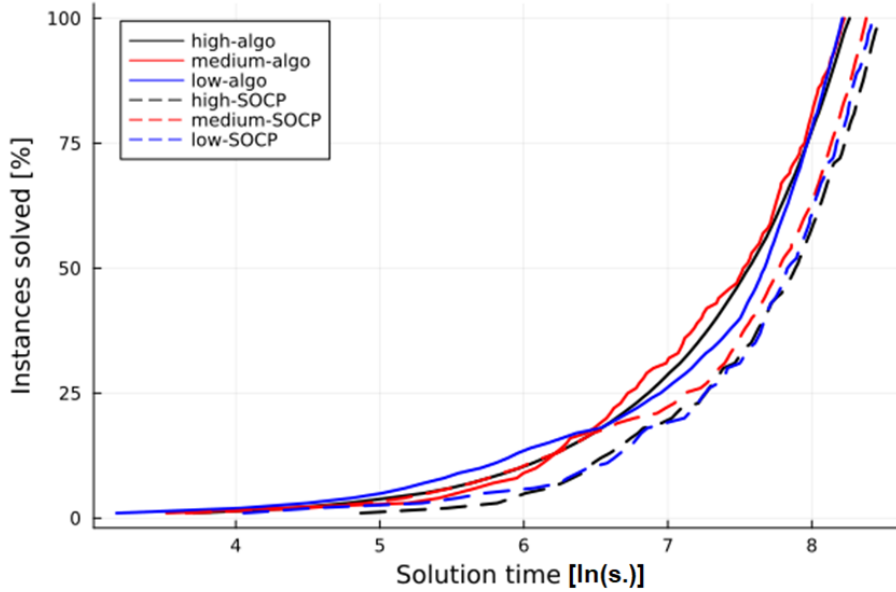


Figure 3.6: Case 2, 240-bus, 24-hours: Computational performance curves plotting percentage of instances solved vs. runtime in natural logarithm of seconds of each instance solved.

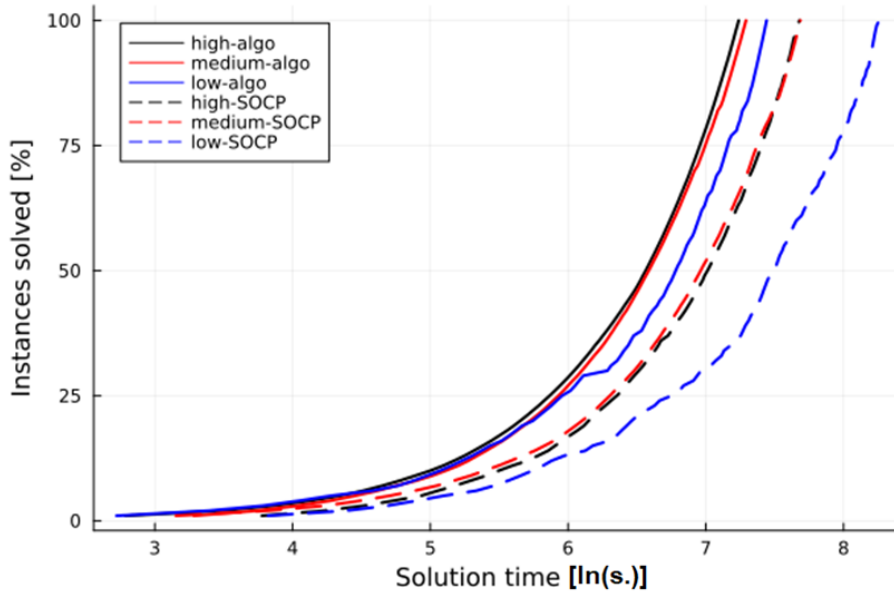


Figure 3.7: Case 3, 118-bus, 24-hours: Computational performance curves plotting percentage of instances solved vs. runtime in natural logarithm of seconds of each instance solved.

For expository purposes, constraint violations for Case 1 are provided in Fig. 3.8 and Fig. 3.9 for the high-loaded system conditions. As similar patterns are observed for Case 2 and Case 3, solely the results for Case 1 are presented. Constraint violations are computed based on Equation (3-53) for 100 instances,

which are in per unit (p.u.) basis, and violation ranges are plotted accordingly. Note that this metric also demonstrates the deviations with regard to the feasibility of the obtained solutions under the original non-convex AC power flow formulation. It can be observed that albeit some variations per hour, constraint violations under the standard SOCP is in the range of 0.18-0.30 p.u.. Regarding the proposed algorithm the constraint violation range is 0.002-0.010 p.u.. We note that the reduction of constraint violations under the proposed algorithm is an anticipated result because of the fact that the algorithm pushes the solutions towards the boundary of the quadratic relaxation. The latter is in general tends to be tighter than the SOCP relaxation which includes the interior of the cone.

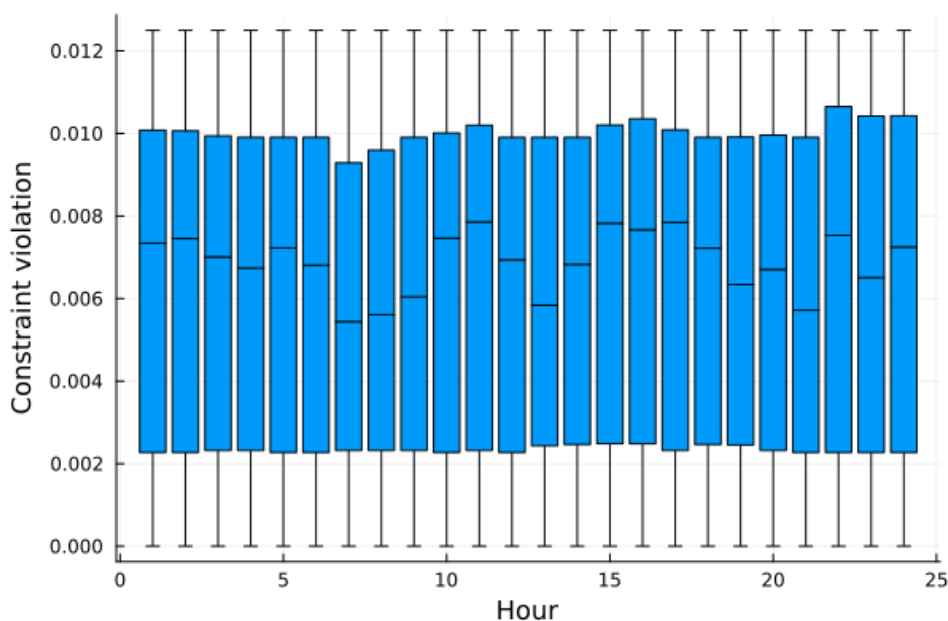


Figure 3.8: Case 1, 5-bus, 24-hours: Constraint violations in p.u. for 100 instances under the algorithm high-loading case.

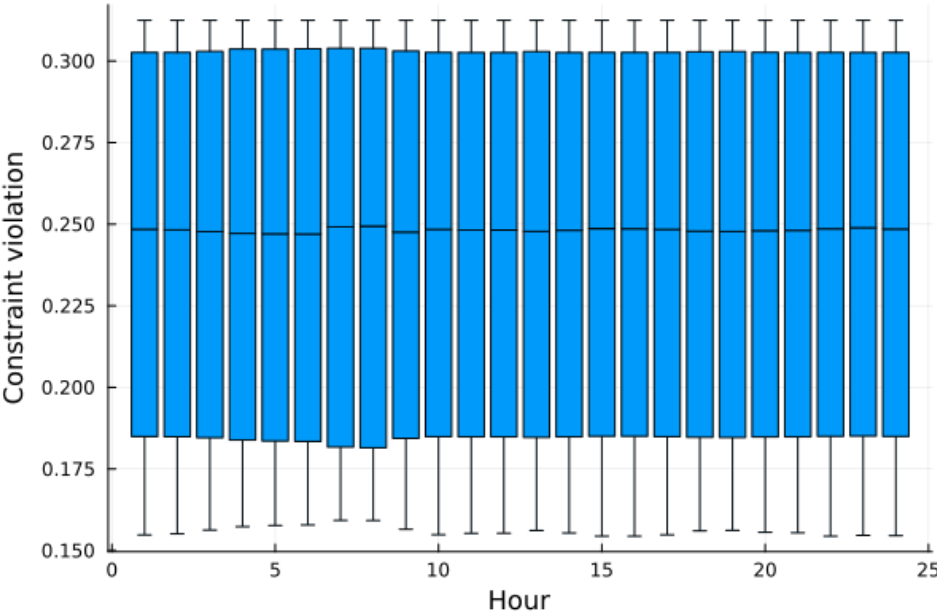


Figure 3.9: Case 1, 5-bus, 24-hours: Constraint violations in p.u. for 100 instances under the SOCP high-loading case.

## 4

# Computational Techniques and Model Accuracy in DSO-TSO Coordination Problems for Congestion and Voltage Management

This Chapter is on the basis of and reusing parts of the journal article, which is under review [**Paper B**] Martin, N. C., & Fanzeres, B. A Two-Level ADMM Algorithm for Multi-Agent DSO-TSO Congestion Management and Voltage Control Coordination with Limited Information Exchange. *In process of publication*. This article is herewith referenced and cited as [140], which may be subject to changes in its final version, and incorporate other numerical experiment settings compared to the content of this Chapter.

We note that the Chapter focuses on the technical aspects of DSO-TSO coordination, and specifically congestion and reactive power or voltage management. A number of sociological, technical and economic challenges need to be addressed for the implementation of DSO-TSO coordination, for which the review [24] can be referred to. Firstly, system operations and dispatch are becoming more complex, for which DERs need to be orchestrated. To this end, accuracy of network information is paramount. Especially distribution networks tend to have limited observability, in particular at low-voltage level. Fairness aspects for the services provided by DERs are also of importance, which need to be addressed. Vulnerability of the network to cyberattacks may increase as a result of more access to network information. Finally, DSO-TSO coordination requires policies and regulations for its implementation. There are various coordination frameworks considered in the literature, which can be mainly classified as TSO-managed, TSO-DSO hybrid-managed or DSO-managed models, depending on which entity is the center of coordination. This Chapter, among others, attempts to bring an equilibrium point of view into the discussion, where DSO and TSO entities are considered without any hierarchy.

## 4.1

### Background for Mathematical Formulations

In this Chapter, a bus injection type, and voltage-based formulation of AC OPF is constructed when applicable. Voltage magnitudes at each bus  $n \in \mathcal{N}$ , are given by  $V_n$ , and are represented by a polar form, such that  $e^{i\theta_n} = \text{Cost}(\theta_n) + i.\text{Sin}(\theta_n)$ , where  $\theta_n$  is the phase angle of the respective bus measured in radians,  $\theta_n \in (-\pi, \pi], \forall n \in \mathcal{N}$ . The notation is simplified

such that instead of  $|V_n|$ , the notification  $V_n$  is used to represent voltage per bus.  $|V_n|$  is the modulus of the complex voltage  $V_n = |V_n|.e^{i.\theta_n}$ . Though not explicitly stated during the Chapter, admittance matrix formulation is on the basis of rectangular coordinates, such that  $\mathbf{Y}_{n,m} = \mathbf{G}_{n,m} + i.\mathbf{B}_{n,m}$ . Balanced, single-phase equivalent model as well as steady-state conditions are assumed throughout. Furthermore, especially transmission networks, tend to have meshed structures, which require additional non-convex constraints in the formulation for the consistency of phase angles [13]. This aspect is not considered and left as a future work.

Moreover, energy storage systems related modelling assumes ideal storage systems. It ignores fast response of such units which can be captured in tighter time scales, varying charging or discharging efficiencies, degradation aspects, etc. The storage systems are assumed to be owned, or operated in such a way that its sole purpose is to contribute to the least-cost operation of the system. The latter is, in practice, possible by bilateral contracts between system operators and storage owners.

Finally, under the decentralised and distributed structures discussed, the agents are assumed to act truthfully and communicate the true value of the computed primal and dual variables.

## 4.2 Introduction

Large-scale penetration of distributed energy resources (DERs) along with network constraints are increasingly causing congestion and voltage problems due to time-varying power flows. The participation of DERs, such as battery energy storage systems (BESSs) and weather-dependent generation, can be located at medium voltage networks, managed by distribution system operators (DSOs). Furthermore, although transmission and distribution systems are physically interconnected, their standalone operations are bounded by their respective jurisdictions. As such, the operators individually do not have full visibility or direct control of the overall power system [22]. Given this interconnectedness, uncoordinated actions of transmission system operators (TSO) and DSOs can jeopardise security of supply, just as their cooperation can result in more efficient operations [141, 22].

In order to mitigate congestion or voltage problems in the respective systems, central-planning-based approaches - reliant on optimisation of transmission and distribution system costs cumulatively - are not realistic or adequate [22]. This setting ignores the individual optimisation of system operators and information-sharing aspects amongst different networks governed by each en-

tity [22]. Conversely, hierarchical or multi-level approaches define one of the entities as a leader in the coordination problem. These approaches assume that at least one of the operators has full knowledge of the other system's constraints [142, 143], and tend to be computationally expensive [24]. Distributed approaches have been proposed in the literature, which allows a collaborative computation between different entities, to attain a system-level objective [99]. It is based on the notion of breaking down a complex mathematical problem into smaller problems which are computed by local agents and coordinated with each other so that an optimal or near-optimal solution to the system objective is achieved. Distributed computation brings in the following main advantages against a centralised computation [13, 144]:

i) Centralised approaches need high bandwidth communication architecture, which tends to be expensive, due to extensive amount of geographically spread data that needs to be aggregated and stored by a central controller. In distributed approaches, local data obtained through sensors and monitoring tools are directly used [99], and a limited amount of data is interchanged amongst sub-systems or with the central controller.

ii) Distributed computation brings in cybersecurity and resilience advantages. In case the central controller disconnects, the whole system operations can be impacted. Distributed computation, however, makes it possible local sub-systems to continue operating in an asynchronous fashion by means of local control functions. This would also be the case if a local sub-controller defaults.

iii) Distributed computation has advantages in terms of network, cost functions and constraints or sensitive measurement data privacy preservation, because these do not need to be or to a limited degree shared between sub-systems or with the central controller.

iv) Distributed computation is more adaptable to topology changes in the system because of re-configuration as a result of faults or dynamic aspects of the power and communication architectures [144]. When, for instance, some local controllers are disconnected, other local controllers can continue normal operations, and distributed OPF can be computed in an asynchronous fashion. In case of a centralised optimisation, if the central controller collapses, then the whole system can be disrupted [144, 145].

v) Distributed computation can potentially be more scalable, due to

ability to perform parallel tasks, and efficient than a centralised one, especially when a large number of sub-systems and vast amounts of network and measurement data involved [13].

The coordination problem involving coordination of multiple DSO-TSO agents can be viewed as seeking for equilibrium operational set-points amongst the involved entities governing their sub-systems, each of which having their own objectives [141]. Reaching to such an equilibrium requires iterations amongst the adjacent entities directly or via a central coordinator to exchange data commonly regarding the interface power flows along with their prices as a signal towards reaching eventually a consensus. The Alternating Direction Method of Multipliers (ADMM) algorithm, as a distributed approach, is a widely used such computational method to handle DSO-TSO coordination problems [146, 147, 148, 141]. The ADMM provides the advantage of performing parallel computing which potentially enhances solution speed [13]. However, the ADMM and its variants require significant penalty parameter tuning and update process, suffering from numerical instability, and their convergence may not be achieved within a reasonable time frame [149, 150]. In addition, DSO-TSO coordination may involve multiple DSOs or TSOs in practice, which can be represented by a multi-block ADMM problem, i.e., a separable problem involving more than two operators when a suitable (Lagrangian) relaxation of the coupling constraints are applied. Multi-block ADMM does not have convergence guarantees [151]. The literature lacks works handling DSO-TSO coordination problem with multiple operators which can warrant convergence at least to a stationary solution.

ADMM method, generally, requires a - possibly virtual - central coordinator to collect and aggregate data provided by each entity and redistribute. To eliminate or reduce such a need while also reducing the data exchange amongst the entities, decentralised versions of ADMM are proposed [144]. These approaches principally rely on exchanging information with the adjacent entity, rather than aggregating exchanged data centrally. This can result in cybersecurity benefits, reduction of data storage needs and computational savings.

Moreover, power flow models describing the laws of physics in these systems, such as Kirchhoff's and Ohm's Law, are with non-linear and non-convex AC power flow constraints, and are demonstrated to be non-deterministic polynomial-time hard (NP-hard) even for radial networks [39], i.e., it cannot be proven whether a solution to the problem can be found in polynomial time. Solution approaches to these models are broadly categorised into i) non-linear methods; ii) convex relaxations or approximations. Non-linear methods seek for

globally or locally optimal solutions directly from the non-convex problem formulation, the main approach being primal-dual interior-point methods (IPM). Convex relaxations or approximations relaxes the power flow equations into convex inequalities to which a global optimum solution to the relaxed problem can be obtained. Linearisation-based techniques as well as second-order cone programming and semi-definite programming-based approaches are categorised in this work under convex relaxations or approximations.

The majority of works in the literature studying DSO-TSO coordination apply a DC approximation to represent power flow for distribution networks. However, DC power flow as a linear approximation to AC are not realistic for distribution systems characterised by high resistance-to-reactance ratios [59, 58].

Yet, system and market operators tend to prefer applying linear programming (LP)-based approaches in practice mainly due to the following motivations [63, 60]: i) LP (and Mixed-integer linear) solvers are more mature and computationally robust compared to other type of solvers based on IPM or convex relaxations, such as SOCP or SDP. Convergence under LP and convex relaxations or approximations is guaranteed in case of a feasible-solution to the problem exists; ii) IPM-based ones are shown to be sensitive to the initialisation and model formulation. Poor choice of the initial points can lead to long computational time or non-convergence. iii) Locational Marginal Prices (LMP) for market-clearing purposes are more straightforward to obtain out of LP problems, and the obtained solutions are more transparent and interpretable.

Other than linear approximations, a recent work [152] applies a second-order cone programming (SOCP) convex relaxation to enhance AC OPF for distribution networks within the context of DSO-TSO coordination in its case study. Yet, under high-loading conditions, when thermal or voltage limits are typically exceeded, leading to congestion or voltage problems, the SOCP can result in large deviations between actual and predicted power flows [14].

To address these computational, network-information exchange-related as well as power flow accuracy challenges for an effective multi-agent DSO-TSO coordination to resolve operational problems jointly, in this work, a distributed decomposition algorithm is proposed based on a minimal information interchange between all entities operating a distribution or transmission network, following a distributed approach. In addition, a decentralised framework is also proposed which removes the need for a central coordinator for exchanging parameters amongst the entities while reducing the quantity of data transfer which may translate into computational savings for large power

systems. More precisely, a two-level nested-loop ADMM is designed [149, 150] which enhances the penalty parameter tuning of standard ADMM and model convergence accordingly. To this end, slack variables are introduced into the coupling constraints between the DSO and the TSO problems. The inner loop updates the Lagrange multipliers of the coupling constraints and the slack variables. Using the solutions from the inner loop, the outer loop updates the sensitivity of the slack variables and the respective penalty parameters. This ADMM process enables mitigation of congestion and voltage problems in the respective systems in a coordinated way. The framework is general enough to address finding an equilibrium amongst multiple DSO-TSO entities. Moreover, in order to improve the computation of interface power flows for a more efficient coordination, a linearisation-based circle approximation and a decomposition algorithm to solve AC OPF is also provided and embedded into the proposed algorithm. This linear approximation is based on a recent work [20], potentially outperforming the standard SOCP in terms of accuracy and computational efficiency, especially under high system-loading conditions characterised by congestion and voltage problems. The results of the devised algorithm are compared with standard ADMM with a standard SOCP as a benchmark.

#### 4.2.1 Objectives and Contributions

The principal objective of this work is to devise a methodology to enhance computational aspects of multi-actor DSO-TSO coordination in day-ahead operational planning for the procurement of ancillary services to handle operational issues regarding congestion and voltage management, address network information-exchange aspects and accuracy of power flow computation at the interface nodes. The contributions of this work are as follows:

1. Different from state-of-the-art DSO-TSO coordination models in the literature, the proposed model co-optimises active and reactive power procurement costs arising from the changes in forecast for, e.g., renewable generation to ensure security of supply by respecting all network constraints involved. The devised framework can handle multiple actors. State-of-the-art techniques are incorporated in modelling enhancing accuracy and computation, such as a linear BESS model, tighter than other known linear formulations without binaries as in [139].
2. To enhance power flow modelling in order to closely align overall involved transmission and distribution system operations for DSO-TSO coordination. To this end, this work implements the method proposed in

the recent work [20] based on a linearisation-based circle approximation of AC power flow. This procedure potentially enhances computational robustness and accuracy of AC OPF compared to, e.g., the standard SOCP. The latter is regarded as a computationally tractable technique with high accuracy at least for normal system conditions [19].

3. To devise an efficient solution procedure for the multi-actor DSO-TSO congestion management and voltage control coordination problem, which is a multi-period time-coupled problem with the presence of energy storage systems. The proposed solution procedure is based on a two-level nested ADMM framework in [150, 149]. This framework protects network or other sensitive data of standalone entities. Different from [150, 149], this work proposes decentralised consensus algorithm inspired from [144] which solely requires exchange of data with the neighbouring subsystems reducing the amount of interchanged data while a central coordinator for this interchange may no longer be needed. Two-level ADMM framework is shown to have convergence guarantees to an approximate stationary solution for multi-block problems, which in the particular context of this work in case of more than two system operator agents are concerned. The works [150, 149] study non-convex AC OPF without any convexification process. This work, however, studies convex approximations and relaxations to the AC OPF within a DSO-TSO coordination problem, where the obtained solutions are global optimal for the convexified problem. Constraint violations compared to the original non-convex formulation are shown to be minimal.

### 4.3

#### Mathematical Formulation

This work considers a general and broad framework with multiple transmission and distribution networks, each of which operated by a TSO or a DSO, respectively. These systems are interconnected via tie-lines, through which active and reactive power flows are exchanged. Single-phase balanced network models are presented. Steady-state conditions, and balanced, single-phase equivalent power flow are assumed throughout. On a stand-alone basis and without considering any coordination between the networks, a transmission system is customarily represented as an infinite source for the distribution system analysis. Similarly, the distribution system is considered as an aggregate load in the transmission system-related analysis [153]. This set-up ignores effects of any potential coordination between these systems. DSO-TSO coor-

dination framework, however, establishes relationship between variables of the transmission and distribution networks at their interfaces.

In the analysed set-up, in this work, TSOs and DSOs coordinate amongst each other to procure ancillary services for i) active power, i.e., with regard to congestion management purposes; ii) reactive power, i.e., for voltage support purposes after the clearance of the day-ahead schedule. This necessity arises because the operators may have an updated forecast on the uncertain variables, such as on renewable generation, towards real-time operations. Each operator has the objective to co-optimize the costs for re-dispatching the units which they operate due to deviations from the day-ahead schedule. This involves remedying potential congestion and voltage problems at a least cost while balancing demand and supply. The set-up is similar to those in [22, 65, 154]. Different from these stated works, this work co-optimises both active and reactive power procurement costs, rather than focusing on one or the other.

### 4.3.1 Subsystem Operation Problem Formulation

This work regards the DSO-TSO cooperation problems from the perspective of finding equilibrium set points for operations of individual DSOs and TSOs in a given interconnected system. To this end, this section presents the non-linear and non-convex optimisation problem as a general problem reflecting each of the DSO and TSO's optimisation problem for their day-ahead operation planning after the settlement of the day-ahead markets.

Such a planning includes re-dispatch of all components based on the most actual forecast for renewable generation and demand and flexibility procurement for congestion management and voltage control for secure operations.

For each entity  $p$ , (DSO or TSO), the optimisation problem is formulated in (4-1) – (4-39). This formulation incorporates all components and flexibility procurement possibilities that each operator can have, though not necessary that they have or utilise these components or options. The formulation also includes the interface nodes of each entity with the adjacent entity, such that  $\mathcal{N}_p = \bar{\mathcal{N}}_p \cup \mathcal{N}_p^\infty$ , where set of nodes belonging to the entity  $\mathcal{N}_p$  contains both local nodes  $\bar{\mathcal{N}}_p$  and its nodes at the interface with other entities  $\mathcal{N}_p^\infty$ .

$$\min_{\Xi_p} \mathbb{C}^J(\cdot) + \mathbb{C}^{int}(\cdot) + \mathbb{C}^B(\cdot) + \mathbb{C}^F(\cdot) + \mathbb{C}^{curt}(\cdot) + \mathbb{C}^c(\cdot) + \mathbb{C}^{sh}(\cdot); \quad (4-1)$$

where:

$$\mathbb{C}^J(\cdot) = \sum_{t \in \mathcal{T}} \left( \sum_{i \in \mathcal{J}_p \cup \mathcal{J}_p^{WP}} \left( C_i \cdot g_{i,t} + C_i^q \cdot (q_{i,t}^+ + q_{i,t}^-) \right) \right); \quad (4-2)$$

$$\mathbb{C}^{int}(\cdot) = \sum_{t \in \mathcal{T}} \left( \sum_{n,m \in \mathcal{N}_p^\infty} \left( C_n^{int} \cdot (p_{n,m,t}^{int,+} + p_{n,m,t}^{int,-}) + C_n^{q,int} \cdot (q_{n,m,t}^{int,+} + q_{n,m,t}^{int,-}) \right) \right); \quad (4-3)$$

$$\mathbb{C}^B(\cdot) = \sum_{t \in \mathcal{T}} \left( \sum_{b \in \mathcal{B}_p} \left( C_b \cdot (g_{b,t}^{cha} + g_{b,t}^{dis}) + C_b^q \cdot (q_{b,t}^+ + q_{b,t}^-) \right) \right); \quad (4-4)$$

$$\mathbb{C}^F(\cdot) = \sum_{t \in \mathcal{T}} \left( \sum_{f \in \mathcal{F}_p} \left( C_f \cdot (g_{f,t}^+ + g_{f,t}^-) \right) \right); \quad (4-5)$$

$$\mathbb{C}^{curt}(\cdot) = \sum_{t \in \mathcal{T}} \left( \sum_{k \in \mathcal{J}_p^{WP}} \left( C_k^{curt} \cdot g_{k,t}^{curt} \right) \right); \quad (4-6)$$

$$\mathbb{C}^c(\cdot) = \sum_{t \in \mathcal{T}} \left( \sum_{c \in \mathcal{C}_p} \left( C_c \cdot (q_{c,t}^+ + q_{c,t}^-) \right) \right); \quad (4-7)$$

$$\mathbb{C}^{sh}(\cdot) = \sum_{t \in \mathcal{T}} \left( \sum_{d \in \mathcal{D}_p} \left( C_d^{psh} \cdot g_{d,t}^{psh} + C_d^{qsh} \cdot q_{d,t}^{qsh} \right) \right); \quad (4-8)$$

subject to:

$$\begin{aligned} & \sum_{i \in \mathcal{J}_n \cup \mathcal{J}_n^{WP}} g_{i,t} - \sum_{d \in \mathcal{D}_n} \hat{g}_{d,t} + \sum_{k \in \mathcal{J}_n^{WP}} (\hat{g}_{k,t}^w - g_{k,t}^{curt}) + \sum_{f \in \mathcal{F}_n} (g_{f,t}^- - g_{f,t}^+) + \\ & \sum_{b \in \mathcal{B}_n} (g_{b,t}^{dis} - g_{b,t}^{cha}) + \sum_{d \in \mathcal{D}_n} g_{d,t}^{psh} - \sum_{m \in \mathcal{N}_{pn} \setminus \{\mathcal{N}_{pn}^\infty\}} p_{n,m,t} + \\ & + \sum_{m \in \mathcal{N}_{pn}^\infty} p_{n,m,t}^{int} = 0, \forall n \in \mathcal{N}_p, t \in \mathcal{T}; \end{aligned} \quad (4-9)$$

$$p_{n,m,t}^{int} = p_{n,m,t}^{int,+} - p_{n,m,t}^{int,-}, \forall n \in \mathcal{N}_p^\infty, \forall m \in \mathcal{N}_{pn}^\infty, t \in \mathcal{T}; \quad (4-10)$$

$$\begin{aligned} p_{n,m,t} = & G_{n,m} \cdot (V_{n,t})^2 + V_{n,t} \cdot V_{m,t} \cdot (-G_{n,m} \cdot \text{Cos}(\theta_{n,m,t}) + \\ & + B_{n,m} \cdot \text{Sin}(\theta_{n,m,t})), \forall m \in \mathcal{N}_{pn}, n \in \mathcal{N}_p, t \in \mathcal{T}; \end{aligned} \quad (4-11)$$

$$\begin{aligned} & \sum_{i \in \mathcal{J}_n \cup \mathcal{J}_n^{WP}} q_{i,t} - \sum_{d \in \mathcal{D}_n} \hat{q}_{d,t} + \sum_{d \in \mathcal{D}_n} q_{d,t}^{qsh} + \sum_{c \in \mathcal{C}_n} q_{c,t} + \sum_{b \in \mathcal{B}_n} q_{b,t} + \\ & - \sum_{m \in \mathcal{N}_n \setminus \{\mathcal{N}^\infty\}} q_{n,m,t} + \sum_{m \in \mathcal{N}_n^\infty} q_{n,m,t}^{int} = 0, \quad \forall n \in \mathcal{N}_p, t \in \mathcal{T}; \end{aligned} \quad (4-12)$$

$$q_{n,m,t}^{int} = q_{n,m,t}^{int,+} - q_{n,m,t}^{int,-}, \forall n \in \mathcal{N}_p^\infty, \forall m \in \mathcal{N}_{pn}^\infty, t \in \mathcal{T}; \quad (4-13)$$

$$q_{i,t} = q_{i,t}^+ - q_{i,t}^-, \forall i \in \mathcal{J}_p \cup \mathcal{J}_p^{WP}, t \in \mathcal{T}; \quad (4-14)$$

$$q_{c,t} = q_{c,t}^+ - q_{c,t}^-, \forall c \in \mathcal{C}_p, t \in \mathcal{T}; \quad (4-15)$$

$$q_{b,t} = q_{b,t}^+ - q_{b,t}^-, \forall c \in \mathcal{C}_p, t \in \mathcal{T}; \quad (4-16)$$

$$\begin{aligned} q_{n,m,t} = & (B_{n,m} - b_{n,m}^{shunt}) \cdot (V_{n,t})^2 - V_{n,t} \cdot V_{m,t} \cdot (G_{n,m} \cdot \text{Sin}(\theta_{n,m,t}) + \\ & B_{n,m}^D \cdot \text{Cos}(\theta_{n,m,t})), \forall m \in \mathcal{N}_{pn}, n \in \mathcal{N}_p, t \in \mathcal{T}; \end{aligned} \quad (4-17)$$

$$(p_{n,m,t})^2 + (q_{n,m,t})^2 \leq (\bar{S}_{n,m})^2, \forall m \in \mathcal{N}_{pn}, n \in \mathcal{N}_p, t \in \mathcal{T}; \quad (4-18)$$

$$(\underline{V}_n)^2 \leq (V_{n,t})^2 \leq (\bar{V}_n)^2, \forall n \in \mathcal{N}_p, t \in \mathcal{T}; \quad (4-19)$$

$$\underline{G}_i \leq g_{i,t} \leq \overline{G}_i, \forall i \in \mathcal{J}_p \cup \mathcal{J}_p^{WP}, t \in \mathcal{T}; \quad (4-20)$$

$$\begin{aligned} -RD_i &\leq g_{i,t} - g_{i,t-1} \leq RU_{i,t}, \\ \forall i \in \mathcal{J}_p \cup \mathcal{J}_p^{WP}, \forall t \in \mathcal{T} \setminus \{1\}; \end{aligned} \quad (4-21)$$

$$\begin{aligned} -RD_i &\leq g_{i,t} - g_{i,0} \leq RU_{i,t}, \\ \forall i \in \mathcal{J}_p \cup \mathcal{J}_p^{WP}, \forall t = 1; \end{aligned} \quad (4-22)$$

$$\underline{Q}_i \leq q_{i,t} \leq \overline{Q}_i, \forall i \in \mathcal{J}_p \cup \mathcal{J}_p^{WP}, t \in \mathcal{T}; \quad (4-23)$$

$$\underline{Q}_c \leq q_{c,t} \leq \overline{Q}_c, \forall c \in \mathcal{C}_p, t \in \mathcal{T}; \quad (4-24)$$

$$\underline{G}_b^{cha} \leq g_{b,t}^{cha} \leq \overline{G}_b^{cha}, \forall b \in \mathcal{B}_p, t \in \mathcal{T}; \quad (4-25)$$

$$\underline{G}_b^{dis} \leq g_{b,t}^{dis} \leq \overline{G}_b^{dis}, \forall b \in \mathcal{B}_p, t \in \mathcal{T}; \quad (4-26)$$

$$\underline{SOC}_b \leq SOC_{b,t} \leq \overline{SOC}_b, \forall b \in \mathcal{B}_p, t \in \mathcal{T}; \quad (4-27)$$

$$\begin{aligned} SOC_{b,t} &= SOC_{b,t-1} + [\eta_b^{cha} \cdot g_{b,t-1}^{cha} - \frac{1}{\eta_b^{dis}} \cdot g_{b,t-1}^{dis}], \\ \forall b \in \mathcal{B}_p, t \in \mathcal{T}; \end{aligned} \quad (4-28)$$

$$g_{b,t}^{cha} \leq (\overline{SOC}_b - SOC_{b,t-1}) / \eta_b^{cha}, \forall b \in \mathcal{B}_p, t \in \mathcal{T}; \quad (4-29)$$

$$g_{b,t}^{dis} \leq (SOC_{b,t-1} - \underline{SOC}_b) \cdot \eta_b^{dis}, \forall b \in \mathcal{B}_p, t \in \mathcal{T}; \quad (4-30)$$

$$g_{b,t}^{dis} \leq \overline{G}_b^{dis} - (\overline{G}_b^{dis} / \overline{G}_b^{cha}) \cdot g_{b,t}^{cha}, \forall b \in \mathcal{B}_p, t \in \mathcal{T}; \quad (4-31)$$

$$\underline{Q}_b \leq q_{b,t} \leq \overline{Q}_b, \forall b \in \mathcal{B}_p, t \in \mathcal{T}; \quad (4-32)$$

$$\sum_{t \in \mathcal{T}} g_{f,t}^+ = \sum_{t \in \mathcal{T}} g_{f,t}^-, \forall f \in \mathcal{F}_p; \quad (4-33)$$

$$0 \leq g_{f,t}^+ \leq \overline{G}_{f,t}^+, \forall f \in \mathcal{F}_p, t \in \mathcal{T}; \quad (4-34)$$

$$0 \leq g_{f,t}^- \leq \overline{G}_{f,t}^-, \forall f \in \mathcal{F}_p, t \in \mathcal{T}; \quad (4-35)$$

$$\frac{g_{f,t}^-}{\overline{G}_f^-} + \frac{g_{f,t}^+}{\overline{G}_f^+} \leq 1, \forall f \in \mathcal{F}_p, t \in \mathcal{T}; \quad (4-36)$$

$$0 \leq g_{k,t}^{curt} \leq \hat{g}_{k,t}, \forall k \in \mathcal{J}_p^{WP}, t \in \mathcal{T}; \quad (4-37)$$

$$0 \leq g_{d,t}^{gsh} \leq \hat{g}_{d,t}, \forall d \in \mathcal{D}_p, t \in \mathcal{T}; \quad (4-38)$$

$$0 \leq q_{d,t}^{qsh} \leq \hat{q}_{d,t}, \forall d \in \mathcal{D}_p, t \in \mathcal{T}; \quad (4-39)$$

where  $\Xi_p = \{g_{i,t}, g_{k,t}^{curt}, q_{i,t}^+, q_{i,t}^-, q_{k,t}^w, g_{d,t}^{psh}, q_{d,t}^{qsh}, g_{b,t}^{cha}, g_{b,t}^{dis}, SOC_{b,t}, g_{f,t}^+, g_{f,t}^-, q_{b,t}^+, q_{b,t}^-, q_{c,t}^+, q_{c,t}^-\} \geq 0 \cup \{p_{n,m,t}, q_{n,m,t}, V_{n,t}, \theta_{n,m,t}, q_{c,t}, q_{b,t}, q_{i,t}\}$  is the set of decision variables for each entity  $p \in \mathcal{P}$ .

The objective (4-1) minimises all operational costs for the operator or subsystem  $p$ , co-optimising both active and reactive power related dispatch and procurement of flexible sources - curtailment of renewable generation, storage sources for active and reactive power, demand response as well as conventional sources of flexibility of conventional components, such as flexible generators,

capacitor banks in distribution grids or shunt capacitors in transmission grids providing voltage support. More precisely: i) marginal costs of conventional and renewable generators' active power, reactive power - represented by the cost function  $\mathbb{C}^J(\cdot)$  in (4-2); ii) active and reactive power import and export costs of sub-system  $p$  through the interface with the adjacent DSO or TSO, represented by the cost function  $\mathbb{C}^{int}(\cdot)$  in (4-3); iii) battery energy storage systems (ESS) active and reactive power costs - described by the cost function  $\mathbb{C}^B(\cdot)$  in (4-4); iv) costs for the demand response provided through flexible loads by increasing and decreasing their demand - described by the cost function  $\mathbb{C}^F(\cdot)$  in (4-5); v) curtailment costs for renewable generation - represented by the cost function  $\mathbb{C}^{curt}(\cdot)$  in (4-6); vi) marginal costs for capacitor banks - represented by the cost function  $\mathbb{C}^c(\cdot)$  in (4-7); vii) active or reactive power load-shedding as a costly last resort instrument (4-8).

Constraint (4-9) is the active power balance equation per node including interface nodes of the respective subsystem  $p$  - conventional generation, forecast renewable generation minus curtailment, load net of active power load-shedding and demand response, active power provided or consumed by storage system, power flow through the respective branch, as well as exported/imported power flow if the node is at the interface with another subsystem.

Constraint (4-10) and (4-13) splits the active and reactive power export/import into two positive variables to appropriately model absolute values, since both positive and negative values represent a cost in the objective function. Similar split is performed for constraints in relation to reactive power provided by conventional and renewable generators (4-14), by capacitor banks (4-15), and by batteries (4-16).

Equation (4-11) defines the active power flow formulation, which follows an AC bus injection type of model with voltage magnitudes at each bus represented in a polar form [19], such that active and reactive power injections per bus at each time period are equal to the total injections and withdrawals at the bus at that time period, i.e.,  $p_{n,t} = \sum_{m \in \mathcal{N}_{pn}} p_{n,m,t}, \forall m \in \mathcal{N}_{pn}, n \in \mathcal{N}_p, t \in \mathcal{T}$ , and,  $q_n = \sum_{m \in \mathcal{N}_{pn}} q_{n,m}, \forall m \in \mathcal{N}_{pn}, n \in \mathcal{N}_p, t \in \mathcal{T}$ . The phase angle  $\theta_{n,m,t}$  is given by:

$$\theta_{n,m,t} = \theta_{n,t} - \theta_{m,t}, \forall m \in \mathcal{N}_{pn}, n \in \mathcal{N}_p, t \in \mathcal{T}; \quad (4-40)$$

Constraint (4-12) is the reactive power balance, between demand minus load-shed, and, supply by conventional, renewable generation, battery, capacitor banks, and reactive power flow per node including interface nodes. Equation (4-17) defines reactive power flow formulation.

Equation (4-18) describes the active and reactive power flow restricted

by apparent power limits. Equation (4-19) limits voltage per node.

Constraint (4-20) – (4-23) is minimum and maximum capacity, ramping, reactive power limits for conventional and weather-dependent generation, respectively. Equation (4-24) sets operational limits for capacitor banks providing reactive power support.

Equations (4-25) – (4-29) model charging, discharging and state-of-charge (SOC) limits, and how SOC of each BESS depending on the SOC of the previous period and charge and discharge quantities multiplied by efficiency factors. BESS operations are typically captured by constraints involving binary variables so that charging and discharging would not occur at the same time. These binaries make the problem mixed-integer and non-convex, which require significant extra computational resources. This work considers a linear formulation without binaries which is proposed in [139]. This formulation is shown to be tighter than other linear battery models in the literature, and expected to provide solutions close to the exact mixed-integer linear model. Non-exclusivity of charging and discharging are reflected in equations (4-29) – (4-31) as in [139]. Equation (4-32) gives reactive power limits of each BESS.

Equation (4-33) – (4-36) are with respect to the flexible loads or demand response, following the formulation in [65], maintaining energy balance of the demand response sources over the analysed horizon to capture the fact that demand remains the same over the studied period but can be shifted to another hour by a percentage. In addition, bounds for the active power increase or reduction by demand response providers and capturing non-exclusivity of load increase and decrease for a given period, are provided respectively.

Equation (4-37) sets curtailment limits of weather-dependent units per hour bounded by generation forecast. Constraints (4-38) and (4-39) give load-shedding limited by active/reactive power demand, respectively.

## 4.4

### Solution Methodology

The problem of each entity  $p$  is non-linear and non-convex due to power flow-related trigonometric variables. In this Section Second-Order-Cone Programming reformulation of each operator’s problem, and proposed ADMM-based methods to obtain equilibrium points for this problem and computational enhancements with a Two-Level ADMM as well as a decentralised implementation are described. In addition, a sequential linearisation for the AC power flow formulation presented.

#### 4.4.1

### Second-Order Cone Programming (Convex) Reformulation of Each Individual Operator's Problem

Following [20], the subsequent transformations are applied to the AC power flow formulation:

$$c_{n,n,t} = (V_{n,t})^2, \quad \forall n \in \mathcal{N}_p, t \in \mathcal{T}; \quad (4-41)$$

$$c_{n,m,t} = V_{m,t} \cdot V_{n,t} \cdot \text{Cos}(\theta_{n,m,t}), \\ \forall m \in \mathcal{N}_{p_n}, n \in \mathcal{N}_p, t \in \mathcal{T}; \quad (4-42)$$

$$s_{n,m,t} = V_{m,t} \cdot V_{n,t} \cdot \text{Sin}(\theta_{n,m,t}), \\ \forall m \in \mathcal{N}_{p_n}, n \in \mathcal{N}_p, t \in \mathcal{T}; \quad (4-43)$$

These transformations result in:

$$p_{n,m,t} = G_{n,m} \cdot c_{n,n,t} - G_{n,m} \cdot c_{n,m,t} + \\ + B_{n,m} \cdot s_{n,m,t}, \quad \forall m \in \mathcal{N}_{p_n}, n \in \mathcal{N}_p, t \in \mathcal{T}; \quad (4-44)$$

$$q_{n,m,t} = (B_{n,m} - b_{n,m}^{\text{shunt}}) \cdot c_{n,n,t} - G_{n,m} \cdot s_{n,m,t} + \\ - B_{n,m} \cdot c_{n,m,t}, \quad \forall m \in \mathcal{N}_{p_n}, n \in \mathcal{N}_p, t \in \mathcal{T}; \quad (4-45)$$

Accordingly, equations (4-46)–(4-48) are obtained:

$$c_{n,m,t} = c_{m,n,t}, \quad \forall m \in \mathcal{N}_{p_n}, n \in \mathcal{N}_p, t \in \mathcal{T}; \quad (4-46)$$

$$s_{n,m,t} = -s_{m,n,t}, \quad \forall m \in \mathcal{N}_{p_n}, n \in \mathcal{N}_p, t \in \mathcal{T}; \quad (4-47)$$

$$c_{n,m,t}^2 + s_{n,m,t}^2 = c_{n,n,t} \cdot c_{m,m,t}, \\ \forall m \in \mathcal{N}_{p_n}, n \in \mathcal{N}_p, t \in \mathcal{T}; \quad (4-48)$$

The equality constraint (4-48) constitutes a non-convex region, since it describes the surface - excluding its interior region - of a rotated second-order cone in four dimensions. This reformulation is exact for radial networks and equivalent to the SDP relaxation; whereas for meshed networks additional constraints need to be included with further specification of voltage angles for exactness [19, 75]. The second-order conic relaxation of this reformulation is provided by the inequality constraint (4-49) yielding a rotated second-order cone now including its interior:

$$c_{n,m,t}^2 + s_{n,m,t}^2 \leq c_{n,n,t} \cdot c_{m,m,t}, \\ \forall m \in \mathcal{N}_{p_n}, n \in \mathcal{N}_p, t \in \mathcal{T}; \quad (4-49)$$

The SOCP final formulation of each entity's problem is provided below - which is convex, and can be solved by a standard off-the-shelf solver. For each entity  $p$ :

$$\min_{\Xi_p} \text{Equation (4-1);} \quad (4-50)$$

subject to:

$$\begin{aligned} \text{Constraints: (4-9), (4-10), (4-12) - (4-16), (4-18) - (4-39),} \\ (4-44) - (4-47), \text{ and (4-49);} \end{aligned} \quad (4-51)$$

#### 4.4.2 DSO-TSO Common Centralised Problem

A DSO-TSO common, centralised problem which co-optimises all TSOs' and DSOs' objectives, given by  $f_p(\cdot), \forall p \in \mathcal{P}$  representing each entity or subsystem, mitigation of congestion and voltage management of embedded systems, subject to all networks constraints of DSOs, TSOs including their interfaces. Note that this centralised formulation is not a realistic or adequate application, because no such centralised entity exists knowing all transmission and distribution system parameters and constraints [22]. Furthermore, if the entities have conflicting interests such a centralised problem may not be directly constructed, except as a multi-objective optimisation problem. In this work, all entities involved have the objective to minimise their cost function which allows defining the central objective of the system as a co-optimisation of costs for all entities subject to their individual operational constraints and power flows at each branch including those linking interface buses of each entity, i.e., tie-lines. Accordingly, the common centralised problem is provided as a benchmark.

The centralised problem involves the so-called global or consensus variables as such they are common to more than one agent and the individual agents need to agree on their value. Accordingly, it can be regarded as an equilibrium-seeking problem on the joint variables, denoted as  $\mathbf{z}$ . Let  $\mathbf{x}_p$  be the vectors of decision variables of each entity  $p \in \mathcal{P}$ .

The centralised problem can be abstracted as follows. Constraint (4-52) comprises objective functions of the  $p$ -entities related problems, respectively. Constraint (4-53) represents the coupling constraints related to the variables at interface nodes and branches. Constraint (4-54) is the distinct feasible space

for each entity.

$$\min_{\mathbf{x}, \mathbf{z}} \sum_{p \in \mathcal{P}} (f_p(\mathbf{x}_p)) \quad (4-52)$$

subject to:

$$\mathbf{x}_p - \mathbf{z} = \mathbf{0}, \forall p \in \mathcal{P}; \quad (4-53)$$

$$\mathbf{x}_p \in \Xi_p, \quad \forall p \in \mathcal{P}; \quad (4-54)$$

### 4.4.3

#### Alternating Direction Method of Multipliers

In order to compute equilibrium set points for all entities [141] considering their objectives and constraints, distributed methods such as ADMM-based methods can be applied. These methods permit preservation of privacy of sensitive and agent-specific data. ADMM, within the context of this work, can also be interpreted as crunching complex and impracticable centralised optimisation problem of the power system, by crunching it into smaller problems and with a limited information interchange amongst the agents.

ADMM is based on the minimisation of the Lagrangian function, - performed on its augmented form -, and update of dual variables. In the ADMM, the primal variable updates are performed in an alternating or sequential manner.

For the ADMM procedure, firstly the centralised problem is transformed into a separable form, which is naturally not separable due to the subsystems coupled with each other via the tie-lines, i.e., the linking constraint (4-54). Additionally, as shown in [141], the common centralised problem can be decomposed into each of the DSOs' and TSOs' sub-problems by relaxing the coupling constraints, and solved in a distributed fashion. When adequate conditions hold, centralised and distributed problems converge to the same optimal solution and objective values.

By creating a local decision copy of the coupling variables  $\tilde{\mathbf{x}}_p^C$  per agent, the centralised problem in a separable form can be formulated as follows.

$$\min_{\mathbf{x}, \mathbf{z}} \sum_{p \in \mathcal{P}} (f_p(\mathbf{x}_p)) \quad (4-55)$$

subject to:

$$\tilde{\mathbf{x}}_p^C - \mathbf{z}_p^C = \mathbf{0}, \forall p \in \mathcal{P}; \quad (4-56)$$

$$\mathbf{x}_p \in \Xi_p, \quad \forall p \in \mathcal{P}; \quad (4-57)$$

where  $\mathbf{x}_p$  includes local variables  $\bar{\mathbf{x}}_p$  and coupling variables  $\tilde{\mathbf{x}}_p^C$ , i.e.,  $\mathbf{x}_p =$

$[\bar{\mathbf{x}}_p, \tilde{\mathbf{x}}_p^C]$ . The vector  $\mathbf{z}_p^C$  consists of global variables linking the same variables duplicated in other subsystems.

The Lagrangian function is constructed as follows, where  $\boldsymbol{\lambda}_p$  is the Lagrange multiplier of (4-56):

$$\mathcal{L}_\rho(\mathbf{x}_p, \mathbf{z}, \boldsymbol{\lambda}_p) = \sum_{p \in \mathcal{P}} (f_p(\mathbf{x}_p) + \boldsymbol{\lambda}_p^T \cdot (\tilde{\mathbf{x}}_p^C - \mathbf{z}_p^C) + \frac{\rho}{2} \cdot \|\tilde{\mathbf{x}}_p^C - \mathbf{z}_p^C\|_2^2), \forall p \in \mathcal{P}; \quad (4-58)$$

Accordingly, at each iteration  $k$ , primal variable update is performed by:

$$\mathbf{x}_p^{k+1} = \operatorname{argmin}_{\mathbf{x}_p} (f_p(\mathbf{x}_p) + \boldsymbol{\lambda}_p^{k,T} \cdot \mathbf{x}_p + \frac{\rho}{2} \cdot \|\tilde{\mathbf{x}}_p^C - \mathbf{z}_p^{k,C}\|_2^2), \forall p \in \mathcal{P}; \quad (4-59)$$

Dual update is performed by:

$$\boldsymbol{\lambda}_p^{k+1} := \boldsymbol{\lambda}_p^k + \rho \cdot (\tilde{\mathbf{x}}_p^{k+1,C} - \mathbf{z}_p^{k+1,C}), \forall p \in \mathcal{P}; \quad (4-60)$$

Let  $(\tilde{\mathbf{x}}_p)_w$  be the  $w$ th variable of  $\tilde{\mathbf{x}}_p^C$ . A mapping from copied coupling variables  $\tilde{\mathbf{x}}_p^C$  onto the global variables  $\mathbf{z}_p^C$  is defined as  $g = G(p, w)$ . Global variable update is performed by calculating the average of all  $(\tilde{\mathbf{x}}_p)_w$  related to  $\mathbf{z}_g$ :

$$\mathbf{z}_g^{k+1} := \frac{\sum_{G(p,w)=g} (\tilde{\mathbf{x}}_p^{k+1,C})_w}{\sum_{G(p,w)=g} \mathbf{1}}, \forall g \in \mathcal{Z}; \quad (4-61)$$

This standard consensus ADMM algorithm stops when the primal and dual residuals in each sub-problem  $p$  is sufficiently small with an error tolerance level of  $\epsilon$ :

$$\|\mathbf{s}^{k+1}\|_2^2 = \rho \cdot \|\mathbf{z}_p^{k+1,C} - \mathbf{z}_p^{k,C}\|_2^2 \leq \epsilon_1, \forall p; \quad (4-62)$$

$$\|\mathbf{r}_p^{k+1}\|_2^2 = \|\boldsymbol{\lambda}_p^{k+1} - \boldsymbol{\lambda}_p^k\|_2^2 \leq \epsilon_2, \forall p; \quad (4-63)$$

#### 4.4.4 Decentralised ADMM

ADMM, in general, requires a central coordinator which collects data from subsystems, and aggregates and redistributes it during the optimisation procedure. In order to mitigate the need for a central coordinator, this work proposes a data exchange framework for the DSO-TSO coordination problem in which data interchange is amongst the neighbouring operator entities, or subsystems. This potentially reduces the communication and data

storage needs, which can make the problem more scalable and computationally efficient especially when realistic large-scale power systems are concerned. This decentralised communication structure is inspired by [144].

The idea of this decentralisation is illustrated in Fig. 4.1 with 1 TSO and 2 DSOs, or 3 subsystems S1, S2 and S3, which are interconnected with one another. Each subsystem has one boundary bus, namely,  $t$ ,  $b$  and  $j$ . The branches connecting  $t - b$ ,  $b - j$  and  $j - t$  are named as tie-lines. Accordingly, power flow constraints at these boundary buses makes the centralised problem not directly separable. For each subsystem, the coupling variables of boundary buses are duplicated, such that set of local variables  $\theta_b, \theta_j, \theta_t$  and copy variables, those having superscripts, are formed.

Standard ADMM communication mechanism is shown in Fig. 4.2. Global variables  $\mathbf{z}^C$  link the duplicated variables in different subsystems. For example,  $z_1^C$  links  $\theta_t, \theta_t^{S1}, \theta_t^{S2}$ . All copy variables calculated are transferred to the central controller, which calculates the values for  $z_1^C, z_2^C, z_3^C$  by taking averages of the copies received, and broadcasts to the subsystems. Detailed procedure of the distributed ADMM with the central controller is outlined in the inner-loop of the *Algorithm 1*.

The proposed decentralised communication strategy, based on [144], the computed values for copy variables related to  $\mathbf{z}^C$  are communicated to the assigned leading subsystem of the corresponding element in  $\mathbf{z}^C$ . The local operator of the leading subsystem computes the respective global variable  $\mathbf{z}^C \in \mathbf{Z}$ , which is the average value of the collected data for the respective consensus variable. This average value is sent back to the subsystems so that they can use this updated value in their computation.

This communication strategy is shown in Fig. 4.3. Details of this decentralised ADMM is presented in the inner-loop of the *Algorithm 2*. It can be observed that the standard ADMM in Fig. 4.2 requires exchange of 18 data points, whereas the proposed decentralised communication in Fig. 4.3 reduces it to 12 data points.

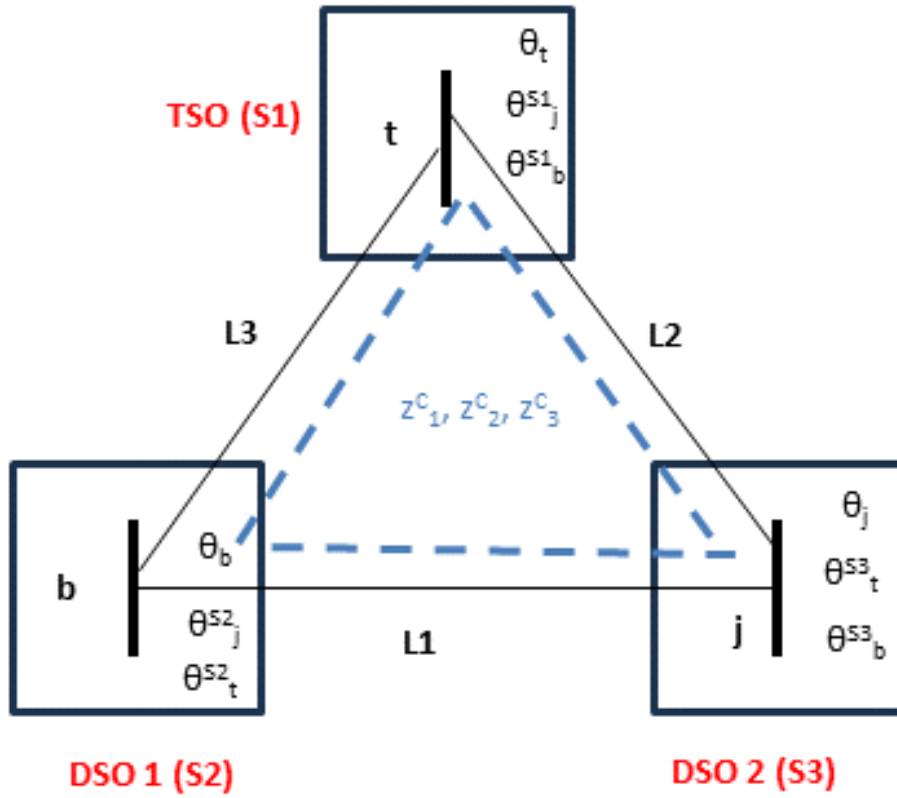


Figure 4.1: Illustration with 3-subsystems.

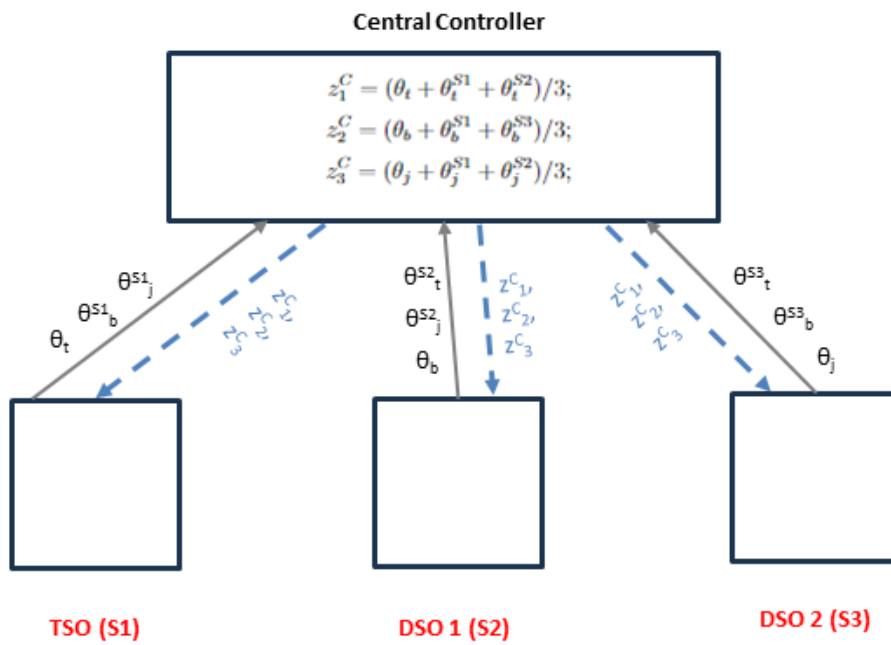


Figure 4.2: Standard ADMM with 3-subsystems.

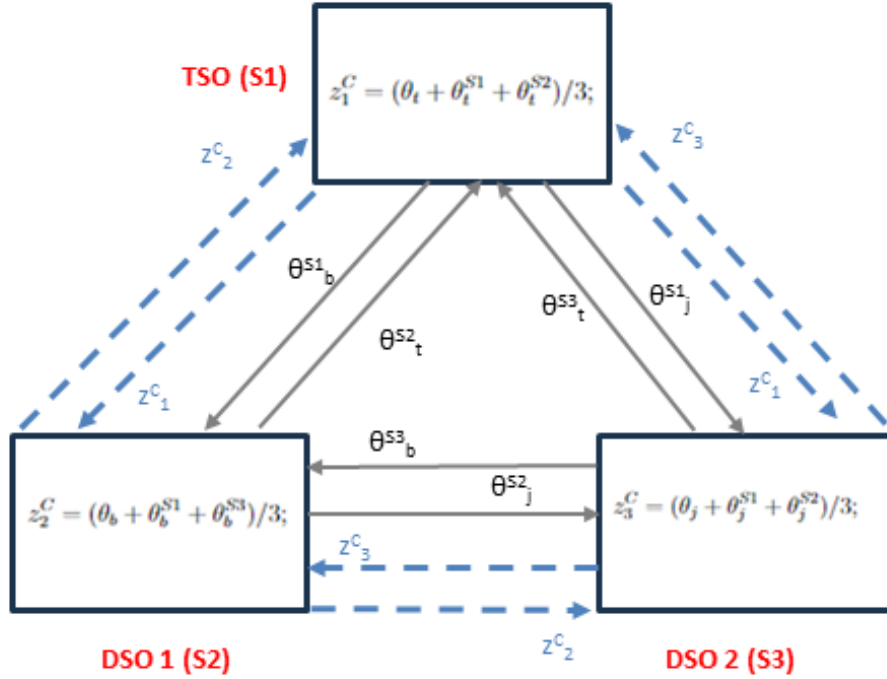


Figure 4.3: Decentralised ADMM with 3-subsystems.

#### 4.4.5

#### Proposed Distributed vs. Decentralised Two-level ADMM Algorithm

*Algorithm 1* outlines the two-level ADMM procedure. Two-level ADMM is a nested loop, consisting of inner and outer loops, procedure searching and updating two different sets of Lagrangian multipliers  $\lambda$  and  $\Lambda$ . Given a fixed  $\Lambda$ , the inner loop updates  $\lambda$  and slack variables  $\varphi$ . Outer loop, on the other hand, updates  $\Lambda$  and its penalty parameter  $\beta$  taking into account the solutions from the inner loop. This procedure, by exerting more control over the update of penalty parameters, is shown to be robust with enhanced convergence properties compared to standard ADMM. Standard ADMM has, in general, a current state-of-the-art limitation of needing significant parameter tuning. The main idea of two-level ADMM is to dualise and penalise slack constraints, and apply a multi-block ADMM to solve Augmented Lagrangian Relaxation (ALR) [149]. This method is shown to converge to an approximate stationary solution even when the problem is non-convex [149].

Regarding the two-level ADMM, slack variables, ( $\varphi$ ), are introduced into the coupling constraints, and it is ensured that slack variables converge to zero,

$\boldsymbol{\varphi} \rightarrow \mathbf{0}$ . Hence, the two-level ADMM is formulated as follows:

$$\min_{\mathbf{x}, \mathbf{z}, \boldsymbol{\varphi}} \sum_{p \in \mathcal{P}} (f_p(\mathbf{x}_p)) \quad (4-64)$$

subject to:

$$\tilde{\mathbf{x}}_p^C - \mathbf{z}_p^C + \boldsymbol{\varphi}_p = \mathbf{0}, \forall p \in \mathcal{P}; \quad (4-65)$$

$$\boldsymbol{\varphi}_p = \mathbf{0} : (\boldsymbol{\Lambda}_p), \forall p \in \mathcal{P}; \quad (4-66)$$

$$\mathbf{x}_p \in \Xi_p, \forall p \in \mathcal{P}; \quad (4-67)$$

Equations (4-65) -(4-66), being coupling constraints, when relaxed the  $p$ -agent problems become separable by agent. Standard consensus ADMM is formulated by relaxing these constraints, and constructing an augmented Lagrangian of the problem. Accordingly, the Lagrangian function is constructed as follows:

$$\begin{aligned} \mathcal{L}_{\rho, \beta}(\mathbf{x}_p, \mathbf{z}, \boldsymbol{\lambda}_p, \boldsymbol{\Lambda}_p) = & \sum_{p \in \mathcal{P}} (f_p(\mathbf{x}_p) + \boldsymbol{\lambda}_p^T \cdot (\tilde{\mathbf{x}}_p^C - \mathbf{z}_p^C + \boldsymbol{\varphi}_p) + \frac{\rho}{2} \cdot \|\tilde{\mathbf{x}}_p^C - \mathbf{z}_p^C + \boldsymbol{\varphi}_p\|_2^2 \\ & + \boldsymbol{\Lambda}_p^T \cdot \boldsymbol{\varphi}_p + \frac{\beta}{2} \cdot \|\boldsymbol{\varphi}_p\|_2^2); \end{aligned} \quad (4-68)$$

Given outer iteration counter  $t$ , at each inner iteration  $k$  primal variable update is performed by:

$$\begin{aligned} \mathbf{x}_p^{k+1} = \operatorname{argmin}_{\mathbf{x}_p} & \left( f_p(\mathbf{x}_p) + \boldsymbol{\lambda}_p^{k,T} \cdot \mathbf{x}_p + \frac{\rho}{2} \cdot \|\tilde{\mathbf{x}}_p^C - \mathbf{z}_p^{k,C} + \boldsymbol{\varphi}_p[k]\|_2^2 + \right. \\ & \left. \boldsymbol{\Lambda}_p^T \cdot \boldsymbol{\varphi}_p[t] + \frac{\beta}{2} \cdot \|\boldsymbol{\varphi}_p[k]\|_2^2 \right), \forall p \in \mathcal{P}; \end{aligned} \quad (4-69)$$

Dual update is performed by:

$$\boldsymbol{\lambda}_p^{k+1} := \boldsymbol{\lambda}_p^k + \rho \cdot (\tilde{\mathbf{x}}_p^{k+1,C} - \mathbf{z}_p^{k+1,C} + \boldsymbol{\varphi}_p[k]), \forall p \in \mathcal{P}; \quad (4-70)$$

Slack parameter update is performed by:

$$\boldsymbol{\varphi}_p[k+1] = (-\boldsymbol{\Lambda}_p[t] - \boldsymbol{\lambda}_p[k] - \rho \cdot (\mathbf{z}_p[k] - \mathbf{z}_p[k]^C)) / (\beta + \rho), \forall p \in \mathcal{P}; \quad (4-71)$$

Global variable update is performed by calculating the average of all  $(\tilde{\mathbf{x}}_p)_w$  related to  $\mathbf{z}_g$ :

$$\mathbf{z}_g^{k+1} := \frac{\sum_{G(p,w)=g} (\tilde{\mathbf{x}}_p^{k+1,C})_w}{\sum_{G(p,w)=g} \mathbf{1}}, \forall g \in \mathcal{Z}; \quad (4-72)$$

Update for the dual of the slack variable is given as follows:

$$\Lambda_p[t+1] = (\Lambda_p[t] + \beta \cdot \varphi_p[k]), \forall p \in \mathcal{P}; \quad (4-73)$$

where  $\rho > 0$  and  $\beta > 0$  are penalty parameters.

---

**Algorithm 1** Two-level Distributed ADMM Algorithm

---

- 0: *Initialisation*:  $\rho \leftarrow \rho_0, \beta \leftarrow 0.5 \cdot \rho_0, t \leftarrow 1$
  - 1: **while** outer stopping criteria not satisfied **do**
  - 2:   initialise  $\lambda[k], \varphi[k], \Lambda[t], k \leftarrow 1$
  - 3:   **while** inner stopping criteria not satisfied **do**
  - 4:     Parallel run **Algorithm 3** for each entities' (subsystems) problems, store optimal values for primal variables  $\tilde{\mathbf{x}}_p^C, \forall p \in \mathcal{P}$
  - 5:     Each subsystem  $p \in \mathcal{P}$  sends  $\tilde{\mathbf{x}}_p^C$  to the central controller.
  - 6:     Slack parameter update: The central controller updates slack parameters via (4-71).
  - 7:     Lagrange multiplier update: Each subsystem updates Lagrange multipliers locally via (4-70).
  - 8:     Consensus update: The central controller updates  $\mathbf{z}_g, \forall g \in \mathcal{Z}$  through (4-72).
  - 9:     The central controller sends  $\mathbf{z}_g$  to each subsystem  $p$ .  
 $k \leftarrow k + 1$
  - 10:   **end while**
  - 11:   Outer-level dual variable update: Each subsystem updates Lagrange multipliers locally via (4-73).
  - 12:   Penalty parameter update: The central controller updates outer-level penalty parameters.  
 $\beta \leftarrow c_\beta \cdot \beta; \rho \leftarrow 2 \cdot \beta$   
 $t \leftarrow t + 1$
  - 13: **end while**=0
- 

#### 4.4.6

##### Stopping Criteria for Two-Level ADMM Algorithm

In this work, the inner loop of the Two-Level ADMM stops if  $\|\varphi[k] - \varphi[k-1]\| \leq \epsilon$  where  $\epsilon$  stands for an error tolerance level. The outer loop of the Algorithm stops if the consensus terms match each other, i.e.,  $\|\mathbf{z}[k] - \mathbf{z}^C[k] + \varphi[k]\| \leq \epsilon$ .

#### 4.4.7

##### Proposed Linearisation-Based Power Flow Algorithm

In order to enhance the solution in computational robustness and accuracy, compared to a standard SOCP which tends to be inaccurate in various

---

**Algorithm 2** Two-level Decentralised ADMM Algorithm

---

0: *Initialisation*:  $\rho \leftarrow \rho_0, \beta \leftarrow 0.5 \cdot \rho_0, t \leftarrow 1$

1: **while** outer stopping criteria not satisfied **do**

2:   initialise  $\lambda[k], \varphi[k], \Lambda[t], k \leftarrow 1$

3:   **while** inner stopping criteria not satisfied **do**

4:     Parallel run **Algorithm 3** for each entities' (subsystems) problems, store optimal values for primal variables  $\tilde{\mathbf{x}}_p^C, \forall p \in \mathcal{P}$

5:     Each subsystem  $p \in \mathcal{P}$  sends  $\tilde{\mathbf{x}}_p^C$  related to the linked  $\mathbf{z}_g$  to its responsible leading subsystem.

6:     Leading subsystem of  $\mathbf{z}_g, p \in \mathcal{P}$  sends  $\tilde{\mathbf{x}}_p^C$  to the respective leading subsystem responsible for that variable.

7:     Slack parameter update: The respective leading subsystem updates slack parameters via (4-71).

8:     Lagrange multiplier update: Each subsystem updates Lagrange multipliers locally via (4-73).

9:     Consensus update: The leading subsystem of  $\mathbf{z}_g$  updates  $\mathbf{z}_g, \forall g \in \mathcal{Z}$  through (4-72).

10:     The leading subsystem sends updated  $\mathbf{z}_g$  to respective neighbouring subsystems  $p$ .  
        $k \leftarrow k + 1$

11:   **end while**

12:   Outer-level dual variable update: Each subsystem updates Lagrange multipliers locally via (4-73).

13:   Penalty parameter update: One leading subsystem updates outer-level penalty parameters, and each leading subsystem sends to neighbouring entities.  
        $\beta \leftarrow c_\beta \cdot \beta; \rho \leftarrow 2 \cdot \beta$   
        $t \leftarrow t + 1$

14: **end while**=0

---

instances with high-system loading conditions resulting in larger deviations from AC-feasible set-points. Also given the fact that for SOCP, the solvers are still less mature than a linear programming solver, a linearisation of power flow formulation procedure is applied as in [20]. As a result of this step, each entity-related problem becomes a linear programming programming. The formulation here is based on the circular formulation with the valid bounds of voltage, i.e.,  $0 \leq c_{n,m,t}^2 + s_{n,m,t}^2 \leq (\bar{V}_n)^2 \cdot (\bar{V}_m)^2, \forall m \in \mathcal{N}_n, \forall n \in \mathcal{N}, t \in \mathcal{T}$ , The algorithm is constructed in the following fashion: In the *Initialisation* step, the algorithm initialises the iteration counter,  $\nu$ , and, the initial set value for discretisation-related variables  $\alpha$  and  $\alpha'$ . A master problem is constructed by (4-74)–(4-78), which includes linearisation for circle approximation of conic constraints. Therefore, each agent's optimisation problem becomes a linear programming problem. The pseudo-code of this decomposition procedure is

presented in *Algorithm 3*.

*Master problem solution:*

$$\text{Solve equation (4-59), which is augmented from (4-1);} \quad (4-74)$$

subject to:

Constraints: (4-9), (4-10), (4-12) – (4-16), (4-20) – (4-39),

$$(4-44) – (4-47), ; \quad (4-75)$$

$$(\underline{V}_n)^2 \leq c_{n,n,t} \leq (\overline{V}_n)^2, \quad \forall n \in \mathcal{N}_p, t \in \mathcal{T}; \quad (4-76)$$

$$-\frac{-\alpha_{n,m,t}^{(\mu)} \cdot p_{n,m,t} + (\overline{S}_{n,m})^2}{\sqrt{(\overline{S}_{n,m})^2 - \alpha_{n,m,t}^{(\mu)2}}} \leq q_{n,m,t} \leq$$

$$\frac{-\alpha_{n,m,t}^{(\mu)} \cdot p_{n,m,t} + (\overline{S}_{n,m})^2}{\sqrt{(\overline{S}_{n,m})^2 - \alpha_{n,m,t}^{(\mu)2}}},$$

$$\forall m \in \mathcal{N}_{p_n}, n \in \mathcal{N}_p, t \in \mathcal{T}, \mu = 0, \dots, \nu; \quad (4-77)$$

$$-\frac{-\alpha'_{n,m,t}^{(\mu)} \cdot c_{n,m,t} + (\overline{V}_n)^2 \cdot (\overline{V}_m)^2}{\sqrt{(\overline{V}_n)^2 \cdot (\overline{V}_m)^2 - \alpha'_{n,m,t}^{(\mu)2}}} \leq s_{n,m,t} \leq$$

$$\frac{-\alpha'_{n,m,t}^{(\mu)} \cdot c_{n,m,t} + (\overline{V}_n)^2 \cdot (\overline{V}_m)^2}{(\overline{V}_n)^2 \cdot (\overline{V}_m)^2 - \alpha'_{n,m,t}^{(\mu)2}},$$

$$\forall m \in \mathcal{N}_{p_n}, n \in \mathcal{N}_p, t \in \mathcal{T}, \mu = 0, \dots, \nu; \quad (4-78)$$

---

**Algorithm 3** Decomposition Algorithm for Each Entity's Problems

---

*Initialisation:*

Set  $\mu \leftarrow 0$ ; Set  $\nu \leftarrow 0$ ;

Set  $\alpha_{n,m,t}^\nu \leftarrow \alpha_{n,m,t}^{\text{ini}}, \forall m \in \mathcal{N}_{p_n}, n \in \mathcal{N}_p, t \in \mathcal{T}$ ;

Set  $\alpha'_{n,m,t}{}^\nu \leftarrow \alpha'_{n,m,t}{}^{\text{ini}}, \forall m \in \mathcal{N}_{p_n}, n \in \mathcal{N}_p, t \in \mathcal{T}$ ;

Solve **master problem** given by (4-74)–(4-78), store its optimal solution  $((p_{n,m,t})^\nu, (q_{n,m,t})^\nu, c_{n,m,t}^\nu, s_{n,m,t}^\nu)$ , and, objective function value  $\text{TotalCost}^{(\nu)}$ ;

*Iteration  $\nu \geq 1$*

**Step 1:** Run **sub-problems**.  $\forall m \in \mathcal{N}_{p_n}, n \in \mathcal{N}_p, t \in \mathcal{T}$ , compute projection of  $(p, q)$  on its respective circular region:  $((p')^{(\nu-1)}, q^{(\nu-1)})$ , where  $(p')^{(\nu-1)} = \overline{S}^2 - (q^2)^{(\nu-1)}$ . Similarly compute projection of  $(c, s)$  on its respective circle:  $(c')^{(\nu-1)}, s^{(\nu-1)}$  where  $(c')^{(\nu-1)} = \overline{V}_n^2 \cdot \overline{V}_m^2 - (s^2)^{(\nu-1)}$ . Set  $\alpha^{(\nu)} \leftarrow (p')^{(\nu-1)}$ . Set  $(\alpha')^{(\nu)} \leftarrow (c')^{(\nu-1)}$ . Store  $\alpha^{(\nu)}, \alpha'^{(\nu)}$ ;

**Step 2:** If  $\text{Gap} \leq \epsilon$ , then stop. Otherwise, go to **Step 3**;

**Step 3:**  $\forall \mu = 1, \dots, \nu$ , solve master problem consisting of (4-74)–(4-78). Store its optimal solution  $((p_{n,m,t})^{(\nu)}, (q_{n,m,t})^{(\nu)}, c_{n,m,t}^{(\nu)}, s_{n,m,t}^{(\nu)})$ , and, objective function value,  $\text{TotalCost}^{(\nu)}$ . Set  $\nu \leftarrow \nu + 1$ . Go to **Step 1**.

---

## 4.5

### Numerical Experiments

In order to demonstrate the computational capability of the proposed approach, in this section, a comparison amongst a centralised solution to the DSO-TSO joint problem as a benchmark, a distributed approach based on a standard ADMM as well as a two-level ADMM with different penalty parameters are provided.

#### 4.5.1

##### Motivating Example

This motivating example is based on a 7-bus system consisting of 3 generators and 4 loads as depicted in Fig. 4.4. Data for generators and branches are provided in Table 4.1. In order to illustrate the key aspects of the proposal, the analysis is performed on one-hour, inelastic demand and by considering a DC-power flow formulation without considering any flexibility in the system.

Two cases studied, Case 1 and Case 2, are composed of the partition of the 7-bus system into two and three sub-systems, respectively. Table 4.2 and Fig. 4.4 show what this partition entails. Case 1 considers that the buses B5 and B4 are linked with a branch with the same characteristics as, e.g., the line L5. Standard ADMM and 2-level ADMM are applied under different choices of the penalty parameter  $\rho > 0$  with error tolerance of  $\epsilon = 10^{-4}$ . Fig. 4.5 shows the convergence rate of Case 1, and Table 4.3 presents both Case 1 and Case 2 with different values of  $\rho$ . The results indicate that the choice of  $\rho$  plays a significant role in the convergence rate, a value of 8 giving the best result in Case 1. The same  $\rho$ , such as of value 8, can result in different convergence speed in different cases. A poor choice of  $\rho$  can lead to non-convergence, as observed in Case 2 at a value of 2. These observations support earlier findings, e.g., in [144].

Table 4.3 also demonstrates that the number of blocks, i.e., decision entities, for the ADMM procedure impacts the convergence results. 3-block ADMM, in this study Case 2 with 3 subsystems, does not have convergence guarantees, whereas Case 1 has such guarantees. Despite the fact that both

cases converge, Case 1 requires much less number of iterations than Case 2. Number of global variables also plays a role in the convergence performance. Case 1 has 3 global variables and Case 2 has 6 global variables, and accordingly it has less number of data exchange and iterations to reach to a consensus.

The convergence performance of a 2-level ADMM against a standard ADMM is reported in Table 4.3. Two-level ADMM number of iterations are represented as total iterations for comparability, since these are repeated after the outer loop run. In general, computational time is impacted by number of iterations needed, which is relatively high, e.g., for Case 2 with 3 subsystems with  $\rho = 2$ . The two-level ADMM depicts a superior performance, especially in Case 2 where standard ADMM needs a significantly larger number of iterations even when the penalty parameter is relatively well-tuned, e.g.  $\rho = 100$  in Case 2. Noted is also that the the outer-level iterations of two-level ADMM do not need a significant computational effort, as they principally compute parameters for next iterations. The solution quality is also preserved with a moderate error tolerance level of  $\epsilon = 10^{-4}$ , towards which the number of iterations can be sensitive to. Fig. 4.6 illustrates that, albeit the fact that both for standard ADMM and two-level ADMM the same initialisation is applied with a neutral assignment of zero to each consensus variables, 2-level ADMM quickly reaches to a tighter optimality gap after 6 iterations to below  $10^{-2}$  accuracy. ADMM needs 11 iterations to reach such a level. Two-level ADMM shows larger fluctuations or jumps over the subsequent iterations. It is most likely due to the fact that the outer loop in the two-level ADMM exerts control on the inner loop, and provides feedback which becomes of essence when the subsequent iterations do not improve. This control and feedback results in jumps, which reach to a more stable situation until the next feedback arrives. Standard ADMM, lacking such a manager, remains stable for possibly a long time without any improvement.

Moreover, Table 4.3 also reports two-level ADMM under a decentralised communication strategy. We note that the proposed decentralised ADMM would not reduce the number of iterations needed for the ADMM computation, since the exchanged parameter values would be the same amongst the subsystems. Reduction of communication bottleneck may translate into computational savings. Although some time savings have been reported compared to standard distributed two-level ADMM, the benefits can potentially be more pronounced for large system related computation.

In terms of coordination aspects, looking into the Case 2 with 3 subsystems, subsystem S2 is reliant on the interface flows from the other two systems to be able to serve the demand within its jurisdiction of 300 MW

in total whereas it has a total generation capacity of 200 MW. Particularly, with the given demand and generation parameters, S2 would ideally receive an active power flow of 121.88 MW from S3. In case the actions of these two subsystems are uncoordinated, in a situation of congestion, e.g., due to a surge in demand in S3, or alternatively weather conditions causing a lower-than-anticipated renewable generation by G3 S2 may not be able to serve the demand within its system. Similarly, S1 is a net power provider for S2 through their interface. Hence, uncoordinated operations of interconnected systems can cause high system costs as a whole due to emergency actions which can be required. Moreover, an effective coordination can enhance access to lower-cost generation from adjacent subsystems, giving rise to efficiency.

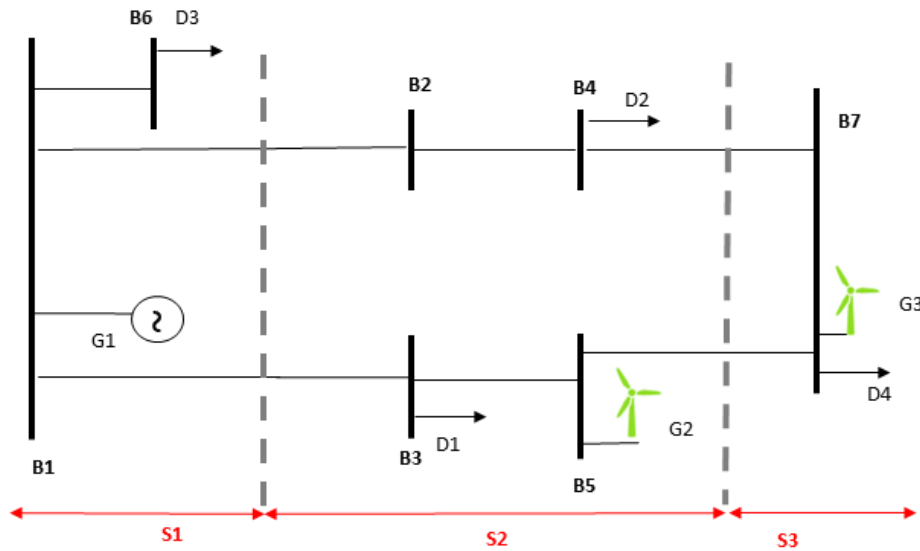


Figure 4.4: 7-bus system with 3 sub-systems.

Table 4.1: 7-Bus system branch data.

Lines	From	To	$x$ [p.u.]	FMax [MW]	Demand node	Demand [MW]
L1	1	2	0.6	150	D1	150
L2	1	3	0.6	150	D2	150
L3	2	4	0.1	150	D3	10
L4	3	5	0.1	150	D4	10
L5	4	7	0.1	150		
L6	1	6	0.1	150		
L7	5	7	0.1	150		

Table 4.2: 7-Bus system 2-Case studies.

Case Nb.	Subsystems	Tie-lines	Nb. global var.
1	S1=1,6 S2 = 2, 3, 4, 5	L1 and L2	3
2	S1=1,6 S2=2,3,4,5 S3=7	L1 and L2 L5 and L7	6

Table 4.3: 7-Bus system computational results.

Case 1 2 sub-systems	Comput. time [s.]	Nb. iterat.	Nb. outer loop iterat.	Convergence yes/no
$\rho = 2$				
Standard ADMM	22.804	284	-	yes
2-level ADMM	6.318	50	10	yes
2-level ADMM decentral	6.060	50	10	yes
$\rho = 8$				
Standard ADMM	11.835	49	-	yes
2-level ADMM	5.272	40	7	yes
2-level ADMM decentral	5.159	40	7	yes
$\rho = 100$				
Standard ADMM	18.510	234	-	yes
2-level ADMM	5.895	48	8	yes
2-level ADMM decentral	5.676	48	8	yes
<b>Case 2 3 sub-systems</b>				
$\rho = 2$				
Standard ADMM	102.628	1000	-	no
2-level ADMM	102.228	917	6	yes
2-level ADMM decentral	93.642	917	6	yes
$\rho = 8$				
Standard ADMM	118.961	978	-	yes
2-level ADMM	61.216	416	6	yes
2-level ADMM decentral	51.777	416	6	yes
$\rho = 100$				
Standard ADMM	49.448	398	-	yes
2-level ADMM	38.481	221	5	yes
2-level ADMM decentral	29.446	221	5	yes

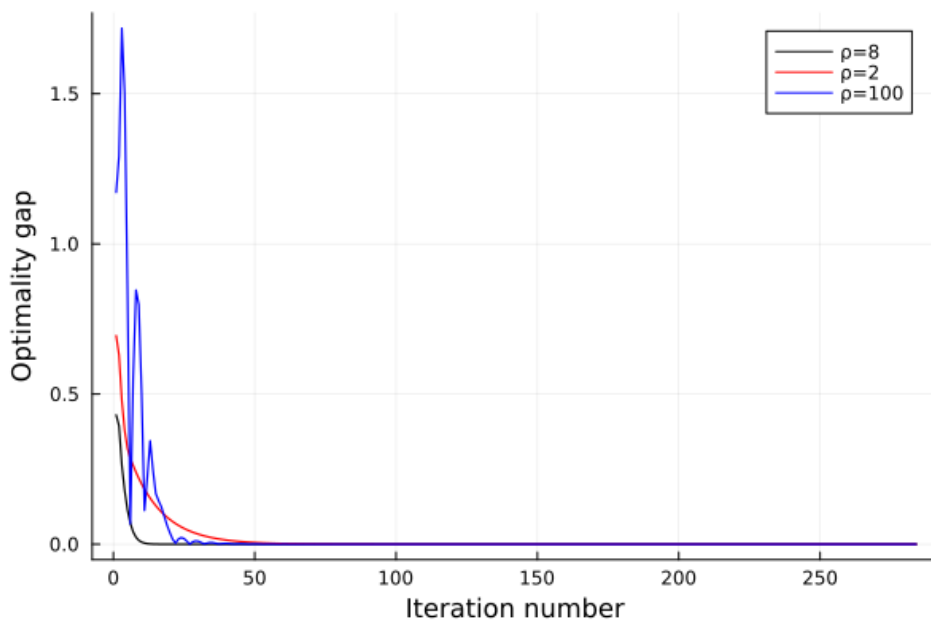


Figure 4.5: Case 1 with 2 sub-systems: Optimality gap per iteration for standard ADMM results with different values of  $\rho$ .

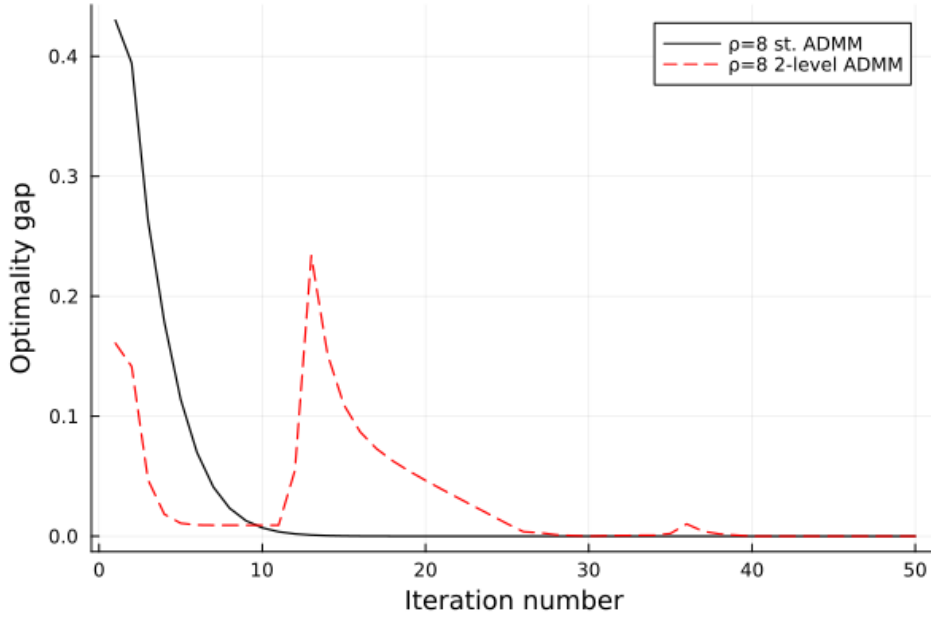


Figure 4.6: Case 1 with 2 sub-systems: Optimality gap per iteration standard ADMM vs. 2-level ADMM results with  $\rho = 8$ .

#### 4.5.2

##### Case Study on IEEE 118-bus system connected with two 33-bus systems

In this Section, a two-level network with a high-voltage (HV) transmission and medium-voltage (MV) distribution level networks are considered. At the HV level, a modified IEEE 118-bus test transmission system, which is based on the American Electric Power System in the U.S. Midwest, is studied to highlight congestion and voltage aspects with high penetration of renewable generation, in which wind and solar farms of 4.264 GW of rated power is considered. This system is comprised of 186 transmission lines, 28 conventional of which 9 hydro power plant as well as 26 weather-dependent generation - wind and solar - facilities.

At the MV level, two radial distribution systems based on a modified 33-bus test system in order to be able to co-operate via tie-lines jointly with the 118-bus system [155], with an identical topology. These distribution systems are connected to the interface nodes 4 and 8 of the transmission network, respectively. The two distribution networks are connected through the nodes 144 and 178. We note that interconnection amongst DSOs may not be common in the current power systems, though is observed for instance at the border regions of the Netherlands and Belgium. In addition, in Europe not only cross-border interconnections amongst transmission networks are stimulated, but also such interconnection cross-border possibilities at distribution level are explored [156]. The distribution systems in this Case Study operate as

'active distribution systems' in the sense that they are capable of providing bottom-up flexibility with their aggregated resources towards the transmission system. Conversely, transmission system is also able to transfer or consume power through the interface with the distribution systems. The tie-lines of each system can host 55 MW of active power between transmission and distribution and 25 MW between the two distribution networks. Two generators are placed at nodes 140 and 151 for the first distribution network and 173 and 184 of the second distribution network, for which the numbering is based on the total system of 184 nodes. Each of the first generation facility is considered to be weather-based with an aggregated rated capacity of 45 MW. The conventional generation facilities are with a capacity of 30 MW each and a marginal costs for active power of 9.33 EUR-106.24 EUR per MWh depending on the unit type. Marginal costs for all weather-based generation in the system is assumed to be zero. Marginal costs for reactive power are assumed to be 20% of those for active power, which is a simplification. In general, reactive power markets exist in some jurisdictions, such as the United Kingdom, which can be used as a benchmark for marginal price of reactive power.

Four of aggregated energy storage systems with homogeneous technical specifications, each of which of a total of 30 MWh capacity, 6 MW of rated power, are placed at nodes 120, 121 and 140 related to the first distribution network (S2) as well as node 173 connected to the second distribution network (S3). The average charge and discharge efficiencies are assumed to be at 86.6% and 97.2%, with an operational cost of 0.1 EUR MWh. respectively, as in [157]. The maximum and minimum state-of-charge (SOC) is set at 80% and 20% of the capacity, respectively.

This interconnected systems with one transmission and two distribution subsystems are considered to accommodate an hourly peak demand of 5.742 GW.

24-hours of operations of the respective systems with varying renewable output as well as demand are modelled, as in Fig. 4.7. Parallel with [152], voltage limits at all nodes are considered to be 0.95 p.u. and 1.05 p.u. <sup>1</sup>

Parallel with the implementation of a two-level ADMM in [149], the outer penalty parameter  $\beta$  is initialised at 1000.0, and its multiplier  $c_\beta$  is chosen as 6.0. In order to illustrate sensitivity to the choice of the parameters, the results under different choice of constant and variable penalty parameters at each iteration are also presented. An upper bound of 1.0e8 is considered in order to avoid numerical failures for the solver due to potentially large penalties and

<sup>1</sup>All simulations are run on an Intel® Core i7-8550U CPU, 1.99 GHz with 8 GB of RAM machine under JuMP® and CPLEX® solver.

dual variables. Outer level dual variables are bounded by  $\pm 1.0e8$ . Both primal and dual variables are initialised at 0.0 as a neutral starting point.

Tolerance parameter for the stopping criteria is set at  $\epsilon = 10^{-5}$ , unless otherwise indicated.

#### 4.5.2.1

##### Simplified case with two-subsystems and three-subsystems

Firstly, a simplified version of the full Case is presented in order to gain some insights on computational aspects without complexities of time-coupling, flexibility provision and power flow accuracy. A DC power flow is implemented over an hour of operations. In order to run a two-subsystem Case, the second DSO related to sub-system S3 is removed.

Table 4.4 shows the computational results for two subsystems consisting of IEEE 118-bus transmission system connected with one 33-bus distribution system. Standard ADMM does not converge after 1,000 iterations, which requires a significant computational effort. Two-level ADMM, on the other hand, converges within less than one fifth of number of iterations, saving more than 80% of computational resources. A decentralised computing of two-level ADMM, however, did not lead to any savings but rather to a slight increase of computational time in this relatively simple study. Table 4.5 demonstrates the computational performance of the algorithms for three subsystems consisting of IEEE 118-bus transmission system connected with two 33-bus distribution systems in a similar settings as in the earlier two-subsystem case. As in the previous case, Standard ADMM does not converge after 1,000 iterations Two-level ADMM reaches to a convergence after about 10% of the iterations for standard ADMM, and within 56% of the time. A decentralised computing of two-level ADMM depicts some gradual time savings, by 3.1%.

Table 4.4: IEEE-118-bus transmission system coupled with one IEEE-33 bus distribution system; DC power flow 1-hour without flexible resources computational results for  $\rho = 8$ .

Case 118 bus + 1x 33 bus 2 sub-systems	Comput. time [s.]	Nb. iterat.	Nb. outer loop iterat.	Convergence yes/no
Standard ADMM	147.439	1000	-	no
2-level ADMM	26.440	197	14	yes
2-level ADMM decentral	26.551	197	14	yes

Table 4.5: IEEE-118-bus transmission system coupled with two IEEE-33 bus distribution systems; DC power flow 1-hour without flexible resources computational results for  $\rho = 8$ .

Case 118 bus + 2x 33 bus 3 sub-systems	Comput. time [s.]	Nb. iterat.	Nb. outer loop iterat.	Convergence yes/no
Standard ADMM	162.198	1000	-	no
2-level ADMM	90.618	105	40	yes
2-level ADMM decentral	87.799	105	40	yes

#### 4.5.2.2

#### Full case with DSO-TSO three-subsystems with flexibility resources and AC power flow, 24-hours operations

This sub-section reports the full implementation results of the proposal with a full model involving flexible resources mainly at the distribution level, AC power flow and 24-hours of operations. The model, in its centralised formulation, has 71,376 variables and 123,308 constraints (including 36,768 non-negativity constraints for variable definitions).

Fig. 4.8 and Fig. 4.9 report the active and reactive power flows at interface nodes. Fig. 4.10 shows how the state-of-charge (SOC) of the storage system, located at node 120 connected to S2, evolves over time. Fig. 4.11 demonstrates the evolution of the SOC for the storage system 2 per hour, which is very similar to storage system 3 and 4. The latter are not explicitly plotted due to similar behaviour. Because of the assumption that renewable generation and demand pattern is homogeneous at every sub-system, and hence not depicting other weather conditions or demand, these three storage facilities show a similar change of SOC, though with slightly varying quantities.

It is observed that there are differences in terms of quantities of active and reactive power injected or withdrawn at each interface node, despite two homogeneous active distribution systems, first of which being S2 and second being S3, coupled to the transmission systems, with a difference of base demand, S2 with 6.3 MW and S3 with 4.2 MW, and the number of storage facilities. S2 operates three storage units at nodes 120, 121 and 140, whereas S3 operates 1 storage unit at node 173.

Following the demand and generation structure given in Fig. 4.7, night hours of  $0h - 6h$ , with low renewable generation coupled with low demand result in the highest flow of reactive power between S1, representing the TSO, and S2.

High renewable generation hours,  $10h - 15h$ , lead to relatively large quantities of especially active power flow from S1, TSO, to both DSOs's subsystems, S2 and S3. It is because of the fact that TSO, lacking any storage in its network, makes use of energy storage systems located at DSO

nodes. Another observation is that during these hours the interface flows, both active and to a large extent reactive power, is steady owing to the impact of storage which creates a bridge between low and high generation hours. We note that albeit the fact that a tight formulation is chosen based on state-of-the-art techniques in the literature [139] to avoid binaries for capturing not simultaneous charging and discharging, the results showed that this could not be entirely prevented. In fact, in hour 22 characterised by low generation and declining demand, for storage 1 this was the case which is reflected in the SOC by netting charging power of 1.69 MW and discharging power of 2.73 MW for the respective hour. For the same hour and with regard to storage 2, charging power of 2.77 MW and discharging power of 2.46 MW were netted.

On the other hand, peak-load evening hours,  $16h - 19h$ , and thereafter with relatively low renewable generation, reactive power injections and withdrawals demonstrate largest fluctuations at every interface node. These hours are characterised by a higher need of voltage control especially at the transmission level, which is at least partly provided by active distribution networks.

Looking into the interaction between the two DSOs, one can observe that the active power flow direction is mainly from S3 into S2 especially during night hours supporting for low generation to serve a larger demand at S2.

Moreover, capacitors are placed at every node with relatively high marginal costs in order to illustrate the capability of renewable and storage facilities for reactive power support. It is observed that capacitors are hardly activated in any of the hours. Therefore, the bottom-up flexibility is capable to help transmission system for voltage management purposes without having the need to rely on conventional means for voltage control, such as shunt capacitors or capacitor banks.

Overall, the flows at interfaces are sizeable, and during some hours they are towards their limits, stipulating that flexible distribution systems can play a significant role in active power congestion and voltage management at the TSO as well as the adjacent DSOs, by optimising the power flows at the interface of the respective networks. This highlights the importance of power flow modelling so that the limits and flexibility of the power system can more efficiently be exploited, in particular at the interface. Furthermore, in this setting, aggregated energy storage facilities in distribution networks is observed to act as a key player for coordination.

Table 4.6 summarises the computational results of the described numerical experiments. Standard ADMM couple with a standard SOCP is provided as a benchmark. The proposed algorithms-related results, namely Algorithm 1 with a distributed two-level ADMM with a sequential-linearisation based

circle approximation algorithm given by *Algorithm 1*, as well as the same but a decentralised one, *Algorithm 2* are provided. Optimality gap is reported as in [150], defined such that  $Opt.Gap = \frac{|TotalCostOptimal - TotalCostAlgorithm|}{TotalCostAlgorithm}$ , where  $TotalCostOptimal$  is the optimal objective value of the centralised solution and the  $TotalCostAlgorithm$  is the total cost obtained out of the algorithm.

A time limit of 10,800 seconds is set for all cases. Implementation is repeated with different penalty parameters,  $\rho = 8, 12, 100$ , choice of which did hardly make any impact on the outcome. As such, the results for  $\rho = 8$  is presented in the Table 4.6, which is comparable with outcomes with other choices of  $\rho$ .

Standard ADMM with SOCP remained divergent, and was able to run 152 iterations within the time limits. The bounds hardly improved over the iterations, which conclude with a high optimality gap of 41.79%, almost the same level as its start. Two-level ADMM with sequentially linearised power flows, on the other hand, resulted in a tighter optimality gap, albeit not within the pre-set tolerance level of  $10^{-5}$ , from engineering point of view may be in an acceptable range depending on the implementation, such as for a large distributed power flow case study in [144]. Furthermore, two-level ADMM with a decentralised data communication structure with again the same linearisation-based power flow embedded resulted in a possibility of iterating 5.2% more within the given time limits, leading to a gradual improvement of optimality gap by 0.02 percentage points. Two-level distributed algorithm requires a total of data exchange of 144 variables per iteration, being 50-50% primal and dual both for inner and outer iterations, whereas decentralised algorithm needs an exchange of 96 variables with the same composition, saving one-third of data communication. The consensus variables chosen to be exchanged are  $c_{n,m}, \forall n \in \mathcal{N}_p, m \in \mathcal{N}_p^\infty, p \in \mathcal{P}$ , and  $s_{n,m}, \forall n \in \mathcal{N}_p, m \in \mathcal{N}_p^\infty, p \in \mathcal{P}$  in the implementation, which do not reveal any sensitive information about the content of the data.

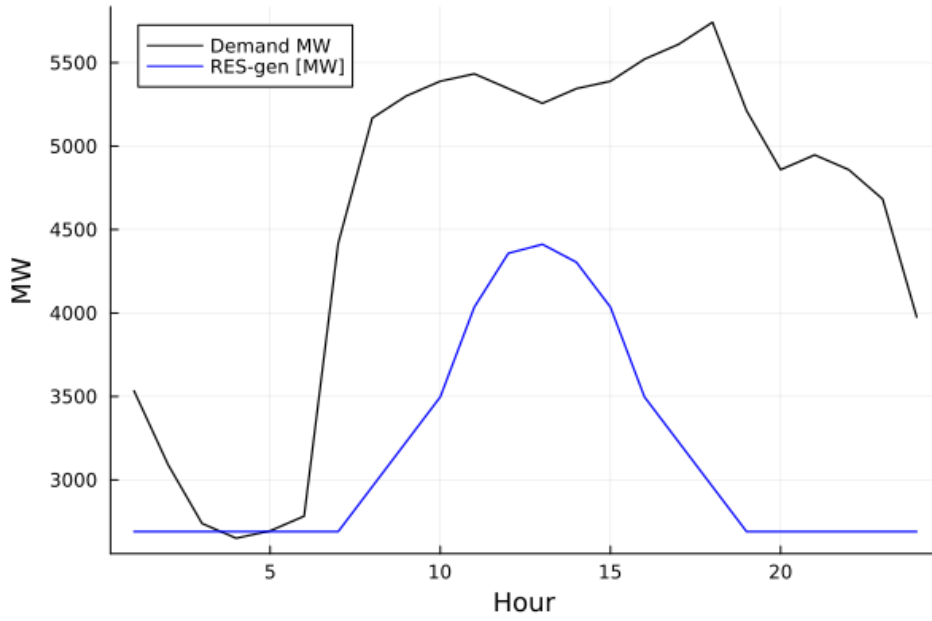


Figure 4.7: Total demand and renewable generation per hour in MW.

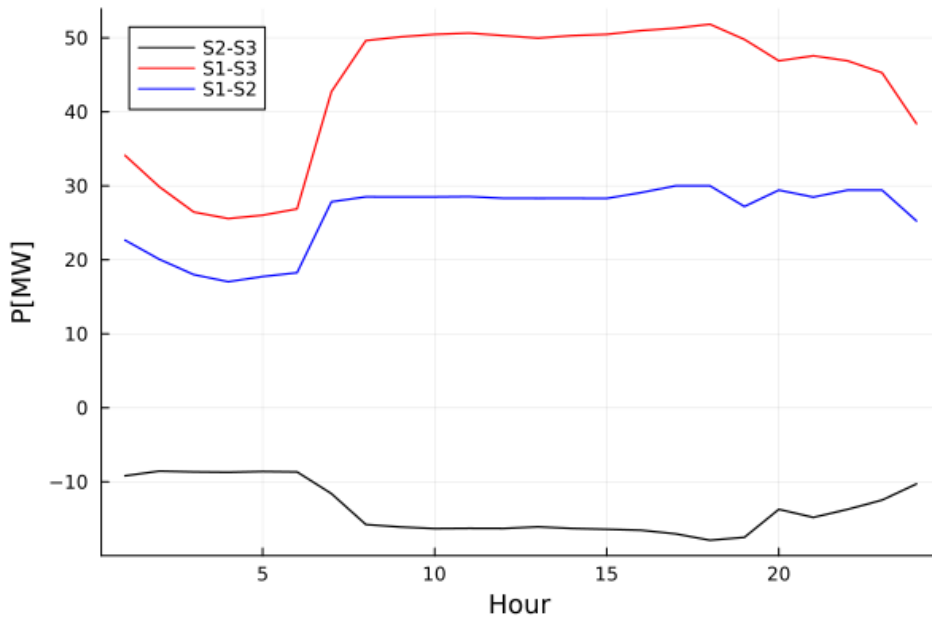


Figure 4.8: Active power flow  $P$  per hour at the interface nodes between subsystems in MW.

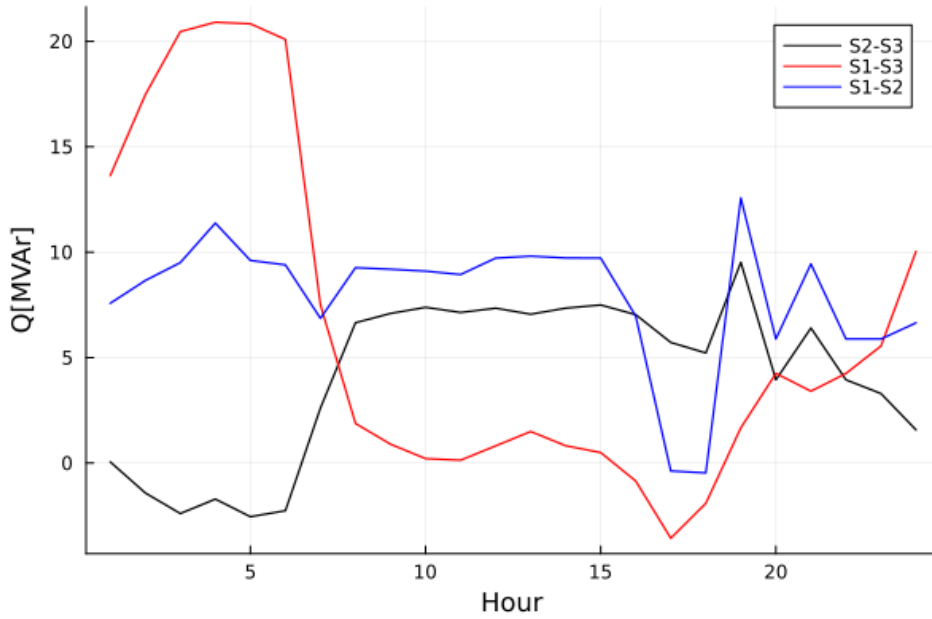


Figure 4.9: Reactive power flow  $Q$  per hour at the interface nodes between subsystems in MVar.

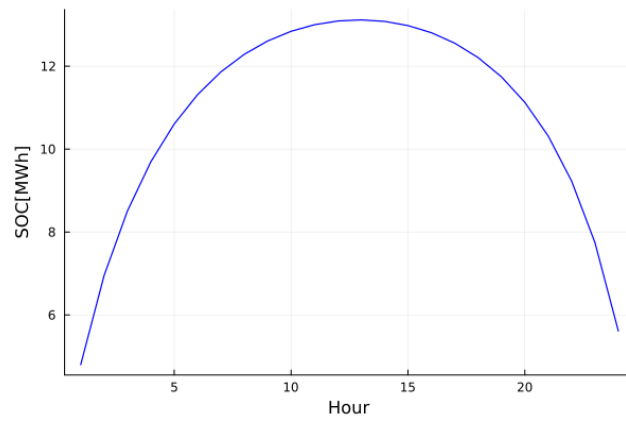


Figure 4.10: SOC [MWh] storage system-1 per hour at the distribution systems.

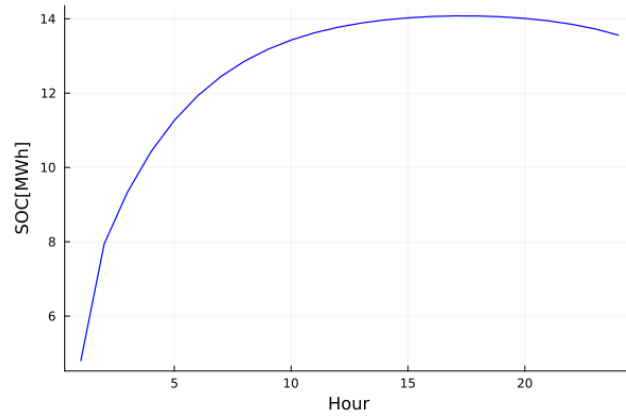


Figure 4.11: SOC [MWh] storage system-2 per hour at the distribution systems, representative also for storage system-3 and 4.

Table 4.6: IEEE-118-bus transmission system coupled with two 33-bus distribution systems; AC power flow 24-h with flexible resources computational results: 'Two-level ADMM with Linearisation-Algorithm 1 & 2 vs. 'Standard ADMM with Standard SOCP'

Case 118 bus + 2x 33 bus 3 sub-systems	Comput. time [s.]	Nb. iterat.	Nb. outer loop iterat.	Optimality gap
Standard ADMM & SOCP	10,800	152	-	41.79%
2-level ADMM Algo. 1	10,800	231	5	8.78%
2-level ADMM decentral Algo. 2	10,800	243	6	8.76%

### 4.5.2.3

#### Value of DSO-TSO coordination

To illustrate the no coordination case, constant flows are assumed between the subsystems - S1-S2 of 30 MW, S1-S3 of 55 MW and S2-S3 of -10MW - based on bilateral agreements. Accordingly, each subsystem ignores the state of one another. This results in a curtailment of 108.51 MW of renewable generation per hour in the overall system as well as total system costs of \$ 515,911.42. By incorporating coordination of DSO-TSO systems according to the presented framework, the renewable generation curtailment reduces to 82.86 MW per hour, representing a decrease by 23.63%. Total system costs decrease to \$ 367,402.32, corresponding to a drop of 28.79%.

## 5

# Computational Techniques and Model Accuracy in Energy and Reserve Pricing for Power Systems with Non-Convex Costs

This Chapter reuses the publication, [**Paper C**] Martin, N. C., & Fanzeres, B. (2023). Stochastic risk-averse energy and reserve scheduling and pricing schemes with non-convexities and revenue caps. *Electric Power Systems Research*, 225, 109858. [**Paper A**], which is herewith referenced and cited as [29]. A related publication supporting the conclusions is [**Paper D**] Martin, N. C., & Fanzeres, B. (2023, September). A Stochastic Risk-Averse Model to Price Energy in Pool-Based Electricity Markets with Non-Convex Costs and Revenue Caps. In *2023 International Conference on Smart Energy Systems and Technologies (SEST)* (pp. 1-6). IEEE. The latter is referenced as [18].

In general, it is assumed throughout the Chapter that the market clearing results may not be binding for market participants, such that they may have an incentive to deviate if they can not recover their costs.

A particular aspect of the structure of electricity production systems is that planning, operation, and market clearing are intrinsically linked [158]. More precisely, electricity market clearing is derived from the solution of a welfare-maximising scheduling and operation of the system assets to meet demand. In general, the models applied to this end are suitably formulated as Mixed-Integer Linear Programming (MILP) problems. In this context, binary variables capture the generators' operating characteristics, such as start-up and no-load costs [159]. For a MILP problem, however, the feasibility space is non-convex, which hampers the derivation of marginal prices as Lagrange multipliers of demand and supply balance equations. Fixing binaries in the MILP problem or relaxing the integrality constraints to obtain marginal prices are widely applied. It is at a cost, since for some instances, it might be preferable for generators to deviate from the dispatch decisions of the system operator, as otherwise their overall (non-convex) costs may not be entirely covered by delivering energy at the marginal price provided by the market operator [159]. Debatable out-of-market mechanisms, such as uplift schemes as side payments, are used in several markets around the globe in order to properly remunerate generators due to their non-convex cost structure. These payments are intended to capture the opportunity costs for generators when the dispatch decisions are followed. Uplift payments, however, may distort price signals for entry into the market, as they are discriminatory among players and

only known *ex-post* [160].

Accordingly, the convex hull pricing approach proposed in technical literature revolves around an uplift payment minimising mechanism, which determines prices through the Lagrangian dual of the original MILP problem. This approach is, however, considered to be computationally expensive while giving limited intuition into the resulting prices [161]. On the other hand, the European Union has recently intensely debated on imposing revenue caps to limit windfall profits of generation companies by virtue of abnormal market and system conditions [162]. Because of a surge in fuel prices, particular high-cost gas generators become price-setters, handing over high electricity prices to consumers, while the actual fuel costs of low-cost technologies are hardly affected. In this context, revenue caps are out-of-market mechanisms intending to reallocate windfall profits from generators to consumers.

Most electricity markets follow a day-ahead deterministic clearing process that entails decisions with respect to the commitments of generators along with the scheduling of energy and reserves. These commitments are determined following a contingency analysis to prevent extreme events, such as blackouts. Moreover, reserves provide an excess capacity allocation, on top of the expected load, and a prompt availability mechanism against adverse operating events, e.g., loss of energy or errors in net demand forecasting. Co-optimisation of energy and reserves can lower the cost of providing energy, as such a mechanism sets the price for energy and reserve simultaneously and determines the optimal resource allocation while ensuring security in supply [33]. U.S. markets are examples of such a market setup. Energy price reflects the marginal cost of supplying an incremental amount of load, at the same time meeting the reserve requirements. The reserve price, on the other hand, refers to the marginal cost of an additional unit of providing reserve and the opportunity cost of not committing to energy delivery.

Such a deterministic market clearing mechanism has been increasingly challenged by stochastic power output from renewable sources and proactive demand. In fact, inconsistent outcomes have been observed between scheduling and pricing under the deterministic setting when used as a proxy for a stochastic reality [28]. Moreover, high system balancing-costs are incurred, triggered by large forecast errors for renewable generation sources [163]. Stochastic market-clearing processes, nevertheless, provide a better-informed [164] – if not an ‘ideal’ set-up to accommodate renewables and schedule for reserves [122] – sequential decision-making framework for the system operator [31].

From a procedural viewpoint, in the first stage of these models, the

operator determines the day-ahead commitments, nominal operative points along with reserve allocations, and demand response resources on the basis of a renewable production forecast. In the second stage, the operator makes use of the resources allocated at the day-ahead (first) stage to adjust the system's operative state in order to meet an updated net demand forecast close to real-time operation. In addition, system operators are concerned with the risk of not being able to provide the energy demanded by customers. In case high renewable generation uncertainty is coupled with outages, this risk amplifies, motivating the consideration of risk aversion in the market-clearing process [165, 166].

To overcome these challenges, in this work, a novel market-clearing process is designed that co-optimises energy and reserve in a stochastic risk-averse framework enabling robust decision-making for system operators, and endogenously ensures cost recovery for generation companies. The process is built upon a primal-dual formulation with the objective of mitigating the system operator's uplift payments by minimising the optimality gap between the MILP and the Lagrangian dual of the corresponding linear program when integrality constraints are relaxed. Accordingly, the rationale of such a market clearance is to minimally diverge from the welfare-maximising economic-dispatch solution while ensuring cost recovery for market agents taking into account their non-convex cost structure endogenously to the clearing procedure [116]. We highlight that a similar approach has been studied in technical literature in [167] within a deterministic setting, and in [116] considering a stochastic clearing procedure, but both without co-optimising and pricing energy and reserves and explicitly characterising the system operator's aversion to risk. Finally, we highlight that the resulting formulation for the market-clearing process falls into the class of a Mixed Integer Bi-Linear Programming (MIBLP) problem, challenging to be handled efficiently using standard optimisation algorithms or off-the-shelf solvers. Therefore, to enhance the computational capability in solving the proposed market-clearing procedure, in this work, a hybrid binary expansion and McCormick envelope-based algorithm is proposed. The efficiency of the algorithm is demonstrated in a large system case study based on the IEEE-118 bus test system.

### 5.0.1

#### **Objectives and Contributions to the Literature**

The contributions of this work are principally linked to the following strands of literature: i) reflecting uncertainties in electricity market design; ii) pricing and recovering non-convex cost structures; and iii) handling bi-linear

optimisation problems. These literature strands will be outlined in the next sub-sections.

### 5.0.1.1

#### Reflecting Uncertainties into Electricity Market Design

Three principal design options are discussed in the technical literature for taking into account the uncertainty in sequential electricity markets, i.e. day-ahead, intra-day, and balancing markets, as described in [164, 168]. Deterministic design with new products – e.g., flexible ramp and operating residual demand curves – incorporates flexibility taking into account implicitly the impact of uncertainty; represented by [169, 170, 28]. Robust design which ensures feasibility for outcomes within any given uncertainty realisation within an *a-priori*-defined uncertainty set; represented by [171, 31, 165]. Stochastic design models day-ahead and real-time markets as a two-stage model where the dispatch decisions are taken prior to day-ahead and in anticipation of the real-time uncertain realisation. A principal advantage of a stochastic market-clearing procedure is in terms of overall operative costs, which tend to be lower than, e.g., in a deterministic framework with operational reserves [164].

### 5.0.1.2

#### Pricing and Recovering Non-Convex Cost Structures

Energy prices supposedly provide incentives and signals for profit-maximising generators to adhere to the commitment and dispatch decisions of the system operator [159]. Non-convexities present in the cost structure due to units' operating features, however, imply that the optimal choice for the generator may be to deviate from these dispatch decisions, as otherwise its costs recovery, e.g., start-up and no-load costs, may not be fully covered by selling energy at marginal prices. For instance, a fast-ramping unit dispatched at its minimum operation limit may not receive sufficient income to cover its non-convex start-up costs, when marginal prices are the sole source of payment. Additionally, from an economic perspective, equilibria in markets with non-convexities may not exist [172]. Out-of-market mechanisms, such as uplift schemes as side-payments, are used in several markets around the globe, e.g., European and US markets, in order to appropriately remunerate generation companies and remove incentives to deviate from the central dispatch decisions. These payments would capture the opportunity cost, as the difference between the profit-maximising solution for the generation company, i.e., a self-scheduling solution, and the total revenue obtained from the social-welfare-maximising solution of the system operator. However, uplift payments

may distort price signals for entry into the market as they are only evaluated and disclosed *ex-post* to the operation.

For transparency reasons, a widely studied approach in the technical literature has an objective to mitigate uplift payments while maintaining a reasonable-costly operation. For instance, in the so-called Convex Hull (CH) method [161], prices are evaluated based on the gradient of the estimated convex envelope obtained, e.g., using Lagrangian Relaxation. The convex hull prices are then those which maximise the mixed-integer and non-smooth Lagrangian dual problem. More specifically, a convex hull is constructed by replacing the cost function of each generation company with its convex envelope and the constraint set of the problem by its convex hull. Although various methods - e.g., sub-gradient, bundle, and cutting plane - have been studied in the technical literature to handle the challenges in computing prices based on the CH method, most of them do not guarantee global optimal solution in polynomial time [159], thus the CH method is referred to be, in general, computationally prohibitive [173]. Alternatively, A different approach has been discussed in [167] that tackles the cost-recovery issue directly and explicitly. More specifically, the objective is to commit and dispatch the system assets as close as possible to its resulting pricing solutions. This is achieved by relaxing the integrality conditions of the binary unit commitment variables with their continuous analogs and obtaining the duality gap between the primal problem and the dual, relaxed problem, subject to the combination of both the primal and dual problem constraints. In order to ensure cost recovery, additional constraints are added to enforce for each generation company a market revenue sufficient to cover its non-convex cost structure. In this work, we follow this latter approach to design the proposed market-clearing process.

### 5.0.1.3

#### Linearisation of Bi-linear Terms

Since cost recovery for generators is imposed in the commitment and scheduling problem, a non-convex, bi-linear term emerges in the market-clearing formulation. Such optimisation problems with bi-linear terms along with mixed integer variables may not be efficiently solved by commercial solvers or standard optimisation algorithms [34]. Furthermore, such problems are typically NP-hard [35]. Accordingly, bi-linear terms are commonly linearised for tractability purposes. Binary expansion is amongst the most common methods applied in the technical literature [174]. Its precision is highly impacted by the step size chosen by the decision-maker, and, albeit a smaller step size implies a higher precision, it can be computationally prohibitive and configures only

an approximation to the original bi-linear formulation [116]. Recently, several hybridisations and combinations of relaxation procedures, such as McCormick envelopes [111] within the binary expansion process have been studied aiming at enhancing the computational capability and solution quality of bi-linear optimisation problems [175, 114]. In Section 5.2, we leverage this hybridisation technique to construct an efficient solution approach to the proposed bi-linear market-clearing procedure.

#### 5.0.1.4 Objectives and Contributions

Despite the relevance of the aforementioned technical literature, earlier works studying efficient pricing mechanisms in markets with participants with non-convex cost structures, in general, focus on deterministic or risk-neutral frameworks, and omit the reserve scheduling and compensation. In this work, we extend this literature by exploring the impact of a risk-averse structure on the market-clearing process, with a particular focus on the trade-off between expected operation cost and the risk of short-term demand-supply imbalances, inferring how to price energy and reserves guaranteeing cost recovery for generation companies. From a computational viewpoint, aiming at enhancing the computational capability to handle the proposed bi-linear market-clearing process, a hybrid method combining McCormick envelopes and binary expansion is designed.

The intention of the paper is to be as general as possible, and it arguably selects desirable design aspects, such as co-optimisation of energy with reserves as well as some issues raised in practice, such as risk-averse decision-making process of system operators, and, windfall profits and cost recovery of generators. In terms of market-design, the United Kingdom (UK) electricity market design is the closest real-world application, where revenue caps and a nodal market has been in discussion and under consideration.

In summary, the contributions of this work are fourfold:

1. To extend [116, 167, 31] to a multi-commodity environment and their endogenous clearance of reserves and scale-up the numerical analysis to larger power networks to gain insights on realistic systems.
2. To consider a risk aversion profile to the market operator for meeting demand and supply in an uncertain renewable power generation environment, mimicking the daily decision process of system operators in practice.

3. To compare the market outcomes from the perspective of provision of cost recovery guarantee for the generation companies under the following schemes: i) at the day-ahead stage including energy and reserves; ii) in expectation; iii) per scenario; iv) uplift covering all the shortages with regard to energy; and v) revenue cap. The latter is of practical interest in view of market design debate, especially in the European Union and the United Kingdom.
4. To design an efficient procedure to tackle the bi-linear terms based on a hybrid approach combining McCormick envelopes with binary expansion in order to improve the computational compatibility to handle the market-clearing process. The proposed hybrid McCormick and binary expansion procedure is novel, at least in power system applications.

## 5.1

### Stochastic Energy and Reserve Market Clearing Model with Cost Recovery

One of the main objectives of this work is to propose a risk-averse market-clearing process that efficiently balances reasonable-costly energy and reserves scheduling to meet demand with an endogenous cost-recovery guarantee for generation companies, thus explicitly mitigating the side payments in the market. For this purpose, we leverage primal-dual interdependence and identify a least-duality gap solution with (non-convex) cost recovery. In this section, we carefully describe the proposed market-clearing process. Firstly, Section 5.1.1 presents the (primal) formulation that identifies the least-cost commitment and energy and reserves scheduling under uncertainty. This primal model formulation is very close to how it is implemented by system operators in their daily activities. Then, Section 5.1.2 indicates the process to formulate the dual problem of the non-convex problem presented in Section 5.1.1. Further on, Section 5.1.3 discusses different cost-recovery structures for generation companies. Finally, Section 5.1.4 resumes the proposed market-clearing process formulated as a MIBLP problem.

#### 5.1.1

##### Primal Formulation

It is assumed that all generators are price-takers in this study. In addition, a linear cost structure is assumed. Similar to most stochastic market-clearing formulations studied in the technical literature, the presented primal model is stated as a two-stage mixed-integer linear program. Structurally, the first stage defines the day-ahead commitment of each conventional unit and energy

and reserves scheduling to meet demand, complying with different technical constraints, and the second stage is in the view of the real-time energy

production and delivery [31, 32].

$$\begin{aligned}
 \min_{\Xi} \quad & (1 - \Lambda) \cdot \left[ \sum_{t \in \mathcal{T}} \left( \sum_{i \in \mathcal{J}} \left( \lambda_i^E \cdot g_{i,t}^{DA} + \lambda_i^U \cdot r_{i,t}^U \right. \right. \right. \\
 & \left. \left. \left. + \lambda_i^D \cdot r_{i,t}^D + \lambda_{i,t}^{SU} + \lambda_{i,t}^{SD} \right) \right. \right. \\
 & \left. \left. + \sum_{s \in \mathcal{S}} \phi_s \cdot \left( \sum_{i \in \mathcal{J}} \left( \lambda_i^E \cdot \left( \delta_{i,s,t}^+ - \delta_{i,s,t}^- \right) \right. \right. \right. \right. \\
 & \left. \left. \left. + \sum_{d \in \mathcal{D}} \left( \lambda_d^{shed} \cdot l_{d,s,t}^{shed} \right) \right) \right) \right] \\
 & + \Lambda \cdot \left[ \beta + \frac{1}{1 - \varphi} \sum_{s \in \mathcal{S}} \phi_s \cdot \gamma_s^{CVaR} \right]; \tag{5-1}
 \end{aligned}$$

subject to:

$$u_{i,t} \cdot G_i^{min} \leq g_{i,t}^{DA} + r_{i,t}^U \leq u_{i,t} \cdot G_i^{max}, \quad : (\mu_{i,t}^{Umin}, \mu_{i,t}^{Umax}) \quad \forall i \in \mathcal{J}, t \in \mathcal{T}; \tag{5-2}$$

$$u_{i,t} \cdot G_i^{min} \leq g_{i,t}^{DA} - r_{i,t}^D, \quad : (\mu_{i,t}^{Dmax}) \quad \forall i \in \mathcal{J}, t \in \mathcal{T}; \tag{5-3}$$

$$\begin{aligned}
 \sum_{i \in \Psi_n} g_{i,t}^{DA} - \sum_{d \in \mathcal{D}_n} g_{d,t} + \sum_{k \in \Psi_n} w_{k,t}^{DA} \\
 - \sum_{m \in \mathcal{N}_n} B_{n,m} (\theta_{n,t}^{DA} - \theta_{m,t}^{DA}) = 0, \quad : (\lambda_{n,t}^{DA}) \\
 \forall n \in \mathcal{N}, t \in \mathcal{T}; \tag{5-4}
 \end{aligned}$$

$$\begin{aligned}
 -\bar{F}_{n,m} \leq B_{n,m} (\theta_{n,t}^{DA} - \theta_{m,t}^{DA}) \leq \bar{F}_{n,m}, \\
 : (\eta_{n,m,t}^{DAmin}, \eta_{n,m,t}^{DAmax}) \quad \forall m \in \mathcal{N}_n, n \in \mathcal{N}, t \in \mathcal{T}; \tag{5-5}
 \end{aligned}$$

$$\lambda_{i,t}^{SU} \geq (u_{i,t} - u_{i,0}) \cdot K_i^{SU}, \quad : (\mu_{i,t}^{SU}) \quad \forall i \in \mathcal{J}, t = 1; \tag{5-6}$$

$$\lambda_{i,t}^{SD} \geq (u_{i,0} - u_{i,t}) \cdot K_i^{SD}, \quad : (\mu_{i,t}^{SD}) \quad \forall i \in \mathcal{J}, t = 1; \tag{5-7}$$

$$\lambda_{i,t}^{SU} \geq (u_{i,t} - u_{i,t-1}) \cdot K_i^{SU}, \quad : (\mu_{i,t}^{SU}) \\
 \forall i \in \mathcal{J}, t \in \mathcal{T} \setminus \{1\}; \tag{5-8}$$

$$\lambda_{i,t}^{SD} \geq (u_{i,t-1} - u_{i,t}) \cdot K_i^{SD}, \quad : (\mu_{i,t}^{SD}) \\
 \forall i \in \mathcal{J}, t \in \mathcal{T} \setminus \{1\}; \tag{5-9}$$

$$\theta_{n=ref,t}^{DA} = 0, \quad : (\gamma_t) \quad \forall t \in \mathcal{T}; \tag{5-10}$$

$$\delta_{i,s,t}^+ \leq r_{i,t}^U, \quad : (\sigma_{i,s,t}^{Umax}) \quad \forall i \in \mathcal{J}, s \in \mathcal{S}, t \in \mathcal{T}; \tag{5-11}$$

$$\delta_{i,s,t}^- \leq r_{i,t}^D, \quad : (\sigma_{i,s,t}^{Dmax}) \quad \forall i \in \mathcal{J}, s \in \mathcal{S}, t \in \mathcal{T}; \tag{5-12}$$

$$w_{k,s,t}^{spill} \leq w_{k,s,t}^{scen}, \quad : (\alpha_{k,s,t}^{max}) \quad \forall k \in \mathcal{WP}, s \in \mathcal{S}, t \in \mathcal{T}; \tag{5-13}$$

$$l_{d,s,t}^{shed} \leq g_{d,t}, \quad : (\omega_{d,s,t}^{max}) \quad \forall d \in \mathcal{D}, s \in \mathcal{S}, t \in \mathcal{T}; \tag{5-14}$$

$$\begin{aligned}
 -\bar{F}_{n,m} \leq B_{n,m} (\theta_{n,w,t}^{RT} - \theta_{m,w,t}^{RT}) \leq \bar{F}_{n,m}, \\
 : (\eta_{n,m,t}^{RTmin}, \eta_{n,m,t}^{RTmax}) \quad \forall m \in \mathcal{N}_n, n \in \mathcal{N}, t \in \mathcal{T}, s \in \mathcal{S}; \tag{5-15}
 \end{aligned}$$

$$\begin{aligned} & \sum_{i \in \Psi_n} (\delta_{i,s,t}^+ - \delta_{i,s,t}^-) + \sum_{d \in \mathcal{D}_n} l_{d,s,t}^{\text{shed}} + \sum_{k \in \Psi_n} (w_{k,s,t}^{\text{scen}} \\ & - w_{k,t}^{\text{DA}} - w_{k,s,t}^{\text{spill}}) = \sum_{m \in \mathcal{N}_n} B_{m,n} \left( (\theta_{n,s,t}^{\text{RT}} - \theta_{m,s,t}^{\text{RT}}) \right. \\ & \left. - (\theta_{n,t}^{\text{DA}} - \theta_{m,t}^{\text{DA}}) \right), : (\lambda_{n,s,t}^{\text{RT}}) \quad \forall n \in \mathcal{N}, t \in \mathcal{T}, s \in \mathcal{S}; \end{aligned} \quad (5-16)$$

$$\theta_{(n=\text{ref}),s,t}^{\text{RT}} = 0, \quad : (\gamma_{s,t}^{\text{RT}}) \quad \forall t \in \mathcal{T}, s \in \mathcal{S}; \quad (5-17)$$

$$w_{k,t}^{\text{DA}} \leq W_k^{\text{max}}, \quad : (\mu_{k,t}^{\text{WP}}) \quad \forall t \in \mathcal{T}, k \in \mathcal{WP}; \quad (5-18)$$

$$r_{i,t}^U \leq \bar{R}_i, \quad : (\pi_{i,t}^U) \quad \forall i \in \mathcal{J}, t \in \mathcal{T}; \quad (5-19)$$

$$r_{i,t}^D \leq \underline{R}_i, \quad : (\pi_{i,t}^D) \quad \forall i \in \mathcal{J}, \forall t \in \mathcal{T}; \quad (5-20)$$

$$\sum_{i \in \mathcal{J}} r_{i,t}^U \geq \bar{R}_t^{\text{sys}}, \quad : (\pi_t^{\text{Usys}}) \quad \forall t \in \mathcal{T}; \quad (5-21)$$

$$\sum_{i \in \mathcal{J}} r_{i,t}^D \geq \underline{R}_t^{\text{sys}}, \quad : (\pi_t^{\text{Dsys}}) \quad \forall t \in \mathcal{T}; \quad (5-22)$$

$$\begin{aligned} \gamma_s^{\text{CVaR}} + \beta \geq & \left[ \sum_{t \in \mathcal{T}} \left( \sum_{i \in \mathcal{J}} (\lambda_i^E \cdot g_{i,t}^{\text{DA}} + \lambda_i^U \cdot r_{i,t}^U + \right. \right. \\ & \left. \left. + \lambda_i^D \cdot r_{i,t}^D + \lambda_{i,t}^{\text{SU}} + \lambda_{i,t}^{\text{SD}}) + \left( \sum_{i \in \mathcal{J}} (\lambda_i^E \cdot (\delta_{i,s,t}^+ - \delta_{i,s,t}^-) \right) \right. \right. \\ & \left. \left. + \sum_{d \in \mathcal{D}} (\lambda_d^{\text{shed}} \cdot l_{d,s,t}^{\text{shed}}) \right) \right], \quad : (\pi_s^{\text{dualCVaR}}) \quad \forall s \in \mathcal{S}; \end{aligned} \quad (5-23)$$

$$\begin{aligned} -RD_i \leq g_{i,t} - g_{i,t-1} \leq RU_{i,t}, \quad & : (\mu_{i,t}^{\text{RD}}, \mu_{i,t}^{\text{RU}}) \\ & \forall i \in \mathcal{J}, \forall t \in \mathcal{T} \setminus \{1\}; \end{aligned} \quad (5-24)$$

$$\begin{aligned} -RD_i \leq g_{i,t} - g_{i,0} \leq RU_{i,t}, \quad & : (\mu_{i,t}^{\text{RD}}, \mu_{i,t}^{\text{RU}}) \\ & \forall i \in \mathcal{J}, \forall t = 1; \end{aligned} \quad (5-25)$$

$$\begin{aligned} -RD_i \leq g_{i,t} - g_{i,t-1} + \delta_{i,s,t}^+ - \delta_{i,s,t}^- - \delta_{i,s,t-1}^+ \\ + \delta_{i,s,t-1}^- \leq RU_{i,t}, \quad & : (\mu_{i,t}^{\text{RDRT}}, \mu_{i,t}^{\text{RURT}}) \\ & \forall i \in \mathcal{J}, \forall t \in \mathcal{T} \setminus \{1\}; \end{aligned} \quad (5-26)$$

$$\begin{aligned} -RD_i \leq g_{i,t} - g_{i,0} + \delta_{i,s,t}^+ - \delta_{i,s,t}^- - \delta_{i,s,0}^+ \\ + \delta_{i,s,0}^- \leq RU_{i,t}, \quad & : (\mu_{i,t}^{\text{RDRT}}, \mu_{i,t}^{\text{RURT}}) \\ & \forall i \in \mathcal{J}, \forall t = 1. \end{aligned} \quad (5-27)$$

where  $\Xi = \{g_{i,t}^{\text{DA}} \geq 0, \theta_{n,t}^{\text{DA}}, r_{i,t}^U \geq 0, r_{i,t}^D \geq 0, \delta_{i,s,t}^+ \geq 0, \delta_{i,s,t}^- \geq 0, \theta_{n,s,t}^{\text{RT}}, w_{k,s,t}^{\text{spill}} \geq 0, l_{d,s,t}^{\text{shed}} \geq 0, u_{i,t} \in \{0, 1\}, \lambda_{i,t}^{\text{SU}} \geq 0, \lambda_{i,t}^{\text{SD}} \geq 0, w_{k,t}^{\text{DA}} \geq 0, \beta, \gamma_s^{\text{CVaR}} \geq 0\}$  is the set of decision variables, thus (5-1)–(5-27) falls into the class of Mixed-Integer Linear Programming (MILP) problems. The objective function (5-1) minimises a risk-adjusted functional of the total cost to supply energy, consisting of energy, up and down reserves, start-up and shut-down of the units, and load shedding

costs. By virtue of its technical and computational properties, we employ a quantile-based risk functional, known as the Conditional Value-at-Risk (CVaR) [120], to capture the risk aversion in the certainty equivalent social-welfare maximisation problem. For a given percentile  $\varphi \in (0, 1)$ , the CVaR measures the average of the  $1 - \varphi$  worst-valued scenario realisations. Accordingly, the commitment and scheduling model aims at identifying a decision vector that minimises the convex combination of risk-neutral expected and risk-averse measure (CVaR) of system costs for supplying energy,  $(1 - \Lambda) \cdot E[\cdot] + \Lambda \cdot CVaR_\varphi(\cdot)$ . The  $\Lambda \in [0, 1]$  represents a risk-averse parameter. More specifically, a low (high) value of  $\Lambda$  implies a low (high) weight given to risk aversion and a high (low) weight to expected system cost, respectively.

The set of constraints (5-2) - (5-10), (5-18) - (5-22) and (5-24) - (5-25) are in relation to the day-ahead stage. More specifically, (5-2) is the minimum generation and maximum capacity bounds for energy and reserve dispatch. These bounds are multiplied by binary variables, indicating that those constraints are active if the respective units are scheduled to start-up, or otherwise their dispatch and reserve provision are enforced to be zero. Constraint (5-3) ensures that the difference between energy dispatch and downward reserve cannot exceed the lower limit of generation. Similarly, binaries capture the on/off status of these units. The remaining equations are regarding power balance in day-ahead including the wind power generation scheduling (5-4), minimum and maximum flow limits for each transmission line - represented by from and to each node - (5-5), start-up costs when units are to be turned-on are represented in (5-6) and (5-8), and shut-down costs when units are to be turned-off (5-7) and (5-9), and reference angle (5-10). Constraints (5-11) - (5-12) limit the real-time re-dispatch given by up and downward adjustments by allocated reserves in the DA-stage. Equation (5-13) is in relation to the wind spill limited by actual - i.e., RT - wind scenarios. Equation (5-14) shows the load shed - which comes into play in case some demand cannot be supplied, e.g. caused by underproduction of wind - bounded by the maximum load. Equation (5-15) sets the power flow limits of each transmission line in RT, and (5-16) describes the power balance in RT presented in terms of adjustments which should balance out. Equation (5-17) shows the reference angle for the RT power generation. Equation (5-18) is wind production plant DA dispatch bounded by its capacity. Equation (5-19) and (5-20) are up and down reserve provision limits, respectively, of each generator and time period. Equations (5-21) and (5-22) are minimum amount of total upwards and downwards reserves required by the system operator to safeguard the power system for each time period. Equation (5-23) is with regard to the definition of CVaR. Equations (5-24)–(5-27) are

with regard to ramping up and down limits of each generator (first two at day-ahead and last two at real-time stages), respectively.

The market operator clears the market and sets the energy price (Lagrange multiplier of the balance constraint (5-4) for the DA and (5-16) for the RT), as well as up and down reserve prices (multipliers of the constraints (5-21) and (5-22)). The market operator also decides through this optimisation model which generators are to be dispatched for 1-day ahead based on the wind production scenarios available at the time of decision.

### 5.1.2

#### Dual Formulation

By relaxing the integrality constraints with regard to the binary variables, i.e.,  $0 \leq u_{i,t} \leq 1 : \left( \mu_{i,t}^{binary} \right), \forall i \in \mathcal{J}, t \in \mathcal{T}$  - the dual formulation of the

relaxed version of the primal problem can be obtained.

$$\begin{aligned}
\max_{\Xi^{dual}} & \sum_{t \in \mathcal{T}} \left( \sum_{i \in \mathcal{J}} (-\mu_{i,t}^{binary} - \mu_{i,t}^{RD} \cdot RD_i - \mu_{i,t}^{RU} \cdot RU_i + \right. \\
& - \underline{R}_i^D \cdot \pi_{i,t}^D - \bar{R}_i^U \cdot \pi_{i,t}^U) - \sum_{s \in \mathcal{S}} \left( \sum_{i \in \mathcal{J}} \mu_{i,s,t}^{RDRT} \cdot RD_i + \right. \\
& - \mu_{i,s,t}^{RURT} \cdot RU_i) + \sum_{k \in \mathcal{WP}} (-W_k^{max} \cdot \mu_{k,t}^{WP}) + \\
& + \sum_{k \in \mathcal{WP}, s \in \mathcal{S}} (-w_{k,s,t}^{scen} \cdot \alpha_{k,s,t}^{max}) + \sum_{k \in \Psi_n, s \in \mathcal{S}} (w_{k,s,t}^{scen} \cdot \lambda_{n,s,t}^{RT}) + \\
& + \sum_{d \in \mathcal{D}, s \in \mathcal{S}} (-g_{d,t} \cdot \omega_{d,s,t}^{max}) + \sum_{d \in \mathcal{D}_n, n \in \mathcal{N}} (g_{d,t} \cdot \lambda_{n,t}^{DA}) + \\
& + \sum_{n \in \mathcal{N}, m \in \mathcal{N}_n, s \in \mathcal{S}} (-\bar{F}_{n,m} \cdot (\eta_{n,m,t}^{DAmin} + \eta_{n,m,t}^{DAmax} + \\
& + \eta_{n,m,s,t}^{RTmin} + \eta_{n,m,s,t}^{RTmax})) + \underline{R}_t^{sys} \cdot \pi_t^{Dsys} + \bar{R}_t^{sys} \cdot \pi_t^{Usys} \Big) + \\
& \left( \sum_{i \in \mathcal{J}} (-K_i^{SU} \cdot u_{0,i} \cdot \mu_{i,t=1}^{SU} + K_i^{SD} \cdot u_{i,0} \cdot \mu_{i,t=1}^{SD} + \right. \\
& + \mu_{i,t=1}^{RD} \cdot g_{0,i} - \mu_{i,t=1}^{RU} \cdot g_{0,i}) + \sum_{s \in \mathcal{S}} \left( \sum_{i \in \mathcal{J}} \mu_{i,s,t=1}^{RDRT} \cdot (g_{0,i} + \right. \\
& + \delta_{0,t=1}^+ - \delta_{i,t=1}^-) \Big); \tag{5-28}
\end{aligned}$$

subject to:

$$\begin{aligned}
& \lambda_i^E \cdot (1 - \Lambda) - \mu_{i,t}^{Umin} + \mu_{i,t}^{Umax} - \mu_{i,t}^{Dmax} - \lambda_{n,t}^{DA} \\
& + \sum_{s \in \mathcal{S}} (\pi_s^{dualCVaR}) - \mu_{i,t}^{RD} + \mu_{i,t+1}^{RD} + \mu_{i,t}^{RU} - \mu_{i,t+1}^{RU} \\
& + \sum_{s \in \mathcal{S}} (-\mu_{i,s,t}^{RDRT} + \mu_{i,s,t+1}^{RDRT} + \mu_{i,s,t}^{RURT} - \mu_{i,s,t+1}^{RURT}) \\
& \geq 0, : g_{i,t}^{DA}, \forall i \in \Psi_n, t \in \mathcal{T} \setminus \{1\}; \tag{5-29}
\end{aligned}$$

$$\begin{aligned}
& \lambda_i^E \cdot (1 - \Lambda) - \mu_{i,t}^{Umin} + \mu_{i,t}^{Umax} - \mu_{i,t}^{Dmax} - \lambda_{n,t}^{DA} \\
& + \sum_{s \in \mathcal{S}} (\pi_s^{dualCVaR}) - \mu_{i,t}^{RD} + \mu_{i,t}^{RU} \\
& + \sum_{s \in \mathcal{S}} (-\mu_{i,s,t}^{RDRT} + \mu_{i,s,t}^{RURT}) \\
& \geq 0, : g_{i,t}^{DA}, \forall i \in \Psi_n, t = T; \tag{5-30}
\end{aligned}$$

$$\begin{aligned}
& \lambda_i^U \cdot (1 - \Lambda) + \mu_{i,t}^{Umax} - \mu_{i,t}^{Umin} + \sum_{s \in \mathcal{S}} (-\sigma_{i,s,t}^{Umax} + \\
& + \pi_s^{dualCVaR} \cdot \lambda_i^U) + \pi_{i,t}^U - \pi_t^{Usys} \geq 0, \\
& : r_{i,t}^U, \forall i \in \mathcal{J}, t \in \mathcal{T}, s \in \mathcal{S}; \tag{5-31}
\end{aligned}$$

$$\begin{aligned}
& \lambda_i^D \cdot (1 - \Lambda) + \mu_{i,t}^{Dmax} + \sum_{s \in \mathcal{S}} (-\sigma_{i,s,t}^{Dmax} + \pi_s^{dualCVaR} \cdot \lambda_i^D) \\
& + \pi_{i,t}^D - \pi_t^{Dsys} \geq 0, : r_{i,t}^D, \forall i \in \mathcal{J}, t \in \mathcal{T}; \tag{5-32}
\end{aligned}$$

$$\phi_s \cdot \lambda_i^E \cdot (1 - \Lambda) + \lambda_{n,s,t}^{RT} + \sigma_{i,s,t}^{Umax} + \pi_s^{dualCVaR} \cdot \lambda_i^E$$

$$\begin{aligned}
 & -\mu_{i,s,t}^{RDRT} + \mu_{i,s,t+1}^{RDRT} + \mu_{i,s,t}^{RURT} - \mu_{i,s,t+1}^{RURT} \geq 0, \\
 & : \delta_{i,s,t}^+, \quad \forall i \in \Psi_n, t \in \mathcal{T} \setminus \{1\}, s \in \mathcal{S}; \tag{5-33}
 \end{aligned}$$

$$\begin{aligned}
 & \phi_s \cdot \lambda_i^E \cdot (1 - \Lambda) + \lambda_{n,s,t}^{RT} + \sigma_{i,s,t}^{Umax} + \pi_s^{dualCVaR} \cdot \lambda_i^E \\
 & - \mu_{i,s,t}^{RDRT} + \mu_{i,s,t}^{RURT} \geq 0, \\
 & : \delta_{i,s,t}^+, \quad \forall i \in \Psi_n, t = T, s \in \mathcal{S}; \tag{5-34}
 \end{aligned}$$

$$\begin{aligned}
 & -\phi_s \cdot \lambda_i^E \cdot (1 - \Lambda) - \lambda_{n,s,t}^{RT} + \sigma_{i,s,t}^{Dmax} + \mu_{i,s,t}^{RDRT} \\
 & - \mu_{i,s,t+1}^{RDRT} - \mu_{i,s,t}^{RURT} + \mu_{i,s,t+1}^{RURT} - \pi_s^{dualCVaR} \cdot \lambda_i^E \\
 & \geq 0, : \delta_{i,s,t}^-, \quad \forall i \in \Psi_n, t \in \mathcal{T} \setminus \{1\}, s \in \mathcal{S}; \tag{5-35}
 \end{aligned}$$

$$\begin{aligned}
 & -\phi_s \cdot \lambda_i^E \cdot (1 - \Lambda) - \lambda_{n,s,t}^{RT} + \sigma_{i,s,t}^{Dmax} + \mu_{i,s,t}^{RDRT} \\
 & - \mu_{i,s,t}^{RURT} - \pi_s^{dualCVaR} \cdot \lambda_i^E \\
 & \geq 0, : \delta_{i,s,t}^-, \forall i \in \Psi_n, t = T, s \in \mathcal{S}; \tag{5-36}
 \end{aligned}$$

$$\begin{aligned}
 & \alpha_{k,s,t}^{max} + \lambda_{n,s,t}^{RT} \geq 0, \\
 & : w_{k,s,t}^{spill}, \forall i \in \Psi_n, t \in \mathcal{T}, s \in \mathcal{S}; \tag{5-37}
 \end{aligned}$$

$$\begin{aligned}
 & \phi_s \cdot \lambda_{d,t}^{shed} \cdot (1 - \Lambda) + \lambda_{n,s,t}^{RT} + \omega_{d,s,t}^{max} + \pi_s^{dualCVaR} \cdot \lambda_d^{shed} \\
 & \geq 0, : l_{d,s,t}^{shed}, \forall d \in \mathcal{D}_n, t \in \mathcal{T}, s \in \mathcal{S}; \tag{5-38}
 \end{aligned}$$

$$\begin{aligned}
 & -\lambda_{n,t}^{DA} + \sum_{s \in \mathcal{S}} (\lambda_{n,s,t}^{RT}) + \mu_{k,t}^{WP} \geq 0, \\
 & : w_{k,t}^{DA}, \forall k \in \Psi_n, t \in \mathcal{T}, s \in \mathcal{S}; \tag{5-39}
 \end{aligned}$$

$$\begin{aligned}
 & 1 - \Lambda - \mu_{i,t}^{SU} + \sum_{s \in \mathcal{S}} (\pi_s^{dualCVaR}) \geq 0, \\
 & : \lambda_{i,t}^{SU}, \forall i \in \mathcal{J}, t \in \mathcal{T}, s \in \mathcal{S}; \tag{5-40}
 \end{aligned}$$

$$\begin{aligned}
 & 1 - \Lambda - \mu_{i,t}^{SD} + \sum_{s \in \mathcal{S}} (\pi_s^{dualCVaR}) \geq 0, \\
 & : \lambda_{i,t}^{SD}, \forall i \in \mathcal{J}, t \in \mathcal{T}, s \in \mathcal{S}; \tag{5-41}
 \end{aligned}$$

$$\begin{aligned}
 & -G_i^{max} \cdot \mu_{i,t}^{Umax} + G_i^{min} \cdot \mu_{i,t}^{Umin} + G_i^{min} \cdot \mu_{i,t}^{Dmax} + \\
 & + \mu_{i,t}^{bin} + K_i^{SU} \cdot \mu_{i,t}^{SU} + -K_i^{SU} \cdot \mu_{i,t+1}^{SU} - K_i^{SD} \cdot \mu_{i,t}^{SD} + \\
 & + K_i^{SD} \cdot \mu_{i,t+1}^{SD} \geq 0, \\
 & : u_{i,t}, \forall i \in \mathcal{J}, t \in \mathcal{T} \setminus \{T\}; \tag{5-42}
 \end{aligned}$$

$$\begin{aligned}
 & -G_i^{max} \cdot \mu_{i,t}^{Umax} + G_i^{min} \cdot \mu_{i,t}^{Umin} + G_i^{min} \cdot \mu_{i,t}^{Dmax} + \\
 & + \mu_{i,t}^{bin} + K_i^{SU} \cdot \mu_{i,t}^{SU} - K_i^{SD} \cdot \mu_{i,t}^{SD} \geq 0, \\
 & : u_{i,t}, \forall i \in \mathcal{J}, t = T; \tag{5-43}
 \end{aligned}$$

$$\begin{aligned}
 & \sum_{m \in \mathcal{N}_n} B_{n,m} \cdot \left( -\lambda_{n,t}^{DA} + \lambda_{m,t}^{DA} + \sum_{s \in \mathcal{S}} (\lambda_{n,s,t}^{RT} - \lambda_{m,s,t}^{RT}) + \right. \\
 & \left. + \eta_{n,m}^{DAmax} - \eta_{m,n}^{DAmax} - \eta_{n,m}^{DAmin} + \eta_{m,n}^{DAmin} \right) = 0, \\
 & : \forall n \in \mathcal{N} \setminus \{n = ref\}, t \in \mathcal{T}; \tag{5-44}
 \end{aligned}$$

$$\sum_{m \in \mathcal{N}_n} B_{n,m} \cdot \left( -\lambda_{n,t}^{DA} + \lambda_{m,t}^{DA} + \sum_{s \in \mathcal{S}} (\lambda_{n,s,t}^{RT} - \lambda_{m,s,t}^{RT}) + \right)$$

$$\begin{aligned}
 & + \eta_{n,m}^{DAmax} - \eta_{m,n}^{DAmax} - \eta_{n,m}^{DAmin} + \eta_{m,n}^{DAmin} \Big) + \\
 & + \gamma_t = 0, \\
 & \quad : \theta_{n,t}^{DA}, \forall n \in \{n = ref\}, t \in \mathcal{T}; \tag{5-45}
 \end{aligned}$$

$$\begin{aligned}
 & \sum_{m \in \mathcal{N}_n} B_{n,m} \cdot \left( \lambda_{n,s,t}^{RT} - \lambda_{m,s,t}^{RT} + \eta_{n,m,s,t}^{RTmax} - \eta_{m,n,s,t}^{RTmax} + \right. \\
 & \left. - \eta_{m,n,s,t}^{RTmin} + \eta_{n,m,s,t}^{RTmin} \right) + \gamma_{t,s}^{RT} = 0, \\
 & \quad : \theta_{n,s,t}^{RT}, \forall \{n = ref\}, t \in \mathcal{T}, s \in \mathcal{S}; \tag{5-46}
 \end{aligned}$$

$$\begin{aligned}
 & \Lambda \cdot (\phi_s / (1 - \varphi)) - \pi_s^{dualCVaR} \geq 0, \\
 & \quad : \gamma_s^{CVaR}, \forall s \in \mathcal{S}; \tag{5-47}
 \end{aligned}$$

$$\Lambda - \sum_{s \in \mathcal{S}} (\pi_s^{dualCVaR}) = 0, : \beta; \tag{5-48}$$

where  $\Xi_{dual} = \{\mu_{i,t}^{Umin} \geq 0, \mu_{i,t}^{Umax} \geq 0, \mu_{i,t}^{Dmax}, \lambda_{n,t}^{DA}, \eta_{n,m,t}^{DAmin} \geq 0, \eta_{n,m,t}^{DAmax} \geq 0, \mu_{i,t}^{SU} \geq 0, \mu_{i,t}^{SD} \geq 0, \gamma_t, \sigma_{i,s,t}^{Umax} \geq 0, \sigma_{i,s,t}^{Dmax} \geq 0, \alpha_{k,s,t}^{max} \geq 0, \omega_{d,s,t}^{max} \geq 0, \eta_{n,m,t}^{RTmin} \geq 0, \eta_{n,m,t}^{RTmax} \geq 0, \lambda_{n,s,t}^{RT} \geq 0, \gamma_{s,t}^{RT}, \mu_{k,t}^{WP} \geq 0, \pi_{i,t}^U \geq 0, \pi_{i,t}^D \geq 0, \pi_{i,t}^{Usys} \geq 0, \pi_{i,t}^{Dsys} \geq 0, \pi_s^{dualCVaR} \geq 0, \mu_{i,t}^{RD} \geq 0, \mu_{i,t}^{RU} \geq 0, \mu_{i,s,t}^{RDRT} \geq 0, \mu_{i,s,t}^{RURT} \geq 0\}$  is the set of dual decision variables.

### 5.1.3 Cost Recovery

In this work, similar to the framework in [167, 116], we study different cost recovery structures so that the generation companies would have sufficient incentives to remain in the market and follow the system operator's dispatch decisions. Different than those works, nevertheless, we also take into account any shortfalls with regard to the reserve allocations in the DA-stage.

#### 5.1.3.1 Cost Recovery per Scenario (CRPS)

Constraint (5-49) warrants that generation companies would not incur any losses under any scenario  $s \in \mathcal{S}$ . Therefore, for each generator  $i \in \Psi_n$  and scenario  $s \in \mathcal{S}$ , we impose that:

$$\begin{aligned}
 & \sum_{t \in \mathcal{T}} \left[ \left( \lambda_{n,t}^{DA} - \lambda_i^E \right) \cdot g_{i,t}^{DA} - \lambda_{i,t}^{SU} - \lambda_{i,t}^{SD} + \left( \pi_{i,t}^{Usys} - \lambda_i^U \right) \cdot r_{i,t}^U + \left( \pi_{i,t}^{Dsys} - \lambda_i^D \right) \cdot r_{i,t}^D \right. \\
 & \left. + \left( \delta_{i,s,t}^+ - \delta_{i,s,t}^- \right) \cdot \left( \lambda_{n,s,t}^{RT} / \phi_s - \lambda_i^E \right) \right] \geq 0. \tag{5-49}
 \end{aligned}$$

### 5.1.3.2

#### Cost Recovery in Expectation (CRIE)

Similar to (5-49), constraint (5-50) ensures that all the generation companies participating in the market recover their costs for supplying energy and reserves in DA-Stage and RT-Stage, but in expectation. More specifically, for a given generator  $i \in \Psi_n$ , we ensure:

$$\sum_{t \in \mathcal{T}} \left[ \left( \lambda_{n,t}^{DA} - \lambda_i^E \right) \cdot g_{i,t}^{DA} - \lambda_{i,t}^{SU} - \lambda_{i,t}^{SD} + \left( \pi_{i,t}^{U_{sys}} - \lambda_i^U \right) \cdot r_{i,t}^U + \left( \pi_{i,t}^{D_{sys}} - \lambda_i^D \right) \cdot r_{i,t}^D + \sum_{s \in \mathcal{S}} \phi_s \cdot \left( \delta_{i,s,t}^+ - \delta_{i,s,t}^- \right) \cdot \left( \lambda_{n,s,t}^{RT} / \phi_s - \lambda_i^E \right) \right] \geq 0. \quad (5-50)$$

### 5.1.3.3

#### Cost recovery in DA-stage including reserves (CRDARES)

Constraint (5-51) ensures that the generators do not incur shortfalls when scheduled for provision of energy and reserves taking into account only the DA-Stage. As some electricity markets do not have an RT-Stage, this cost-recovery scheme provides a comparison against the other two aforementioned schemes. Therefore, for a given  $i \in \Psi_n$ ,

With regard to the CRDARES scheme, Equation (5-51) is added to the main problem, while the other constraints of the main problem with regard to real-time are maintained. The intuition is that the system operator takes a (risk-averse) day-ahead and real-time scheduling decision based on the real-time scenarios and considering a cost recovery guarantee during the day-ahead stage only. Hence, no cost recovery guarantees are given regarding the real-time stage. This is parallel with one of the schemes proposed by the reference [116], and it is maintained for comparability reasons. In addition, revenue cap discussions in the European Union revolves around the day-ahead markets. This makes CRDARES as a relevant scheme in practice as well.

$$\sum_{t \in \mathcal{T}} \left[ \left( \lambda_{n,t}^{DA} - \lambda_i^E \right) \cdot g_{i,t}^{DA} - \lambda_{i,t}^{SU} - \lambda_{i,t}^{SD} + \left( \pi_{i,t}^{U_{sys}} - \lambda_i^U \right) \cdot r_{i,t}^U + \left( \pi_{i,t}^{D_{sys}} - \lambda_i^D \right) \cdot r_{i,t}^D \right] \geq 0. \quad (5-51)$$

### 5.1.3.4 Revenue Cap (REVCAP)

The REVCAP is adapted from the recently proposed European revenue cap scheme which limits the income for generation companies from the day-ahead stage triggered by high-cost gas generators impacting market clearing prices. We note that this is only considered to be applied to DA energy markets, which has been criticised, among others, due to its potential impact on the other markets, such as intraday and balancing markets, etc.

The constraint (5-52) ensures that not only the marginal (variable) costs of generators are covered but also their long-term costs,  $\lambda_i^{LT}$ , evaluated as a technology-specific cap, differentiating among which generator of which technology can earn at a maximum, as outlined in [162]. The maximum income of low-cost technologies – such as wind, solar, nuclear, etc., is capped so that the most they can earn from the day-ahead market is limited to their overall costs, which includes a depreciation value of their long-term costs plus possibly a mark-up. The Levelised Cost of Electricity<sup>1</sup> (LCOE) is used for this purpose. LCOE is regarded as the fair amount a generator needs to earn back in order to break-even their lifetime costs [176]. Within the illustrated revenue cap mechanism, the market-clearing process and uniform market price remain unchanged. As an out-of-market procedure, the revenue exceeding the cap of each generator is redistributed to consumers to mitigate their overall high expenses under abnormal market and system conditions.

Fig. 5.1 illustrates this technology-specific cap mechanism and (5-52) presents the constraints to be imposed in the market clearing procedure for each generator  $i \in \Psi_n$ .

<sup>1</sup>Typically estimated as the average total cost of producing electricity over the power plant lifetime.

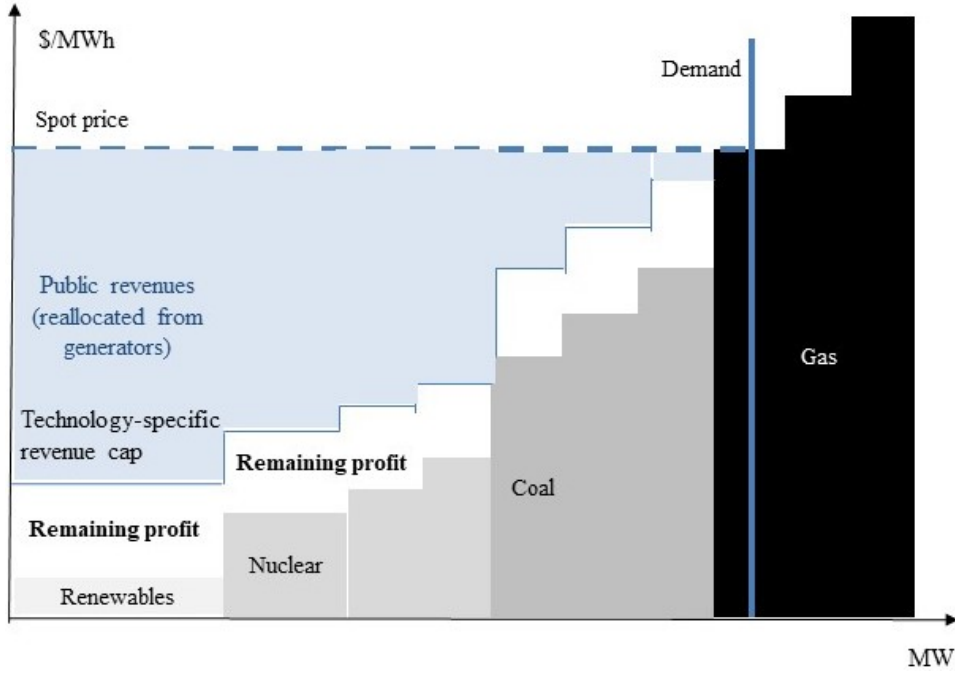


Figure 5.1: Technology-specific revenue cap, adapted from [162].

$$\sum_{t \in T} \left[ \left( \lambda_{n,t}^{DA} - \lambda_i^E \right) \cdot g_{i,t}^{DA} - \lambda_{i,t}^{SU} - \lambda_{i,t}^{SD} - \lambda_i^{LT} \right] \geq 0. \quad (5-52)$$

From a procedural perspective, under the REVCAP case, it is proposed in this paper firstly to perform the market-clearing process including constraint (5-52). Then, as an out-of-market mechanism, revenues exceeding the total costs of generators based on the LCOE are reallocated from generators to consumers.

### 5.1.4 Risk-Averse Market-Clearing with Cost Recovery

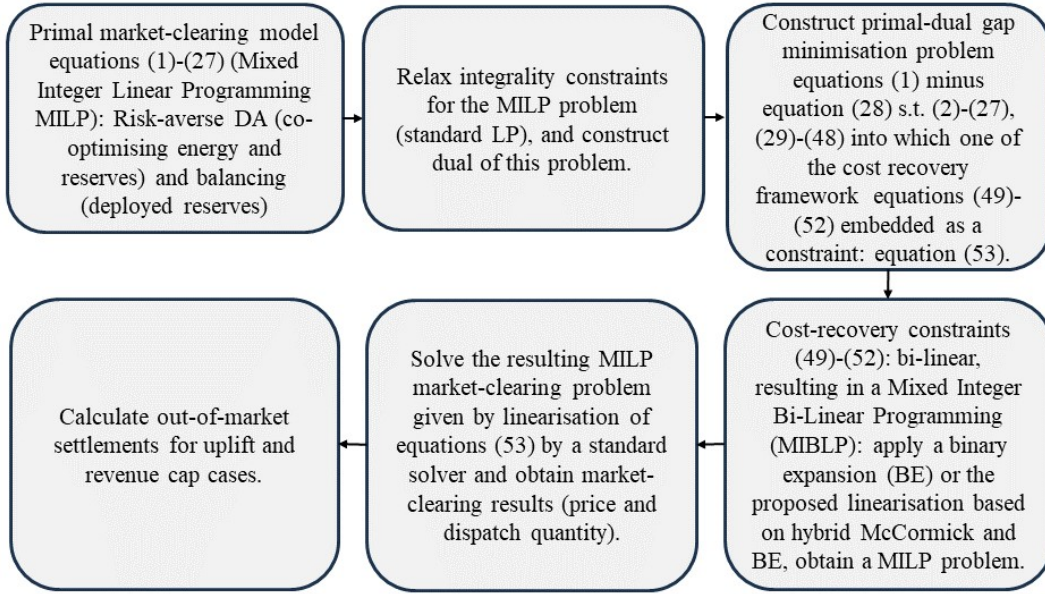


Figure 5.2: Flowchart of the proposed model.

Following the discussion in Sections 5.1.1–5.1.3, the proposed risk-averse market-clearing procedure with cost-recovery guarantees is presented in (5-53). A flowchart of the proposed model is also provided in Figure 5.2. It is based on the primal-dual interdependence which aims at minimising the duality gap between ‘*the risk-adjusted least-cost energy and reserve provision*’ and ‘*market price setting under the continuous relaxation of the non-convex (binary) variables*’.

$$\begin{aligned}
 & \min_{\Xi, \Xi_{dual}} \text{Equation (5-1) minus Equation (5-28)} \\
 & \text{subject to:} \\
 & \text{Primal Constraints: (5-2) – (5-27)} \\
 & \text{Dual Constraints: (5-29) – (5-48)} \\
 & \text{Cost Recovery Constraint: one of (5-49) – (5-52).} \quad (5-53)
 \end{aligned}$$

It is worth highlighting that the market-clearing procedure formulation is within the class of Mixed-Integer Bi-Linear Programming (MIBLP) models, which might not be efficiently solved by available off-the-shelf solvers or standard optimisation algorithms. Therefore, next, we present an efficient solution approach for handling the bi-linear terms in (5-53) based on the hybridisation of McCormick envelopes and binary expansion.

## 5.2

### Solution Methodology: Hybrid McCormick Envelopes and Binary Expansion

We note that the market-clearing formulation in (5-53) is a non-convex optimisation problem due to the bi-linear terms associated with the cost-recovery constraints. Bi-linear terms arise when two decision variables multiply each other, which is the case in the cost-recovery constraints with the product between the clearing-price and cleared-quantity variables. Such problems, classified as NP-hard [35, 108], might not be efficiently solved through available off-the-shelf solvers; and linearisation of these terms is often applied. In this section, we provide a two-step linearisation approach by combining McCormick envelopes and Binary Expansion (BE) approaches to recast the non-convex optimisation problem into a MILP formulation, which can be solved efficiently by leveraging state-of-the-art mixed-integer optimisation algorithms.

Formally, the main idea is to extend the standard binary expansion framework [174, 177] with the inclusion of McCormick envelopes. More specifically, firstly, note that the bi-linear terms encompass DA and/ or RT dispatch or reserve-related variables for which operational feasibility limits their values. Therefore, a binary expansion can be conveniently performed on these DA, RT, and, reserve-related variables. For expository purposes, we focus the presentation in this section on the bi-linear term composed by  $\lambda_{n,t}^{DA} \cdot g_{i,t}^{DA}$ . Any bounded, real-valued number (e.g.,  $g_{i,t}^{DA} \in [0, G_i^{max}]$ ) can be written as a sum of a fractional with a binary expanded term.

$$g_{i,t}^{DA} = \Delta g_{i,t}^{DA} + \sum_{l \in \mathcal{K}} 2^l \cdot z_{i,t,l}^{(1)}, \quad (5-54)$$

where  $\Delta g_{i,t}^{DA} \in [0, 1]$ ,  $z_{i,t,l}^{(1)} \in \{0, 1\}$  and  $\mathcal{K} = \{0, \dots, \lfloor \log_2(G_i^{max}) \rfloor\}$ . Hence, the bi-linear term can be re-written as follows,

$$\lambda_{n,t}^{DA} \cdot g_{i,t}^{DA} = \Delta g_{i,t}^{DA} \cdot \lambda_{n,t}^{DA} + \sum_{l \in \mathcal{K}} 2^l \cdot z_{i,t,l}^{(1)} \cdot \lambda_{n,t}^{DA}. \quad (5-55)$$

Define  $v_{i,t,l}^{(1)} \in \mathbb{R}$  and  $w_{i,t}^{(1)} \in \mathbb{R}$  such that  $v_{i,t,l}^{(1)} = z_{i,t,l}^{(1)} \cdot \lambda_{n,t}^{DA}$  and  $w_{i,t}^{(1)} = \Delta g_{i,t}^{DA} \cdot \lambda_{n,t}^{DA}$ . Then,

$$\lambda_{n,t}^{DA} \cdot g_{i,t}^{DA} = w_{i,t}^{(1)} + \sum_{l \in \mathcal{K}} 2^l \cdot v_{i,t,l}^{(1)}. \quad (5-56)$$

Further on, we apply the McCormick envelopes relaxation to both bi-linear terms  $v_{i,t,l}^{(1)}$  and  $w_{i,t}^{(1)}$ . Firstly, for each  $l \in \mathcal{K}$ , (5-57)–(5-58) describes the

relaxation for  $v_{i,t,l}^{(1)}$ .

$$\lambda_{n,t}^L \cdot z_{i,t,l}^{(1)} \leq v_{i,t,l}^{(1)} \leq \lambda_{n,t}^U \cdot z_{i,t,l}^{(1)}; \quad (5-57)$$

$$\lambda_{n,t}^L \cdot (1 - z_{i,t,l}^{(1)}) \leq \lambda_{n,t}^{DA} - v_{i,t,l}^{(1)} \leq \lambda_{n,t}^U \cdot (1 - z_{i,t,l}^{(1)}), \quad (5-58)$$

where  $\lambda_{n,t}^L$  and  $\lambda_{n,t}^U$  are, respectively, lower- and upper-bounds on  $\lambda_{n,t}^{DA}$ . Albeit the fact that the bounds for dual variables, e.g.,  $\lambda_{n,t}^{DA}$ , are challenging to define, due to the nature of the problem some assumptions can be made under normal operating conditions. For instance, the highest marginal cost in the system can be considered as the upper bound ( $\lambda_{n,t}^U$ ) and its negative value, the respective lower bound ( $\lambda_{n,t}^L$ ). Furthermore, since  $z_{i,t,l}^{(1)} \in \{0, 1\}$ , the McCormick relaxation (5-57)–(5-58) is exact.

For the second bi-linear term  $w_{i,t} = \Delta g_{i,t}^{DA} \cdot \lambda_{n,t}$ , we apply the same rationale leading to the following set of inequalities.

$$\lambda_{n,t}^L \cdot \Delta g_{i,t}^{DA} \leq v_{i,t,l}^{(1)} \leq \lambda_{n,t}^U \cdot \Delta g_{i,t}^{DA}; \quad (5-59)$$

$$\lambda_{n,t}^L \cdot (1 - \Delta g_{i,t}^{DA}) \leq \lambda_{n,t}^{DA} - v_{i,t,l}^{(1)} \leq \lambda_{n,t}^U \cdot (1 - \Delta g_{i,t}^{DA}). \quad (5-60)$$

Therefore, for instance, for a given generator  $i \in \Psi_n$ , the cost recovery scheme presented in (5-52) can be formulated by the following linear equation,

$$\sum_{t \in \mathcal{T}} \left[ w_{i,t}^{(1)} + \sum_{l \in \mathcal{K}} 2^l \cdot v_{i,t,l}^{(1)} - \lambda_{i,t}^E \cdot g_{i,t}^{DA} - \lambda_{i,t}^{SU} - \lambda_{i,t}^{SD} - \lambda_i^{LT} \right] \geq 0,$$

with  $w_{i,t}^{(1)}$  and  $v_{i,t,l}^{(1)}$  characterised by (5-57)–(5-58) and (5-59)–(5-60), respectively. Two key points worth highlighting related to the benefits of combining McCormick envelopes with BE schemes with respect to using one of them individually. On the one hand, note that the proposed hybrid approach has the same order of complexity as the standard BE scheme recurrently used in the technical literature [174, 177]. Thus, the extension to consider McCormick envelopes does not introduce any additional computational burden to the problem, but guarantees that it covers the whole continuous space on which the bi-linear term is defined, differently from the standard BE scheme in which an *a priori* discretisation (approximation) must be defined. On the other hand, since the relaxation imposed by the McCormick envelopes is exact whenever one of the two terms in the bi-linear expression is within its boundaries, we argue that expression (5-56) is expected to be tightly close to the bi-linear term recurrently. More specifically, the only relaxation in the procedure stems from the first term of (5-54), which accounts for the fractional part of the original variable, i.e., variable  $\Delta g_{i,t}^{DA}$ . It is since the second, binary-

expanded, part is modelled using binary variables, thus at their boundaries by construction. Therefore, due to the tight bounds of  $\Delta g_{i,t}^{DA} \in [0, 1]$ , as opposed to  $g_{i,t}^{DA} \in [0, G_i^{max}]$ , we expected that the solution using the hybrid approach be tightly close to the exact one than applying the McCormick envelopes directly in the original bi-linear term.

Finally, it is important to mention that a similar procedure can be performed into the remaining bi-linear terms in the market-clearing model recasting the original risk-averse market-clearing procedure as a MILP model suitable to be solved using state-of-the-art algorithms for mixed-integer optimisation problems. In the next section, a set numerical experiment is presented to illustrate the applicability of the proposed clearing procedure in two case studies.

### 5.3 Case Study

In this section, we illustrate the effectiveness of the proposed market-clearing procedure using two case studies<sup>2</sup>. In Section 5.3.1, an illustrative, small-scale system is considered and we focus our analysis on the following four distinct setups: (i) risk-neutral, uncongested, and multi-commodity markets; (ii) risk-neutral, uncongested, and energy-only market; (iii) risk-neutral, energy-only market with congestion; and (iv) risk-averse, congested with multi-commodity markets. Furthermore, in Section 5.3.2, the representative IEEE 118-bus test system is considered, where we study the effectiveness of the proposed clearing process under similar setups of the first case study. Finally, in Section 5.3.4, the computational performance of the proposed solution approach is analysed and benchmarked against two BE schemes using the IEEE 118-bus test system.

For expository purposes, we also consider a conventional uplift mechanism, hereinafter referred to as U1, where generators are compensated for any potential revenue shortfall in a DA-energy dispatch-only setup. More specifically, firstly, the optimal binary values are obtained by solving the primal market-clearing problem (5-1)–(5-27). Secondly, the problem is re-solved by having fixed the binaries to the optimal values obtained. The dual variables are calculated accordingly from this convex problem in order to obtain DA and RT energy, and reserve prices. Finally, a unit-specific uplift payment is performed, on top of the payments resulting from the market clearance, as

<sup>2</sup>All numerical experiments are performed on an Intel® Core i7-8550U CPU, 1.99 GHz with 8 GB of RAM machine under JuMP® and CPLEX® solver.

follows:

$$U1 = -\min \left\{ \sum_{t \in \mathcal{T}} \left( \lambda_{n,t}^E \cdot (g_{i,t}^{DA} - \lambda_i^E) - \lambda_{i,t}^{SU} - \lambda_{i,t}^{SD} \right), 0 \right\}.$$

We note that real-time scheduling can be with 15 minutes or higher time granularity in today's electricity markets. The most similar market design to the one described in this paper, such as in the United Kingdom (UK), a time-window of half-an-hour to one-hour time-window is applied before the actual delivery. Given the computationally intensive aspect of the model and difficulties in uncertainty representation involving forecast simulations for every, e.g., 15 minutes or shorter; for expository purposes, a time-window of 1-hour is applied without loss of generality.

### 5.3.1

#### Case Study 1: Illustrative System

This case study is adapted from [116], but with both energy and reserve markets under consideration. Throughout the experiment, we assume two-clearing periods representing a low and high demand level. The illustrative system is made up of 3 buses, 3 transmission lines, 3 conventional generators, and 1 wind power production plant, as shown in Figure 5.3. The related data concerning generation and reserve capacity limits, marginal costs of energy, up and down reserves, start-up and shut-down costs are presented in Table 5.1. Reactance of the lines are at 0.13 p.u., and the capacities are at 200 MW. Uncertainty in renewable energy supply resumes to wind power generation and is represented by means of two scenarios: Scenario 1 (*high*) with a probability of occurrence of 0.6 and scenario 2 (*low*) with 0.4 probability.

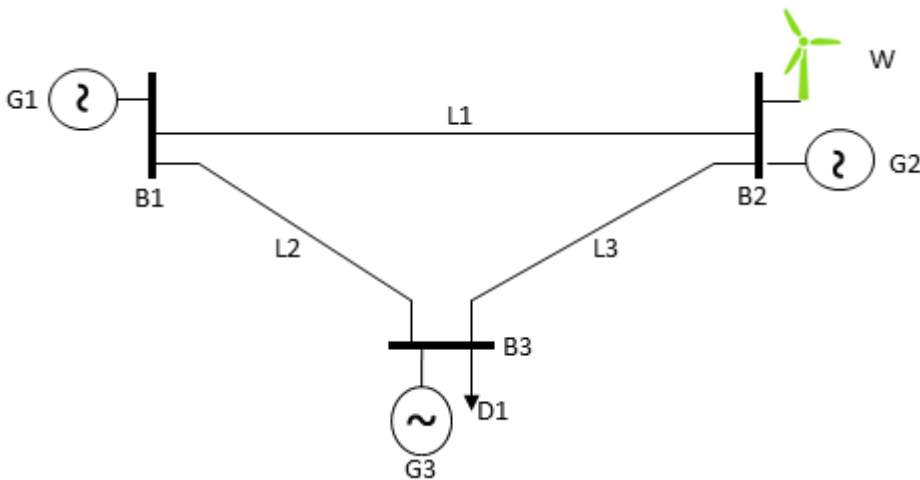


Figure 5.3: Illustrative 3-bus system.

Table 5.1: 3-Bus thermal generation data.

	$G_i^{max}$ [MW]	$G_i^{min}$ [MW]	$\bar{R}_i$ [MW]	$\underline{R}_i$ [MW]	$\lambda_i^E$ [\$/MWh]	$\lambda_i^U$ [\$/MWh]	$\lambda_i^D$ [\$/MWh]	$\lambda_i^{SU}$ [\$]	$\lambda_i^{SD}$ [\$]
G1	95	10	47.50	47.50	20.03	10.02	10.02	101.10	50.55
G2	100	10	50.00	50.00	50.06	25.03	25.03	103.20	51.60
G3	105	10	52.50	52.50	100.01	50.00	50.00	2,001.06	1,000.53

### 5.3.1.1

#### Risk-neutral energy and reserve market

Table 5.2 showcases the resulting DA and RT energy and reserve prices under the different pricing mechanisms analysed. Note that the prices do not vary across scenarios, since no congestion is considered. As anticipated, U1 result in the lowest energy and reserve prices, since the optimisation problem does not inherently impose cost recovery. CRIE yields the lowest price outcomes. In addition, prices under CRDARES are the same as under CRPS. The expected prices for the RT are equal to the DA prices. Table 5.3 presents an overview of consumer payments (*Cons. PMT*), expected cost of supplying energy (*Exp. Cost*) and duality gap (*Dual. GAP*), as a percentage of the expected cost, under the different pricing mechanisms considered. Consumer payments consist of the total cost of energy, reserves, real-time re-dispatch as a function of cleared prices and quantities, as well as start-up and shut-down costs of generators. The cost recovery guarantee represents higher consumer payments than uplift-payment-based approaches. The expected cost of supplying energy in Table 5.3 is calculated from the objective function of the original primal problem, i.e., the social cost of supplying energy. CRDARES depicts the highest costs, whereas U1 and REVCAP yield the least cost.

Table 5.2: Case 1: Energy & Res. Market: DA-energy, reserve, and RT-prices (\$ / MWh).

	DA-Energy		DA-Reserve		RT	
Time	$t = 1$	$t = 2$	$t = 1$	$t = 2$	$t = 1$	$t = 2$
CRDARES	20.03	129.42	28.37	10.02	20.03	129.42
CRIE	20.03	114.55	28.37	10.02	20.03	114.55
CRPS	20.03	129.42	28.37	10.02	20.03	129.42
U1	20.03	95.02	25.03	10.02	20.03	95.02
REVCAP	20.03	131.67	28.37	10.02	20.03	100.02

In Table 5.3, a widening duality gap can be interpreted as a decreased social welfare. REVCAP shows the highest duality gap, followed by CRDARES. As U1 is in relation to a convex optimisation problem where the binary values are fixed, its duality gap is, therefore, zero. Table 5.4 illustrates the opportu-

Table 5.3: Case 1: Energy & Res. Market: Consumer payment (\$), Expected cost of supplying energy (\$), and Duality gap (%).

	CRDARES	CRIE	CRPS	U1	REVCAP
<b>Cons. PMT</b>	44,211.25	40,040.48	43,021.31	34,480.17	35,680.57
<b>Exp. Cost</b>	20,711.13	20,401.95	20,406.90	19,884.06	20,703.27
<b>Dual. GAP</b>	3.89%	2.19%	2.99%	-	4.08%

nity cost of each generator, calculated as the difference between the optimal self-scheduling outcome of each generator and the income obtained under each pricing mechanism. The latter is derived from the calculated DA and RT energy and reserve prices under each scheme, and, as it is assumed that the generators are price-takers. It can be observed that without any cost recovery or similar mechanism, there would be relatively high incentives to deviate from market outcomes. This may give rise to generators diverging from truthful bidding principles. Amongst the cost recovery mechanisms, expectedly, REVCAP represents the highest incentive for the generators to deviate from market outcomes, followed by CRDARES. CRIE leads to the highest alignment between the market and the individual unit. Uplift methods, which are usually criticised due to the respective payments are not reflected directly in energy prices, in this case study, also bring a misalignment between self-scheduling and the market. Especially, this results in G1 and G3 having higher incentives to deviate from market outcomes.

Table 5.4: Case 1: Energy & Res. Market: Opportunity cost under different pricing schemes (\$).

	CRDARES	CRIE	CRPS	U1	REVCAP
G1	0.00	0.00	0.00	1,576.58	3,079.25
G2	391.72	0.00	0.00	300.30	0.00
G3	927.02	562.37	955.68	2,051.01	0.00
Total	1,318.74	562.37	955.68	3,927.89	3,079.25

### 5.3.1.2

#### Risk-neutral energy-only market

In this section, we compare the multi-commodity market combined results against an the typical energy-only market design implemented in several power systems worldwide. Table 5.5 showcases the energy prices in this setup. For time period 1, compared to a bi-product - energy and reserve - market in Section 5.3.1.1, the energy-only market depicts higher DA and expected RT energy prices. In the energy and reserve market structure G1 is the price-setter,

though in the energy-only market the price is affected by the marginal cost of G2. For time period 2, as the bi-product market results in a comparatively lower clearing price, the influence of G3 on the price is more pronounced. Table 5.6 showcases the consumer payment, expected cost of supplying energy,

Table 5.5: Case 1: Energy-only market case: DA and RT prices (\$ / MWh).

Time	DA-Energy		DA-Reserve		RT-scen1		RT-scen2	
	t=1	t=2	t=1	t=2	t=1	t=2	t=1	t=2
CRDARES	33.84	119.07	33.84	119.07	20.03	100.01	54.56	147.65
CRIE	33.84	91.95	33.84	91.95	20.03	50.06	54.56	154.79
CRPS	33.84	103.51	33.84	103.51	20.03	50.06	54.56	183.69
U1	20.03	70.04	20.03	70.04	20.03	50.06	20.03	100.01
REVCAP	33.84	120.59	33.84	120.59	20.03	100.01	54.56	151.46

and the duality gap for the energy-only market. Note that, as expected, the consumer payment and expected cost are significantly lower for the energy-only case compared to the bi-product market. At the same time, we highlight that these results may not be entirely comparable, nevertheless since energy-only markets usually require (out-of-market) mechanisms to safeguard the power system and supply security, whose costs are not reflected. In the case of the energy-only market, the duality gap slightly widens as a percentage of the expected cost as compared to a bi-product market, rising from 4.08% to 6.33% in the case of REVCAP. Finally, Table 5.7 is in relation to the opportunity costs of generators. This single-product market depicts substantial differences among different pricing schemes. The level of incentive misalignment is the highest for REVCAP followed by CRDARES.

Table 5.6: Case 1: Energy-only market case: Consumer payment (\$), Expected cost of supplying energy (\$), and Duality gap (%).

	CRDARES	CRIE	CRPS	U1	REVCAP
<b>Cons. PMT</b>	37,405.99	29,476.32	32,822.23	24,250.88	33,551.32
<b>Exp. Cost</b>	13,606.25	13,561.61	13,560.47	13,553.43	13,563.71
<b>Dual. GAP</b>	5.50%	3.68%	4.83%	-	6.33%

Table 5.7: Case 1: Energy-only market case: Opportunity cost under different pricing schemes (\$).

	CRDARES	CRIE	CRPS	U1	REVCAP
G1	104.98	110.23	110.23	-	1,930.79
G2	1,241.08	162.16	162.16	300.30	1,240.72
G3	737.23	812.27	1,254.01	802.26	760.69
Total	2,083.29	1,084.66	1,526.40	1,102.56	3,932.20

### 5.3.1.3

#### Risk-neutral energy and reserve market: congestion case

Now on, we impose congestion in the network system by limiting the line capacities to 50, 170, and 100 MW for lines 1, 2, and 3, respectively. This limitation did not induce changes in the DA-energy prices for the time period 1 under all mechanisms, except U1 which differed per node varying between 20.03 and 32.04 \$/MWh. This results from the fact that the time period is characterised by a low demand level. In time period 2, however, prices differ per node as opposed to the uncongested case. U1 has very high prices, 416.77 \$/MWh and 813.52 \$/MWh for nodes 2 and 3, as a highly costly load-shedding would be necessary at those nodes. From Table 5.8, we note that consumer payment reduces in most cases due to the load-curtailement. Load-shedding costs are not directly included in the consumer expenses under all schemes. U1 gives rise to substantial consumer payments because of significant clearing price increases. High clearing prices under U1 are observed because of the characteristic of U1, in which firstly the optimal binary values are obtained from the primal problem, and then these are fixed at their optimal values, and finally, the primal problem is rerun. This procedure of fixing of binaries leads directly to substantial day-ahead clearing prices per node, driven by load-shedding becoming the marginal driver of price. In other pricing schemes, this is not the case, because binary values are not fixed, and this gives flexibility in the optimisation problem. Marginal costs driving the clearing-price under these schemes come from generators marginal costs directly. Expected costs, on the other hand, do not show too large variations between different pricing schemes. The duality gap widens notably. From Table 5.9, each scheme depicts some incentives to deviate from market outcomes for G1 and G2. G3 would ideally not participate in the market under CRIE if it were self-scheduled. Another conclusion is that not only G1 and G2 but also G3 would have diverging incentives under U1 due to congestion.

Table 5.8: Case 1: Congestion case: Consumer payment (\$), Expected cost of supplying energy (\$) and Duality gap (%).

	CRDARES	CRIE	CRPS	U1	REVCAP
<b>Cons. PMT</b>	33,372.19	28,098.84	35,067.17	133,765.42	29,570.77
<b>Exp. Cost</b>	52,016.66	51,637.66	51,545.24	50,887.44	51,561.87
<b>Dual. GAP</b>	61.57 %	59.67 %	62.03 %	-	60.17 %

Table 5.9: Case 1: Congestion case: Opportunity cost under different pricing schemes (\$).

	CRDARES	CRIE	CRPS	U1	REVCAP
G1	5,320.50	3,803.49	5,867.30	1,677.67	5,610.63
G2	179.22	131.73	171.61	2,297.30	204.74
G3	0.00	2,782.47	1,155.89	3,181.89	0.0
Total	5,499.72	6,717.69	7,194.80	7,156.85	5,815.37

### 5.3.1.4

#### Risk-averse energy and reserve market

For the risk-averse case, we analyse a mean-risk situation by setting  $\Lambda = 0.50$ , giving equal weight to both the risk-neutral expected value solution and the expected shortfall, measured by CVaR. From Table 5.10, one of the findings is that energy prices rise comparatively for the time period 2 under all cases except CRDARES, against the risk-neutral case. The reserve price for time period 2, which represents a peak hour, increases as a result of the risk aversion of the market operator.

Table 5.10: Case 1: Risk aversion case: DA-energy, reserve and RT-prices (\$/MWh).

Method	DA-Energy		DA-Reserve		RT	
	t=1	t=2	t=1	t=2	t=1	t=2
CRDARES	20.03	129.33	28.37	16.02	20.03	129.33
CRIE	20.03	119.07	28.37	16.02	20.03	119.07
CRPS	20.03	119.41	28.37	16.02	20.03	119.41
U1	20.03	100.01	25.03	16.02	20.03	100.01
REVCAP	10.02	131.67	14.18	46.67	10.02	90.01

From Table 5.11, the main conclusion is that both consumer payment and the expected cost of supplying energy increase, which is an anticipated outcome. From Table 5.12, the risk aversion of the system operator creates, in general, higher incentives for all generators to deviate from market clearing results.

We note that a risk-neutral framework takes the average impact of the expected scenarios into account. This differs from a risk-averse framework, in which the tail-risk is also reflected in the decision-making process so that robustness - in case an adverse scenario materialises in reality - can be achieved depending on the choice of confidence level.

In order to illustrate the 'value' of a risk-averse framework, a high-impact unobserved extreme scenario with low wind is assumed to occur as a real-time

Table 5.11: Case 1: Risk aversion case: Consumer payment (\$), Expected cost of supplying energy (\$), and Duality gap (%).

	CRDARES	CRIE	CRPS	U1	REVCAP
<b>Cons. PMT</b>	45,109.56	42,209.70	42,272.88	37,768.35	37,413.04
<b>Exp. Cost</b>	20,785.13	20,761.61	20,604.18	20,260.86	20,786.38
<b>Dual. GAP</b>	2.75%	1.97%	2.86%	-	3.41%

Table 5.12: Case 1: Risk aversion case: Opportunity cost under different pricing schemes (\$).

	CRDARES	CRIE	CRPS	U1	REVCAP
G1	3,022.16	3,021.02	3,024.44	2,778.06	3,323.12
G2	987.79	1,035.55	1,496.60	675.75	0.00
G3	2,828.25	2,376.28	1,764.98	2,001.06	2,915.15
Total	6,838.20	6,432.85	6,286.02	5,454.87	6,238.27

realisation. This is in order to measure the load-shedding in extreme cases. Firstly, a first-stage solution day-ahead scheduling with and without risk-aversion consideration is obtained. The quality of the first-stage solution is evaluated, measured by load-shedding level under risk-neutral and risk-averse frameworks. Without loss of generality, it is also assumed that generators are not fully flexible and cannot increase their generation by more than 50% in real-time compared to their commitment. For a demand level of 320 MW within 1-hour period and considering the expected wind scenarios used in this case study, as in Table 5.13, both frameworks dispatch 95 MW for the wind park at the day-ahead stage. Risk-averse framework, being more conservative, schedules in day-ahead a lower quantity from G2 and a higher one from G3 due to high wind uncertainty, although G3 has a higher marginal cost. Accordingly, risk-neutral framework would need to shed 55 MW of load in real-time in order not being able to re-dispatch sufficiently from especially G3 because of its inflexibility, given low wind generation realisation of 10 MW. In the case of risk-averse framework, the 12.5 MW of load would be shed.

Table 5.13: Case 1: Illustration of benefit of risk-aversion.

	Risk-neutral DA Dispatch MW	Risk-averse DA Dispatch MW	Risk-neutral RT Realisation MW	Risk-averse RT Realisation MW
G1	85	85	95	95
G2	100	65	100	97.5
G3	40	75	60	105
WP	95	95	10	10
Generation Total	320	320	265	307.5
Load-shedding			55	12.5

### 5.3.2

#### Case Study 2: IEEE-118 Test System

Case Study 2 is based on the IEEE-118 test system, adapted to fit the Belgium, Netherlands, Sweden, Germany, and Norway power systems characteristics. The test system consists of 118 buses, 186 transmission lines, 28 conventional generators, and 26 weather-dependent production facilities. We assume three clearing periods representing low, mid, and high load levels. The wind output uncertainty is accounted for after fitting its uncertainty into a Weibull distribution as in [178]. The study uses the estimates by Met Office (UK National Weather Service) as nominal expected values of the distribution. For the characterisation of the wind output, 25 scenarios are randomly sampled. By fitting the actual data to the Weibull distribution, point estimates are obtained. The shape and scale parameters of the distribution are 1.69 and 18.53, respectively. As a congestion case, the capacity of five branches originating from buses 69 and 89 - namely, branches 105, 106, 107, 136, 137 - are reduced: the first three of them to 40 % of their capacity, and the last two to 20% of their capacity. This congestion setup may arguably be restrictive for the normal operation of the network where the generators are more static and not weather-dependent. However, the countries with increased penetration of renewable sources, such as the case in the Netherlands, are observing structural congestion as a new reality.

Table 5.14 shows the overview of consumer payments, expected cost of supplying energy, and duality gap results under different pricing schemes. One can observe that cost-recovery imposed cases have relatively similar results in terms of the expected cost of supplying energy, with CRPS and CRDARES among the highest. As expected, CRPS and CRDARES induce the highest consumer payments, with REVCAP the second lowest and CRIE the lowest. A similar order is also observed with regard to the duality gaps.

Table 5.14: Case 2: Risk-neutral Energy and Reserve: Consumer payment (\$), Expected cost of supplying energy (\$), and Duality gap (%).

	CRDARES	CRIE	CRPS	U1	REVCAP
<b>Cons. PMT</b>	803,202.70	698,943.54	803,202.70	778,414.87	720,080.10
<b>Exp. Cost</b>	332,668.17	309,954.29	333,382.46	309,193.97	309,793.97
<b>Dual. GAP</b>	8.13%	6.10%	8.22%	-	5.25%

We note that the clearing prices under different mechanisms do not show large deviations from each other. RT prices in expectation are equal to the DA prices. For the energy and reserve market risk-neutral case, the market clearing prices for energy are at \$22.10, \$19.96, \$68.98 per MWh for the time periods 1, 2, and 3, respectively. Regarding the energy-only market case, the prices are

\$9.77, \$10.30, \$176.99, respectively. Risk-averse multi-commodity market case clears the prices at \$23.31, \$21.96, \$75.52, respectively. Table 5.15 outlines the average profit per generator under each pricing regime. REVCAP results in the lowest profits per generator for the risk-averse setup. When risk aversion is taken into account, average profit deviations are relatively low. Congestion causes the average profit to almost double, except for the REVCAP case. Congestion case results, as shown in Table 5.16, show very comparable results for all schemes. REVCAP indicates the lowest consumer payments, 32.96% less when compared against CRIE, for instance.

Table 5.15: Case 2: Average profit per generator under different pricing schemes and market, operational case (\$).

	CRDARES	CRIE	CRPS	U1	REVCAP
<b>En.-Res. Markets</b>	9,861.87	10,484.85	9,825.33	9,652.28	8,821.82
<b>Congestion</b>	19,642.55	20,028.43	19,852.69	18,028.43	11,391.84
<b>Energy only</b>	12,379.87	13,638.42	12,300.78	11,999.87	9,853.00
<b>Risk averse</b>	10,567.63	10,572.57	10,566.59	9,573.44	9,082.16

Table 5.16: Case 2: Risk-neutral Energy and Reserve with Congestion: Consumer payment (\$), Expected cost of supplying energy (\$), and Duality gap (%).

	CRDARES	CRIE	CRPS	U1	REVCAP
<b>Cons. PMT</b>	1,410,542.41	1,411,255.44	1,409,872.31	1,408,118.22	945,159.65
<b>Exp. Cost</b>	449,719.47	440,848.83	442,870.54	440,648.93	440,733.93
<b>Dual. GAP</b>	7.78%	7.15%	7.30%	-	7.14%

Congestion case price results, as in Fig. 5.4, indicate large fluctuations, especially around node 69 where a large generator and one of the congested lines are located. The price shock is the highest at hour 3 when the system loading level is the highest. The effect of congestion in the line originating from bus 89 is perceivable also at other nodes, e.g., node 81, severely. Similarly, node 116 shows a large price shock at hour 3. The lost opportunity cost per generator is presented in Fig. 5.5. The energy and reserve risk-neutral market case is the least varying one, whereas the energy-only case shows relatively large opportunity costs for some generators. It is attributable to the fact that co-optimisation of energy and reserves results in a more informed allocation, leading to lower opportunity costs for generators. Congestion gives results in a higher number of outliers with relatively high lost opportunity costs. Since clearing prices are higher in the case of congestion, at some nodes some generators might be willing to dispatch more compared to what is feasible under the central dispatch which considers network constraints. Self-scheduling does not consider network constraints.

Consumer payment, expected cost, and duality gap results for risk-averse energy and reserve case are presented in Table 5.17. Risk aversion gives result in an alignment between the schemes. REVCAP differs from the others in terms of providing the lowest consumer payment. Similarly, Table 5.18 outlines consumer payment, expected cost, and duality gap results for the risk-neutral energy-only case. These are comparable to the bi-commodity case, with orders of magnitude of the schemes being different.

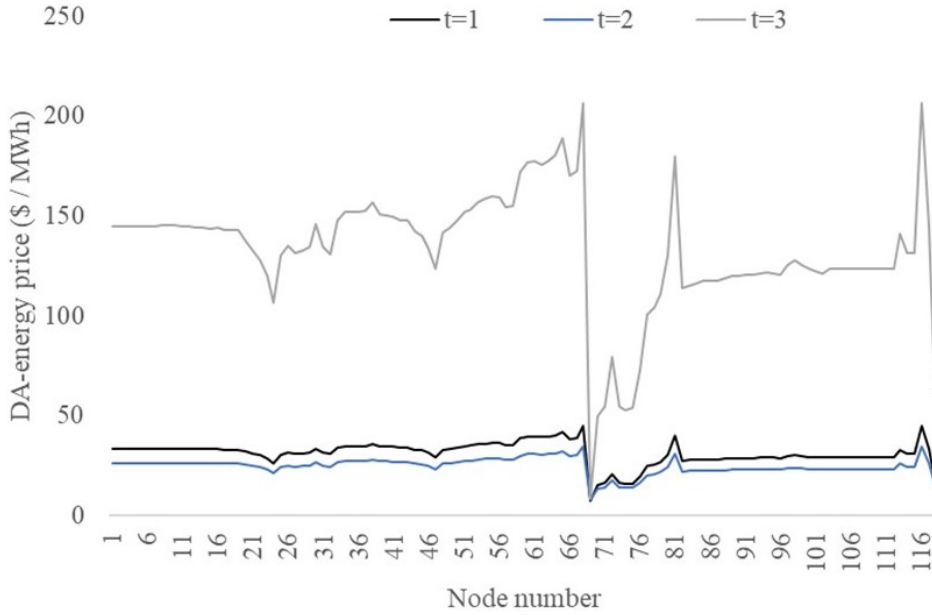


Figure 5.4: Case 2: Congestion DA-energy prices per node (\$ / MWh)

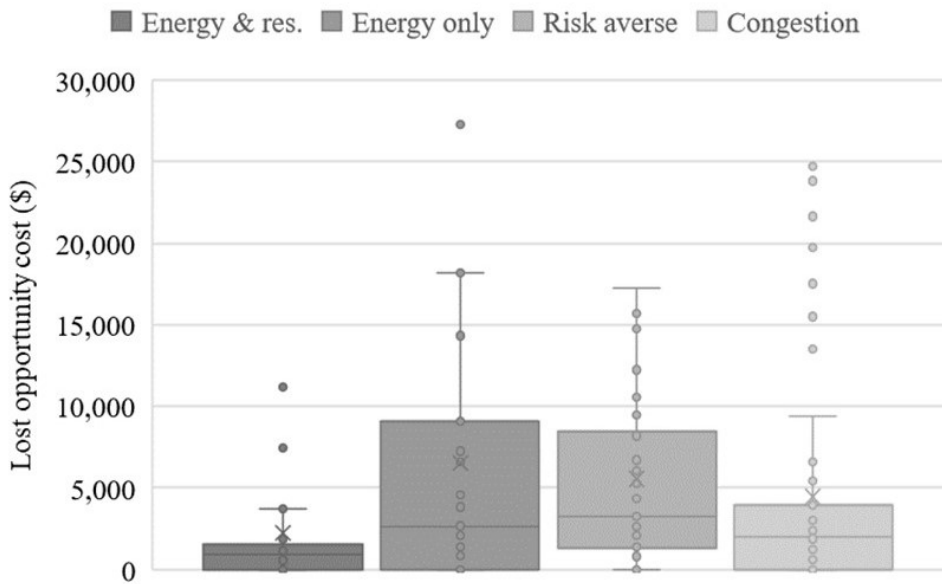


Figure 5.5: Case 2: Lost opportunity cost per generator (\$)

Table 5.17: Case 2: Risk-Averse Energy and Reserve: Consumer payment (\$), Expected cost of supplying energy (\$), and Duality gap (%).

	CRDARES	CRIE	CRPS	U1	REVCAP
<b>Cons. PMT</b>	918,276.30	918,315.38	918,220.19	870,789.82	837,721.03
<b>Exp. Cost</b>	333,139.21	332,911.71	333,139.21	333,099.21	332,799.14
<b>Dual. GAP</b>	5.50%	5.47%	5.50%	-	5.46%

Table 5.18: Case 2: Risk-neutral Energy Only: Consumer payment (\$), Expected cost of supplying energy (\$), and Duality gap (%).

	CRDARES	CRIE	CRPS	U1	REVCAP
<b>Cons. PMT</b>	665,936.97	573,133.70	658,626.21	523,667.28	487,163.65
<b>Exp. Cost</b>	194,866.04	189,450.41	192,726.77	187,177.01	189,260.96
<b>Dual. GAP</b>	5.41%	6.28%	5.47%	-	5.53%

### 5.3.3

#### Case Study 3: GB-29 Bus System

This Case Study is based on [32] as well as [179]. The Great Britain (GB) system comprises 29 buses, 99 transmission lines, 52 generators, and 10 wind farms. These wind generation facilities are connected to buses 1, 2, 3, 4, 6, 7, 11, 19, 20 and 27. Two major generators are located at node numbers 25 and 27. Based on the data, conventional generators have marginal costs varying between 4.42 and 13.0 \$ per MWh. The demand totals to 225.30 GW in the first hour and 444.25 in the second hour, allocated to each node in similar percentages as in [32]. 25 wind scenarios and 2 hours of operations are considered in this analysis. Wind scenarios cover 45% and 22% of the demand within hour 1 and 2, respectively. As a congestion case, the capacity of one of the lines connected to generator 25 is reduced to 60% of its capacity.

Table 5.19 outlines the consumer payments, expected cost of supplying energy and duality gap results under different pricing schemes. The observations are similar to that of Case 2: cost-recovery imposed cases depict comparable results in terms of expected cost of supplying energy and consumer payment. CRPS leads to the highest consumer payments and duality gaps, preceded by CRDARES and CRIE.

Table 5.19: Case 3: Risk-neutral Energy and Reserve: Consumer payment (\$), Expected cost of supplying energy (\$), and Duality gap (%).

	CRDARES	CRIE	CRPS	U1	REVCAP
<b>Cons. PMT</b>	7,800,402.58	6,311,728.35	7,800,539.81	7,859,808.66	6,310,000.00
<b>Exp. Cost</b>	1,656,473.51	1,648,782.12	1,657,447.46	1,645,963.14	1,650,000.00
<b>Dual. GAP</b>	3.57%	2.10%	3.59%	-	1.75%

Congestion case, as described in Table 5.20, do not indicate large deviations amongst the schemes. As in Case 2, REVCAP gives the least consumer payment, which is 8.34 % lower than CRIE.

Table 5.20: Case 3: Risk-neutral Energy and Reserve with Congestion: Consumer payment (\$), Expected cost of supplying energy (\$), and Duality gap (%).

	CRDARES	CRIE	CRPS	U1	REVCAP
<b>Cons. PMT</b>	8,300,654.87	7,684,533.42	8,602,888.23	7,568,823.32	7,043,464.01
<b>Exp. Cost</b>	1,800,394.71	1,750,689.33	1,833,689.11	1,750,622.83	1,750,867.29
<b>Dual. GAP</b>	10.91%	10.82%	10.21%	-	10.79%

The lost opportunity cost per generator is given in Fig. 5.6. As observed for Case 2, the energy and reserve risk-neutral market case is the least volatile, while on average the energy-only case depicts markedly large opportunity costs for some generators. Congestion leads to more outliers.

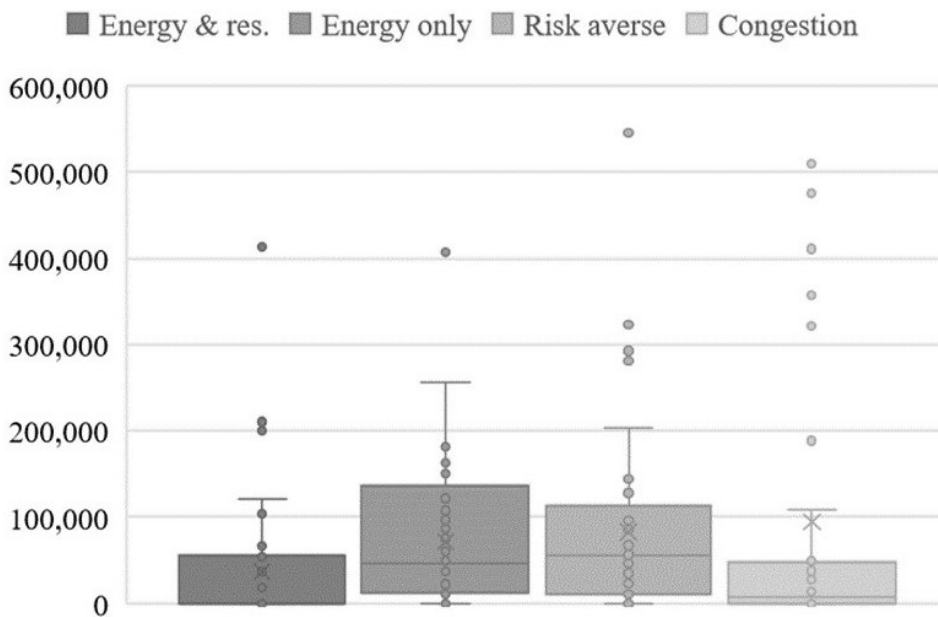


Figure 5.6: Case 3: Lost opportunity cost per generator (x10 \$)

Risk-averse case, as described in Table 5.21, shows that REVCAP gives result to lowest consumer payments. Other schemes provide comparable results. Both Case Study 2 and 3 show that without any cost recovery or similar mechanism, there are incentives to deviate from market outcomes, though to a lesser extent especially when energy and reserve markets are jointly considered, as compared to the Case Study 1.

Table 5.21: Case 3: Risk-Averse Energy and Reserve: Consumer payment (\$), Expected cost of supplying energy (\$), and Duality gap (%).

	CRDARES	CRIE	CRPS	U1	REVCAP
<b>Cons. PMT</b>	8,544,378.99	8,542,627.21	8,541,092.90	8,341,253.40	7,909,060.25
<b>Exp. Cost</b>	1,702,200.19	1,703,699.81	1,702,281.57	1,702,221.21	1,700,561.10
<b>Dual. GAP</b>	6.61%	6.35%	6.40%	-	6.34%

Table 5.22: Case 3: Risk-neutral Energy Only: Consumer payment (\$), Expected cost of supplying energy (\$), and Duality gap (%).

	CRDARES	CRIE	CRPS	U1	REVCAP
<b>Cons. PMT</b>	6,240,329.22	5,990,621.01	6,123,821.12	5,500,299.91	5,201,308.81
<b>Exp. Cost</b>	1,027,829	990,625.41	1,019,653.53	988,235.51	989,320.87
<b>Dual. GAP</b>	6.11%	6.78%	6.01%	-	6.13%

### 5.3.4

#### Computational Analysis: IEEE-118 Test System

Table 5.23 compares the standard BE scheme with a step size discretisation of 20 MW (*large*) and 10 MW (*small*) for energy. These are compared against the proposed hybrid mechanism described in Section 5.2, which blends BE with McCormick envelopes. For expository purposes, the computational analysis is made on the CPRS scheme for the energy and reserve, risk-neutral case. Similar conclusions can be drawn for other schemes. The proposed algorithmic procedure reduces the computational time by roughly 70% and achieves a solution 1.8% lower than the binary expansion small step size case, highlighting the computational capability of the proposed hybrid procedure, both in speed and solution quality.

Table 5.23: Case 2: Computational Analysis

	BE-Large	BE-Small	Hybrid
Nb. of cont.var.	181,928	182,864	170,030
Nb. of bin.var.	15,370	16,106	34,712
Nb. of total var.	197,298	198,970	204,742
Nb. of constraints	415,258	601,088	877,099
Computational time [sec.]	128,596.20	136,025.55	40,774.39
Obj.value [USD]	86,887.28	66,051.66	64,855.45

## 5.4

### Chapter Conclusion

In this paper, a market-clearing procedure is proposed that efficiently balances a reasonable-costly scheduling for the next day’s operation with an endogenous cost-recovery guarantee. Structurally, the rationale is to co-optimize energy and reserves in a stochastic risk-averse framework while endogenously ensuring cost recovery for generation companies. To this end, different income sufficiency schemes are considered: i) warranting DA-energy and reserve-related shortfalls to be covered; ii) providing revenue sufficiency in expectation of the RT scenario realisations; iii) guaranteeing self-sustainability for generators in every ‘credible’ scenario agreed by the market players. These

mechanisms are compared against the existing uplift payments – based on out-of-market compensation schemes, for the DA-stage. A revenue cap, limiting windfall profits for low-cost generators and reallocating them to consumers, is also designed and discussed.

The resulting stochastic market-clearing procedure formulation is within the class of Mixed-Integer Bi-Linear Programming (MIBLP) models, thus challenging to be solved using off-the-shelf solvers or standard optimisation algorithms. Therefore, a hybridisation of McCormick envelopes and binary expansion is proposed to enhance the computational capability to solve the clearing problem. Numerical experiments indicate that the computing time under this solution approach decreases by 70% compared to the standard binary expansion when applied to an instance of the IEEE-118 test system. Two case studies are also conducted to illustrate the effectiveness of the proposed market-clearing procedure. In summary, we observe that:

1. Although the cost-recovery mechanisms are intuitively similar, under a highly uncertain wind power generation environment, as in case study 1, they depict heterogeneous dispatch and price outcomes. This aspect has also been observed by [116]. Moreover, the inclusion of risk aversion results in an increased alignment between the pricing schemes. Revenue cap indicates in almost all cases the lowest consumer payments, which competes mostly with CRIE.
2. Under high uncertainty, mechanisms other than CRPS may not always warrant covering the costs of the generation companies. Nevertheless, such a mechanism may also cause shifts of revenues from the least marginal cost generators toward higher-cost ones. This can also be concluded based on the proposed pricing schemes by [116].
3. In the bi-commodity markets with co-optimising energy and reserves clearing, the costs for safeguarding the power system are more transparently allocated and calculated. This aspect is studied in a recent paper in a different framework [30]. An energy-only market would otherwise require out-of-market mechanisms to settle any real-time deviations.
4. In terms of opportunity costs, some high-cost generators, may not have incentives to enter the market solely based on price signals. They may have high incentives to deviate from market outcomes. This finding is also supported by earlier works, such as [159, 28, 116]. It is shown that consideration of reserve markets and risk aversion may not be sufficient to mitigate these incentives.

Transmission congestion can lead to high market-clearing prices, as observed particularly in Case 1. Future research can look into fairness aspects of uplift or other out-of-market mechanisms, and how to reimburse affected consumers. As a future direction, market power aspects could also be studied.

## 6

### Conclusions, Limitations and Future Perspectives

This Chapter reuses and extends the conclusions in the following publications: [**Paper A**] Martin, N. C., & Fanzeres, B. (2023, June). Linearisation Based Decomposition Method for Circle Approximation in AC Network Constrained Unit Commitment. In 2023 IEEE Belgrade PowerTech (pp. 1-6). IEEE, which is herewith referenced and cited as [20]. [**Paper B**] Martin, N. C., & Fanzeres, B. A Two-Level ADMM Algorithm for Multi-Agent DSO-TSO Congestion Management and Voltage Control Coordination with Limited Information Exchange. *In process of publication*, which is referenced and cited as [140]. [**Paper C**] Martin, N. C., & Fanzeres, B. (2023). Stochastic risk-averse energy and reserve scheduling and pricing schemes with non-convexities and revenue caps. *Electric Power Systems Research*, 225, 109858., which is referenced and cited as [29]. A related publication supporting the conclusions is [**Paper D**] Martin, N. C., & Fanzeres, B. (2023, September). A Stochastic Risk-Averse Model to Price Energy in Pool-Based Electricity Markets with Non-Convex Costs and Revenue Caps. In 2023 International Conference on Smart Energy Systems and Technologies (SEST) (pp. 1-6). IEEE. The latter is referenced and cited as [18].

#### 6.1

##### Overview of conclusions

In this thesis, models and algorithms are developed so that computational capability and model accuracy are improved for

- i) AC Network-constrained Unit Commitment (NC-UC) / optimal power flow (OPF) for standalone normal operations as well as ‘coordinated transmission and distribution system operations to mitigate congestion and voltage problems with a limited network information interchange’;
- ii) locational marginal pricing (LMP) for DC-NCUC for transmission system under non-convex operational decisions and stochastic renewable generation (RES).

The main conclusions and future perspectives are as follows:

### 6.1.1

#### Conclusions, limitations and future perspectives for computational techniques and modelling accuracy for AC UC and OPF

##### *Conclusions*

In this contribution, linked to [Paper A], we proposed a methodology to solve AC-NCUC problems, which is shown to be computationally beneficial especially for solving relatively large network problems, with 118-bus and 240-bus which tend to be state-of-the-art network sizes. This methodology relies on i) quadratic relaxation for the conic formulation, and linearisation of all resulting quadratic constraints, ii) applying an outer approximation based decomposition algorithm to select optimal lines from a continuous set. Since the linearisation procedure in [133] may require a large number of discretisations selected *a priori* along with their enumeration, the proposed procedure in this contribution enhances scalability, given the fact that it solely includes discretisations (tangents) which improve the solution.

We numerically demonstrated the efficiency of the proposed algorithm, which converges after a few iterations. It gives computational savings compared to standard SOCP. For medium-loading conditions, the results are similar to those provided by SOCP, which tend to be precise [129]. With regard to high-loading conditions, under which SOCP results may be less precise, the devised algorithm enhances the solution quality. The latter is measured in this work in terms of how much the original non-convex equality constraint – which describes a cone when relaxed into an inequality constraint – is violated under both solutions. For a low load-level, the load flow related results from the algorithm can be more disperse, though on average provide a higher precision than SOCP.

These main findings are also supported by extensive numerical experiments represented by performance curves, based on simulations by considering randomly drawn instances for important parameters.

##### *Limitations and future perspectives*

Future works can make a comparison between the outer approximation-based approach [91], as applied in this work, against an inner approximation. Furthermore, future works can extend the study in relation to the circumstances under which DC power flow (linear) approximation to an AC system would not perform well. Stability and computational characteristics of the proposal can be analysed in more detail, as low-loading conditions, for example, resulted in a relatively high constraint violation for one of the instances analysed. Some constraint violations can be anticipated for a low system-loading, since the

devised method uses a quadratic relaxation in which the bounds are set at the maximum voltage limits, which might not be tight especially for low-loaded networks. Handling this aspect is left as future work.

Other than these, one of the limitations of the thesis is the potential existence of other convexification techniques which have not been extensively studied though highlighted in Chapter 2 - Methodological Background. As future work, tighter convex relaxations can be sought, and other comparisons can be made with other techniques, such as semi-definite programming or hybrid methods combining SDP-SOCP, also in view of different loading conditions. Potential tightening of quadratic approximation applied in this thesis through a dynamic circle approximation with valid tangents (cuts) is an ongoing work. Another work-in-progress is applying different circle projection methods to the outer approximation algorithm, not only horizontal as in the thesis, but also vertical and diagonal, which may show different characteristics.

Furthermore, extensions of the proposed algorithm with state estimation is a research direction, in which limited observability of distribution systems can be incorporated and studied.

Finally, a limitation of the proposed method is the fact that it ignores meshed aspects of networks, which requires consideration of phase angle consistency-related constraints around orientation of each phase angle, which are non-convex. Future works can extend the proposal by meshed networks. Especially for transmission systems meshing is regarded as an important element for future energy systems, as in the Netherlands, due to security of supply, stability and integration of offshore wind [180]. Because of self-healing technologies being explored for distribution systems, a meshed network structure can be beneficial for, e.g., remote switching and reconfiguration. As such, a meshed structure can also be relevant particularly for future MV distribution grids. Three-phase models for distribution systems is another research direction. An  $N - 1$  security analysis can also be included in future works, and scalability of the model considering this can be analysed.

### 6.1.2

#### **Conclusions, limitations and future perspectives for computational techniques and modelling accuracy for multi-agent DSO-TSO coordination for congestion and voltage management**

##### *Conclusions*

This contribution, linked to [Paper B], investigated the computational, power flow accuracy and network-information exchange benefits of employing a two-level ADMM into which a linearisation-based circle approximation to AC OPF for distribution networks embedded as a nested structure to solve a multi-agent

DSO-TSO coordination problem. Furthermore, a decentralised communication structure is proposed reducing the network information exchange with some computational and other potential benefits, such as less data storage needs and cybersecurity. Multi-agent DSO-TSO coordination can be, e.g., through active distribution networks proving flexibility towards a TSO to optimise scheduling by considering the power flows at the interface. The problem is studied as a multi-period time-coupled coordination problem - given the presence of energy storage systems and demand response - in day-ahead operational planning for the procurement of ancillary services has the objective to handle operational issues regarding congestion and voltage problems jointly. The modelling approach is a general framework consisting potentially of multiple DSOs and TSOs in which the networks can be further decomposed in terms of subsystems or devices. Such a problem constitutes a multi-block problem without any warranty of convergence under a standard ADMM. Note that this time-coupling and AC power flow modelling increases the computational load of the model considerably.

Numerical experiments comparing the computational performance of the proposed procedure with a standard ADMM along with a SOCP-approximation to AC power flow as benchmarks revealed some benefits of the proposal. The results demonstrated that in terms of number of iterations and computational time, two-level ADMM outperforms standard ADMM. It is observed that penalty parameter-tuning is an issue in both standard ADMM and two-level ADMM and results vary depending on their choice. Two-level ADMM is shown to provide convergence or a tighter optimality gap which can be acceptable from an engineering point of view, depending on the application, for a computationally demanding case with time-coupling and AC power flow. For the same case, standard ADMM gives a divergent result for a given number of iterations, and does not seem to converge. In addition, incorporation of the linearisation and decomposition procedure for AC power flow for distribution networks results in computational savings. In terms of network data transfer, interchange of solely active and reactive power flows (or equivalently, parameters related to sinus and cosine functions of nodal voltage) and their dual values with the adjacent operator are needed. Accordingly a need for a central controller is limited.

The value of DSO-TSO coordination is calculated under presented assumptions. Accordingly, when with coordination and without coordination cases compared, it is observed that the renewable generation curtailment decreases by 23.63% and total system costs by 28.79%.

*Limitations and future perspectives*

One limitation of this work is the fact that it ignores the broader perspectives for the implementation of DSO-TSO coordination, where sociological, technical and economic challenges need to be addressed.

Despite demonstrated advantages of a two-level ADMM in this work in terms of parameter control and convergence, necessity to trial-and-error parameter choice may not be entirely eliminated. In practice, one can use experiences from previously run cases. For representative days, with regard to demand and supply conditions for instance, the gained experience on the parameters can be applied to similar days. This procedure can be done on a regular basis, and a database for parameters can be created, and these can be applied as a warm-start of the algorithm, by using techniques such as machine learning and other data-driven methods, which can be a future research direction.

Future works can relax the assumption that agents provide the computed values honestly for exchange variables, include reputation of agents in the modelling, and what can be learned from past data. Machine learning or data-driven methods, such as reinforcement learning, can be considered to be applied, e.g., in order to penalise agents when not acting honestly.

Other than that, auction theoretical aspects can be added into the modelling, with frameworks incentivising truthful bidding of agents.

In addition, though system operators are assumed not to have any hierarchy amongst each other, the implications of a potential hierarchy can be analysed and discussed. Albeit this assumption, the fairness aspects for all agents with further elements, such as fairness of curtailment for consumers, are not taken into account, and left as future work.

Future works can focus on computational benefits of the proposed approach on coordination problems with stochasticity of e.g., generation or load, and mixed-integer variables representing unit commitment. Moreover, despite the fact that two-level ADMM can be a promising approach to handle the multi-agent DSO-TSO coordination problem, some additional implementations can be explored, such as within the context of microgrids. The scalability of the approach in case of a larger number of agents can be investigated. For real systems, further implementation capability might be needed - such as, parallel computing in a cloud service, efficient parallelisation, and data structure, as well as hot start or heuristic strategies. Other decentralised or distributed computational techniques can also be explored for solving DSO-TSO coordination.

Furthermore, general state-of-the art limitation of ADMM models is the necessity of significant penalty parameter-tuning. Two-level ADMM poten-

tially provides more control over the parameter updates, though its trial-and-error based tuning may not be eliminated as also observed in [149, 150]. As a potential future research, one can analyse in more detail relationship between the choice of penalty parameters, and the system characteristics, such as line impedances and loading conditions.

Moreover, iterations of sub-problems in any ADMM model may have diverging computational times amongst each other, leading to waiting by faster sub-problems for the slower ones until a solution is found. Asynchronous versions of two-level ADMM can be explored for computational savings.

Another point is in terms of some jumps in the results per iteration observed within a two-level ADMM modelling, most likely because of the existence of an outer loop providing control and feedback towards the inner loop, which is lacking in a standard ADMM. Implementations along with a 'best upper bound' or similar research directions can be thought of, or blended with a two-level ADMM to achieve a monotonically decreasing optimality gap.

Furthermore, in terms of a managerial consideration, the day-ahead planning problem presented ignores  $N - 1$  security for the transmission system so that it procures sufficient flexibility to re-dispatch in case of a failure of a component. This security constraint is typically included in real system operations [65]. Although this work focuses principally on the network information exchange and coordination for mitigating congestion and voltage problems, it is anticipated that inclusion of  $N - 1$  security would not change the principal conclusions of this work. Nevertheless, this is left as a future work.

Future works can relax assumptions on energy storage systems, such as being ideal, implement granular time scales, varying charging or discharging efficiencies, degradation aspects, etc. Another extension can be by considering storage systems operated by third parties and having own objectives. This latter would require consideration of equilibrium amongst not only system operators but also storage operators. Another observation is that tight formulations in the state-of-the art literature [139] to avoid binaries for capturing not simultaneous charging and discharging, could not entirely prevent this to occur. Since ADMM variants tend not to perform well for mixed-integer OPF problems, such a convex formulation as in [139] is adapted in this work. Future works can consider devising alternative formulations for capturing these mutually exclusive states.

Moreover, demand response modelling can be extended further. For instance, efficiency loss in demand shift due to weather and temperature can be included.

Finally, as in the previous contribution, the proposed power flow computation method tends to be towards exact for radial, single-phase equivalent distribution networks. Especially since transmission systems are commonly in a meshed structure, future works can incorporate (non-convex) constraints related to meshed networks, and study three-phase distribution networks.

### 6.1.3

#### **Conclusions, limitations and future perspectives for computational techniques and modelling accuracy for pricing of non-convex scheduling**

##### *Conclusions*

In this contribution, related to [Paper C]-[Paper D], a market-clearing procedure is proposed that efficiently balances a reasonable-costly scheduling for the next day's operation with an endogenous cost-recovery guarantee. Structurally, the rationale is to co-optimize energy and reserves in a stochastic risk-averse framework while endogenously ensuring cost recovery for generation companies. To this end, different cost recovery schemes are considered. These schemes are compared against the existing uplift payments – based on out-of-market compensation schemes, for the DA-stage. A revenue cap, limiting windfall profits for low-cost generators and reallocating them to consumers, is also designed and discussed. Such a revenue cap is inspired from the European Union discussions revolved around increasing costs for consumers due to a surge in fuel prices.

The resulting stochastic market-clearing procedure formulation is within the class of Mixed-Integer Bi-Linear Programming (MIBLP) models, thus challenging to be solved using off-the-shelf solvers or standard optimisation algorithms. Therefore, a hybridisation of McCormick envelopes and binary expansion is proposed to enhance the computational capability to solve the clearing problem. Numerical experiments indicate that the computing time under this solution approach decreases by approximately 70% compared to the standard binary expansion when applied to an instance of the IEEE-118 test system.

Under case studies presented, it is shown that price computation schemes presented lead to some differences in scheduling and price outcomes. Consideration of a risk aversion by the system operator gives rise to a synchronization of system costs amongst the schemes. Revenue cap indicates in almost all cases the lowest consumer payments, which competes mostly with the scheme 'Cost Recovery in Expectation'. Under high uncertainty, mechanisms other than 'Cost Recovery per Scenario' may not always warrant covering the costs of the generation companies. Nevertheless, such a mechanism may also cause

shifts of revenues from the least marginal cost generators toward higher-cost ones. Furthermore, co-optimising energy and reserves clearing, the costs for safeguarding the power system are more transparently allocated and calculated. An energy-only market would otherwise require out-of-market mechanisms to settle any real-time deviations. It is also shown that transmission congestion can lead to high market-clearing prices.

It is also demonstrated that a risk-averse energy and reserve scheduling can reduce load-shedding significantly, in the illustrated case by 77.3%, in case an unobserved extremely low wind generation scenario occurs.

#### *Limitations and future perspectives*

Not consideration of fairness and market power are amongst the limitations of the thesis, and left as a future work. In particular, future research can look into fairness aspects of uplift or other out-of-market mechanisms, and how to reimburse affected consumers. Revenue adequacy of system operators, and the effect of congestion and contingency can be other research directions. Furthermore, other techniques (e.g., machine learning or data-driven methods for warm-start procedures, decompositions techniques such as ADMM-variants - those which can potentially be applicable for mixed-integer problems) to improve tractability can be studied. In general, the proposed model, because of the computational time required to solve day-ahead market, is not directly practicable in the current market context. The time aspect would be aggravated also considering the fact that modern markets require complex orders as well as increased time granularity of some markets (15-minutes or less). Solution times can also be compared against other methods as future work, such as convex hull techniques, which is considered to be a computationally expensive method.

Another future direction is to analyse a Pareto curve in order for the operators to be able to choose the best risk-weight parameters. Other risk-control techniques, such as robust optimisation can also be studied as described in [181, 182], instead of a CVaR risk-measure.

Finally, future works can study different approaches to reserve pricing, such as in the references [183, 33].

## Bibliography

- [1] Ioannis Kougias et al. “The role of photovoltaics for the European Green Deal and the recovery plan.” In: *Renewable and Sustainable Energy Reviews* 144 (2021), p. 111017.
- [2] Antonio J Conejo and Luis Baringo. *Power system operations*. Vol. 11. Springer, 2018.
- [3] Juan M Morales et al. *Integrating renewables in electricity markets: operational problems*. Vol. 205. Springer Science & Business Media, 2013.
- [4] Pieter Schavemaker and Lou Van der Sluis. *Electrical power system essentials*. John Wiley & Sons, 2017.
- [5] Luis Nando Ochoa and Pierluigi Mancarella. “Bottom-Up Flexibility: Flexibility From the Edge of the Grid [Guest Editorial].” In: *IEEE Power and Energy Magazine* 19.4 (2021), pp. 14–103.
- [6] Ioannis Bouloumpasis, David Steen, et al. “Congestion management using local flexibility markets: recent development and challenges.” In: *2019 IEEE PES Innovative Smart Grid Technologies Europe (ISGT-Europe)* (2019), pp. 1–5.
- [7] Peter Bach Andersen, Junjie Hu, and Kai Heussen. “Coordination strategies for distribution grid congestion management in a multi-actor, multi-objective setting.” In: *2012 3rd IEEE PES Innovative Smart Grid Technologies Europe (ISGT Europe)*. IEEE. 2012, pp. 1–8.
- [8] Swedish Standard. “Voltage characteristics of electricity supplied by public electricity networks.” In: *German Institute for Standardisation: Berlin, Germany* (2010).
- [9] *International Smart Grid Action Network (ISGAN) (2019) [online]* Available at [www.iea-isgan.org/flexibility-in-future-power-systems/](http://www.iea-isgan.org/flexibility-in-future-power-systems/). Tech. rep. ISGAN, 2019.
- [10] Innocent Kamwa. “Dynamic Wide Area Situational Awareness: Propelling Future Decentralized, Decarbonized, Digitized, and Democratized Electricity Grids.” In: *IEEE Power and Energy Magazine* 21.1 (2023), pp. 44–58.

- [11] Baljinnnyam Sereeter, Cornelis Vuik, and Cees Witteveen. “On a comparison of Newton–Raphson solvers for power flow problems.” In: *Journal of Computational and Applied Mathematics* 360 (2019), pp. 157–169.
- [12] Mary B Cain, Richard P O’neill, Anya Castillo, et al. “History of optimal power flow and formulations.” In: *Federal Energy Regulatory Commission 1* (2012), pp. 1–36.
- [13] Daniel K Molzahn et al. “A survey of distributed optimization and control algorithms for electric power systems.” In: *IEEE Transactions on Smart Grid* 8.6 (2017), pp. 2941–2962.
- [14] Gonzalo E Constante-Flores, Antonio J Conejo, and Feng Qiu. “AC network-constrained unit commitment via relaxation and decomposition.” In: *IEEE Transactions on Power Systems* 37.3 (2021), pp. 2187–2196.
- [15] Shaobu Wang et al. “Multifold Insights for Power System Dynamics From Data Assimilation: Meeting Current Challenges.” In: *IEEE Power and Energy Magazine* 21.1 (2023), pp. 36–43.
- [16] J. D. Guy. “Security Constrained Unit Commitment.” In: *IEEE Transactions on Power Apparatus and Systems* PAS-90.3 (May 1971), pp. 1385–1390. DOI: 10.1109/TPAS.1971.292942.
- [17] Jean-Michel Glachant, Paul L. Joskow, and Michael G. Pollitt, eds. *Handbook on Electricity Markets*. First. Edward Elgar Pub, 2021.
- [18] Nuran Cihangir Martin and Bruno Fanzeres. “A Stochastic Risk-Averse Model to Price Energy in Pool-Based Electricity Markets with Non-Convex Costs and Revenue Caps.” In: *2023 International Conference on Smart Energy Systems and Technologies (SEST)*. IEEE. 2023, pp. 1–6.
- [19] Burak Kocuk, Santanu S Dey, and Xu Andy Sun. “Inexactness of SDP relaxation and valid inequalities for optimal power flow.” In: *IEEE Transactions on Power Systems* 31.1 (2015), pp. 642–651.
- [20] Nuran Cihangir Martin and Bruno Fanzeres. “Linearisation Based Decomposition Method for Circle Approximation in AC Network Constrained Unit Commitment.” In: *2023 IEEE Belgrade PowerTech*. IEEE. 2023, pp. 1–6.
- [21] João Silva et al. “Estimating the active and reactive power flexibility area at the TSO-DSO interface.” In: *IEEE Transactions on Power Systems* 33.5 (2018), pp. 4741–4750.

- [22] Muhammad Usman et al. “A novel two-stage TSO–DSO coordination approach for managing congestion and voltages.” In: *International Journal of Electrical Power & Energy Systems* 147 (2023), p. 108887.
- [23] Amin Kargarian et al. “Toward Distributed/Decentralized DC Optimal Power Flow Implementation in Future Electric Power Systems.” In: *IEEE Transactions on Smart Grid* 9.4 (Oct. 2016), pp. 2574–2594. DOI: 10.1109/TSG.2016.2614904.
- [24] Arthur Gonçalves Givisiez, Kyriacos Petrou, and Luis F Ochoa. “A review on TSO-DSO coordination models and solution techniques.” In: *Electric Power Systems Research* 189 (2020), p. 106659.
- [25] Simon Wenzel, Felix Riedl, and Sebastian Engell. “An efficient hierarchical market-like coordination algorithm for coupled production systems based on quadratic approximation.” In: *Computers & Chemical Engineering* 134 (2020), p. 106704.
- [26] Robert Currie et al. “Data privacy for the grid: Toward a data privacy standard for inverter-based and distributed energy resources.” In: *IEEE Power and Energy Magazine* 21.5 (2023), pp. 48–57.
- [27] Mohannad Alkhraijah et al. “PowerModelsADA: A Framework for Solving Optimal Power Flow using Distributed Algorithms.” In: *arXiv preprint arXiv:2304.00639* (2023).
- [28] Jacob Mays. “Quasi-stochastic electricity markets.” In: *INFORMS Journal on Optimization* 3.4 (2021), pp. 350–372.
- [29] Nuran C Martin and Bruno Fanzeres. “Stochastic risk-averse energy and reserve scheduling and pricing schemes with non-convexities and revenue caps.” In: *Electric Power Systems Research* 225 (2023), p. 109858.
- [30] Jiantao Shi et al. “A Scenario-Oriented Approach to Energy-Reserve Joint Procurement and Pricing.” In: *IEEE Transactions on Power Systems* 38.1 (Apr. 2022), pp. 411–426. DOI: 10.1109/TPWRS.2022.3165635.
- [31] Juan M Morales et al. “Pricing electricity in pools with wind producers.” In: *IEEE Transactions on Power Systems* 27.3 (2012), pp. 1366–1376.
- [32] Alexandre Moreira, Bruno Fanzeres, and Goran Strbac. “Energy and Reserve Scheduling under Ambiguity on Renewable Probability Distribution.” In: *Electric Power Systems Research* 160 (July 2018), pp. 205–218. DOI: <https://doi.org/10.1016/j.epsr.2018.01.024>.

- [33] Yun Tiam Tan and Daniel S Kirschen. “Co-optimization of energy and reserve in electricity markets with demand-side participation in reserve services.” In: *2006 IEEE PES power systems conference and exposition*. IEEE. 2006, pp. 1182–1189.
- [34] Tiago Andrade et al. “The p-Lagrangian Relaxation for Separable Nonconvex MIQCQP Problems.” In: *Journal of Global Optimization* 84.1 (Sept. 2022), pp. 43–76. DOI: <https://doi.org/10.1007/s10898-022-01138-y>.
- [35] Mohit Tawarmalani and Nikolaos V. Sahinidis. “Global Optimization of Mixed-Integer Nonlinear Programs: A Theoretical and Computational Study.” In: *Mathematical Programming* 99.3 (Apr. 2004), pp. 563–591. DOI: <https://doi.org/10.1007/s10107-003-0467-6>.
- [36] Geev Mokryani. *Future Distribution Networks*. New York, USA: AIP Publishing, 2022.
- [37] Steven H Low. “Convex relaxation of optimal power flow—Part I: Formulations and equivalence.” In: *IEEE Transactions on Control of Network Systems* 1.1 (2014), pp. 15–27.
- [38] Jacques Carpentier. “Contribution a l’etude du dispatching economique.” In: *Bull. Soc. Fr. Elec. Ser. 3* (1962), p. 431.
- [39] Karsten Lehmann, Alban Grastien, and Pascal Van Hentenryck. “AC-feasibility on tree networks is NP-hard.” In: *IEEE Transactions on Power Systems* 31.1 (2015), pp. 798–801.
- [40] Brian Stott, Jorge Jardim, and Ongun Alsaç. “DC power flow revisited.” In: *IEEE Transactions on Power Systems* 24.3 (2009), pp. 1290–1300.
- [41] Carleton Coffrin and Pascal Van Hentenryck. “A linear-programming approximation of AC power flows.” In: *INFORMS Journal on Computing* 26.4 (2014), pp. 718–734.
- [42] Hermann W Dommel and William F Tinney. “Optimal power flow solutions.” In: *IEEE Transactions on power apparatus and systems* 10 (1968), pp. 1866–1876.
- [43] Saeed Mohammadi, Mohammad Reza Hesamzadeh, and Derek W Bunn. “Distribution locational marginal pricing (DLMP) for unbalanced three-phase networks.” In: *IEEE Transactions on Power Systems* 37.5 (2021), pp. 3443–3457.
- [44] Waqqas A Bukhsh et al. “Local solutions of the optimal power flow problem.” In: *IEEE Transactions on Power Systems* 28.4 (2013), pp. 4780–4788.

- [45] JA Momoh et al. “Challenges to optimal power flow.” In: *IEEE Transactions on Power systems* 12.1 (1997), pp. 444–455.
- [46] Dzung T Phan. “Lagrangian duality and branch-and-bound algorithms for optimal power flow.” In: *Operations Research* 60.2 (2012), pp. 275–285.
- [47] Daniel K Molzahn and Line A Roald. “Towards an AC optimal power flow algorithm with robust feasibility guarantees.” In: *2018 Power Systems Computation Conference (PSCC)*. IEEE. 2018, pp. 1–7.
- [48] Bose Subhonmesh, Steven H Low, and K Mani Chandy. “Equivalence of branch flow and bus injection models.” In: *2012 50th Annual Allerton Conference on Communication, Control, and Computing (Allerton)*. IEEE. 2012, pp. 1893–1899.
- [49] Mesut E Baran and Felix F Wu. “Optimal capacitor placement on radial distribution systems.” In: *IEEE Transactions on power Delivery* 4.1 (1989), pp. 725–734.
- [50] Mesut Baran and Felix F Wu. “Optimal sizing of capacitors placed on a radial distribution system.” In: *IEEE Transactions on power Delivery* 4.1 (1989), pp. 735–743.
- [51] Anya Castillo et al. “A successive linear programming approach to solving the IV-ACOPF.” In: *IEEE Transactions on Power Systems* 31.4 (2015), pp. 2752–2763.
- [52] Byungkwon Park et al. “Sparse tableau formulation for optimal power flow applications.” In: *arXiv preprint arXiv:1706.01372* (2017).
- [53] Andy Sun and Dzung T Phan. “Some Optimization Models and Techniques for Electric Power System Short-term Operations.” In: *Wiley Encyclopedia of Operations Research and Management Science* (2011), pp. 1–17.
- [54] E Robert Bixby et al. “MIP: Theory and practice—closing the gap.” In: *IFIP Conference on System Modeling and Optimization*. Springer. 1999, pp. 19–49.
- [55] Wendel Melo, Marcia Fampa, and Fernanda Raupp. “Two linear approximation algorithms for convex mixed integer nonlinear programming.” In: *Annals of Operations Research* 316.2 (2022), pp. 1471–1491.
- [56] Thomas J Overbye, Xu Cheng, and Yan Sun. “A comparison of the AC and DC power flow models for LMP calculations.” In: *37th Annual Hawaii International Conference on System Sciences, 2004. Proceedings of the*. IEEE. 2004, 9–pp.

- [57] Arild Helseth. “A linear optimal power flow model considering nodal distribution of losses.” In: *2012 9th International Conference on the European Energy Market*. IEEE. 2012, pp. 1–8.
- [58] Zhao Yuan, Mohammad Reza Hesamzadeh, and Darryl R Biggar. “Distribution locational marginal pricing by convexified ACOPF and hierarchical dispatch.” In: *IEEE Transactions on Smart Grid* 9.4 (2016), pp. 3133–3142.
- [59] Konrad Purchala et al. “Usefulness of DC power flow for active power flow analysis.” In: *IEEE Power Engineering Society General Meeting, 2005*. IEEE. 2005, pp. 454–459.
- [60] Zhifang Yang et al. “A linearized OPF model with reactive power and voltage magnitude: A pathway to improve the MW-only DC OPF.” In: *IEEE Transactions on Power Systems* 33.2 (2017), pp. 1734–1745.
- [61] Zhifang Yang et al. “A general formulation of linear power flow models: Basic theory and error analysis.” In: *IEEE Transactions on Power Systems* 34.2 (2018), pp. 1315–1324.
- [62] Dmitry Shchetinin, Tomas Tinoco De Rubira, and Gabriela Hug. “On the construction of linear approximations of line flow constraints for AC optimal power flow.” In: *IEEE Transactions on Power Systems* 34.2 (2018), pp. 1182–1192.
- [63] Sleiman Mhanna and Pierluigi Mancarella. “An exact sequential linear programming algorithm for the optimal power flow problem.” In: *IEEE Transactions on Power Systems* 37.1 (2021), pp. 666–679.
- [64] Lahanda Purage MohashaIsuru Sampath et al. “A trust-region based sequential linear programming approach for AC optimal power flow problems.” In: *Electric Power Systems Research* 165 (2018), pp. 134–143.
- [65] Mohammad Iman Alizadeh and Florin Capitanescu. “A tractable linearization-based approximated solution methodology to stochastic multi-period AC security-constrained optimal power flow.” In: *IEEE Transactions on Power Systems* (2022).
- [66] Rabih A Jabr. “Radial distribution load flow using conic programming.” In: *IEEE transactions on power systems* 21.3 (2006), pp. 1458–1459.
- [67] Stephen P Boyd and Lieven Vandenbergh. *Convex optimization*. Cambridge university press, 2004.

- [68] Javad Lavaei and Steven H Low. “Zero duality gap in optimal power flow problem.” In: *IEEE Transactions on Power systems* 27.1 (2011), pp. 92–107.
- [69] Bernard C Lesieutre et al. “Examining the limits of the application of semidefinite programming to power flow problems.” In: *2011 49th annual Allerton conference on communication, control, and computing (Allerton)*. IEEE. 2011, pp. 1492–1499.
- [70] Somayeh Sojoudi and Javad Lavaei. “Physics of power networks makes hard optimization problems easy to solve.” In: *2012 IEEE Power and Energy Society General Meeting*. IEEE. 2012, pp. 1–8.
- [71] Baosen Zhang and David Tse. “Geometry of feasible injection region of power networks.” In: *2011 49th Annual Allerton Conference on Communication, Control, and Computing (Allerton)*. IEEE. 2011, pp. 1508–1515.
- [72] Subhonmesh Bose et al. “Optimal power flow over tree networks.” In: *2011 49th annual Allerton conference on communication, control, and computing (Allerton)*. IEEE. 2011, pp. 1342–1348.
- [73] Subhonmesh Bose et al. “Quadratically constrained quadratic programs on acyclic graphs with application to power flow.” In: *IEEE Transactions on Control of Network Systems* 2.3 (2015), pp. 278–287.
- [74] Javad Lavaei, David Tse, and Baosen Zhang. “Geometry of power flows and optimization in distribution networks.” In: *IEEE Transactions on Power Systems* 29.2 (2013), pp. 572–583.
- [75] Somayeh Sojoudi and Javad Lavaei. “On the exactness of semidefinite relaxation for nonlinear optimization over graphs: Part I.” In: *52nd IEEE Conference on Decision and Control*. IEEE. 2013, pp. 1043–1050.
- [76] Naum Z Shor. “Quadratic optimization problems.” In: *Soviet Journal of Computer and Systems Sciences* 25 (1987), pp. 1–11.
- [77] Xiaoqing Bai et al. “Semidefinite programming for optimal power flow problems.” In: *International Journal of Electrical Power & Energy Systems* 30.6-7 (2008), pp. 383–392.
- [78] Ramtin Madani, Somayeh Sojoudi, and Javad Lavaei. “Convex relaxation for optimal power flow problem: Mesh networks.” In: *IEEE Transactions on Power Systems* 30.1 (2014), pp. 199–211.
- [79] Baosen Zhang and David Tse. “Geometry of injection regions of power networks.” In: *IEEE Transactions on Power Systems* 28.2 (2012), pp. 788–797.

- [80] Hamid Mahboubi and Javad Lavaei. “Analysis of semidefinite programming relaxation of optimal power flow for cyclic networks.” In: *2018 IEEE Conference on Decision and Control (CDC)*. IEEE. 2018, pp. 3203–3210.
- [81] Vyacheslav Kungurtsev and Jakub Marecek. “A two-step pre-processing for semidefinite programming.” In: *2020 59th IEEE Conference on Decision and Control (CDC)*. IEEE. 2020, pp. 384–389.
- [82] Cédric Josz and Didier Henrion. “Strong duality in Lasserre’s hierarchy for polynomial optimization.” In: *Optimization Letters* 10.1 (2016), pp. 3–10.
- [83] Jiawang Nie. “Optimality conditions and finite convergence of Lasserre’s hierarchy.” In: *Mathematical programming* 146 (2014), pp. 97–121.
- [84] Daniel K Molzahn and Ian A Hiskens. “Mixed SDP/SOCP moment relaxations of the optimal power flow problem.” In: *2015 IEEE Eindhoven PowerTech*. IEEE. 2015, pp. 1–6.
- [85] Xiaolong Kuang et al. “Approximating the ACOPF problem with a hierarchy of SOCP problems.” In: *2015 IEEE Power & Energy Society General Meeting*. IEEE. 2015, pp. 1–5.
- [86] David E Bernal et al. “Alternative regularizations for Outer-Approximation algorithms for convex MINLP.” In: *Journal of Global Optimization* 84.4 (2022), pp. 807–842.
- [87] Ignacio Quesada and Ignacio E Grossmann. “An LP/NLP based branch and bound algorithm for convex MINLP optimization problems.” In: *Computers & chemical engineering* 16.10-11 (1992), pp. 937–947.
- [88] Lijie Su et al. “Improved quadratic cuts for convex mixed-integer nonlinear programs.” In: *Computers & Chemical Engineering* 109 (2018), pp. 77–95.
- [89] Chris Coey, Miles Lubin, and Juan Pablo Vielma. “Outer approximation with conic certificates for mixed-integer convex problems.” In: *Mathematical Programming Computation* 12.2 (2020), pp. 249–293.
- [90] Welington de Oliveira. “Regularized optimization methods for convex MINLP problems.” In: *Top* 24.3 (2016), pp. 665–692.
- [91] Marco A. Duran and Ignacio E. Grossmann. “An Outer-Approximation Algorithm for a Class of Mixed-Integer Nonlinear Programs.” In: *Mathematical Programming* 36.3 (Oct. 1986), pp. 307–339. DOI: <https://doi.org/10.1007/BF02592064>.

- [92] Roger Fletcher and Sven Leyffer. “Solving mixed integer nonlinear programs by outer approximation.” In: *Mathematical programming* 66 (1994), pp. 327–349.
- [93] Jagadisan Viswanathan and Ignacio E Grossmann. “A combined penalty function and outer-approximation method for MINLP optimization.” In: *Computers & Chemical Engineering* 14.7 (1990), pp. 769–782.
- [94] S Tosserams et al. “An augmented Lagrangian relaxation for analytical target cascading using the alternating direction method of multipliers.” In: *Structural and multidisciplinary optimization* 31 (2006), pp. 176–189.
- [95] Sambuddha Chakrabarti et al. “Security constrained optimal power flow via proximal message passing.” In: *2014 Clemson university power systems conference*. IEEE. 2014, pp. 1–8.
- [96] Antonio J Conejo, Francisco J Nogales, and Francisco J Prieto. “A decomposition procedure based on approximate Newton directions.” In: *Mathematical programming* 93 (2002), pp. 495–515.
- [97] Giulio Binetti et al. “Distributed consensus-based economic dispatch with transmission losses.” In: *IEEE Transactions on Power Systems* 29.4 (2014), pp. 1711–1720.
- [98] Yu Zhang and Georgios B Giannakis. “Distributed stochastic market clearing with high-penetration wind power.” In: *IEEE Transactions on Power Systems* 31.2 (2015), pp. 895–906.
- [99] Yu Yang et al. “A survey of admm variants for distributed optimization: Problems, algorithms and features.” In: *arXiv preprint arXiv:2208.03700* (2022).
- [100] Stephen Boyd, Neal Parikh, and Eric Chu. *Distributed optimization and statistical learning via the alternating direction method of multipliers*. 2011.
- [101] Tomaso Erseghe. “Distributed optimal power flow using ADMM.” In: *IEEE transactions on power systems* 29.5 (2014), pp. 2370–2380.
- [102] Andy X Sun, Dzung T Phan, and Soumyadip Ghosh. “Fully decentralized AC optimal power flow algorithms.” In: *2013 IEEE Power & Energy Society General Meeting*. IEEE. 2013, pp. 1–5.

- [103] Sindri Magnússon, Pradeep Chathuranga Weeraddana, and Carlo Fischione. “A distributed approach for the optimal power-flow problem based on ADMM and sequential convex approximations.” In: *IEEE Transactions on Control of Network Systems* 2.3 (2015), pp. 238–253.
- [104] Euhanna Ghadimi et al. “Optimal Parameter Selection for the Alternating Direction Method of Multipliers (ADMM): Quadratic Problems.” In: *IEEE Transactions on Automatic Control* 60.3 (Sept. 2014), pp. 644–658. DOI: [10.1109/TAC.2014.2354892](https://doi.org/10.1109/TAC.2014.2354892).
- [105] Jonathan Eckstein and Wang Yao. “Augmented Lagrangian and Alternating Direction Methods for Convex Optimization: A Tutorial and some Illustrative Computational Results.” In: *RUTCOR Research Reports* 32.3 (Dec. 2012), p. 44.
- [106] Antonio J Conejo, Miguel Carrión, Juan M Morales, et al. *Decision making under uncertainty in electricity markets*. Vol. 1. Springer, 2010.
- [107] John R Birge and Francois Louveaux. *Introduction to stochastic programming*. Springer Science & Business Media, 2011.
- [108] Akshay Gupte et al. “Solving Mixed Integer Bilinear Problems using MILP Formulations.” In: *SIAM Journal on Optimization* 23.2 (2013), pp. 721–744. DOI: <https://doi.org/10.1137/110836183>.
- [109] Leslie Richard Foulds, Dag Haugland, and Kurt Jørnsten. “A bilinear approach to the pooling problem.” In: *Optimization* 24.1-2 (1992), pp. 165–180.
- [110] Faiz A Al-Khayyal and James E Falk. “Jointly constrained biconvex programming.” In: *Mathematics of Operations Research* 8.2 (1983), pp. 273–286.
- [111] Garth P. McCormick. “Computability of Global Solutions to Factorable Nonconvex Programs: Part I – Convex Underestimating Problems.” In: *Mathematical Programming* 10.1 (Dec. 1976), pp. 147–175. DOI: <https://doi.org/10.1007/BF01580665>.
- [112] Joseph K Scott, Matthew D Stuber, and Paul I Barton. “Generalized mccormick relaxations.” In: *Journal of Global Optimization* 51.4 (2011), pp. 569–606.
- [113] Matteo Fischetti and Michele Monaci. “A branch-and-cut algorithm for mixed-integer bilinear programming.” In: *European Journal of Operational Research* 282.2 (2020), pp. 506–514.

- [114] Pedro M. Castro. “Tightening Piecewise McCormick Relaxations for Bilinear Problems.” In: *Computers & Chemical Engineering* 72 (Jan. 2015), pp. 300–311. DOI: <https://doi.org/10.1016/j.compchemeng.2014.03.025>.
- [115] Débora C Faria and Miguel J Bagajewicz. “Novel bound contraction procedure for global optimization of bilinear MINLP problems with applications to water management problems.” In: *Computers & chemical engineering* 35.3 (2011), pp. 446–455.
- [116] Farzaneh Abbaspourtorbati et al. “Pricing Electricity Through a Stochastic Non-Convex Market-Clearing Model.” In: *IEEE Transactions on Power Systems* 32.2 (Mar. 2017), pp. 1248–1259. DOI: 10.1109/TPWRS.2016.2569533.
- [117] Harry Markowitz. *PORTFOLIO SELECTION. EFFICIENT DIVERSIFICATION OF INVESTMENTS. BY HARRY M. MARKOWITZ.* Yale University Press, 1971.
- [118] Rüdiger Schultz and Stephan Tiedemann. “Risk aversion via excess probabilities in stochastic programs with mixed-integer recourse.” In: *SIAM journal on optimization* 14.1 (2003), pp. 115–138.
- [119] Philippe Artzner et al. “Coherent measures of risk.” In: *Mathematical finance* 9.3 (1999), pp. 203–228.
- [120] R. Tyrrell Rockafellar and Stanislav Uryasev. “Conditional Value-at-Risk for General Loss Distributions.” In: *Journal of Banking & Finance* 26.7 (July 2002), pp. 1443–1471. DOI: [https://doi.org/10.1016/S0378-4266\(02\)00271-6](https://doi.org/10.1016/S0378-4266(02)00271-6).
- [121] Anya Castillo et al. “The Unit Commitment Problem With AC Optimal Power Flow Constraints.” In: *IEEE Transactions on Power Systems* 31.6 (Nov. 2016), pp. 4853–4866. DOI: 10.1109/TPWRS.2015.2511010.
- [122] PJM. *Energy Price Formation Senior Task Force – Price Formation.* Tech. rep., Dec. 2018.
- [123] M. Paredes et al. “Benders’ Decomposition of the Unit Commitment Problem with Semidefinite Relaxation of AC Power Flow Constraints.” In: *Electric Power Systems Research* 192 (Mar. 2021), p. 106965. DOI: <https://doi.org/10.1016/j.epsr.2020.106965>.
- [124] Abhinav Verma. *Power grid security analysis: An optimization approach.* Jan. 2010.

- [125] Morteza Ashraphijuo et al. “A strong semidefinite programming relaxation of the unit commitment problem.” In: *2016 IEEE 55th Conference on Decision and Control (CDC)*. IEEE. Dec. 2016, pp. 694–701.
- [126] Ran Quan, Jin-bao Jian, and Yun-dong Mu. “Tighter relaxation method for unit commitment based on second-order cone programming and valid inequalities.” In: *International Journal of Electrical Power & Energy Systems* 55 (Feb. 2014), pp. 82–90.
- [127] Alvaro Gonzalez-Castellanos, David Pozo, and Aldo Bischi. “Stochastic unit commitment of a distribution network with non-ideal energy storage.” In: *2019 International Conference on Smart Energy Systems and Technologies (SEST)*. IEEE. Sept. 2019, pp. 1–6.
- [128] Pierre Bonami, Mustafa Kiliç, and Jeff Linderoth. “Algorithms and software for convex mixed integer nonlinear programs.” In: *Mixed integer nonlinear programming*. Springer, Jan. 2012, pp. 1–39.
- [129] Alvaro González-Castellanos, David Pozo, and Aldo Bischi. “Distribution System Operation with Energy Storage and Renewable Generation Uncertainty.” In: *Handbook of Optimization in Electric Power Distribution Systems*. Springer, Jan. 2020, pp. 183–218.
- [130] Conor Murphy, Alireza Soroudi, and Andrew Keane. “Information Gap Decision Theory-Based Congestion and Voltage Management in the Presence of Uncertain Wind Power.” In: *IEEE Transactions on Sustainable Energy* 7.2 (Nov. 2015), pp. 841–849. DOI: 10.1109/TSTE.2015.2497544.
- [131] Salar Fattahi et al. “Conic relaxations of the unit commitment problem.” In: *Energy* 134 (Sept. 2017), pp. 1079–1095.
- [132] Han Wang, Shariq Riaz, and Pierluigi Mancarella. “Integrated techno-economic modeling, flexibility analysis, and business case assessment of an urban virtual power plant with multi-market co-optimization.” In: *Applied Energy* 259 (Feb. 2020), p. 114142.
- [133] Rodrigo Moreno, Roberto Moreira, and Goran Strbac. “A MILP model for optimising multi-service portfolios of distributed energy storage.” In: *Applied Energy* 137 (Jan. 2015), pp. 554–566.
- [134] Hande Y Benson and Ümit Sağlam. “Mixed-integer second-order cone programming: A survey.” In: *Theory Driven by Influential Applications*. Sept. 2013, pp. 13–36.

- [135] Burak Kocuk, Santanu S Dey, and X Andy Sun. “Strong SOCP relaxations for the optimal power flow problem.” In: *Operations Research* 64.6 (Dec. 2016), pp. 1177–1196.
- [136] Linfeng Yang et al. “Projected mixed integer programming formulations for unit commitment problem.” In: *International Journal of Electrical Power & Energy Systems* 68 (June 2015), pp. 195–202.
- [137] James E Price and John Goodin. “Reduced network modeling of WECC as a market design prototype.” In: *2011 IEEE Power and Energy Society General Meeting*. July 2011, pp. 1–6.
- [138] Elizabeth D Dolan and Jorge J Moré. “Benchmarking optimization software with performance profiles.” In: *Mathematical programming* 91 (2002), pp. 201–213.
- [139] David Pozo. “Linear battery models for power systems analysis.” In: *Electric Power Systems Research* 212 (2022), p. 108565.
- [140] Nuran C Martin and Bruno Fanzeres. “A Two-Level ADMM Algorithm for Multi-Agent DSO-TSO Congestion Management and Voltage Control Coordination with Limited Information Exchange.” In: *in process of publication* (2024).
- [141] Luciana Marques et al. “Grid impact aware tso-dso market models for flexibility procurement: Coordination, pricing efficiency, and information sharing.” In: *IEEE Transactions on Power Systems* 38.2 (2022), pp. 1918–1931.
- [142] David Pozo, Enzo Sauma, and Javier Contreras. “Basic Theoretical Foundations and Insights on Bilevel Models and Their Applications to Power Systems.” In: *Annals of Operations Research* 254.1–2 (July 2017), pp. 303–334.
- [143] Yuting Mou, Anthony Papavasiliou, and Philippe Chevalier. “A bi-level optimization formulation of priority service pricing.” In: *IEEE Transactions on Power Systems* 35.4 (2019), pp. 2493–2505.
- [144] Yamin Wang, Lei Wu, and Shouxiang Wang. “A fully-decentralized consensus-based ADMM approach for DC-OPF with demand response.” In: *IEEE Transactions on Smart Grid* 8.6 (2016), pp. 2637–2647.
- [145] Ziang Zhang, Navid Rahbari-Asr, and Mo-Yuen Chow. “Asynchronous distributed cooperative energy management through gossip-based incremental cost consensus algorithm.” In: *2013 North American Power Symposium (NAPS)*. IEEE. 2013, pp. 1–6.

- [146] Hanspeter Höschle et al. “An ADMM-based method for computing risk-averse equilibrium in capacity markets.” In: *IEEE Transactions on Power Systems* 33.5 (2018), pp. 4819–4830.
- [147] Yunfeng Wen et al. “Synergistic operation of electricity and natural gas networks via ADMM.” In: *IEEE Transactions on Smart Grid* 9.5 (2017), pp. 4555–4565.
- [148] Jiajia Yang et al. “A fully decentralized distribution market mechanism using ADMM.” In: *2019 IEEE Power & Energy Society General Meeting (PESGM)*. IEEE. 2019, pp. 1–5.
- [149] Kaizhao Sun and Xu Andy Sun. “A two-level ADMM algorithm for AC OPF with global convergence guarantees.” In: *IEEE Transactions on Power Systems* 36.6 (2021), pp. 5271–5281.
- [150] Terrence WK Mak et al. “Learning regionally decentralized ac optimal power flows with admm.” In: *IEEE Transactions on Smart Grid* (2023).
- [151] Krešimir Mihić, Mingxi Zhu, and Yinyu Ye. “Managing randomization in the multi-block alternating direction method of multipliers for quadratic optimization.” In: *Mathematical Programming Computation* 13.2 (2021), pp. 339–413.
- [152] Gregorio Muñoz-Delgado et al. “Integrated transmission and distribution system expansion planning under uncertainty.” In: *IEEE Transactions on Smart Grid* 12.5 (2021), pp. 4113–4125.
- [153] Piyush A Sharma, Abheejeet Mohapatra, and Ankush Sharma. “A Novel Interior-Exterior Approach for the TSO-DSO based Bilevel Optimal Power Flow.” In: *IEEE Transactions on Power Systems* (2023).
- [154] Mohammad Iman Alizadeh et al. “Uncertainty-Aware TSO-DSO Coordination Methodology for Transmission Voltages Control.” In: *2023 IEEE Belgrade PowerTech*. IEEE. 2023, pp. 1–6.
- [155] A Gonzalez-Castellanos, D Pozo, and A Bischi. “Online appendix for book chapter: Distribution System Operation with Energy Storage and Renewable Generation Uncertainty.” In: *Zenodo* (2019).
- [156] Bushra Canaan and Djaffar Ould Abdeslam. *Bericht 3.4.1, 3.4.2: Cross-border interconnection possibilities in the distribution level (low-voltage grid), available at: <https://www.res-tmo.com>*. Tech. rep. RES-TMO, Dec. 2022.
- [157] Mariana Resener et al. *Handbook of optimization in electric power distribution systems*. Springer, 2020.

- [158] Mingguo Hong et al. “Electricity market and operations reliability.” In: *2012 IEEE Power and Energy Society General Meeting*. IEEE. 2012, pp. 1–7.
- [159] Bowen Hua and Ross Baldick. “A convex primal formulation for convex hull pricing.” In: *IEEE Transactions on Power Systems* 32.5 (2016), pp. 3814–3823.
- [160] Shaobo Zhang and Kory W Hedman. “Conditions for ramp rates causing uplift.” In: *2019 North American Power Symposium (NAPS)*. IEEE. 2019, pp. 1–6.
- [161] Panagiotis Andrianesis et al. “Computation of Convex Hull Prices in Electricity Markets With Non-Convexities Using Dantzig-Wolfe Decomposition.” In: *IEEE Transactions on Power Systems* 37.4 (July 2022). DOI: 10.1109/TPWRS.2021.3122000.
- [162] Ryan Alexander et al. *What to Cap? Emergency Interventions in the European Electricity and Gas Market*. Tech. rep. EPICO, Sept. 2022.
- [163] Huajie Gu, Ruifeng Yan, and Tapan Saha. “Review of system strength and inertia requirements for the national electricity market of Australia.” In: *CSEE Journal of Power and Energy Systems* 5.3 (2019), pp. 295–305.
- [164] Jalal Kazempour, Pierre Pinson, and Benjamin F Hobbs. “A stochastic market design with revenue adequacy and cost recovery by scenario: Benefits and costs.” In: *IEEE Transactions on Power Systems* 33.4 (2018), pp. 3531–3545.
- [165] Marco Zugno and Antonio J Conejo. “A robust optimization approach to energy and reserve dispatch in electricity markets.” In: *European Journal of Operational Research* 247.2 (2015), pp. 659–671.
- [166] Alexandre Moreira, Bruno Fanzeres, and Goran Strbac. “An Ambiguity Averse Approach for Transmission Expansion Planning.” In: *IEEE PowerTech 2019* (June 2019), pp. 1–6. DOI: 10.1109/PTC.2019.8810864.
- [167] Carlos Ruiz, Antonio J. Conejo, and Steven A. Gabriel. “Pricing Non-Convexities in an Electricity Pool.” In: *IEEE Transactions on Power Systems* 27.3 (Aug. 2012), pp. 1334–1342. DOI: 10.1109/TPWRS.2012.2184562.

- [168] Erik Ela et al. “Electricity Markets and Renewables: A Survey of Potential Design Changes and their Consequences.” In: *IEEE Power and Energy Magazine* 15.6 (Nov. 2017), pp. 70–82. DOI: 10.1109/MPE.2017.2730827.
- [169] Beibei Wang and Benjamin F. Hobbs. “Real-Time Markets for Flexiramp: A Stochastic Unit Commitment-Based Analysis.” In: *IEEE Transactions on Power Systems* 31.2 (Mar. 2016), pp. 846–860. DOI: 10.1109/TPWRS.2015.2411268.
- [170] Congcong Wang, Peter Bao-Sen Luh, and Nivad Navid. “Ramp Requirement Design for Reliable and Efficient Integration of Renewable Energy.” In: *IEEE Transactions on Power Systems* 32.1 (Jan. 2017), pp. 562–571. DOI: 10.1109/TPWRS.2016.2555855.
- [171] Geoffrey Pritchard, Golbon Zakeri, and Andrew Philpott. “A Single-Settlement, Energy-Only Electric Power Market for Unpredictable and Intermittent Participants.” In: *Operations Research* 58.4-part-2 (July 2010), pp. 1210–1219. DOI: <https://www.jstor.org/stable/40793317>.
- [172] Paul Gribik, William W. Hogan, and Susan Pope. “Market-Clearing Electricity Prices and Energy Uplift.” In: *Cambridge, MA* (Dec. 2007).
- [173] Hung-po Chao. “Incentives for Efficient Pricing Mechanism in Markets with Non-Convexities.” In: *Journal of Regulatory Economics* 56.1 (Aug. 2019), pp. 33–58. DOI: 10.1007/s11149-019-09385-w.
- [174] Luiz Augusto Barroso et al. “Nash Equilibrium in Strategic Bidding: A Binary Expansion Approach.” In: *IEEE Transactions on Power Systems* 21.2 (May 2006), pp. 629–638. DOI: 10.1109/TPWRS.2006.873127.
- [175] Leonardo Salsano de Assis et al. “A Piecewise McCormick Relaxation-based Strategy for Scheduling Operations in a Crude Oil Terminal.” In: *Computers & Chemical Engineering* 106 (Nov. 2017), pp. 309–321. DOI: <https://doi.org/10.1016/j.compchemeng.2017.06.012>.
- [176] Jonathan Bosch, Iain Staffell, and Adam D. Hawkes. “Global Levelised Cost of Electricity from Offshore Wind.” In: *Energy* 189 (Dec. 2019), p. 116357. DOI: <https://doi.org/10.1016/j.energy.2019.116357>.
- [177] Bruno Fanzeres, Alexandre Street, and David Pozo. “A Column-and-Constraint Generation Algorithm to Find Nash Equilibrium in Pool-Based Electricity Markets.” In: *Electric Power Systems Research* 189 (Dec. 2020), p. 106806. DOI: <https://doi.org/10.1016/j.epsr.2020.106806>.

- [178] Fatma Gül Akgül, Birdal Şenoğlu, and Talha Arslan. “An Alternative Distribution to Weibull for Modeling the Wind Speed Data: Inverse Weibull Distribution.” In: *Energy Conversion and Management* 114 (Apr. 2016), pp. 234–240. DOI: <https://doi.org/10.1016/j.enconman.2016.02.026>.
- [179] KRW Bell et al. “Test system requirements for modelling future power systems.” In: *IEEE PES General Meeting*. July 2010, pp. 1–8.
- [180] TENNET. *Target grid, available at: <https://www.tennet.eu/target-grid>*. Tech. rep. TENNET, Apr. 2024.
- [181] Karthik Natarajan, Dessislava Pachamanova, and Melvyn Sim. “Constructing risk measures from uncertainty sets.” In: *Operations research* 57.5 (2009), pp. 1129–1141.
- [182] Alexander Schied\*. “Risk measures and robust optimization problems.” In: *Stochastic Models* 22.4 (2006), pp. 753–831.
- [183] Deqiang Gan and Eugene Litvinov. “A lost opportunity cost model for energy and reserve co-optimization.” In: *IEEE Power Engineering Society Summer Meeting*, vol. 3. IEEE. 2002, pp. 1559–1564.